



University  
of Glasgow

<https://theses.gla.ac.uk/>

Theses Digitisation:

<https://www.gla.ac.uk/myglasgow/research/enlighten/theses/digitisation/>

This is a digitised version of the original print thesis.

Copyright and moral rights for this work are retained by the author

A copy can be downloaded for personal non-commercial research or study,  
without prior permission or charge

This work cannot be reproduced or quoted extensively from without first  
obtaining permission in writing from the author

The content must not be changed in any way or sold commercially in any  
format or medium without the formal permission of the author

When referring to this work, full bibliographic details including the author,  
title, awarding institution and date of the thesis must be given

Enlighten: Theses

<https://theses.gla.ac.uk/>  
[research-enlighten@glasgow.ac.uk](mailto:research-enlighten@glasgow.ac.uk)

PHASE DISTRIBUTION AND FLOW CHARACTERISTICS  
OF ISOTHERMAL CO-CURRENT TWO-PHASE FLOW IN  
HORIZONTAL PIPES

DY

SHAWKI ASSAAD HARKLY, B.Sc., A.R.T.C.

A THESIS

PRESENTED FOR THE PH.D., DEGREE

OF THE UNIVERSITY OF GLASGOW.

February, 1966.

ProQuest Number: 10656449

All rights reserved

INFORMATION TO ALL USERS

The quality of this reproduction is dependent upon the quality of the copy submitted.

In the unlikely event that the author did not send a complete manuscript and there are missing pages, these will be noted. Also, if material had to be removed, a note will indicate the deletion.



ProQuest 10656449

Published by ProQuest LLC (2017). Copyright of the Dissertation is held by the Author.

All rights reserved.

This work is protected against unauthorized copying under Title 17, United States Code  
Microform Edition © ProQuest LLC.

ProQuest LLC.  
789 East Eisenhower Parkway  
P.O. Box 1346  
Ann Arbor, MI 48106 – 1346



ACKNOWLEDGEMENT.

The author wishes to convey his deep gratitude to Professor A.S.T. Thomson, D.Sc., Ph.D., A.R.T.C., for the facilities offered in carrying out the experiments in the Royal Technical College Laboratories.

He is also indebted to Professor A.W. Scott, B.Sc., Ph.D., A.R.T.C., and Mr. A.M. Laird, D.Sc., A.R.T.C., for their helpful advice and supervision.

INDEX.

	Page.
Nomenclature	2
Abstract.	iv
CHAPTER I - REVIEW OF PREVIOUS WORK.	
Introduction.	1
(a) Gas-Liquid Flow.	2
Discussion	19
(b) Vapour-Liquid Flow.	11
Discussion	12
(c) Turbulent mass transfer in Liquid-Solids suspensions.	13
(d) Air-Solid flow in pipes.	14
General Discussion.	15
CHAPTER II - APPARATUS.	
Apparatus	17
General Layout	17
Mixing Chamber	19
Experimental pipe section.	19
Quick closing cocks.	20
Sampling	21
"Knife" traversing mechanism.	24

	Page.
<b>CHAPTER III - PROCEDURE.</b>	
Procedure	25
Sampling technique	26
Velocity measurement technique	28
Effect of relative velocity	29
Microflash photographs	30
Air-water velocity ratio tests.	30
<b>CHAPTER IV - DEVELOPMENT OF FLOW/PATTERNS.</b>	
Development of flow patterns	32
For $1\frac{1}{2}$ " I.D. Pyrex pipe	33
Flow mechanism affecting forms of flow.	35
Flash photograph	36
Conclusions.	37
<b>CHAPTER V - PHASE DISTRIBUTION.</b>	
Liquid entrainment	38
Experimental results.	38
Entrained liquid in gas phase.	39
Water concentration in the air stream	40
Results of tests on $1\frac{1}{2}$ " I.D. Glass pipe	
Constant air variable water plotting	40
Constant water variable air "	41
Results of tests on $1\frac{1}{2}$ " I.D. steel pipe	42
Results of tests on 1" I.D. Steel pipe	42
Effect of surface tension reduction.	43

	Page.
Horizontal traverses.	43
$45^\circ$ traverses.	43
General picture of concentration distribution.	44
Discussion of experimental results.	44
Pipe size effect.	46
Effect of reduction of surface tension.	47
Theoretical analysis of phase distribution.	49
Concentration distribution in circular pipe.	51
Modification of the theoretical treatment.	55
Correlation of theory and experimental results.	58
Comparison between theoretical and experimental values.	67
Thickness of laminar sublayer and its relation to the distribution of phases.	66
Conclusions.	69
 CHAPTER VI - VELOCITY DISTRIBUTION.	
Introduction	70
Experimental Results	70
Discussion of results.	73
Correlation of results.	72
Mixing length calculations.	73
Formula used for $\epsilon$	77
Plane of zero shear.	78

	Page.
<b>CHAPTER VII - PRESSURE DROP.</b>	
Introduction	79
Experimental results.	79
Pressure Drop Prediction	
(1) Friction Coefficients concept.	80
(2) Prediction of pressure drop by analogy with Prandtl mixing length.	82
(3) Determination of relative velocity.	87
Correlation of pressure drop results by a method analogous to gas-solid formula.	89
<b>GENERAL DISCUSSION AND CONCLUSIONS.</b>	
Flow patterns.	90
Concentration distributions.	91
Velocity distribution	92
Pressure drop prediction	93
<b>REFERENCES.</b>	95
<b>APPENDIX I - Tables of flow rates.</b>	100
<b>APPENDIX II - Calculation of results.</b>	105
<b>APPENDIX III - Development of equations.</b>	110
Thickness of laminar boundary sublayer.	115
<b>APPENDIX IV - Calculated results for concentration distribution in a vertical traverse.</b>	116
<b>APPENDIX V - Velocity distribution correlations.</b>	128
<b>APPENDIX VI - Pressure drop.</b>	130
Calculation of slip between phases.	135

NOMENCLATURE.

$A, B, A', B', A^*, B^*$ .	Constants.
$Q$	Concentration $\text{lb/ft}^3$ (air).
$C_a$	Concentration at a point.
$C_V$	Volumetric Concentration $\text{ft}^3/\text{ft}^3$ (air).
$D_p, d$ .	Pipe diameter. $\text{ft.}$
$D_d$	Drop diameter microns.
$f$	Coefficient of friction.
$F_N$	Pseudo Number.
$g$	Gravitational acceleration $\text{ft/sec}^2$ .
$G$	Mass Flow velocity $\text{lb/ft}^2 \text{sec.}$
$J_{\mu}, G_x$	Bessel Functions.
$K$	Von Karman Universal Constant.
$L$	Length of the pipe $\text{ft.}$
$l$	Mixing Length.
$M_0, M_0$	Constants.
$N, P_g, S$	Constants.
$Q$	Volume rate of flow. $\text{ft}^3/\text{sec.}$
$r$	radius $\text{ft.}$
$r_0$	Pipe radius. $\text{ft.}$
$Re$	Reynolds Number.
$R$	Ratio of cross section of either phase to total cross section.

$s$	Slip $\frac{V_0}{V_L}$
$t$	time sec.
$U_2$	Friction velocity. ft./sec.
$u, v$	Velocity (average) ft./sec.
$V$	Volume. $\text{ft}^3$ .
$w$	Fall velocity. ft/sec.
$W$	Rate of flow. lb/sec.
$W_0$	Weber Number.
$W_0, W_0'$	Height of pipe empty and full. lb.
$x$	Cross section $\text{ft}^2, \text{in}^2$ .
$y$	Distance from the wall. ft.
$\zeta$	$\frac{\omega}{\rho K u_f}$

Greek Plots.

$\alpha$	$\equiv$	$(\frac{\Delta P}{\Delta L})_{T.P.}/(\frac{\Delta P}{\Delta L})_L$
$\beta$	$\equiv$	<u>momentum transfer coefficient</u> <u>mass transfer coefficient.</u>
$\beta'$	$\equiv$	Vol. ratio of phases.
$\frac{\Delta P}{\Delta L}$	$\equiv$	Pres. drop along the pipe. lb/ft. <sup>3</sup>
$\phi$	$\equiv$	Ratio of areas occupied by the phases.
$\psi$	$\equiv$	Parameter. $\sqrt{\frac{(\frac{\Delta P}{\Delta L})_L}{(\frac{\Delta P}{\Delta L})_g}}$
$\eta$	$\equiv$	$\frac{\lambda_{T.P.}}{\lambda g}$
$\epsilon$	$\equiv$	Coefficient of turbulent viscosity.
$\tau$	$\equiv$	Shear stress. lb/ft. <sup>2</sup>

$\mu$	=	Absolute viscosity.	poisen.
$\nu$	=	Kinematic viscosity.	ft <sup>2</sup> /sec.
$\sigma$	=	Surface tension	1b/ft. or dyne/cm.
$\rho$	=	Density	lb/ft. <sup>3</sup>
$\theta$	=	Angle.	
$\mu$	=	Coefficient of friction	= 42

Suffixes.

T.P. Two phases.

g, l (l) Gas and liquid respectively.

M Momentum.

S Mass transfer.

w Water.

t Top part of pipe.

b Bottom part of pipe.

m Mixture of two phases.

ABSTRACT.

A review of the work already done on co-current gas-liquid two-phase flow in horizontal pipes indicated that many of the conclusions reached and empirical formulae presented were based more on visual observations than on actual experimental measurements. The present research was initiated in an attempt to get by experimentation a clearer picture of the fundamental characteristics of this complex type of flow.

The special apparatus and technique developed for measuring velocity, density and phase distribution over the pipe cross-section and the pressure drop along the pipe are described and the procedure outlined.

The results are presented mainly in graphical form.

From the results it has been possible to follow the changing pattern from the stratified form to the fully dispersed annular flow, through a series of modes which have hitherto been ill-defined as annular flow.

The distribution of water entrained in the air stream is given in the form of concentration curves, a form which has not previously been used in gas-liquid flow. According to the rates of flow covered these curves have two quite distinct forms, the first, for low and moderate flow rates is exponential, and the second, for high rates, is tending progressively towards a symmetrical form. Correlations between the experimental results and a semi-empirical form gives agreement within  $\pm 25\%$  which at this stage, considering the complexity of the problem, is considered satisfactory.

Velocity measurement by Pitot tube method has been used conservatively and its limitations discussed. The graphs presented show a similarity between entrained liquid particles in a gas stream and suspended solid particles in a liquid stream. The correlation of results is given and discussed in the light of turbulence concepts. Explanation of experimental findings are given.

A study of the different ways of correlating pressure drops is made and although it yields promising results, yet it also indicates that the application of the fundamentals of turbulent flow is oversimplified and fails to give reasonable prediction of pressure drops.

A treatment of pressure drop using Fanning formula and applying the mean density of the core proves to be adequate within the range of experiments and it is suggested that such method may be used successfully if the mean density of the dispersed gas stream is predicted according to the semi-empirical formula given.

A correlation analogous to those proposed for gas-solid flow is presented and shows satisfactory results within  $\pm 10\%$ .

CHAPTER I.

REVIEW OF PREVIOUS WORK.

## INTRODUCTION.

Interest in two-phase two-component co-current flow has increased rapidly during the last twenty years. Although investigations of the characteristics of this type of flow were begun a century ago, only recently has progress been made in this field, due mainly to widening fields of application in engineering as in water tube boilers, refrigerators, petroleum refineries and chemical engineering generally.

The fact that progress has been slow is readily understood when one considers the number of variables involved. These are, the ratio of the phase flow rates, the diameter and position of the pipe, surface tension and viscosity of the liquid and the slip velocity between the phases.

Several attempts have been made to correlate the experimental results. But all theoretical attempts to analyse such flow have been based on the treatment of each phase separately and have involved many assumptions.

Two-phase flow investigations have been carried out in four different fields:-

- (a) Gas-liquid flows in horizontal and vertical pipes.
- (b) Vapour-liquid flow.
- (c) Gas-solid flow.
- (d) Liquid-solid flow.

(a) Gas-Liquid Flow:

This is the field in which most work has been done by previous investigators.

Boelter and Kepner (12) investigated experimentally air-water and air-oil co-current flow in pipes. They showed that pressure drop for given air-oil ratios and constant air flow rate would be proportional to  $\frac{1}{\rho_g}^{1.0}$ .

$$\left(\frac{\Delta P}{\Delta L}\right)_{T.P.} = \lambda \frac{G^2}{\rho D g}$$

where  $\lambda$  is independent of  $\rho$ .

Using Blesius equation, they correlated their results as

$$\left(\frac{\Delta P}{\Delta L}\right)_{T.P.} = -0.158 \frac{\mu^{1/4} G^{7/4}}{D^{7/4} g \rho} \quad A-1$$

Liquid viscosity effect was studied and it was concluded that  $\left(\frac{\Delta P}{\Delta L}\right)_{T.P.}$  varied as  $\mu^{0.6}$ .

They also suggested that:

$$\left(\frac{\Delta P}{\Delta L}\right)_{T.P.} = f [Re_l, Re_g, Fr, We] \quad A-2$$

Considering  $\frac{1}{Fr \times We} = \frac{\sigma g^2}{\rho u^4}$  as a modulus for the capillary waves formation, they showed that the velocity to sustain capillary waves on the water surface was 0.75 ft./sec.

Martinelli and co-workers (46) carried out extensive tests with 1" diameter glass and  $\frac{1}{2}"$  diameter galvanised pipes using air and eight different liquids with isothermal flow ranging from all liquid to all air in the pipe.

Also, surface tension was reduced by adding detergents but this did not appear to change the pressure drop.

Visual and photographic observations were made which revealed the following modes of flow:

- (1) Bubble flow in which air flowed on the top part of the mixture in form of bubbles.
- (2) Stratified flow in which the liquid flowed along the bottom without disturbances and air in the top part.
- (3) Wavy stratified when waves appeared at the interface.
- (4) Slugging flow where successive slugs of water and air passed along the tube.
- (5) Annular flow in which the liquid flowed along the pipe wall while the gas filled the central core.

At very low liquid flow rates the type of flow changed to annular without passing into a region of slugging form. In their theoretical analysis, the following assumptions were made:

- (a) The static pressure drop for a liquid phase must be equal to that of gaseous phase.
- (b) The cross section occupied by the liquid and gas was equal to the total cross section of the pipe.

Using the ordinary friction formulae, two-phase pressure drop could be expressed as

$$\left(\frac{\Delta P}{\Delta L}\right)_{T.P.} = \left(\frac{\Delta P}{\Delta L}\right)_g \left[ 1 + \alpha^{\frac{1}{4}} \left( \frac{u_1}{u_g} \right)^{0.083} \left( \frac{P_g}{P_1} \right)^{0.416} \left( \frac{G_L}{G_g} \right)^{0.75} \right]^{2.4} - A-3$$

for turbulent-turbulent gas-liquid flow which is the most common case in practice.

They gave similar formulae for other possible combinations of gas-liquid flows.

They claimed pressure drop predictions of  $\pm 30\%$  from experimental results.

Armand(3), investigated the physical phenomena taking place in two-phase flow in horizontal pipes. By weighing the test section of the pipe he was able to estimate the ratio of the areas occupied by each phase from

$$\phi = \frac{Xg}{X} = \frac{W_o - W}{W_o}$$

In addition, tests were carried out to determine the distribution of phases by the use of sampling tubes and a special "knife" sampler which allowed the phase distribution to be measured in horizontal sections formed by moving the mechanism across the section. A high speed camera was used and the different flow patterns reported were almost the same as reported by Martinelli, except for the fact that as annular flow developed the entrainment of water droplets in the core became important.

For the prediction of pressure drop with annular flow where air moves separately in the core, he obtained a correlation based on the ratio  $\phi$

$$\left( \frac{\Delta P}{\Delta L} \right)_{T.P.} = \left( \frac{\Delta P}{\Delta L} \right)_l \frac{A}{(1 - \phi)^n} \quad A-4$$

in which the value of  $n$  was dependent on the value of  $1 - \phi$ . To complete the pressure drop prediction  $(1 - \phi)$  was expressed as a function of  $Re$  and  $Fr$  for air only (superficial).

Equation A-3 gave satisfactory agreement with experimental results taken from tests on 26 mm. and 56 mm. diameter pipes.

Lockhart and Martinelli(44) developed a method for correlating their results in a simpler way than A-2. Their correlation was based on the same assumptions as in the earlier work by Martinelli(36), and on the application of this non-dimensional expression  $\Psi$ ,  $\phi$  where

$$\Psi = \sqrt{\frac{(\frac{\Delta P}{\Delta L})_L}{(\frac{\Delta P}{\Delta L})_g}}$$

$$\phi = \frac{x_g}{x}$$

and

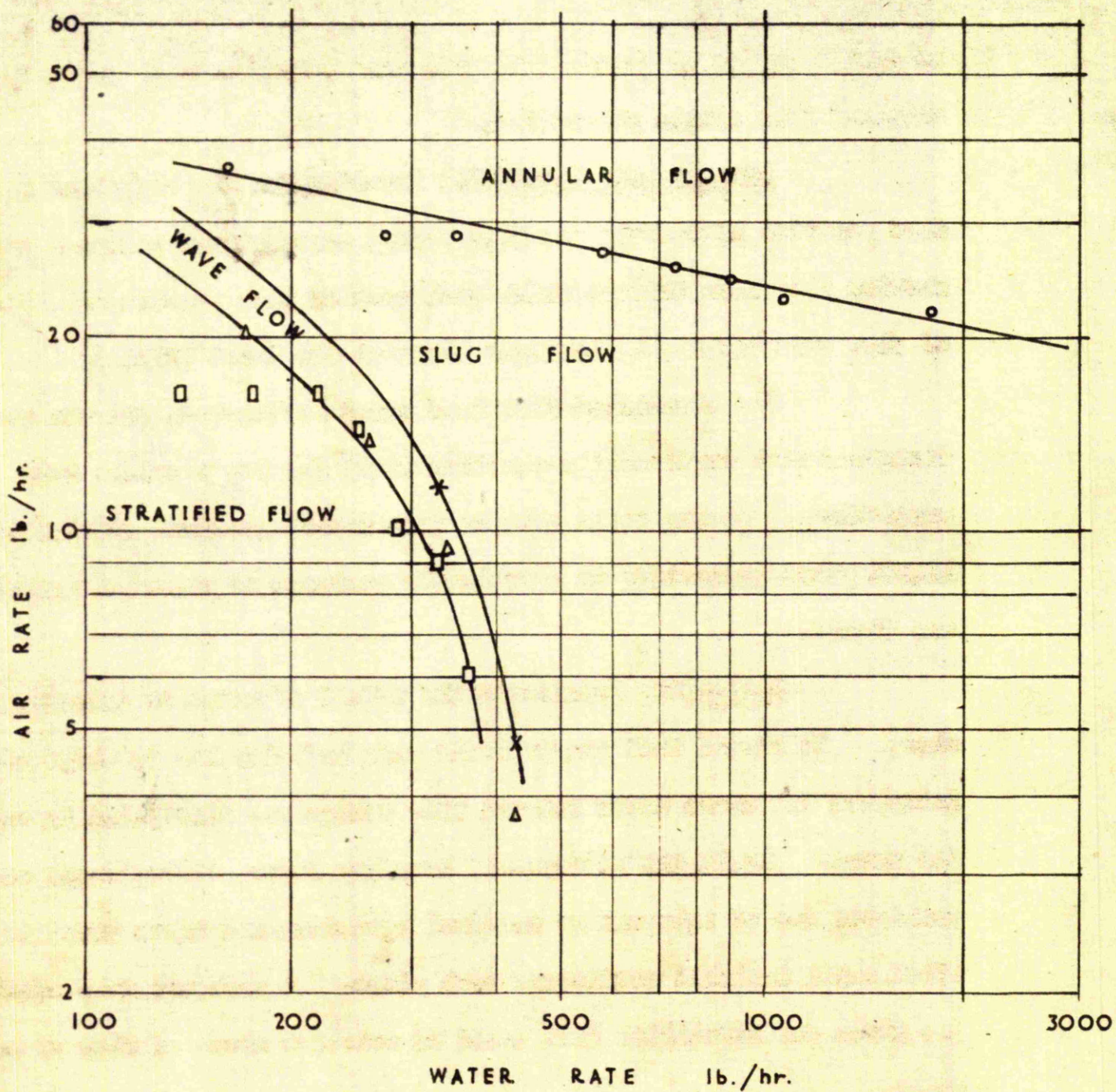
$$\Psi = f(\phi) \quad A - 5$$

The value of  $\phi$  was obtained by trapping a sample between two quick closing cocks and measuring the amount of water in the pipe.

Bergelin(9) discussed generally two-phase flow and indicated the method to be used in estimating pressure drops using equation A-4 and based his method on a chart relating  $\phi$  and  $\Psi$  as well as  $(\frac{\Delta P}{\Delta L})_L$ ,  $(\frac{\Delta P}{\Delta L})_g$ , the latter two functions were given by Martinelli.

Also, he observed mass transfer between the phases. Utilizing the conception of superficial Reynolds number and friction factor obtained from equation

FIG. 1 : LIMITS OF VARIOUS TYPES OF FLOW  
CO-CURRENT FLOW OF AIR & WATER  
IN ONE-INCH TUBES.



○ JENKINS                      □ HOLDEN  
 △ × GAZLEY AND BERGELIN

Fig. 1

$$\left( \frac{\Delta P}{\Delta L} \right)_{T.P.} = \frac{\lambda}{d} \cdot \rho_g \cdot \frac{U_g^2}{2g} \quad \text{A-6}$$

he gave a series of curves that bore some relation to friction factor obtained from single phase flow.

Bergelin and Gazley(11) investigated the different modes of flow reported previously and from visual observations produced a chart showing the range through which each mode of flow persisted. The regions of flow were defined by boundary lines on the Chart (Fig.1).

The stratified flow form was investigated, but the results disagreed with Martinelli's equation (A-3) for the pressure drop prediction. It was found that an interfacial gradient existed in the liquid phase indicating an irreversible exchange of momentum between gas and liquid.

Gazley(22) considered the effect of waves on interfacial shear. He stated that energy would pass undiminished to water with smooth interface but where waves existed some energy was dissipated in sustaining the waves. As in the aerodynamic boundary layer, disturbances would be initiated due to internal or external agencies, and those would be amplified until unstable conditions took place. A pressure drop equation was given for stratified flow based on relative areas of flow of each phase.

Bergelin, Kegel, Carpenter and Gazley(10) carried out tests with air-water mixtures in a vertical tube. Their results compared with Martinelli's correlation (A-3) within  $\pm 30\%$ .

Jenkins(32) was able to correlate his experimental data, obtained with annular flow, to within 40% of Lockhart and Martinelli formula A-4, but found that his data fell within 5% of the best line through each liquid rate, thus indicating that some factor is missing from the formula.

Kosterin(37) represented the different modes of flow and carried out investigations on the influence of pipe size and position on hydraulic resistance. He tried a correlation of his results by giving a series of curves for  $(\gamma - \beta_y)$  where  $\gamma = \frac{\lambda_{T.P.} (\text{at } R_e)}{\lambda g}$   
and  $\lambda_{T.P.} = \frac{\pi^2 g d^5}{G_{T.P.}^2} \cdot \rho_{T.P.} \cdot \left( \frac{\Delta P}{\Delta L} \right)_{T.P.}$  — A-6

$R_e$  is considered as a fictitious Reynolds number for air when it flows inside the pipe,

$$\text{and } \beta_y = \frac{16 G_{T.P.}}{g \pi^2 D^5 [\rho_g \times \beta' + \rho_w (1 - \beta')]^2}$$

$\lambda_{T.P.}$  was shown to be 20-30% higher than single phase values with the bigger difference at lower superficial velocities.

Middella(66) tests were made to determine the pressure drop in the flow of air-water and steam-water mixtures through horizontal pipes. Several curves were given showing the relationship between friction factor and velocity of the air for smooth brass pipes of 25, 36 mm. diameter. Attempts were made to establish a theoretical basis for these results but no reliable theory was found nor did Martinelli's formula prove satisfactory. He concluded that two phase flow is too complex to be solved

by a simple formula.

Johnson and Abou-Sabieh(22) extended the work of Garley by making visual observations of the different flow patterns at higher water rates. They pointed out the existence of mass transfer between phases at high air flow.

Also, non-isothermal flow in horizontal pipes was studied which yielded results that were compared with Martinelli's correlations.

To measure the "slip" between the two phases, i.e., the ratio between gas to water velocities, quick closing cocks were used.

Abrenson(1) in a research on liquid film cooling for jets' nozzles, found that ripples may take place at a certain air velocity and water flow rate. When the liquid thickness becomes greater than the laminar boundary layer, the effect of turbulence in the main stream would give rise to waves at the interface.

Writing down the velocity and thickness of boundary layer in non-dimensional expressions he suggested a method for calculations.

Chisholm(15) made a careful study to two-phase flow by adopting the concepts of turbulence and using the findings of Armand.

He assumed (a) Annular flow, where a water film wets the whole circumference of the pipe; (b) an air core which is uniformly dispersed with water droplets flowing with the same speed as air; (c) same mixing length for single and two phase flow.

Starting from the fundamental Prandtl equation for shear stress in a turbulent flow and a suggested velocity distribution diagram where the core velocity curve incorporated no laminar sublayer due to

waves at the interface, he obtained an expression for the slip between the two phases.

Proceeding from that expression and using Armand's(3) results he was able to give a more rational, though much involved equation for pressure drop in horizontal or inclined tubes.

$$\left(\frac{\Delta P}{\Delta L}\right)_{T.P.} = B \frac{\lambda}{2gD} \left[ (1-\beta') \frac{W}{X} \right]^2 \cdot \frac{1}{\rho_L} \left( \frac{X}{X_L} \right)^2 - A \cdot 7$$

He claimed for tests carried on a 2" I.D. pipe a closer agreement between theory and experimental results than had hitherto been possible.

Laird(38) investigated in a special apparatus the effect of waves moving on the boundary of a pipe in the laminar flow region. His apparatus allowed him to study the effect of frequency, wave length and amplitude on the hydraulic resistance. He found that friction losses increased to 40 times the value obtained with wave-free flow.

He explained the phenomenon of the instability of the water surface in two-phase flow by suggesting that if the energy is absorbed continuously, the disturbed region will grow and turbulent flow would take place, but if the disturbing energy is dissipated faster than it is supplied, laminar flow would exist. Annular flow is to be expected when the interfacial shear stresses are sufficient to support the liquid layer.

Discussion.

Work on two phase flow in circular pipes has indicated considerable complexity. Several methods have been used for tackling the problem.

The method of Martinelli, which has been followed by a number of investigators, was based on Gasturstadt's formula(21), and provided an empirical method for predicting the pressure drop in annular flow without undue concern regarding flow mechanism, *viz.*, effect of turbulence, momentum and mass transfer on the flow structure.

The different patterns of flow was one of the main points raised in most investigations, with annular flow receiving most attention. The hypothetical form of annular flow, which considered a core of air and a layer of water on the walls was used for correlations. Armand and Kosterin indicated that this idealised flow would exist only in a small range and that the main annular flow comprises a layer of liquid on the walls with a core of air dispersed with water droplets.

Difference in core density due to liquid entrainment was considered theoretically by Chisholm but, due to lack of experimental data, theory was applied with numerous assumptions which rendered its application limited.

The other approach of Borgelin or Kosterin was based on the application of the usual friction equations and incorporated some fictitious non-dimensional groups. This method, however, may prove a promising way for correlating the results if allowances were made for some factors neglected.

The outstanding work of Laird, although not directly connected with two phase flow, has emphasized the importance of interfacial waves on hydraulic resistance. Unfortunately this work was confined to the viscous air flow, and the work required extensions to the turbulent range.

### (b) Vapour-Liquid Flow.

As a fundamental branch of two phase flow in engineering, liquid-vapour flow is of interest since it occurs frequently in water tube boilers, refrigerators and refrigerating machines. So a brief summary of work done in this field is included.

Bottomley(13) gave a paper on the flow of evaporating water through tubes.

Armand and Treshchew(4) made use of former theory developed by the first(3) and stated the effect of steam pressure in the case of boilers. The pressure drop was predicted from

$$\left(\frac{\Delta P}{\Delta L}\right)_{T.P} = \left(\frac{\Delta P}{\Delta L}\right)_L \cdot \frac{0.025 \beta + 0.005}{(1 - \beta)^{1.75}} \quad \text{for } \beta > 0.9$$

where  $\beta$  is the boiler pressure. An agreement within 20% was quoted for experimental results.

Shehuab(57) made a comprehensive study of the two phase flow in vertical tube boilers. By assuming a certain shape of flow in vertical steam generators which involved bubbles of steam with separating layers of water. He developed equations of motion and of pressure drop,

the latter in two parts; one due to the zones of steam bubbles and the other due to the water layers. The net lifting force was shown to be a function of the ratio between the steam velocity and the water velocity in the annulus.

Burnell(14), investigated adiabatic flow of steam-water mixtures in pipes. By adopting Bottomley's method(13), he showed that large deviations existed between his results and the theory. The discrepancies were attributed to the assumption of no relative velocity between steam and water.

Turner(43) presented theoretical methods for calculating adiabatic flow of evaporating liquids in pipes. By adopting both continuity and momentum balance equations he obtained an expression for pressure drops. His formula was adapted for the different flow patterns possible. For small tubes up to 0.218" diameter, theory and experimental results agreed well, while in larger pipes the measured values were lower than predicted. The interface velocity ratio increased to 1.2 at certain outlet conditions from the pipe. He found the wall shear force per unit area to be a function of liquid velocity and density.

#### Discussion.

Theoretical analysis of vapour-water 2-phase flow was similar to gas-liquid flow except for the fact that due to continuous evaporation the ratio vapour/liquid rates of flow changed along the pipe and rendered the problem more complicated. Bottomley's work was proved later by Burnell to lack generalization due to neglect of the effect of "slip".

between phases.

Shokwah's approach was interesting and gave a clearer physical picture of the flow but some of the assumptions need more investigation.

Lanning's work was indicated later to incorporate an incorrect factor which rendered his equations unapplicable at high steam pressure.

The importance of the effect of velocity ratio was realised by many of these authors.

#### Turbulent Mass Transfer in Liquid Solid Suspensions.

Mass transfer in suspended sediment in channel was investigated by V.A. Venoni(65) and later by Ismail(31). The experimental data were used to study the effects of the presence of sand in suspension on the characteristics of the flow. They showed that the universal constant of turbulent exchange  $K$  as given by Von Karman(64) decreases with the increase of suspended material. Ismail showed that the ratio between momentum transfer coefficient and mass transfer coefficient was greater than unity but varied according to the size of sand used. The value of the momentum transfer coefficient is affected by the presence of sand only through the change in  $K$ .

Laursen and Lin in a discussion of Ismail's paper did not agree with the author's conclusions. They maintained:-

1.  $K$  is not sufficiently defined to enable rational conclusions to be drawn.
2. that  $\beta$  is equal or less than unity.

### Air-Solid Flow in Pipes.

Suspension of solids in gas is fundamentally the same problem as liquid in gas and air in the case of dispersed flow except for the fact that solid particles would behave differently because of the absence of surface tension.

Gasterstadt(21) defined pressure-drop in transport of solids suspended in air by a formula depending on the ratio of the pressure drop with the solid suspension, to that with air alone at the same velocity. Cramp(16) recognised the effect of particle velocity on the equations of motion. Wood and Bailey gave a detailed analysis of the momentum transfer between the conveying air and the solids. They concluded that the path of the particles appears to be a series of leaps due to aerodynamic forces and gravity effects. Regarding the nature of solid flow Korn(36) suggested three separate classifications. If the solids are light and are acted upon by a steep velocity gradient, there is little contact with the pipe walls and the bulk of material would be carried by the central portion of the air in the pipe. If the particles are extremely small, the velocity would reach air velocity and the mixture will behave as a true fluid. Vogt and White(63) used dimensionless pressure drops ratio  $\alpha$  of Gasterstadt to correlate the results and to eliminate size effect of the particles and of the pipes.

Hariu and Molstad(26) studied the transport of solids in vertical pipes. They considered the pressure drop as the sum of the pressure drop due to the carrier gas and the pressure drop due to the solids.

Discussion.

Work on liquid-solid suspension was used to test the general developments in the turbulence hypothesis by different scientists. Experimenting with liquid-solid mixtures it was found that turbulence was suppressed due to solids existing in the liquid flow, shown by decrease in value of Von Karman's universal constant K. The lines followed in this case would be helpful to analyse air-liquid flow.

With air-solid suspensions the correlations were much the same as were used by Martinelli and other investigators, i.e., predicting the pressure drop without deep understanding of the change in the mechanism from that corresponding to single phase.

General Discussion.

It is not surprising that the mechanics of two-phase flow being so complicated that none of the previous investigators attempted any method of correlation that would tie up the fundamental characteristics of two-phase flow.

They were only touched upon by the different authors and Armand alone tried some measurements of the distribution of phases.

The main type of annular flow which is considered most likely in a co-current gas-liquid flow is the one indicated by Armand and Kosterin, viz., a layer of liquid on the tube wall and a core of gas dispersed with liquid droplets.

In the present work phase distribution and a study of the fundamentals of such a flow was made to get a clearer understanding of the facts that control its mechanism.

Mass transfer in liquid-solids flow as has been given, would be helpful to clarify some of the aspects involved in the study of two-phase flow.

CHAPTER II.

APPARATUS.

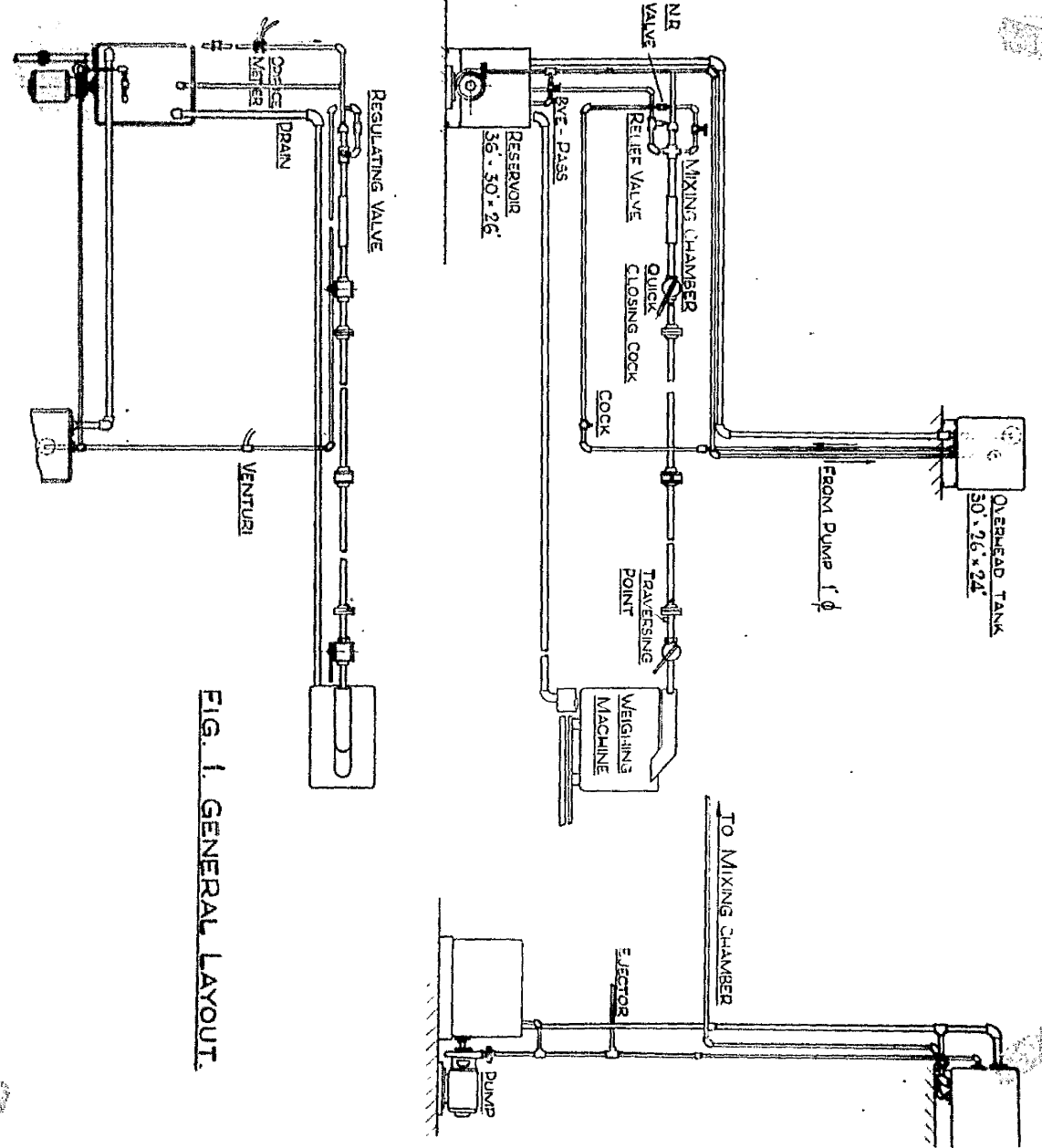
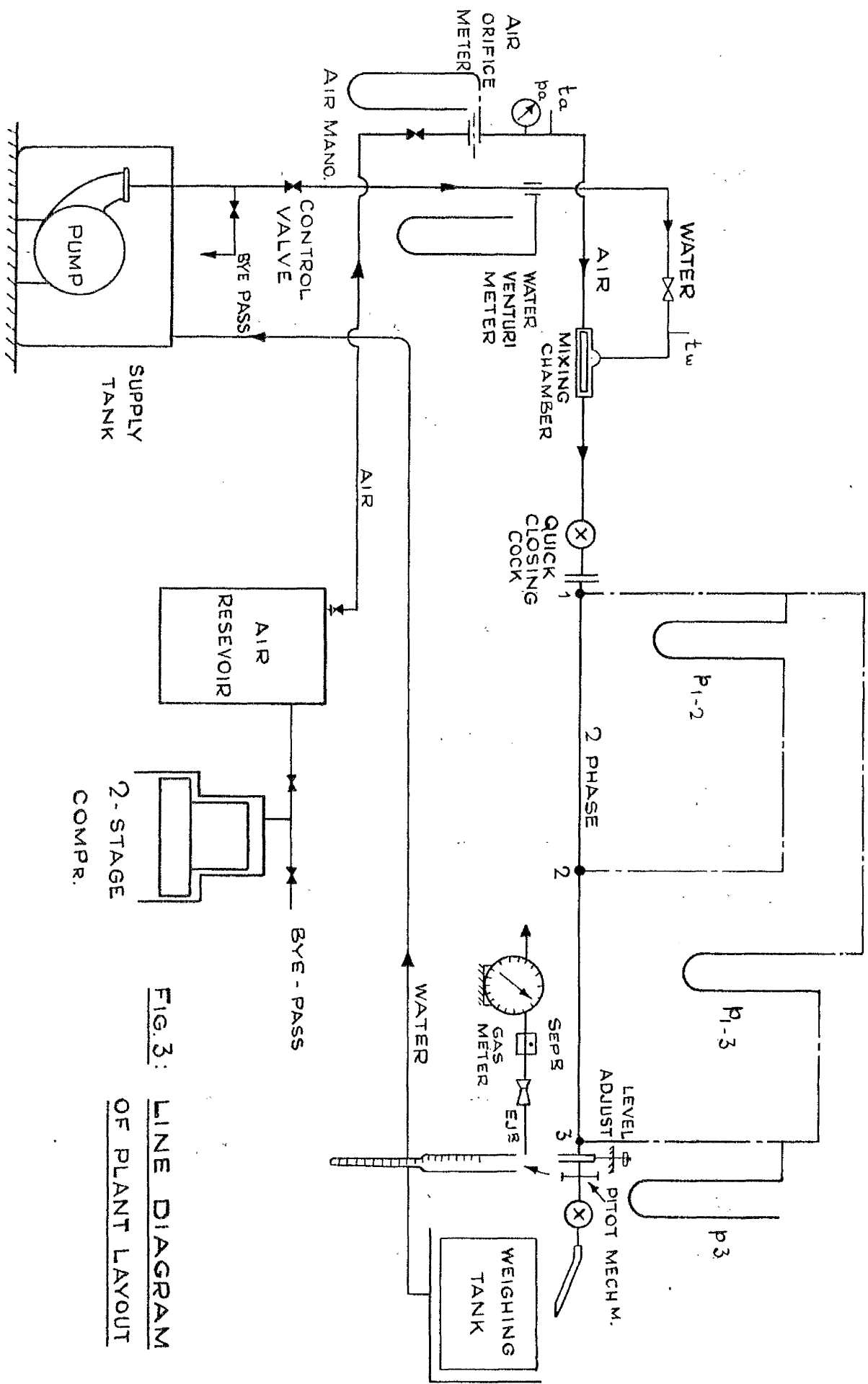


FIG. I. GENERAL LAYOUT.

Fig. II



Apparatus.

The apparatus was designed with the following objects in view:-

1. To establish the different patterns of flow and to observe how they are developed and initiated.
2. To record the pressure drops along the experimental pipe.
3. To determine the slip between water and air, i.e., ratio between air and water velocities of flow.
4. To plot the distribution of the phases.

General Layout.

The general features of the piping are shown in Fig.2, and a line diagram of the system in Fig.3.

Air was supplied from a two-stage electrically driven, constant speed air compressor of maximum capacity 200 cu.ft./min. free air. A by-pass on the discharge side was used to regulate the flow of air to the apparatus. Air passed through a reservoir which damped air pressure fluctuations and separated any oil or water vapour.

A regulation valve and an orifice meter were fixed in the air pipe, also a pressure gauge and a thermometer were used to record the orifice downstream pressure and temperature.

The orifice meter was made according to the German Standard (1931) (49). Three orifice plates, 5/16", 1/2" and 5/8" diameter were used to cover the whole range of air discharge.

Each orifice was calibrated in a water pipe line and the coefficients of discharge against Reynolds numbers are shown in Fig. 6.

As a check, a standard Pitot tube was used to traverse the whole section of the pipe and the air discharge was calculated by multiplying ring areas and corresponding velocities. The readings agreed well.

The water circuit consisted of a reservoir, a circulating pump and overhead tank. Pump discharge was regulated until an overflow from the overhead tank was maintained thus ensuring constant head.

A venturi was used to indicate the water flow rate during the experiment. Before each test its reading was checked, by weighing the water at the end of the experimental tube. The venturi reading was indicated by a carbon tetrachloride manometer.

A non-return valve, fitted before the mixing chamber served to isolate the water system when the pressure rose due to shutting off the quick closing cocks. A regulating valve on the water line from the overhead tank was used at the mixing point.

Water separated from the air was weighed when required, and returned back to the reservoir. Such a system made possible the use of liquids having different characteristics. Also, a very steady liquid flow was attained. However, for high flow rates in the 1" diameter pipe experiments, the head was found insufficient and the pump was used to supply the liquid directly to the mixing chamber. It was possible to obtain fairly constant discharge by using the by-pass valve. The test pipe was connected by a rubber tube to the mixing chamber and one adjustable hinging point was provided at the other end, so that the tube

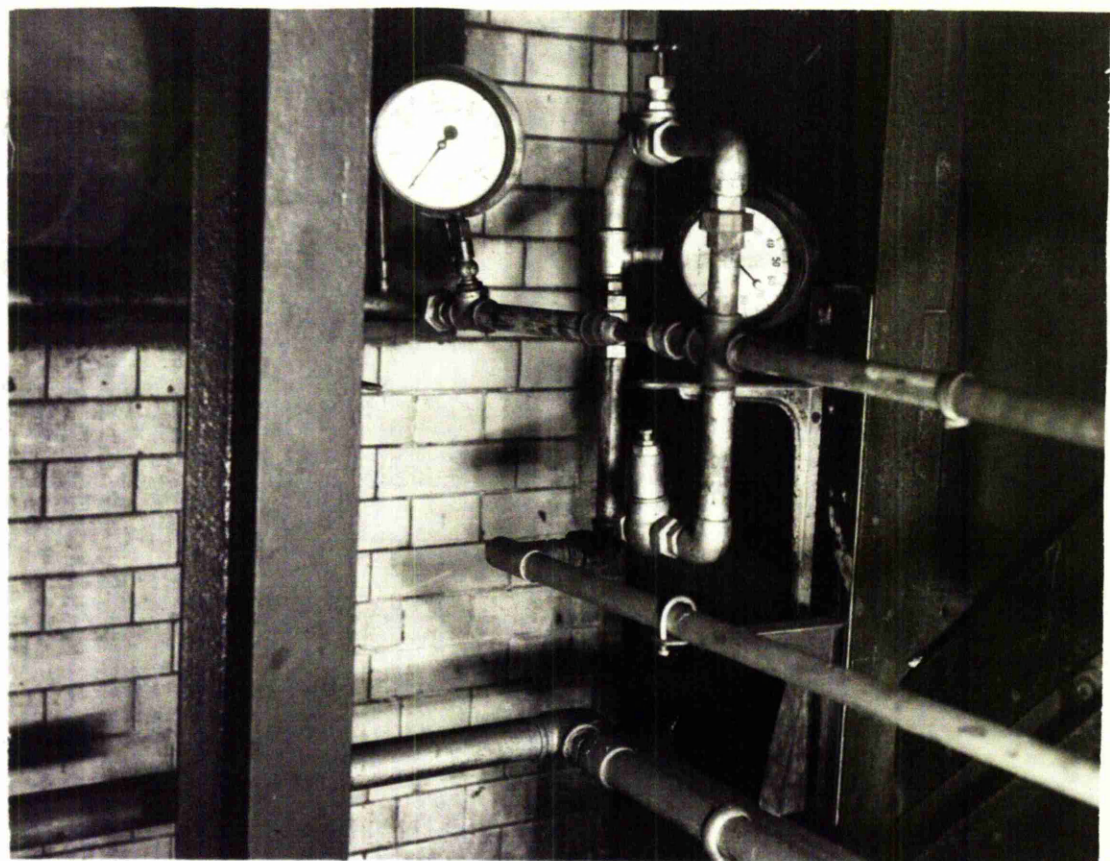


Fig. 7

could be brought horizontal or tilted slightly for draining after the quick closing cocks were used.

#### Mixing Chamber.

Several mixing chambers were tried before building the apparatus. In some of them air was admitted through the pipe and water injected at different angles on it.

It was found that for stability and repeatability the most satisfactory arrangement was similar to Gazley's (22). It consisted of an inner tube surrounded by an outer one leaving an annular space between. The water passed through the annulus and the air entered through the inner tube. Fig. 7.

A relief valve was connected to the mixing chamber to avoid pressure from building up when the quick closing cocks were used.

#### Experimental Pipe Section.

Pipes,  $1\frac{1}{2}$ " and  $2\frac{1}{2}$ " inside diameter were used in the study. For the  $1\frac{1}{2}$ " I.D. size a glass tube and an old "rusty" steel tube were used. For the 1" I.D. size a perspex tube was used, followed by 1" I.D. steel one. The glass and perspex pipes allowed visual observations to be made and also they represented the characteristics of smooth pipes while the steel tubes enabled the study for rough pipes to be made.

The  $1\frac{1}{2}$ " I.D. "Pyrex" glass pipe consisted of two sections, each 6 ft. in length. The sections were carefully aligned with a brass pressure tapping insert, so that no obstruction would take place

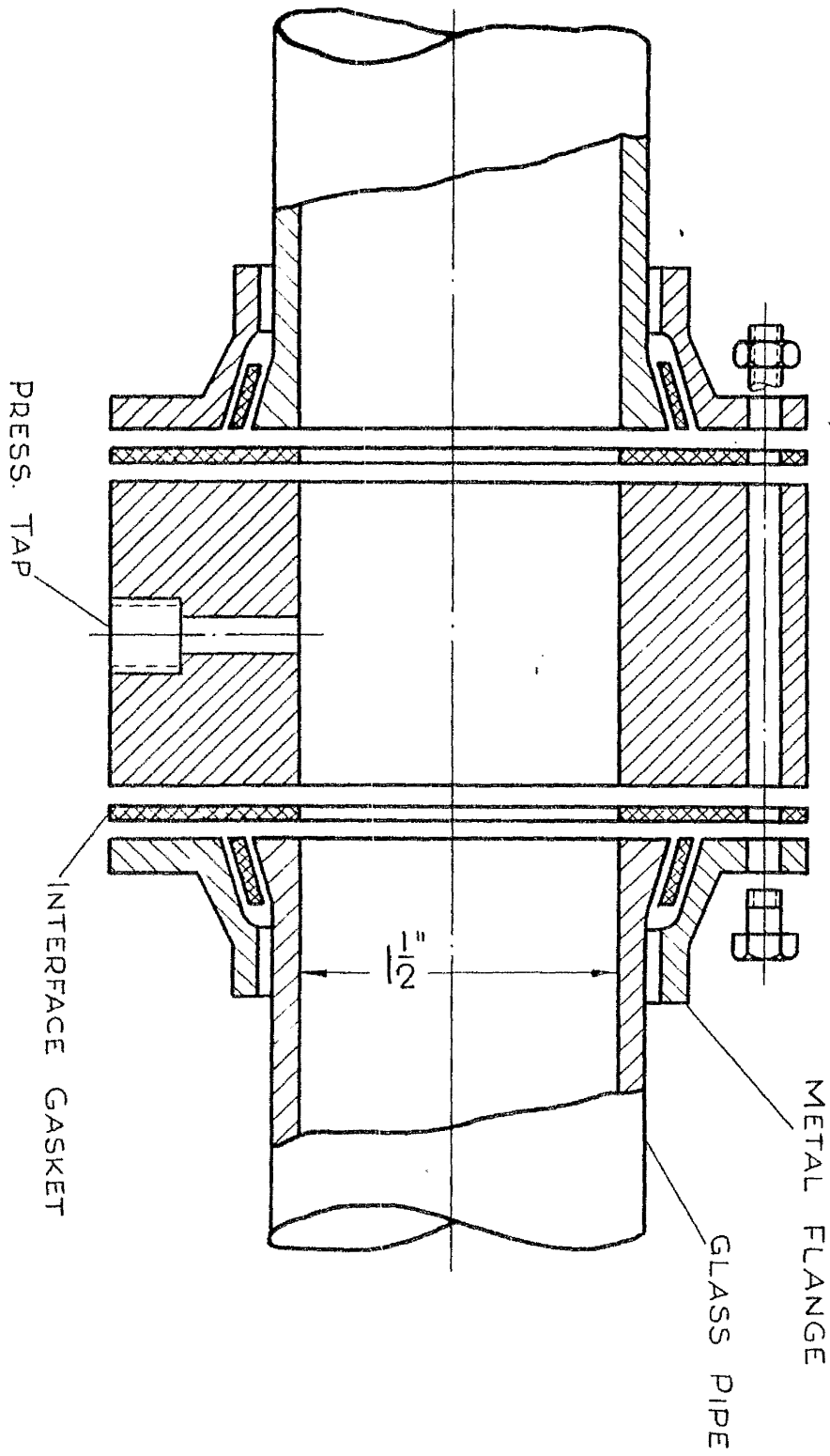
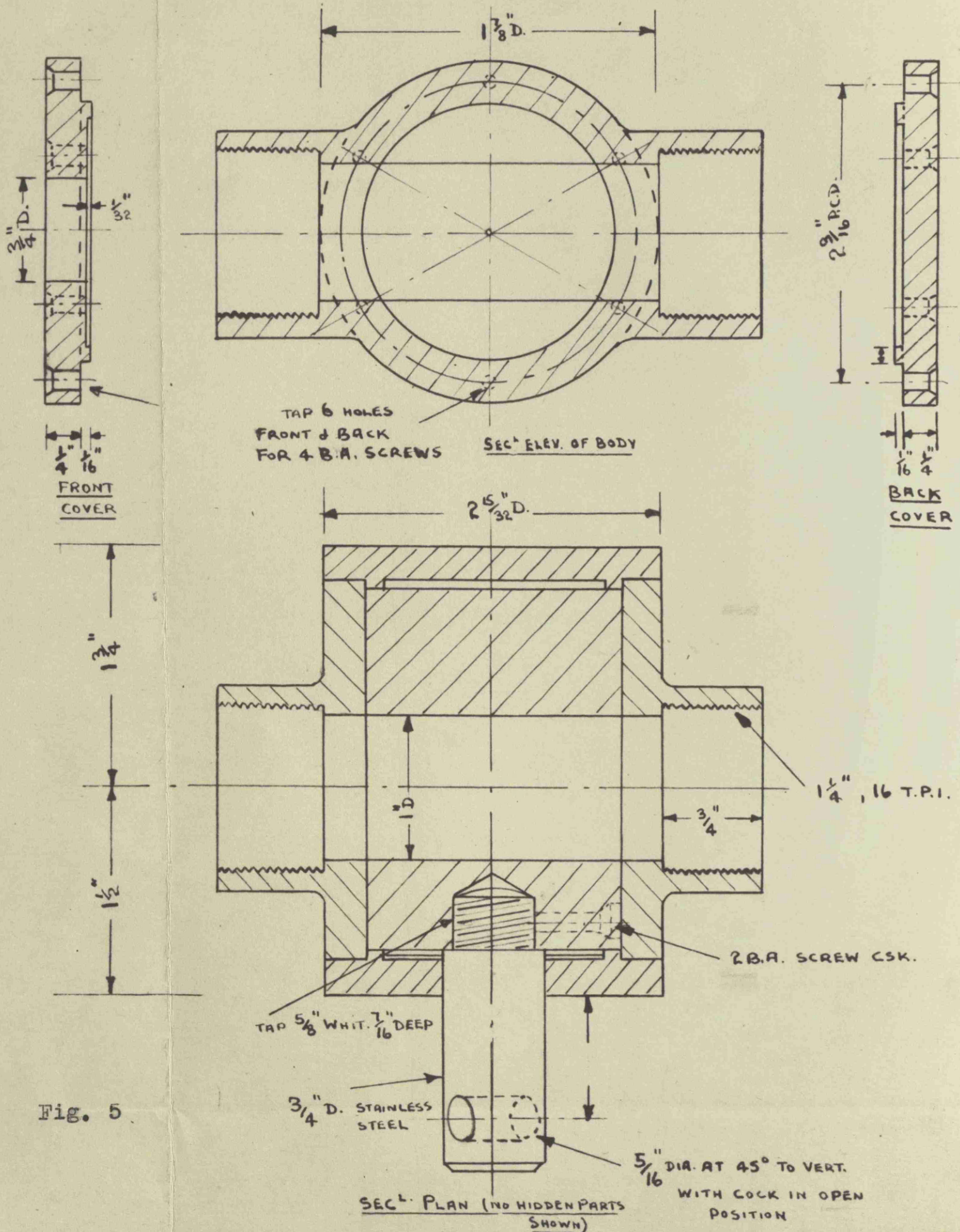


FIG. 4. DIAGRAM OF PIPE COUPLING  
AND PRESSURE TAP INSERT.

Fig. 4

FIG 5 : 1" CLOSING COCK FULL SIZE



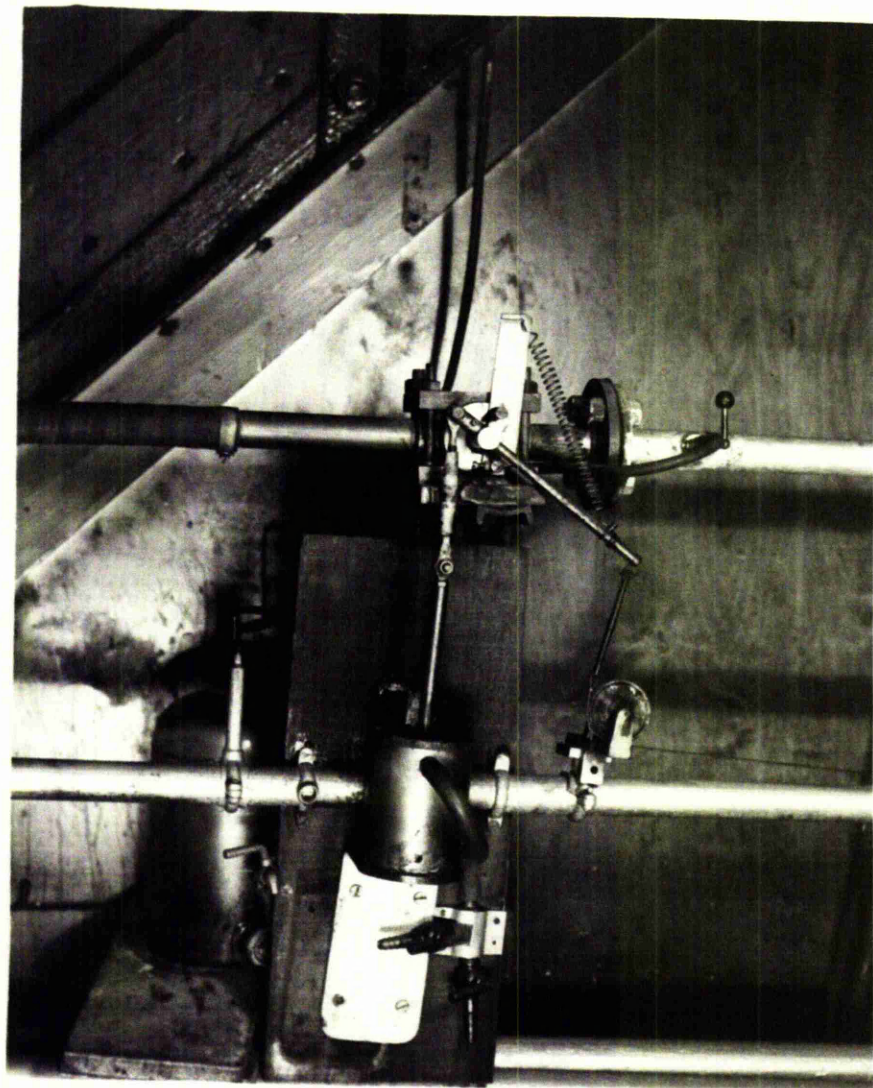


Fig. 5A

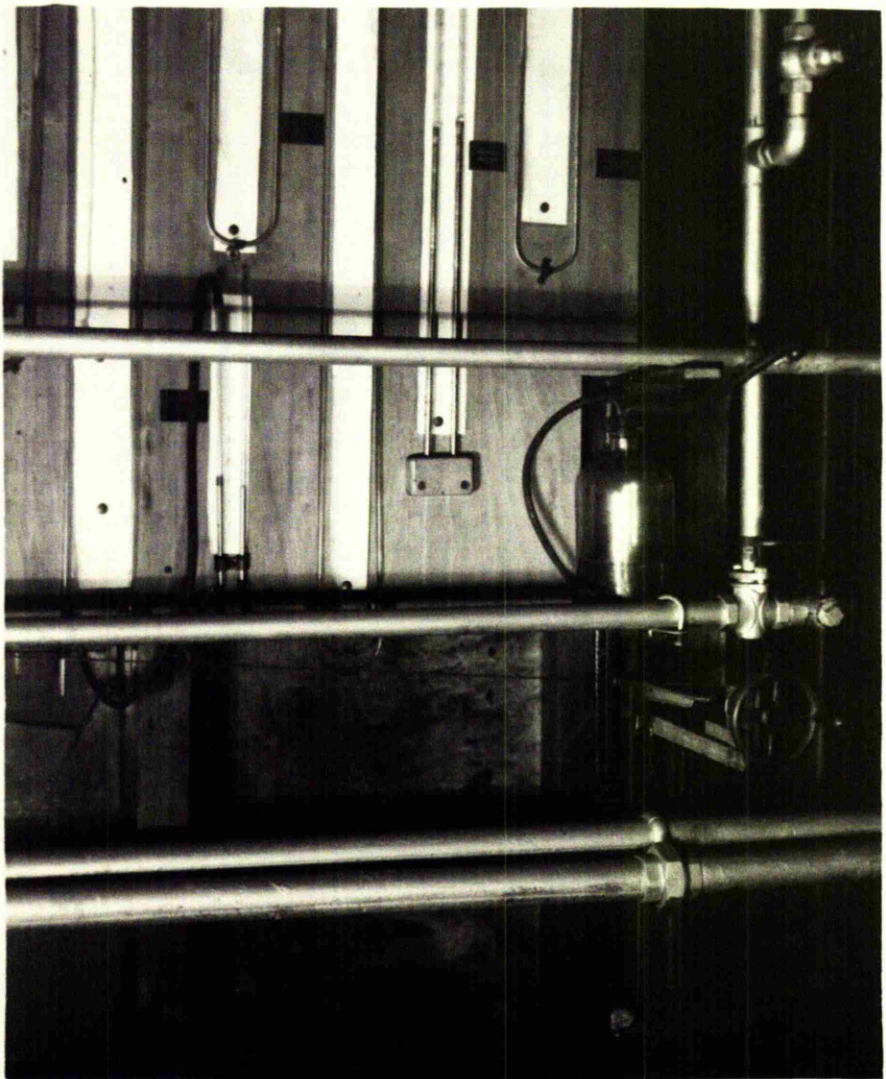


Fig. 5B

FIG. 6: COCK, TRIPPING ARRANGEMENT

DOTTED LINES SHOW COCKS IN  
FULLY CLOSED POSITION

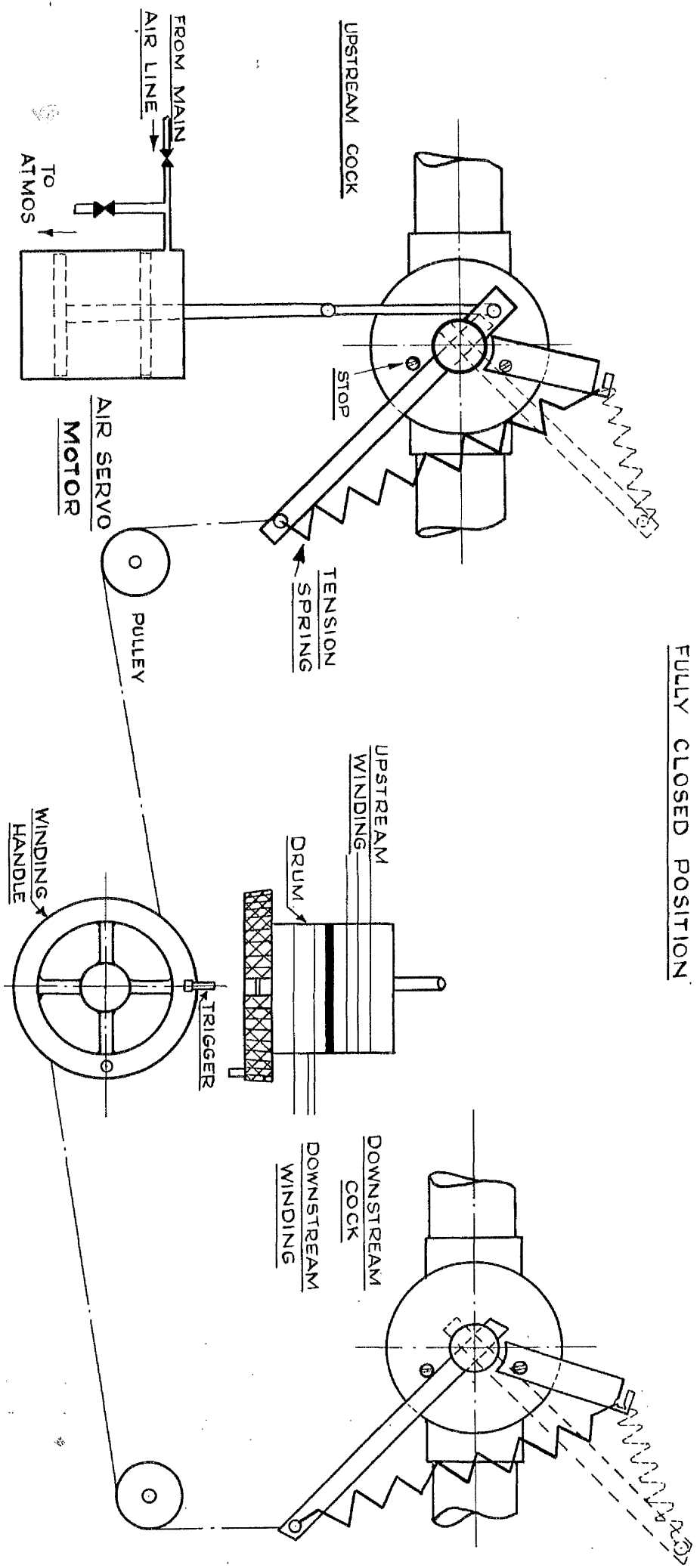


Fig. 6

at the junction of the pipe sections, Fig. 4. Pressure tappings were taken at upstream(1), central(2), and downstream(3), points. The distance between (1) and (3) was 21.5" in the case of 1" pipes and 22.85" for 1 $\frac{1}{2}$ " glass and steel pipes. The exact diameters were:-

for nominal 1 $\frac{1}{2}$ " pyrex pipe exact I.D. was 1.500 in.							
" " " steel "	" "	" "	" "	" "	" 1.565 "	" "	
" " " 1" perspex "	" "	" "	" "	" "	" 0.992 "	" "	
" " " steel "	" "	" "	" "	" "	" 1.002 "	" "	

#### Quick Closing Cocks.

Two specially designed cocks were used at each end of the test pipe to trap a sample of the flow, thus determine the water flow area and hence the velocities of air and water. Construction details are shown in Figs. 5, 5A and 5B.

The cocks were made of brass and were drilled to exactly the same diameter as the inner diameter of the pipe in order to ensure non-interrupted flow when the cocks were open.

The clearance between the valve body and the liner core was kept to minimum allowing a running fit (less than 0.001"). After machining they were tested for leakage, and it was found that with such small clearance and with a coating of grease and graphite no leakage took place under pressure up to 50 lb/in.<sup>2</sup>.

The cocks were spring loaded and both were connected to a drum and trigger as shown in Fig. 6, so that both cocks would be closed

instantly and simultaneously when the trigger is released.

To overcome the resistance to closure due to pressure build-up in the up-stream side of the cock, a small servo piston cylinder was attached to the inlet valve lever.

The servo cylinder consisted of a 3" diameter steel piston fitted in a brass cylinder. The top side of the cylinder could be connected either to atmosphere or to main air pipe, through two small valves. So before triggering, the servo cylinder is connected to the main air pipe and then the trigger was released. The servo motor would pull down the lever and as the valve is shut the resistance would increase but at the same time air pressure being higher would mean bigger force from servomotor. This arrangement was found effective and provided instantaneous valve closure.

Because of the big forces acting on the inlet valve, it was mounted in a special bracket which allowed rigid fixing against any longitudinal movement but allowed tilting of the pipe.

#### Sampling.

To find the distribution of phases, a special sampling tube was used. It was made of stainless steel tube bent at 90° and the end was tapered to knife edge to minimise interruption. The diameter of the tube was chosen to give minimum obstruction and at the same time avoid choking due to water drops entering during sampling. After many trials the best results were obtained by using a 3 mm. O.D. stainless steel tube

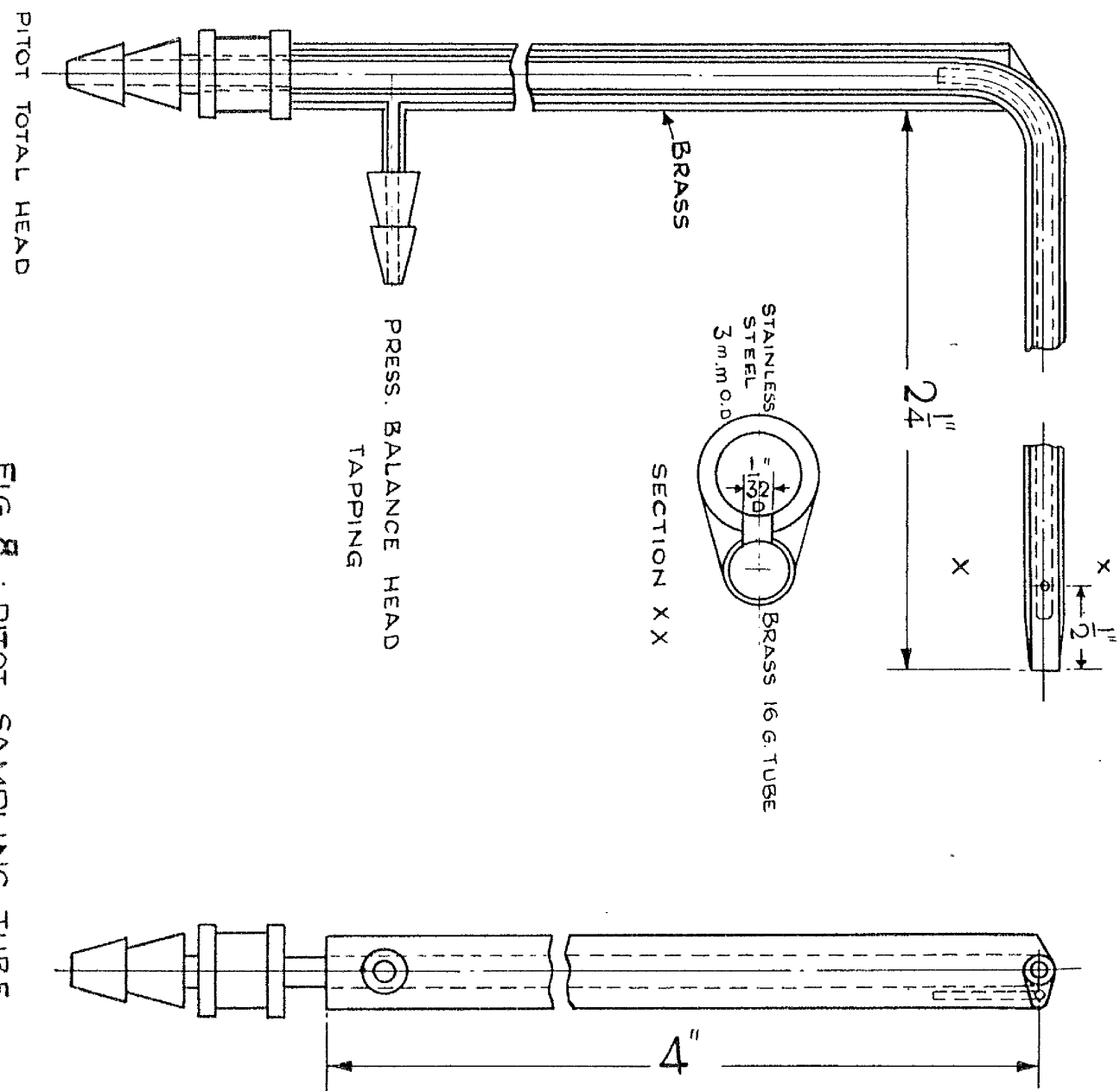
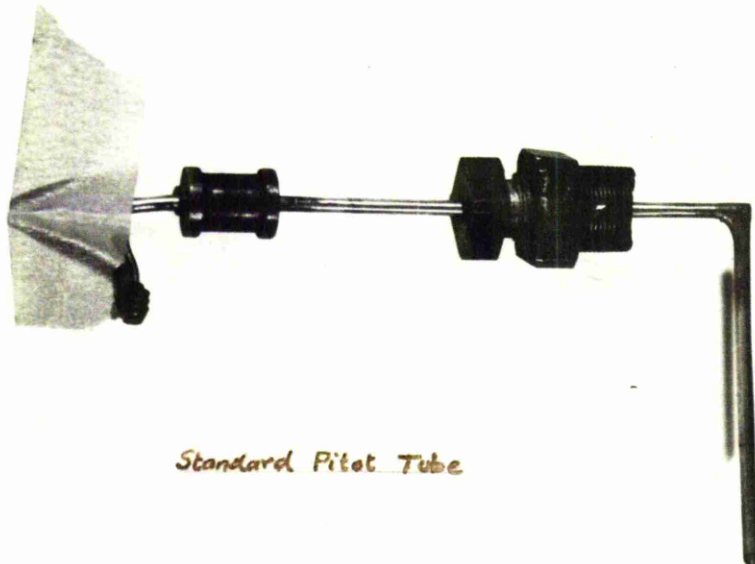


Fig. 8



Sampling Tube



Standard Pitot Tube

Fig. 8A

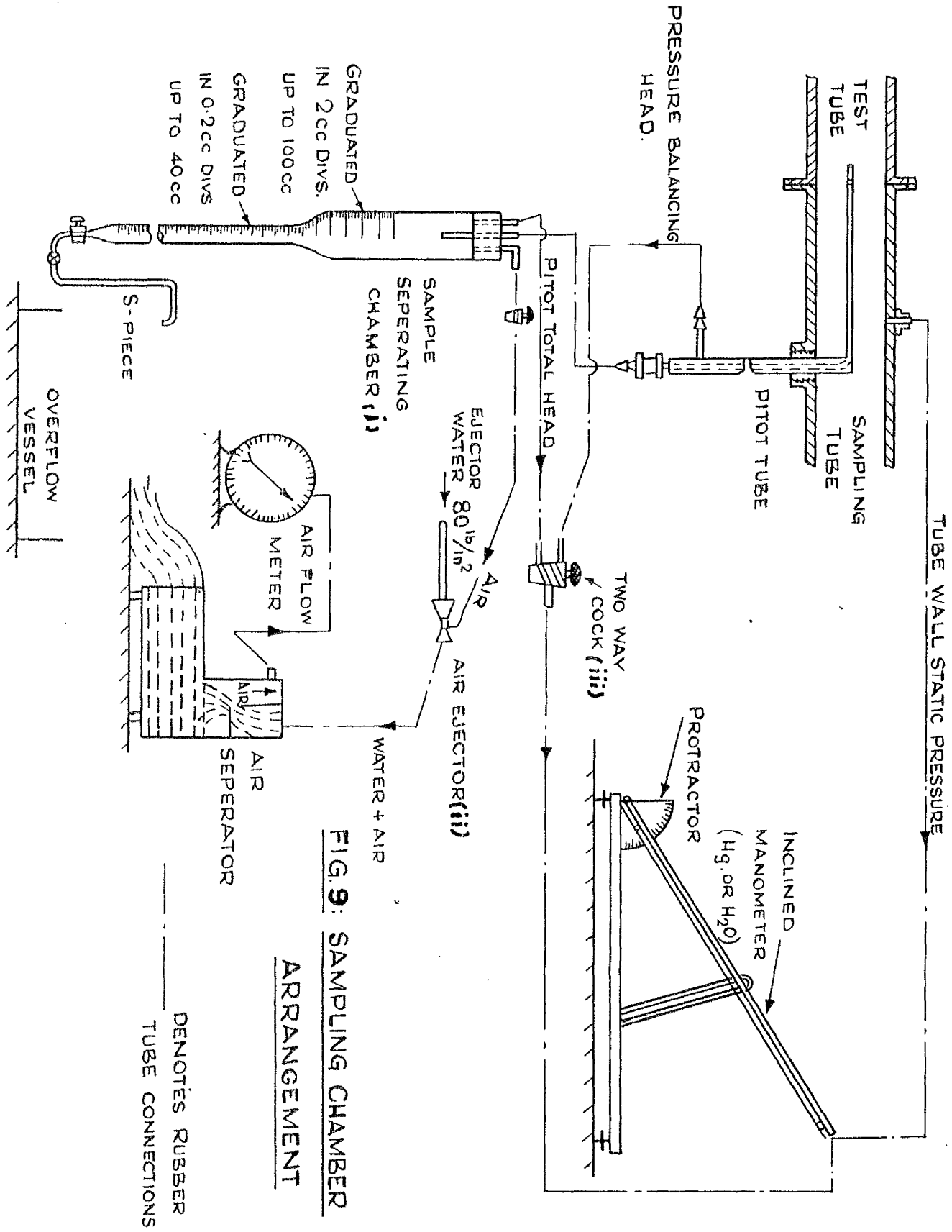


Fig. 9

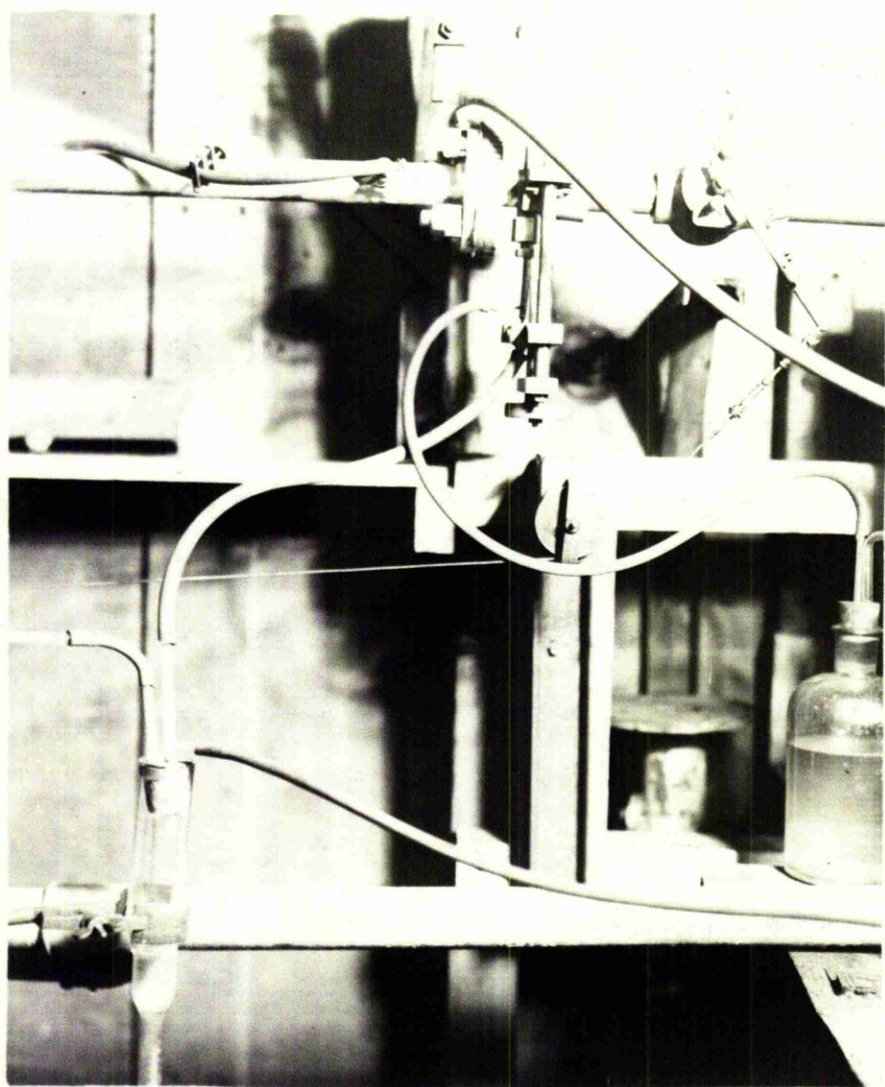


Fig. 9A

(0.086 I.D.). Also, it proved suitable and rigid enough to stand the high velocities that had to be measured.

The tube construction is shown in Fig. 8 and Fig. 8A. Pressure recording point near the tip of the stainless steel tube was made by jointing a  $1/16"$  O.D. (16 G) brass pipe and drilling a  $1/32"$  hole through and then sealing the brass tube at the end as well as the hole on its outer wall. The brass tube, open end passed through in a  $1/4"$  O.D. brass pipe which acted as a closed space from which this pressure was tapped off for measurement.

The  $1/4"$  O.D. part passed through a gland machined so that when screwed in place it was flush with the pipe circumference. The pressure thus recorded was used to equalise the head near the tip of the tube with the static pressure when a sample was drawn in the sampling tube.

The two phase sample was discharged through a graduated special separating chamber (i) where the water content was separated, and could be measured in a certain time interval.

A stopcock at the bottom was used to empty this chamber. The top rubber stopper had one connection to the two-way cock leading to the inclined manometer, a second to a stop cock and then the ejector suction, the third was connected to the sampler. The chamber was fitted at a level lower than the pipe, to allow a sample to flow smoothly under gravity effect once it entered the tube. An s-shaped piece of copper tubing with a regulating cock maintained the level of water constant when total head measurements were made, Fig. 9 and Fig. 9A.

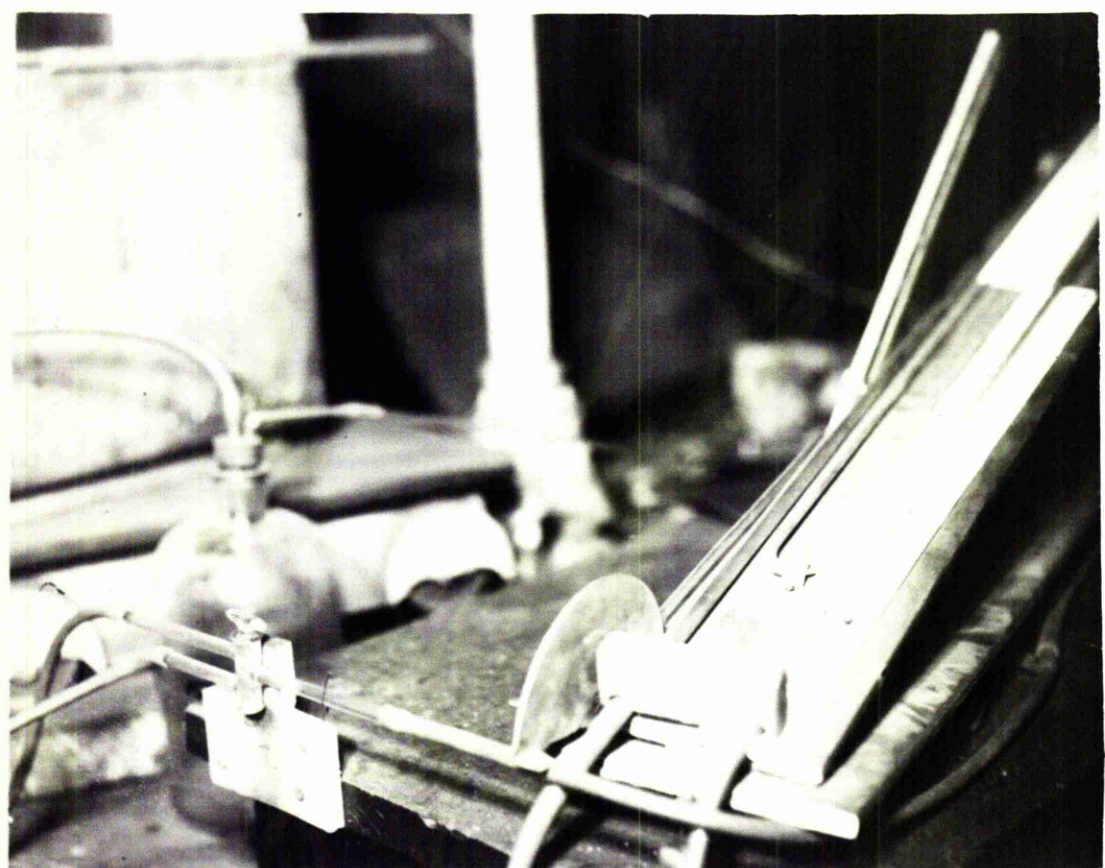


Fig. 9B

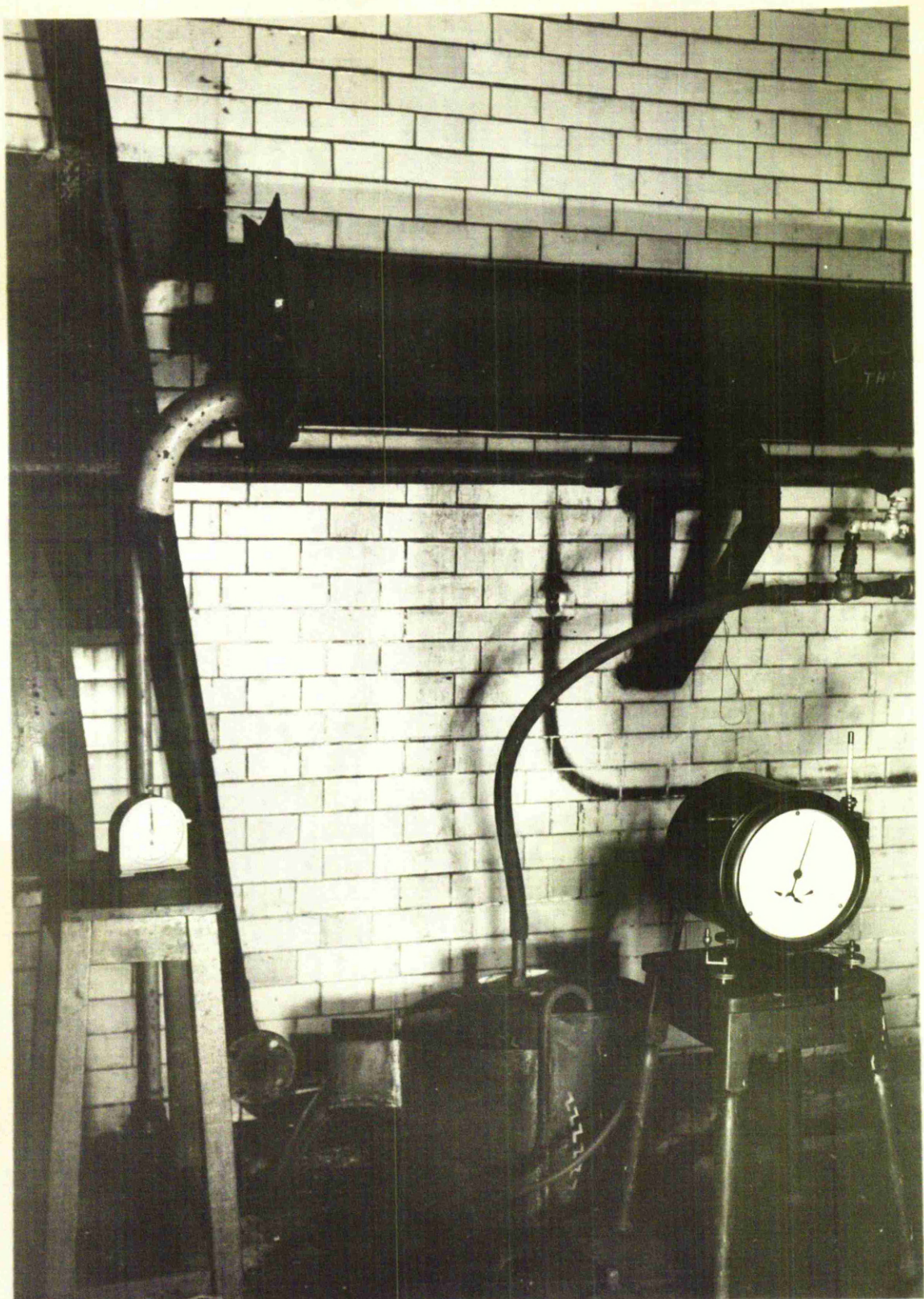


Fig. 9C

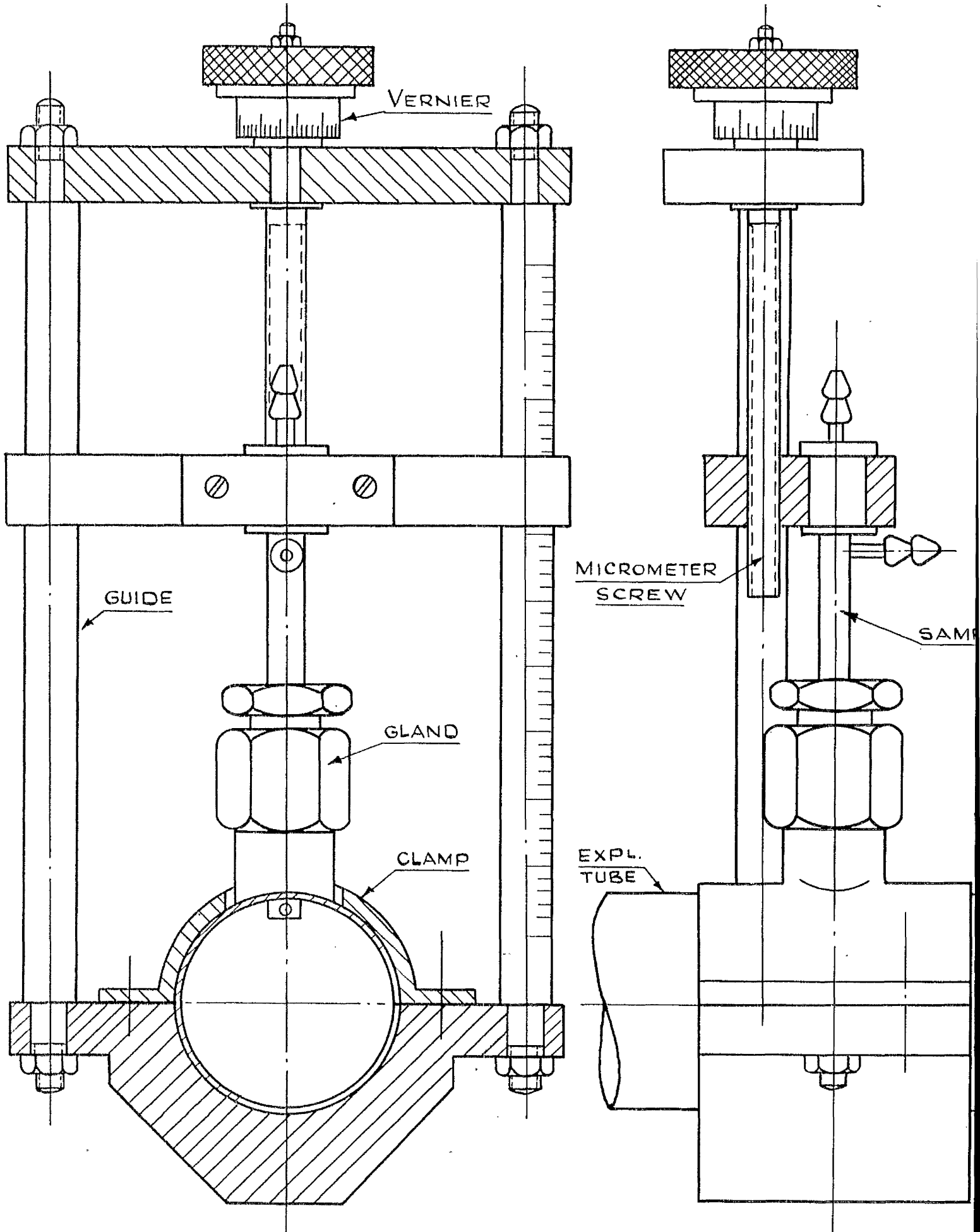
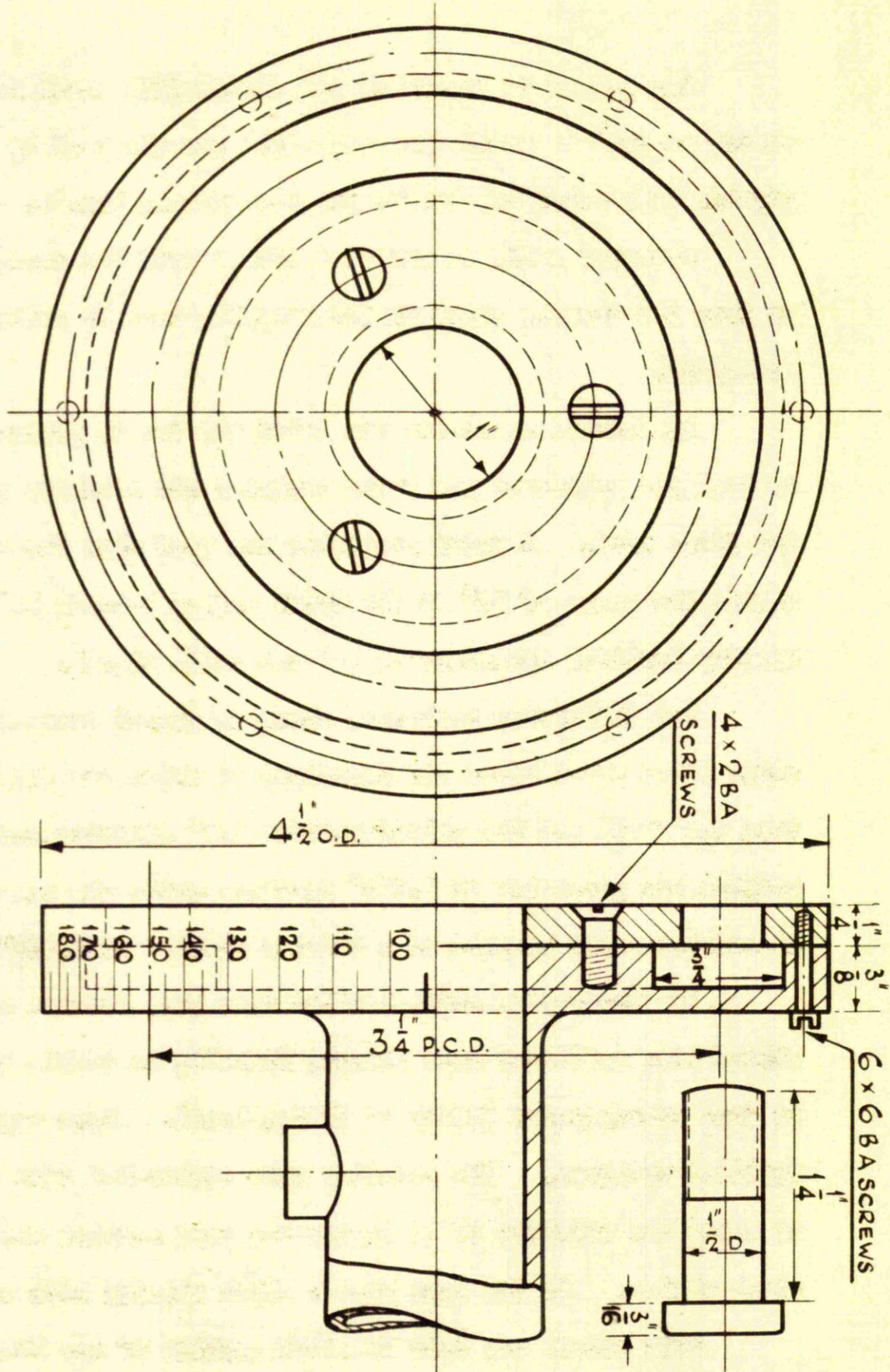


Fig. 10: SAMPLING TRVERSE SET-UP

**FIG. 10A : FLANGE FOR PIOT SET-UP. (FULL SIZE)**



**Fig. 10A**

Air passed to the water jet ejector (ii) which was connected to an air separator vessel from which air was measured by a gas meter capable of reading 0.1 cu.ft. per revolution, Fig. 9G.

Pressure could be recorded either from the separating chamber or from the tapping point on the sampling tube by using the two way cock (iii).

An Askania manometer was tried but due to pressure fluctuations an inclined manometer was found superior and accurate enough to record the Pitot head. A water manometer was used when the recorded head was within the range of 36° at different angles between 12° - 70°, then a mercury inclined manometer at 12° was used, Fig. 9H.

The traversing mechanism shown in Fig. 10 consisted of a micrometer screw which moved the crosshead to which the Pitot-sampling tube was fixed and was guided between 1/2" diameter rods. One of the columns was graduated to 0.025" readings while the knurled head on the micrometer screw coupled to a vernier divided to 0.001".

The traversing mechanism and tube were mounted on a brass pipe which had a specially made flange, Fig. 10A, to enable traversing to be done at any angle (every 5° if required). Zero angle referred to vertical traverse. The sampling tube horizontal side was long enough to allow the entrance to go inside the test section whether smooth or rough piping. On the same pipe a quick closing cock was fitted.

This set-up was made to allow testing of any kind of piping of the same diameter without changing the end pipe or the quick closing cock position.

"Knife" Traversing Mechanism.

A modified apparatus from that designed by Armand(3) was used to find the distribution of phases at high water and low air flow rates.

Results found by this method were not included and were considered not accurate enough to represent a true sample from the core.

CHAPTER III.

PROCEDURE.

Procedure.

Preliminary tests were made with air alone to find the friction coefficient of the pipes. By using a standard Pitot tube made according to Prandtl standards, traverses were made at the end of the test pipe for the same air flows as were used later in case of two-phase flow to allow comparison between velocity profiles.

The curves of velocity distribution thus made compared favourably with Nikuradse's results.

Air was admitted and water pump started with the overflow of the top tank (in the case of 1.1/2" I.D. pipe only) so adjusted to maintain constant level and the water flow through the pipe was controlled by the valve on the water line. Air was measured by the reading of the orifice meter, and pressure and temperature of the air at the orifice.

Water was run directly from the pump in the case of 1" I.D. pipe and in both cases the water discharge was read by the venturi meter. Before each test the carbon-tetrachloride readings were checked by weighing the discharge in a weighing machine.

An hour was allowed with all the settings kept the same until steady conditions were obtained.

The inclined manometer was set to a certain level and the velocity head was read when a steady reading was attained.

The two way cock was turned to record the balancing pressure, and the cock leading to ejector was opened. The amount of suction was changed by a clamp on the rubber tubing while the bottom cock on separating chamber was kept closed.

Ejector suction was adjusted until a pressure balance between static pressure and tip of the sampler was achieved.

Air in the sample was recorded by taking the time for 0.5 cu.ft. to pass through the gas meter, and the water collected in the graduated separator was measured in 5 minutes intervals.

This procedure was repeated for each position of the traverse which was made in 0.1" steps.

During every complete traverse air pressure and temperature as well as water temperature were recorded several times to ensure steady conditions.

Series of constant water-variable air rates were taken. For every air rate 4 water flows were tested. The values of these rates are given in Table I, in Appendix I.

Although the method of sampling was not a complicated one, yet so many adjustments had to be done at the same time that it was difficult for one experimenter to keep all the different controls such that steady conditions could be maintained all the time. Thus every traverse (15 reading for  $1\frac{1}{2}$ " pipes) took nearly three hours.

#### Sampling Technique.

Sampling was made at the end of the tested pipe and since the pressure drops for the two halves of the pipe were always the same it was assumed that no acceleration and no fundamental change in the flow patterns would take place.

When a true sample is required from a stream of air-water mixture, velocity of sampling should be equal to flow velocity. If the latter is greater than air, stream lines will curve away from the tube while the water particles, by their high inertia will go through the tube end thus a higher concentration will be recorded than the actual one. The opposite would happen if sampling velocity is higher than flow velocity.

In the construction of the sampling tube, velocity pressure head at the tube end ought to be equalised (by applying suction in the separating chamber) to static pressure. Although there was a slight pressure drop between pitot tube tip and the tapping point yet it gave satisfactory results.

The tube was checked against a standard Pitot tube. Sampling velocity was calculated by dividing the air quantity passing through the gas meter by the cross section of the sampler (exact internal diameter was measured in the metrology laboratory and was of an average value 0.081").

The average ratio between flow velocity and sampling velocity was  $0.8 \sim 1.05$  which was considered a satisfactory evidence of the validity of the method. It is interesting to note that this method was somewhat similar to a technique developed and used to determine the dust content in flue gases(19). The author was not aware of this until after the technique was developed and all the difficulties were overcome.

Pressure measurements were made at three points on the test pipe section and settling bottles were used to trap the liquid from lodging in the line.

Pressures were measured on either water or mercury manometers. Traverses were mostly made in the vertical plane, but some were taken at 45° and in the horizontal plane.

Surface tension was reduced, to test its effect on the distribution of phases, by adding Lissapol in various quantities. Below 40 dynes/cm., severe foaming took place and the measurements were not accurate and were discarded.

To determine surface tension a "Do Novy Balance" apparatus was used which enabled its estimation directly in dynes/cm. It determines the force required to detach a platinum-iridium ring of 4cm. circumference from the liquid surface.

#### Velocity Measurement Technique.

Measurement of velocity was accomplished from the head indicated by the Pitot tube on the inclined manometer.

The velocity at the point was calculated using the density of the mixture as obtained from the sampling process and applying the formula

$$h = \rho_m \frac{u^2}{2g}$$

This method of measurement was used by Halbrom(24) for measuring the velocity in air-water mixtures in a study of entrainment in high speed currents of water.

To check the method of velocity measurement, it was applied to the case of single phase air flow. A standard Prandtl tube was fixed in the stream to give the velocity traverse across the pipe by the usual method, then the sampling-Pitot tube was fixed in and a sample of air was drawn in. Velocity of sampling was determined by dividing the air flow rate given by the gas meter over the cross-section of the pipe which gave the velocity of sampling. This sampling velocity compared very favourably with the flow velocity.

For two-phase flow, the sampling velocity based on gas-liquid volumes and the calculated head velocity were checked against each other for several tests and the agreement was satisfactory.

#### Effect of Relative Velocity between Water Particles and Air-Stream

The effect of relative velocity between water particles and air should be considered in the evaluation of the mixture velocity at the point of measurement.

T. Baron and others(7) discussed the relative velocities in two-phase flow and estimated that at a Reynolds' number  $R_d = 10^6$  in a 2<sup>1/2</sup> I.D. pipe, for zero relative velocity the particle diameter should not exceed about 6 microns.

In the present investigation, due to the lack of information regarding water particle size and size distribution, it was decided to use the empirical formula developed by Hinkle(27) for the case of air-solid flow to the present problem.

$$v_{rd} = 1.41 \quad v_g \quad D_p^{0.3} \quad (D_p \text{ in ft})$$

(a) Applying the formula of Hinkle and using the estimated drop size shown in Chapter V, the relative velocity estimated varied from 7 ~ 15% of the air stream velocities.

The exact equation for velocity determination would be

$$h = \frac{U^2}{2g} [\rho_a (1 - c_L) + \frac{C_L}{K} \rho_L]$$

$$\& K = \frac{U_L}{U_g}$$

Results appearing in Appendix II, will show that, due to uncertainties regarding the relative velocity, drop size and size distribution together with the small effect which relative velocity has for the drop sizes estimated within the experimental range, are taken to justify using the simple expression

$$h = \rho_m \frac{U^2}{2g}$$

#### Micro Flash Photographs and Visual Observations.

These were made to reveal the flow pattern and to substantiate the possible discussion of flow patterns from the concentration curves.

#### Air-Water Velocity Ratio Test.

Quick closing cocks were used in the case of 1" I.D. pipes for this purpose and the sampling tube was substituted by a small cock used to empty the pipe after the two cocks were closed.

Before doing these tests conditions were allowed to steady then the cocks on the main pressure measuring lines were closed. Air to servo-motor was connected, the trip mechanism was triggered and immed-

mediately after the cocks were shut down, the pump motor was switched off thus preventing pressure building up in the water line.

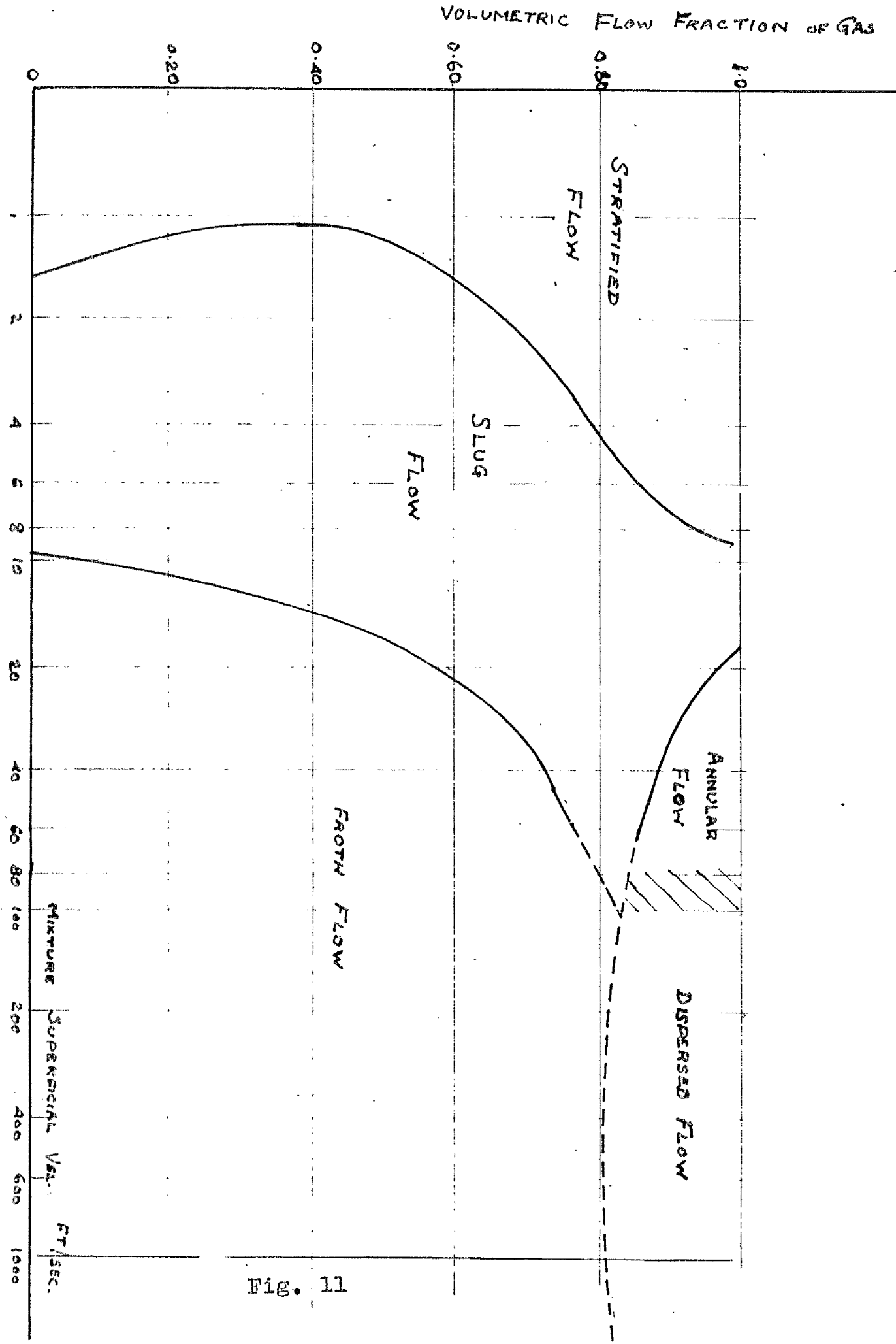
The relief valve at the "mixing chamber" kept the air pressure well below 50 lb./in.<sup>2</sup>.

To measure the water quantity in the test section the tube was tilted by means of a thimble screw at the downstream end. Five minutes were allowed at least for the tube to drain completely, and water ~~was~~ collected, was weighed to an accuracy of 0.02 gms.

Drops lying on the tube walls may cause error in determining the exact quantity of water in the pipe sections. A chemical method was tried which was mainly based on adding a diluting strong acidic solution and mixing it to the water lying inside the pipe by a small circulating pump between two points at the two ends of the test section. Then a sample was drawn and by titration the amount of water added was calculated. This method proved to be promising but due to troubles in the pumping lines the first method had to be used.

CHAPTER IV.

DEVELOPMENT OF FLOW PATTERNS.



LIMITS OF VARIOUS TYPES OF TWO-PHASE FLOW [KOSTERIN]

Development of Flow Patterns.

In previous studies of two-phase flow, much attention has been paid to the development of successive patterns of flow since each pattern required different treatment when predicting pressure drop and hydraulic resistance.

Martinelli(46) gave a macroscopic analysis for the successive stages of two-phase flow while Gazley(22) and Johnson(33) suggested a quantitative basis for the different types.

Armand(3) stated that although high speed photography was tried it only served to show the highly complex nature of two-phase flow in horizontal pipes.

Kosterin(37) used photographic technique, and experimented with several pipe sizes (1" - 4" I.D.) and also different positions of the tubes. The different patterns of flow were plotted for various pipes on a single graph summed by Hughes and Evans(30). These are shown in Fig. II which partially eliminated the effect of pipe size. It was concluded that the boundaries of various types of flow of the mixture of air and water were a function of diameter and position of the tube as well as of the volume flow fraction of the gas. It would be noted from this graph that pure annular flow existed in a rather doubtful narrow region and dispersed flow dominated the whole range of annular flow zone. Because of so much confusion in the interpretation of results obtained mainly by visual observations the present analysis of flow patterns were based essentially on sampling of the core aided by stroboscopic visualisation and micro-flash photography.

For  $\frac{3}{4}$ " I.D. "Pyrex" Pipe:

Fixing the water rate at 12.63 lb./ft.<sup>2</sup> sec., and allowing air to flow at a rate of 1.7 lb./ft.<sup>2</sup> sec., gave stratified flow. Capillary waves were observed on the water surface which became irregular as the air flow increased. When air flow was increased to 4.2 lb./ft.<sup>2</sup> sec., these waves were torn off and some of the water drops struck the upper surface. Some of the drops fell back while others stuck to the wall and were dragged by the air at a much reduced velocity. Also, the liquid at the bottom of the tube tended to spread on the lower part of the pipe until ultimately it joined with the built up layer on the top wall. In the connecting zone the layer seemed to move in waves when seen under stroboscopic lighting.

At air flow of 14.3 lb./ft.<sup>2</sup> sec., liquid covered the entire surface of the tube forming a layer which decreased in thickness from bottom of the section to the top. On increasing air flow in successive steps visual observation showed little change in the flow form but the concentration curves underwent some changes suggesting the existence of a layer on the top wall that increased in thickness until it became thick enough to give mass transfer to the core. Under these conditions the concentration curve became almost symmetrical.

Also, from similar tests carried out on a 2" I.D. "poropex" tube it can be concluded that the apparent annular flow visually observed would be formed in the following steps:-

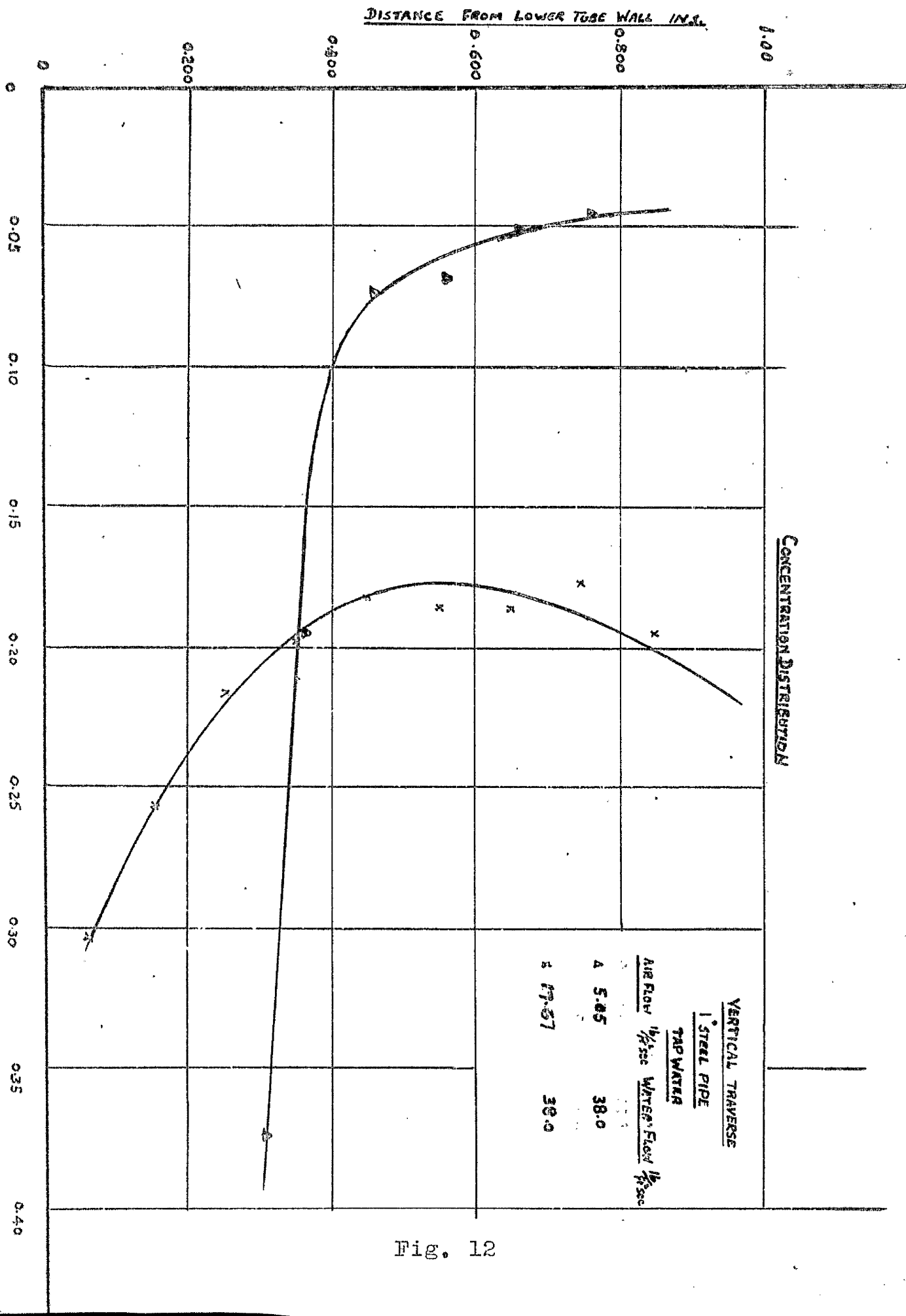


Fig. 12

1. Stratified flow existed in the pipe at low air flow  $3.8 \text{ lb./ft.}^2 \text{ sec.}$  and water flow of  $14.2 \text{ lb./ft.}^2 \text{ sec.}$  The water moved along the bottom of the pipe with air above; waves were observed at the gas liquid interface which depended on the relative velocity between the flowing phases. Water particles shot irregularly to the upper wall where some of these drops adhered.

2. At higher water flow  $38 \text{ lb./ft.}^2 \text{ sec.}$  and at the same air rate the flow pattern changed to what may be described as "Sluggish Stratified". The mixture flowed along the pipe, the stratified nature was still predominant, but it was accompanied by variations in velocity and depth of water layer which took place at about 4ft. intervals along the pipe. The film on the bottom curved along the bottom half of the pipe.

3. At air flow of  $5.05 \text{ lb./ft.}^2 \text{ sec.}$  and water flow  $38 \text{ lb./ft.}^2 \text{ sec.}$  the bottom water film climbed up to connect with the upper film to form a wetting layer on the pipe wall which was varying in thickness. Flow still had a pulsating characteristic.

Mass transfer continued when water flow increased so producing higher concentration of dispersed liquid in the air core. Concentration distribution for the range mentioned above is shown in Fig.12.

4. At high air flow  $17.6 \text{ lb./ft.}^2 \text{ sec.}$  and the same water flow  $38 \text{ lb./ft.}^2 \text{ sec.}$  the whole circumference was wetted by a thin water film and the core was fully dispersed with very fine water drops. Only this latter form could be treated as true dispersed annular flow.

It may be concluded that the annular flow observed by previous experimenters does not exist with the idealized conception of uniform liquid annulus and concentric gas core. Various forms of apparent annular flow persist with varying distribution of water particles in the core until the major part of liquid is entrained in the core and the liquid layer on the wall becomes thin. The liquid layer then could be suggested to be uniform.

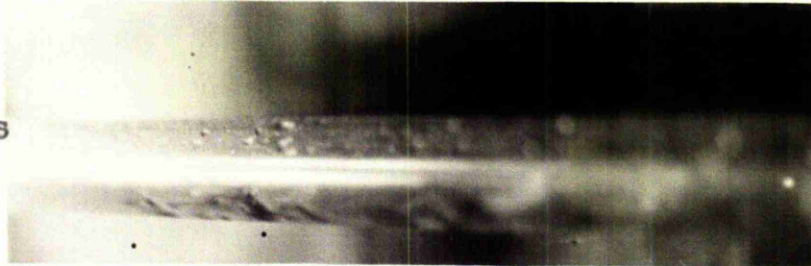
#### Flow Mechanisms Affecting the Successive Forms of Flow.

Starting with air flowing at the top of the liquid, waves would be initiated by the effect of relative velocity at the interface. Kenlogan(34) has given a theoretical treatment of the wave formation which was based on boundary layer theory. His work was confined to the laminar case which holds only for the lowest velocities here reported. The air velocity is higher than that of the water layer existing at the bottom half of the pipe. Velocity distribution over the pipe section will vary from plane to plane over the pipe section. Such a variation in velocity distribution suggests that the liquid surface would undergo a varying shear action from point to point and hence there would be a tendency for a complementary shear to exist inside the liquid itself, giving rise to forces in the circumferential direction. Such lifting forces would act against gravity and would explain the spreading of the water layer on the walls. This secondary motion in the "unsymmetrical" channel when a water layer existed at the bottom of the pipe was reported by Nilluradze (47), in his

1" I.D. Perspex Pipe .

A

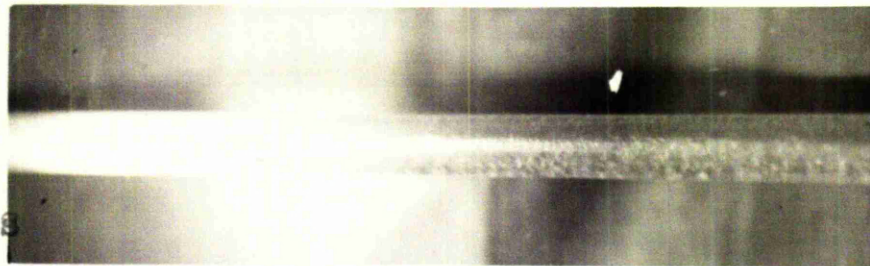
Air Flow = **3.6**  
lb/ft<sup>2</sup>s  
Water " = **13.5**  
lb/ft<sup>2</sup>s



stratified

B

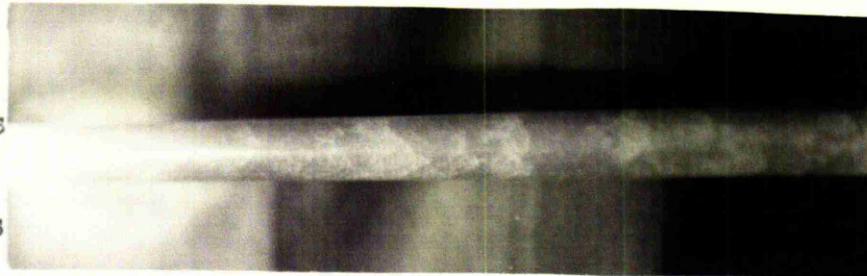
Air Flow = **8.95**  
lb/ft<sup>2</sup>s  
Water " = **13.5**  
lb/ft<sup>2</sup>s



annular

C

Air flow = **9.3**  
lb/ft<sup>2</sup>s  
Water " = **36**  
lb/ft<sup>2</sup>s



sluggish annular

D

Air flow = **12.7**  
lb/ft<sup>2</sup>s  
Water " = **36**  
lb/ft<sup>2</sup>s

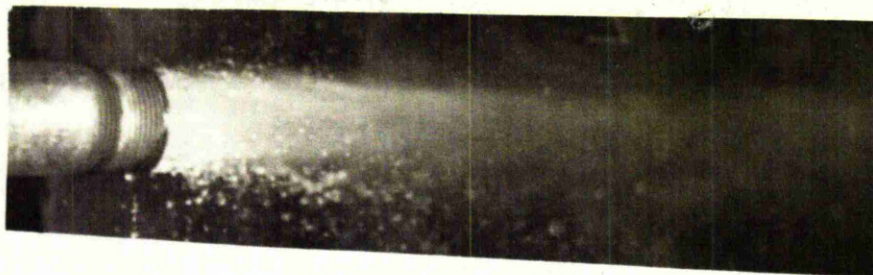


annular

Fig. 13

1½" I.D. Glass Pipe

A



Air Flow       $46/\text{ft}^3$   
= 15.05

Water Flow      "  
= 37.9

B



Air Flow      "  
= 12.85

Water Flow      "  
= 47

C



Air Flow      "  
= 10.9

Water Flow      "  
= 43.8

D



Air Flow      "  
= 9.4

Water Flow      "  
= 41.4

Fig. 14

experiments on triangular and rectangular ducts. The ultimate cause of this secondary action may be that in planes where the shearing stress is greater at the boundary, the fluid will flow to zones of lower shearing stress thus reducing the velocity at the former plane and increasing it at the corners, so that the shearing stress is evened out.

The formation of the upper layer, however, is primarily due, as previously stated, to mass transfer of liquid particles to the top wall.

#### Flash Photograph.

From Figs.13 A, B, C, and D, which show the successive developments in flow patterns for 1" perspex pipes when air flow increased from 1 lb./ft.<sup>2</sup> sec., up to 10 lb./ft.<sup>2</sup> sec. Fig.13A shows stratified flow with waves on the surface, while Fig.13B indicates quite clearly the transfer of water drops from the water surface upwards. Fig.13C, D, show the shape of waves that can be observed also under stroboscopic lighting. It may be noted here that the use of variable frequency stroboscopic lighting was unsatisfactory because it did not synchronize these waves and most possibly that they are made of big waves with smaller waves superimposed on them.

The shape of the two phase stream issuing at the end of the pipe was made by the help of microflash and shown in Figs.14 A, B, C, and D. These were made for 1 $\frac{1}{2}$ " I.D. glass pipes. The flow rates are indicated on the graphs and again they show distinctively how the water is divided

into drops mixed with the air and a water layer on the walls flowing with a reduced velocity.

#### Conclusions.

It can be stated, therefore, that there is practically no definite line of demarcation between the different forms of flow which depend on external conditions, (e.g., vibrations) and on the stabilizing or calming sections, particularly in horizontal pipes. Annular flow originated due to mass transfer from liquid at the bottom of the pipe, (in case of stratified flow). Only with highly developed turbulence in the core was symmetrical annular dispersed flow established.

CHAPTER V.

PHASE DISTRIBUTION.

Liquid Entrainment in the Gas in Co-current  
Gas-Liquid Two-Phase Flow.

In a general study of two-phase flow in pipes, the density of the mixture of gas and entrained liquid drops plays an important part.

Only Dr. Chisholm(15) recognized that effect and included it in his theoretical treatment of pressure drop prediction in water tube boilers. His analysis was based mainly on the very limited data given by Armand(3).

In the present work, experimental values of water concentration and its distribution in the continuous phase were measured and the results were analysed with a view to providing means of predicting the distribution of entrained liquid in the gas phase as well as an evaluation of its amount.

Experimental Results.

Tests were carried out for two pipe sizes  $\frac{1}{2}$ " I.D. and 1" I.D. pipes.

Air flow rates were:

3 ~ 12                           lb/min. for the  $\frac{1}{2}$ " I.D. pipes.

and 1.7 ~ 9.6                   lb/min. for the 1" I.D. pipes.

while water flow rates were

4.67 ~ 35                           lb/min. for both pipes.

Traverses were made mainly in the vertical plane but some horizontal and  $45^\circ$  traverses were also taken. Except where otherwise stated it may be assumed that vertical transverses are meant.

Distance from the bottom wall ins.

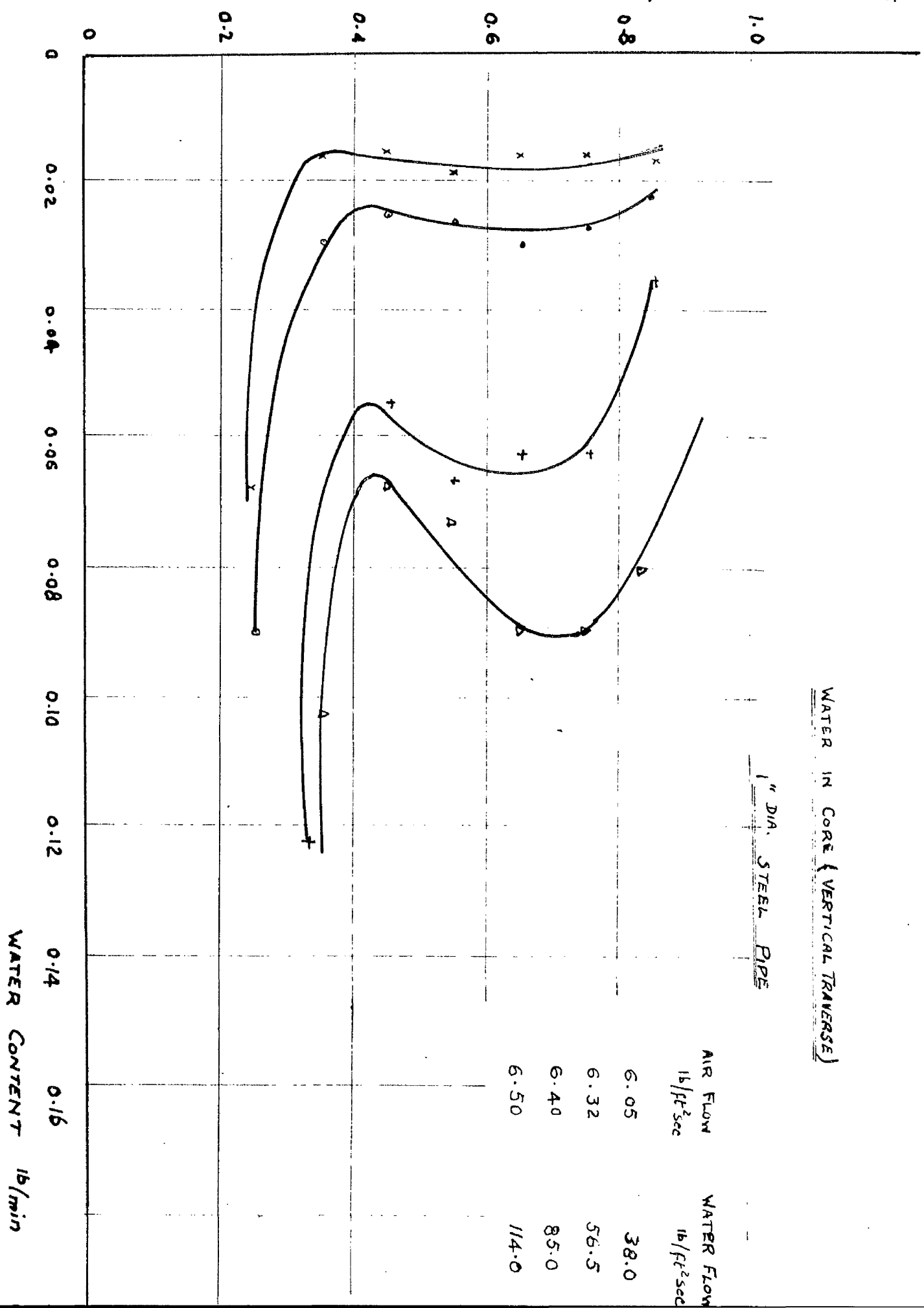


Fig. 15

Concentration was usually evaluated by noting the discharge values of each phase from the sampling tube in a given time. The method of calculation is detailed in Appendix II.

#### Entrained Liquid in the Gas Phase.

The amount of water flowing in the gas stream increased from the top wall to a certain point in the vertical plane and then decreased again until on approaching the water layer at the bottom wall it increased rapidly towards the water boundary.

For the same air-flow, increasing the water flow resulted in increasing the thickness of the water layer at the bottom and the variation in entrained liquid along the line of traverse also increased. These characteristics held for both pipes and are illustrated in Fig.15.

At very high air flow rates in the case of 1" I.D. pipe, increase of water flow did not result in any appreciable increase of bottom layer thickness which could be explained by an increase in the liquid entrainment and possibly by a more uniform thickness of water layer round the walls.

It might be emphasised that the information gleaned from the water quantity measurements using the sampling tube, allows the evaluation of the water quantity passing at the various points in the sections and so, by integration, gives a picture of the distribution of the water flow. It becomes possible, then, to distinguish between the quantity of water entrained in the air and the quantity flowing on the tube wall.

CONCENTRATION DISTRIBUTION - CONSTANT AIR, VARIABLE WATER.

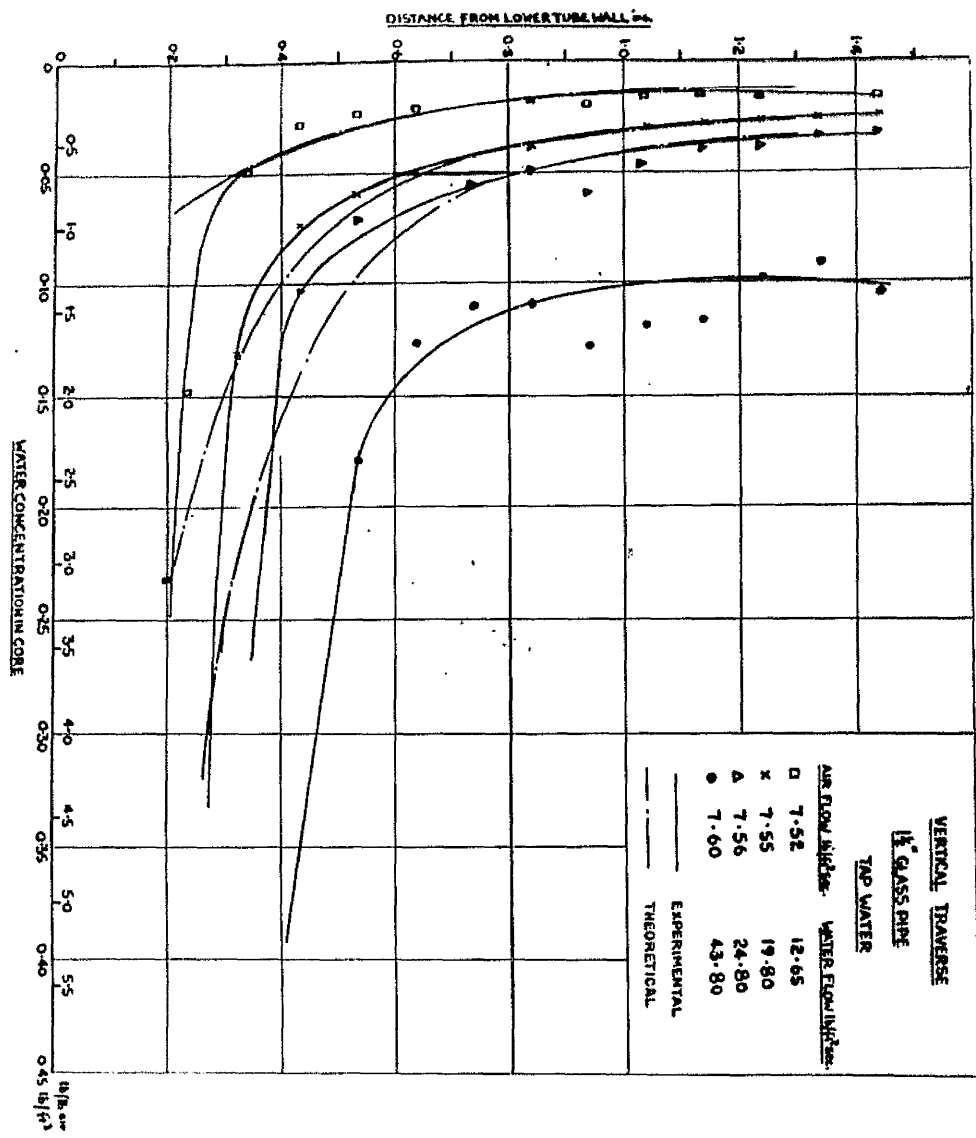


Fig. 16

**CONCENTRATION DISTRIBUTION - CONSTANT AIR, VARIABLE WATER**

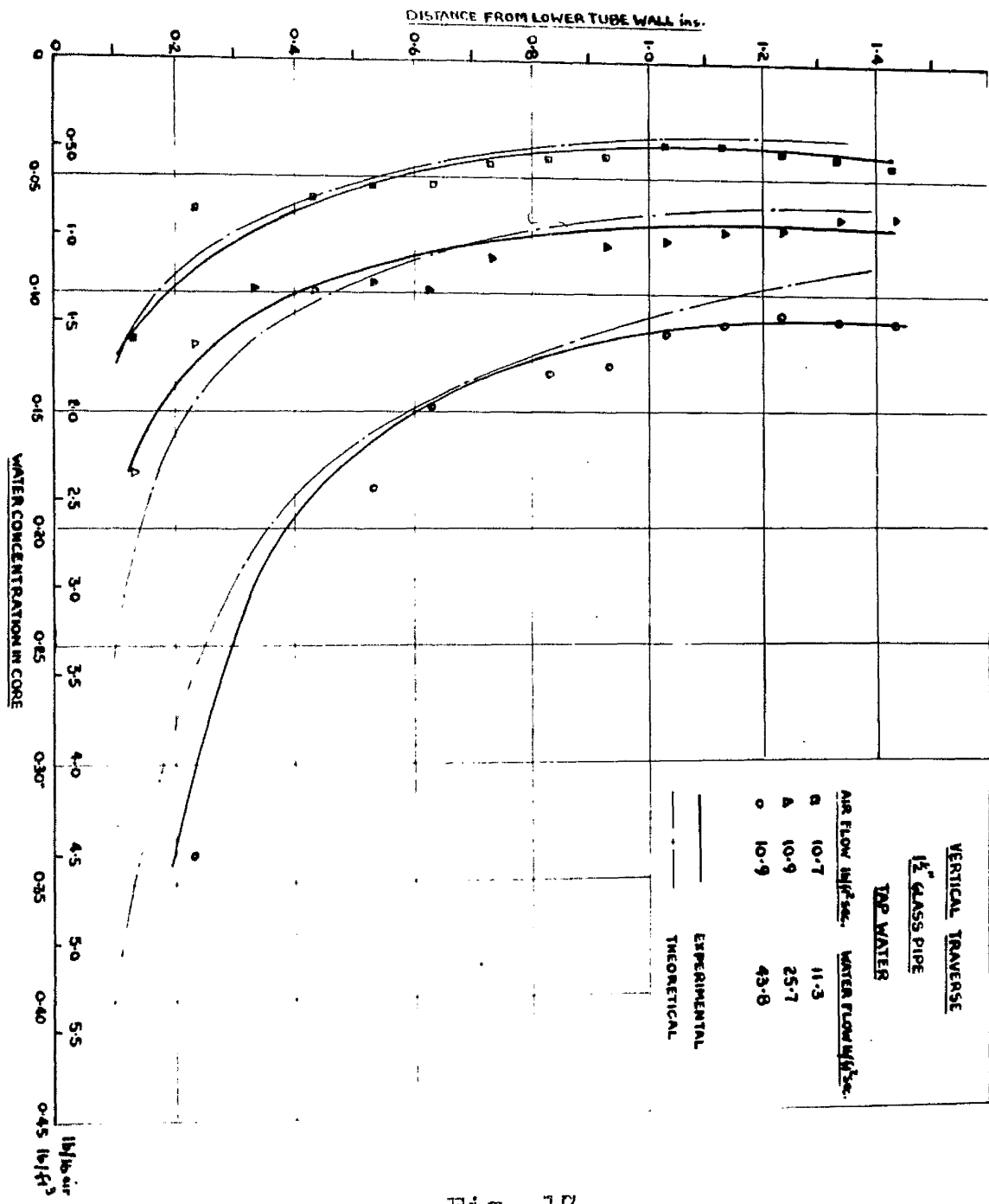


Fig. 17

CONCENTRATION DISTRIBUTION - CONSTANT AIR, VARIABLE WATER

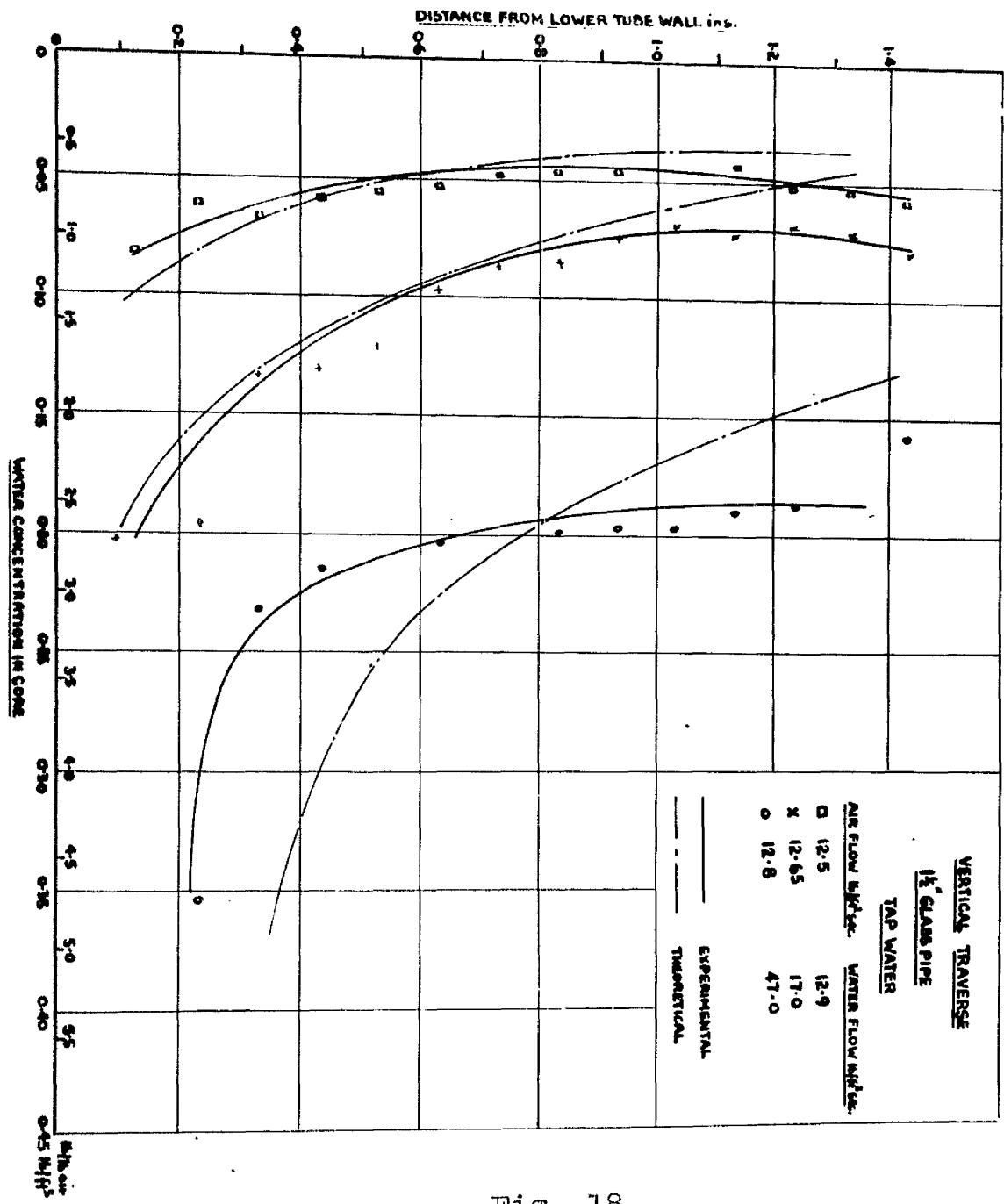


Fig. 18

CONCENTRATION DISTRIBUTION - CONSTANT AIR, VARIABLE WATER

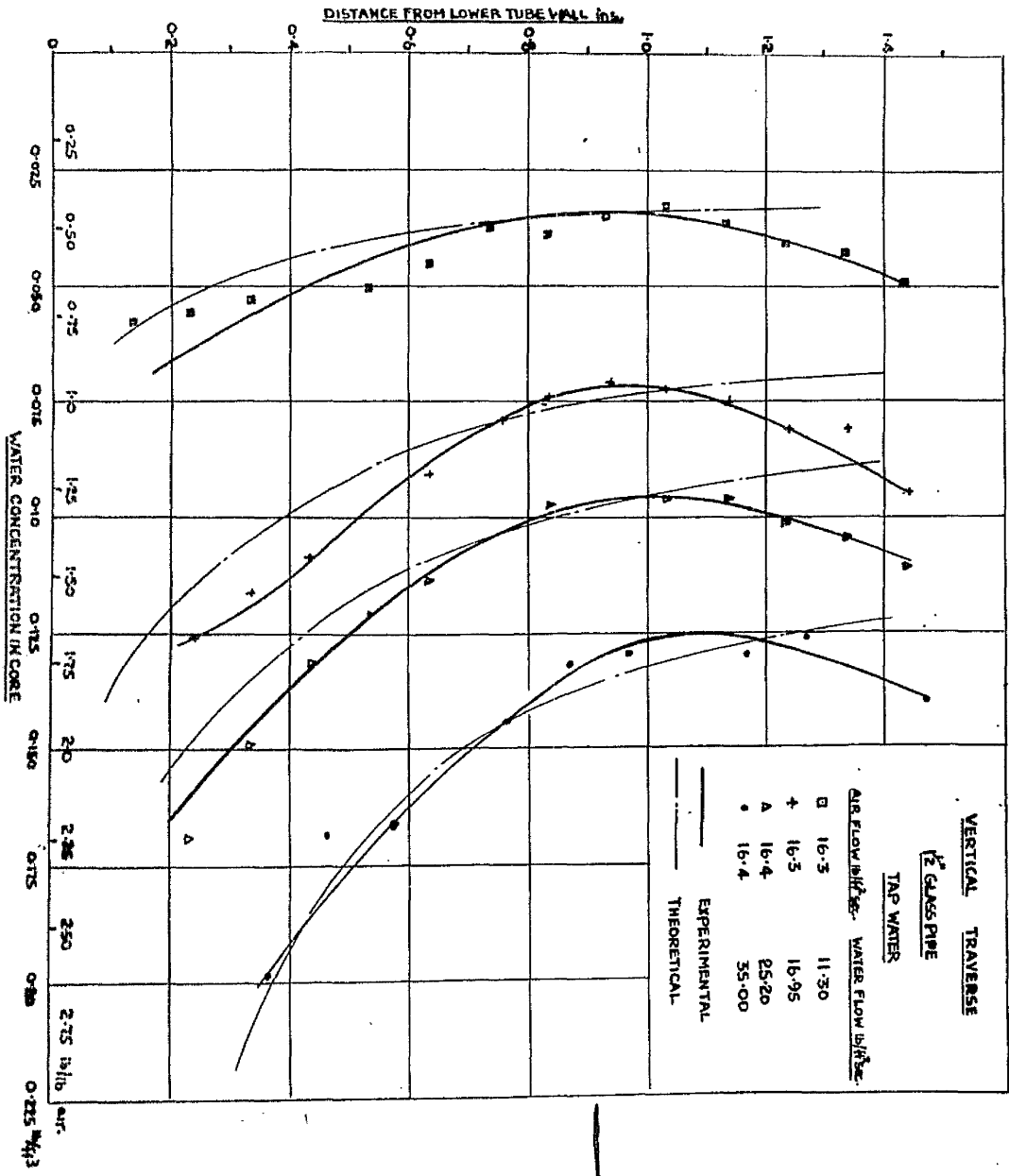


Fig. 19

### Water Concentration in the Air Stream.

When it is required to determine the influence of water entrainment on flow characteristics such as density distribution, it becomes necessary to associate water quantity with air mass flow rate.

Thus the system of plotting adopted in subsequent figures shows the concentration of entrained water in the air, i.e., the weight of water per pound or per cubic foot of air to a base of distance from the tube wall.

### Results of Tests on 1½" Glass Pipe.

#### Vertical Traverses.

#### Constant Air-Variable Water Plotting.

Representative curves are given in Figs. 16-19 which cover the whole range of air and water flow.

It should be noted that the flow rates quoted hereafter for both air and water are based upon the full tube cross-section.

At an average air flow of 7.56 lb./ft.<sup>2</sup> sec. the increase of water flow from 12.05 lb./ft.<sup>2</sup> sec. to 19.8 lb./ft.<sup>2</sup> sec. resulted in an increase of water concentration in the air but with little change in the shape of the graph. The thickness of the layer at the bottom increased as the water was increased, and at the highest water flow rate of  $^{43}$  1 lb./ft.<sup>2</sup> sec. it could be seen that it occupied nearly one third of the tube diameter.

The points generally seem to follow the exponential pattern but at high water flow rates it can be seen that a marked deviation from this form at the centre part of the tube takes place.

CONCENTRATION DISTRIBUTION - CONSTANT WATER, VARIABLE AIR

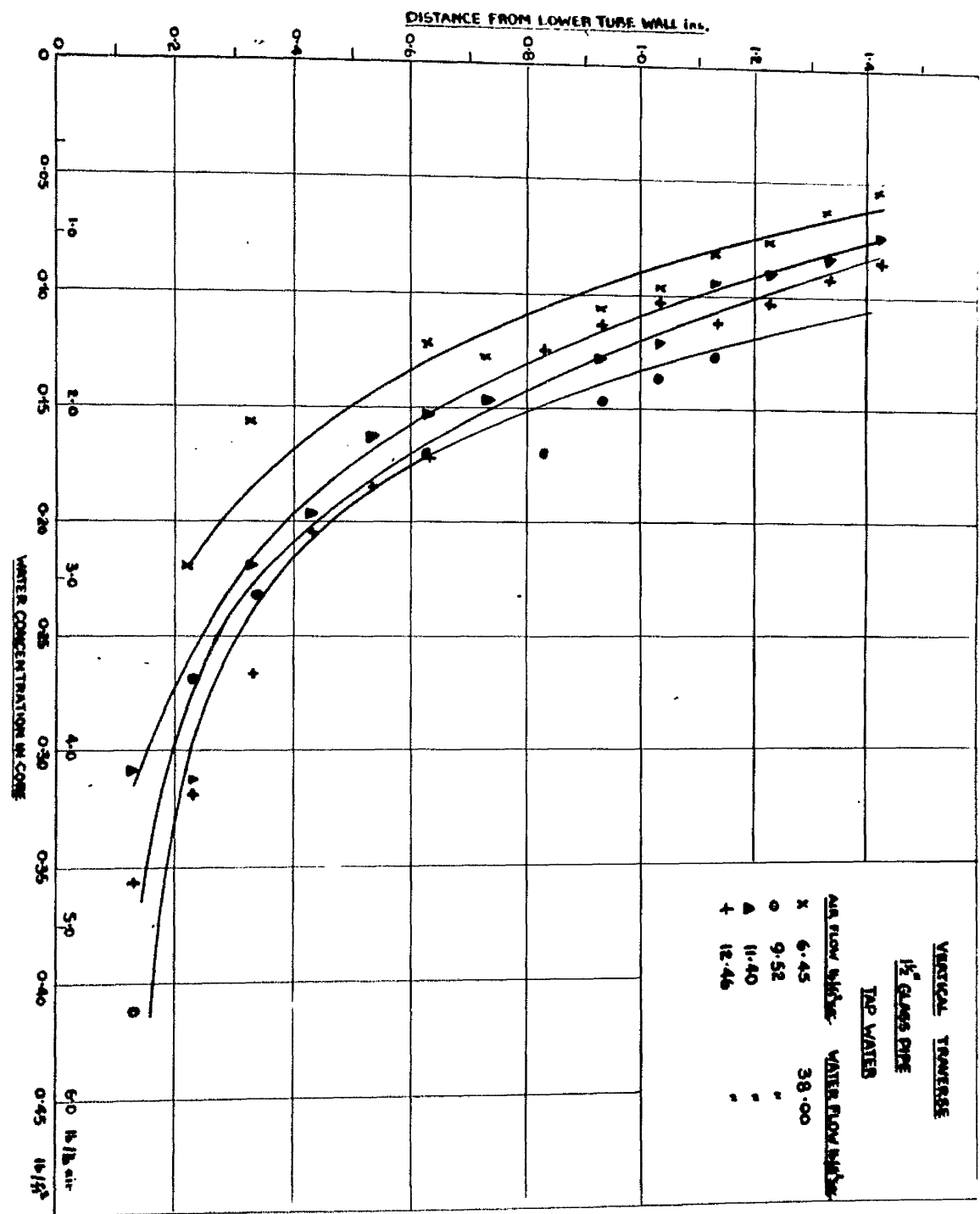


Fig. 20

At an air flow of 10.9 lb./ft.<sup>2</sup> sec. the concentration distribution follows the same shape but the values for approximately the same water flow as in the previous curves show an increase in the value of concentration at the different points of the traverse. Here the most noticeable feature is that the thickness of the bottom layer has decreased appreciably. Also it is noted that at a water flow of 43.8 lb./ft.<sup>2</sup> sec. the top part of the concentration curve is almost vertical implying nearly constant concentration values.

With an air flow of 12.6 lb./ft.<sup>2</sup> sec. the concentration values are unaltered for the lower part of the traverse but show an increase at the top.

At 16.3 lb./ft.<sup>2</sup> sec. air flow, the values of concentration for the lower part of the tube again remain unchanged but the concentration at the top shows a marked increase and the curves tend to take a symmetrical form.

#### Constant Water-Variable Air.

The concentration distribution curves are regrouped to show the effect of variation of air flow when water flow was nearly constant. Concentration graphs are shown in Fig.20. It can be seen that all the graphs have the usual exponential form, for the range plotted. An interesting feature is the tendency within that range towards limiting curve as the air rates increase. This merely confirms the comments made on the constant air-variable water graphs and as would be expected, still

CONCENTRATION DISTRIBUTION - CONSTANT AIR, VARIABLE WATER

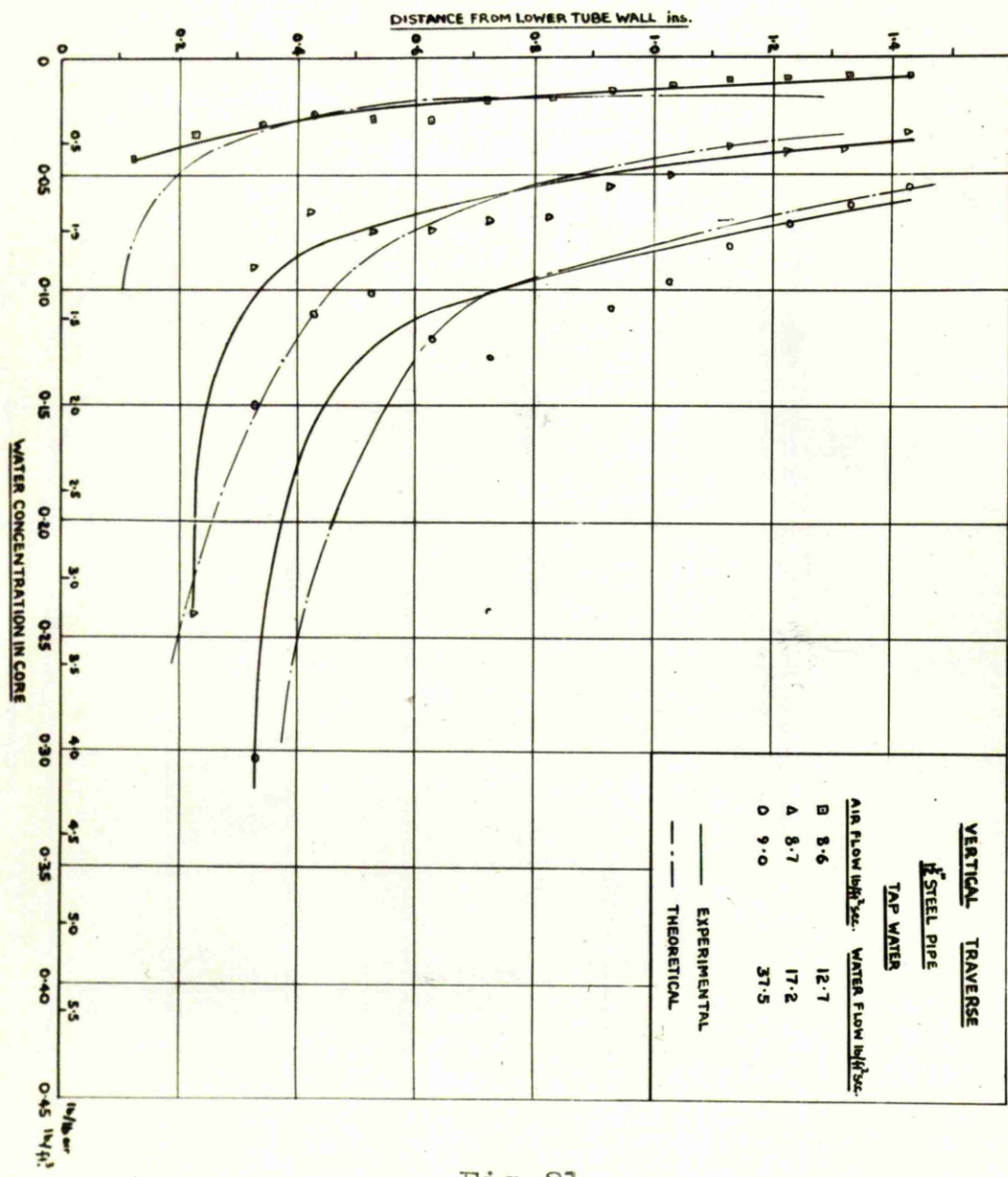


Fig. 21

CONCENTRATION DISTRIBUTION - CONSTANT AIR, VARIABLE WATER.

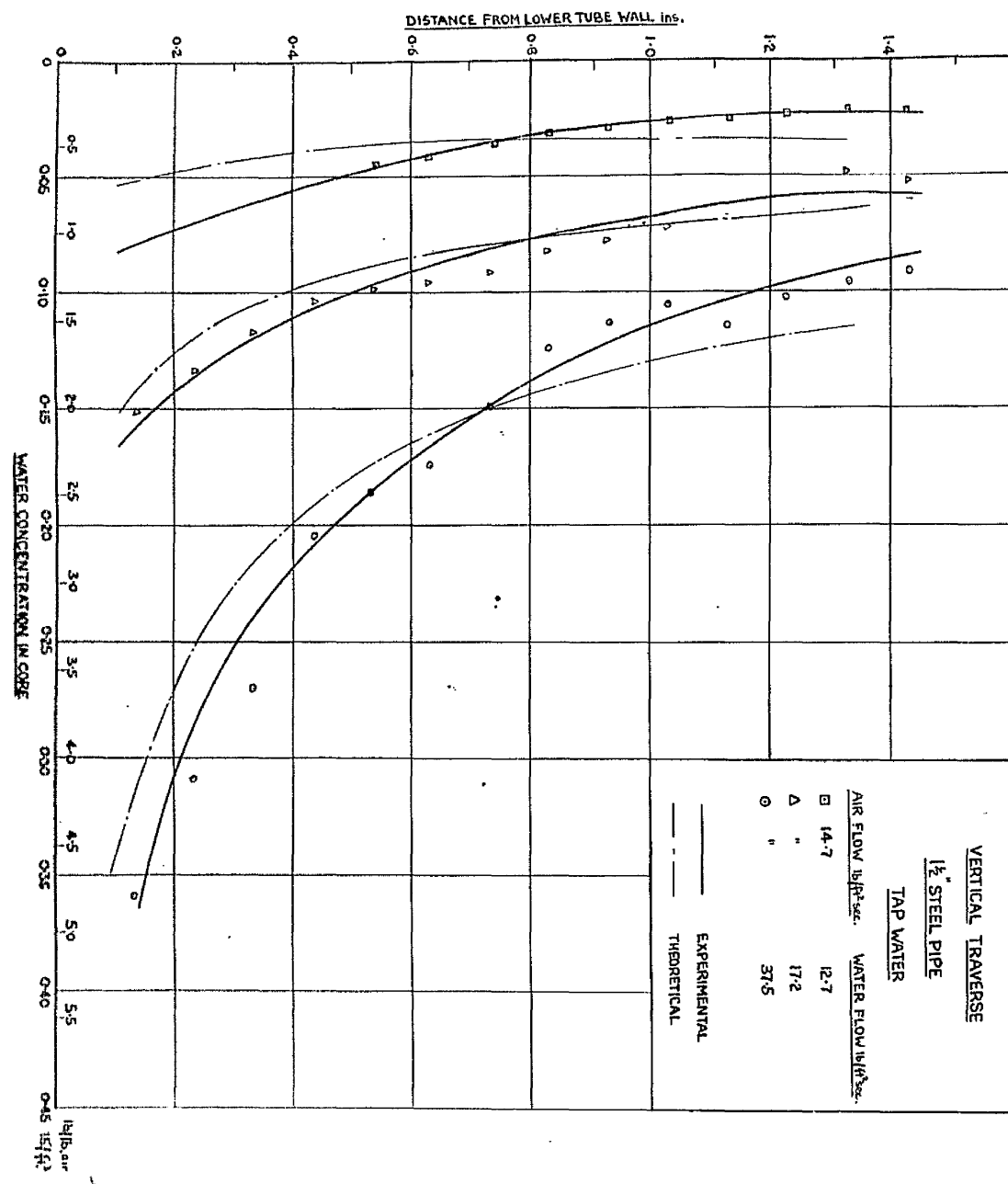


Fig. 22

CONCENTRATION DISTRIBUTION - CONSTANT AIR, VARIABLE WATER

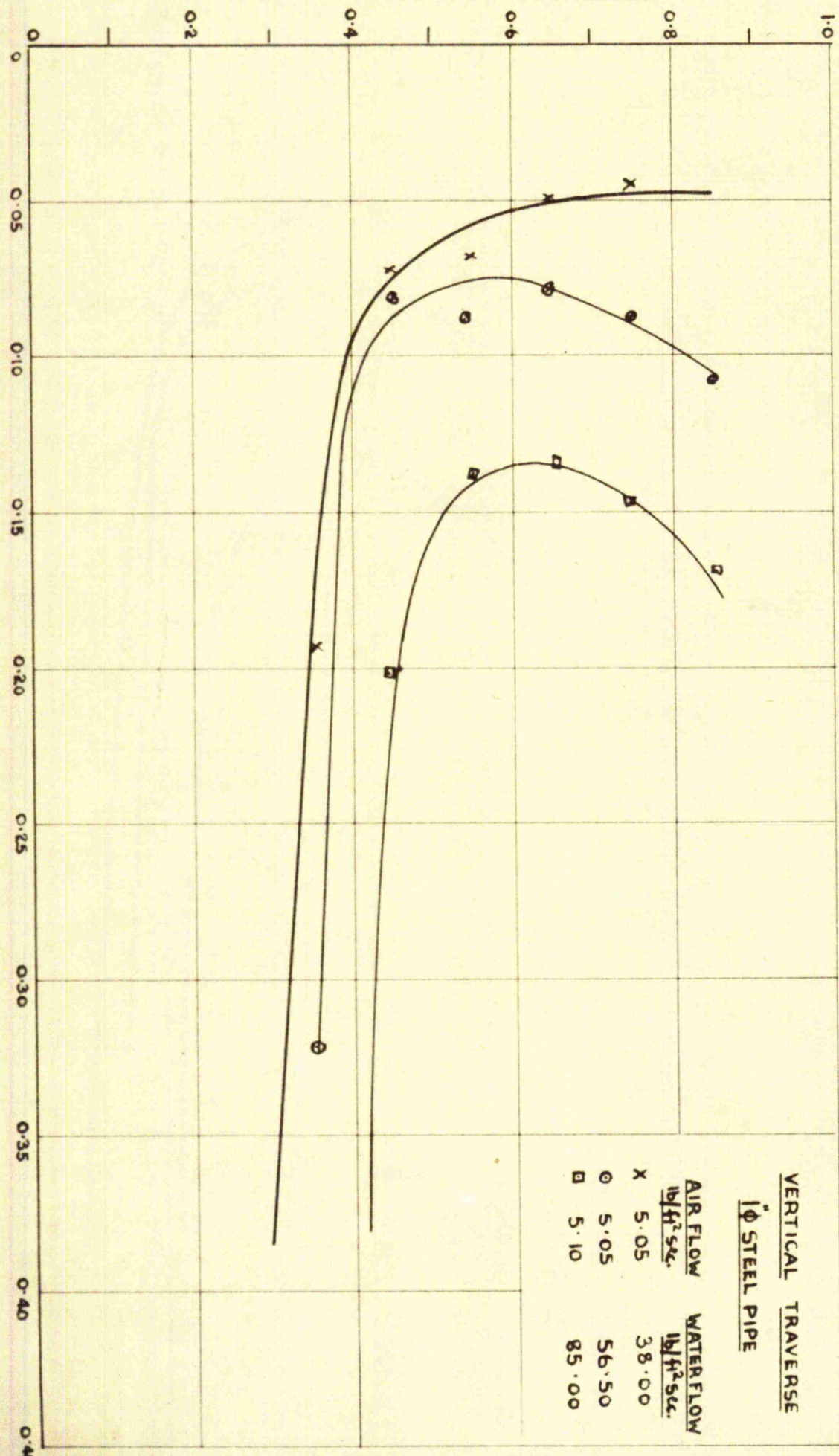


Fig. 23

CONCENTRATION DISTRIBUTION - CONSTANT AIR, VARIABLE WATER

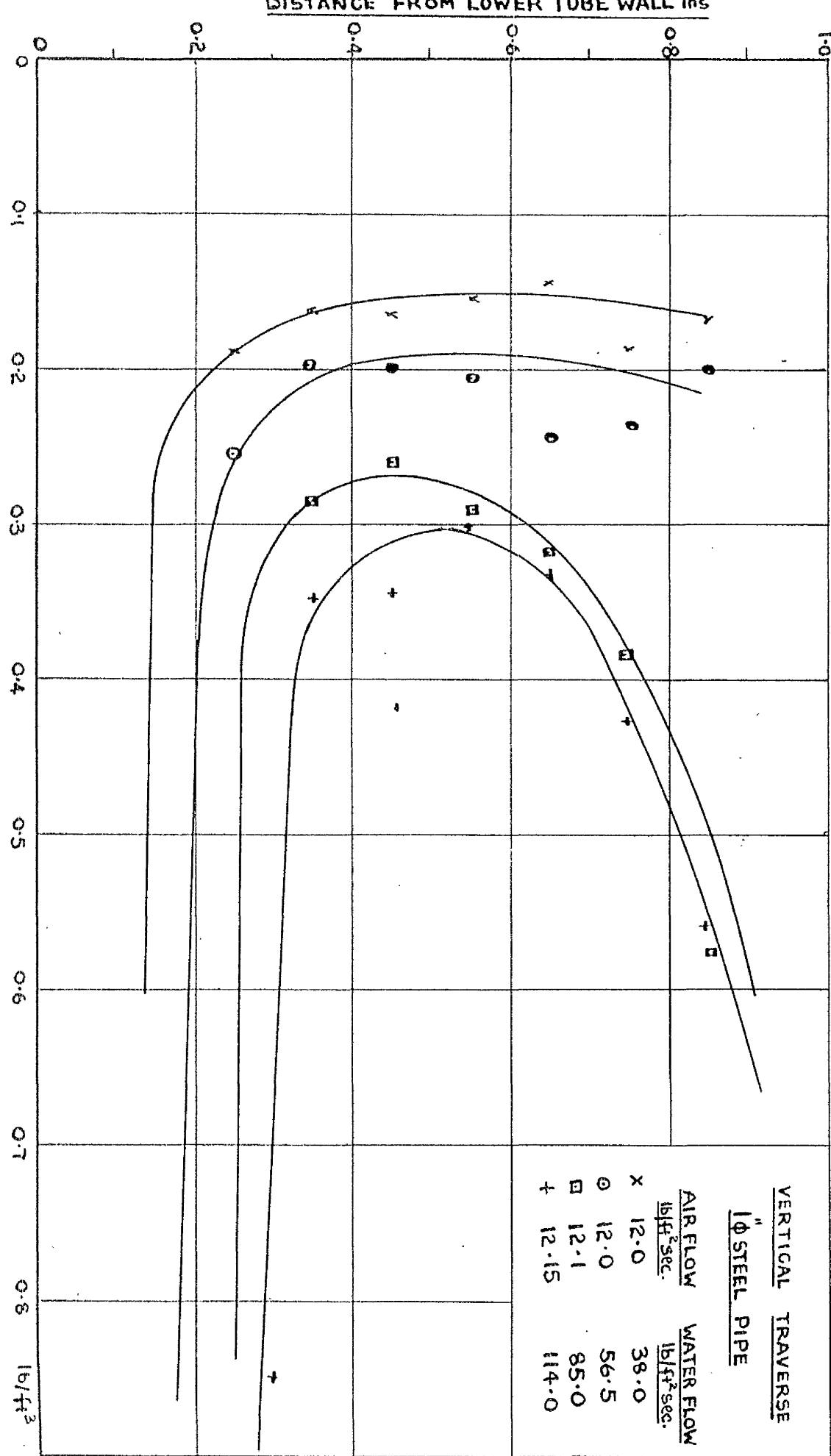


Fig 24

higher air flow rates would produce curves having the same values in the lower part of the tube but with increasing concentration in the upper half.

#### 1 $\frac{1}{2}$ " I.D. Steel Pipe.

These concentration distribution graphs are presented in Figs. 21 and 22 for 1 $\frac{1}{2}$ " steel pipe. They show little difference when compared with the glass pipe. At high air flow, however, there is no suggestion of increasing concentration at the top of the section, the exponential form persisting throughout the range of experiments. The characteristic constancy of concentration in the bottom part of the traverse at high air flow rates found with the glass pipe, is also evident in this case.

#### 1" Steel Pipe.

Tests carried out for the 1" I.D. steel pipe were intended primarily to reveal the effect of pipe size on the phenomenon of liquid entrainment.

At an average air flow of 5.05 lb./ft.<sup>2</sup> sec. Fig. 23, and water circulation of 38 lb./ft.<sup>2</sup> sec., the usual shape of exponential distribution is evident, but at high water flows the curves turn over at the top indicating high concentration at the upper wall. From Fig. 24, it can be seen clearly that the increase in concentration near the top is affected also by the increase of air flow. The thickness of the water layer at the bottom of the pipe increases until at 86 lb./ft.<sup>2</sup> sec. it nearly fills the bottom half of the pipe. (Fig. 23)

CONCENTRATION DISTRIBUTION - CONSTANT AIR, VARIABLE WATER

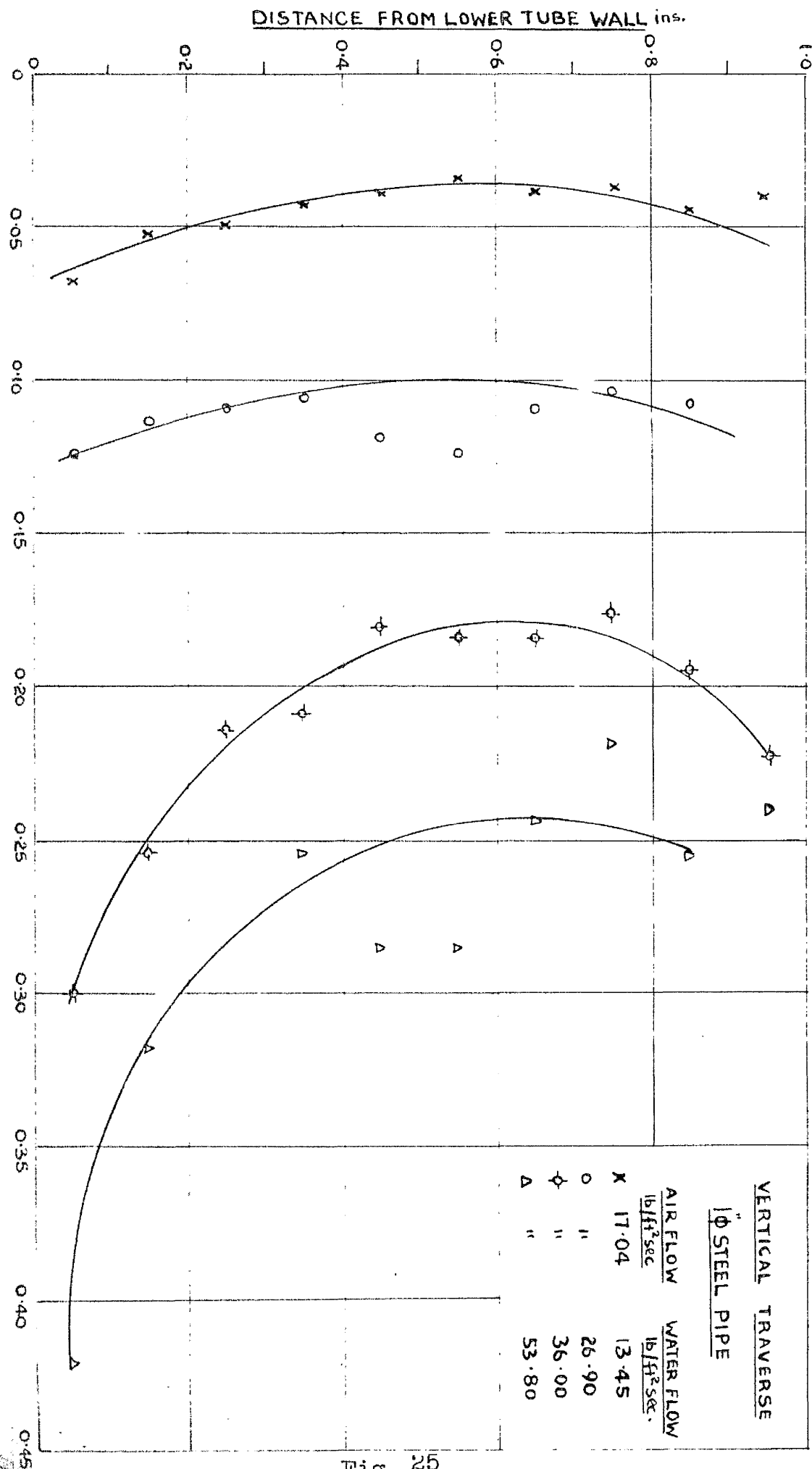


Fig. 25

CONCENTRATION DISTRIBUTION - CONSTANT AIR, VARIABLE WATER

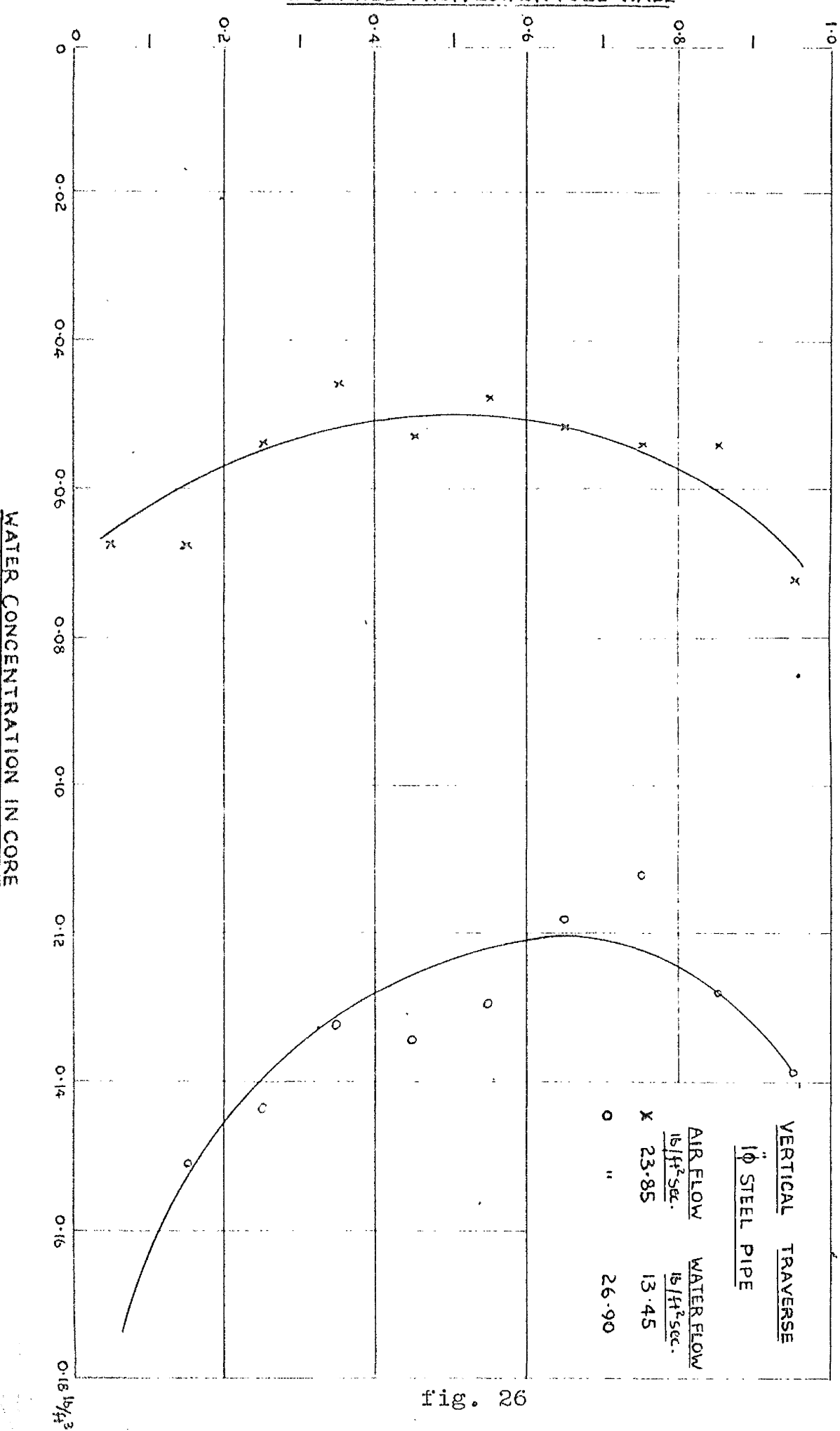


fig. 26

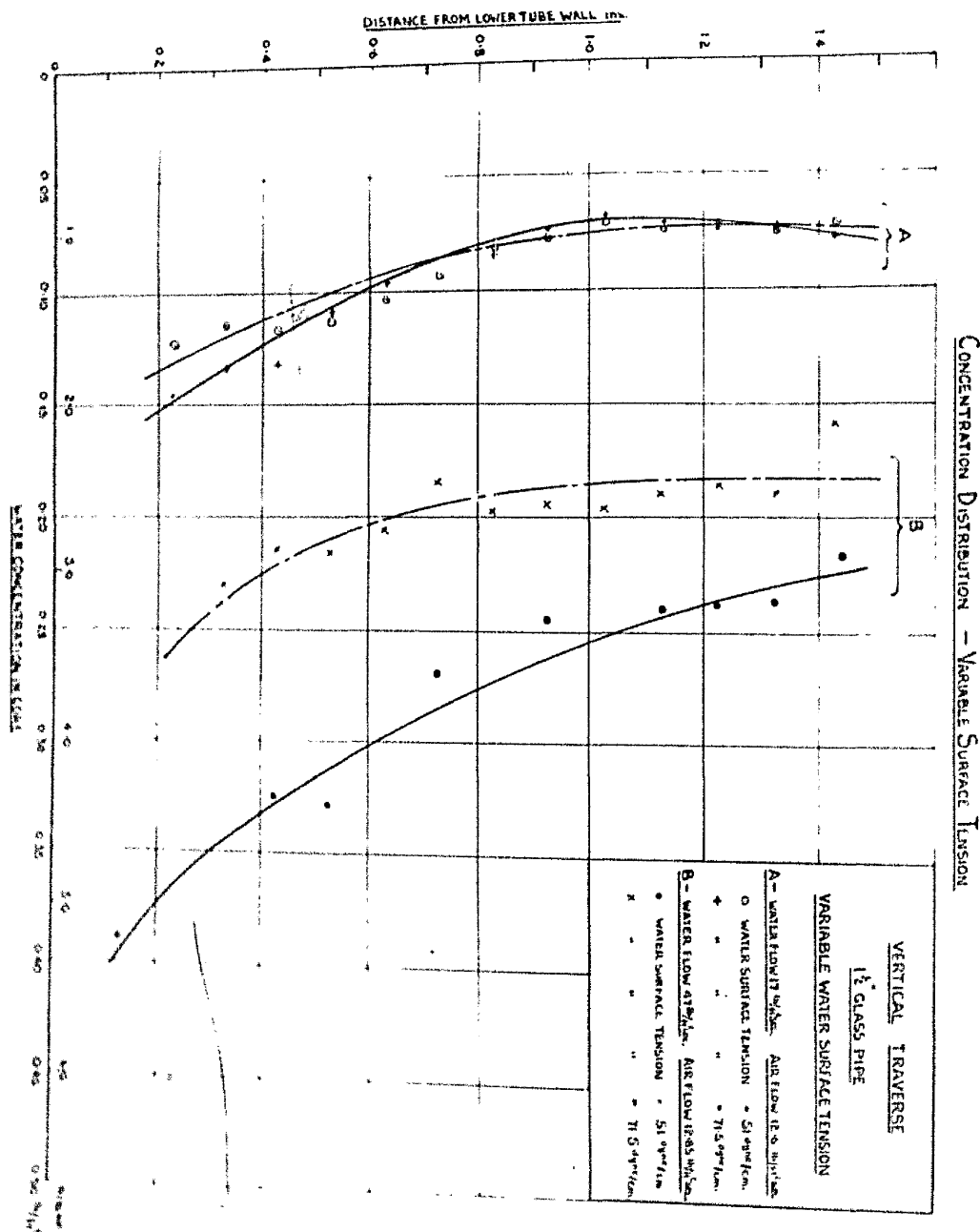


Fig. 27

CONCENTRATION DISTRIBUTION - CONSTANT AIR, VARIABLE WATER S.I.

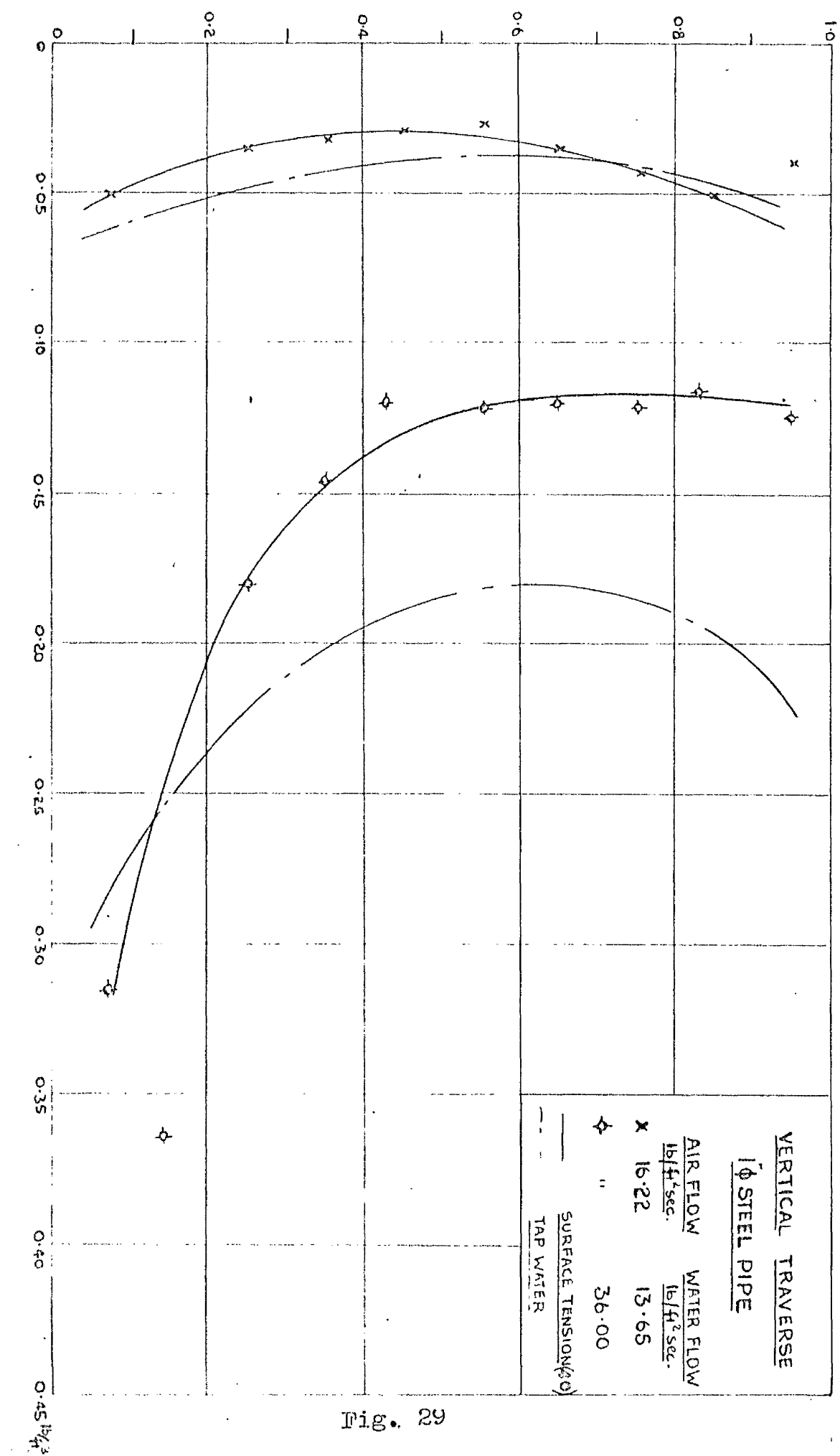


Fig. 29

CONCENTRATION DISTRIBUTION - CONSTANT AIR, VARIABLE WATER

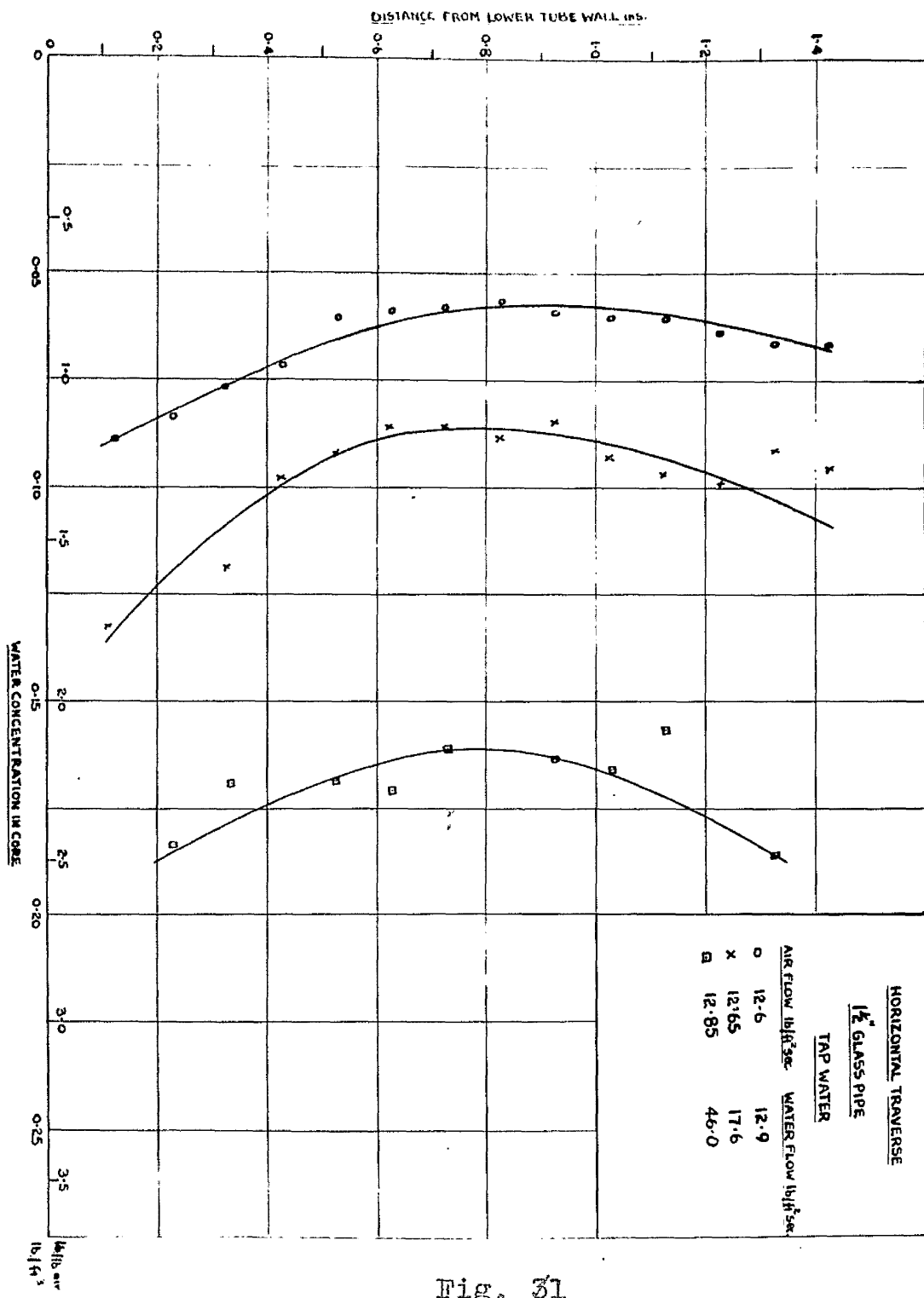
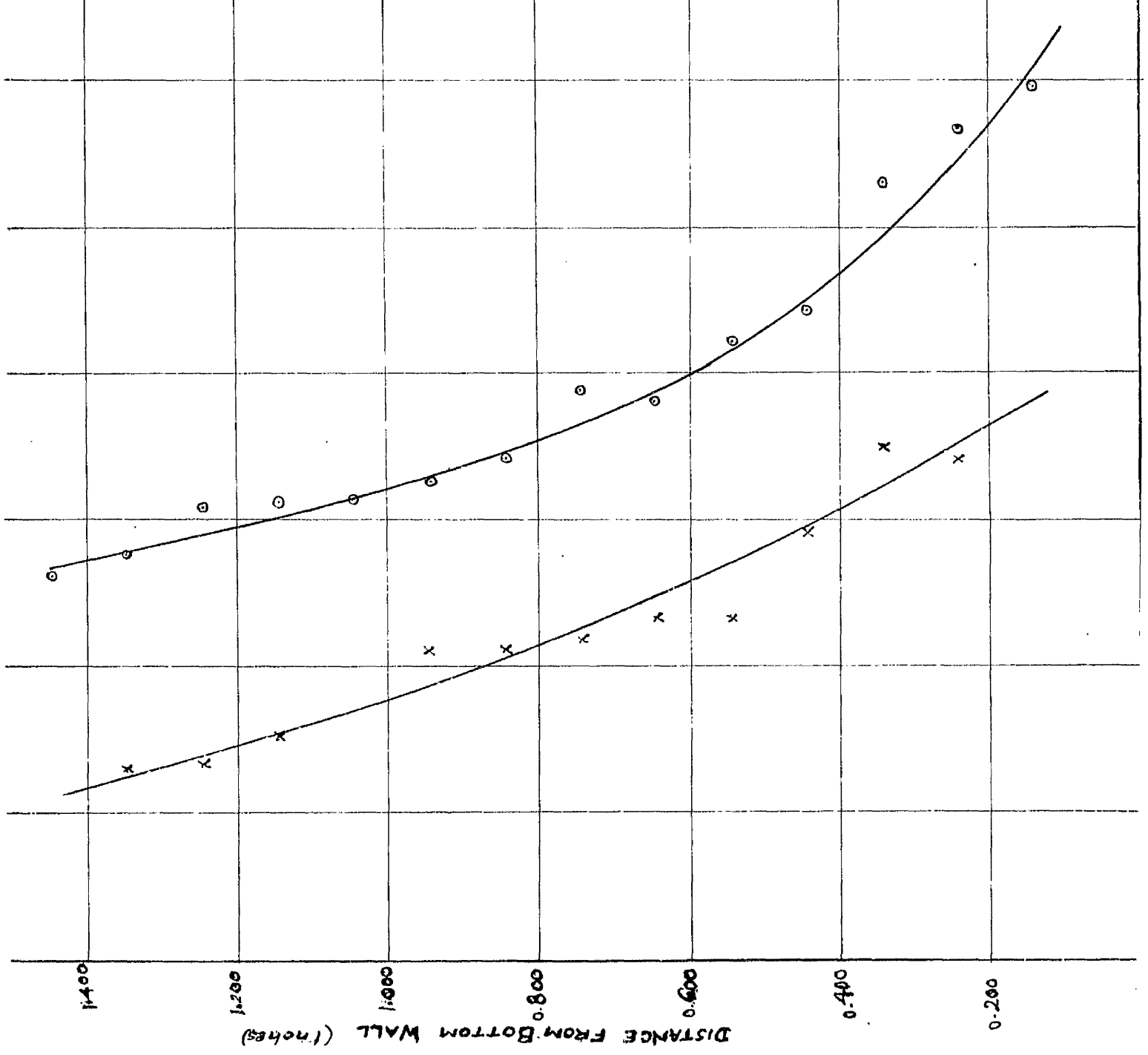


Fig. 31

CONCENTRATION DISTRIBUTION

45° TRAVERSE  
 1½" STEEL PIPE  
 TAP WATER  
 AIR FLOW  
 $\text{lb}/\text{ft}^2 \cdot \text{sec}$   
 8.4      12.6  
 14.6      12.6



At high air flow rates in the range 17.04 to 23.85 lb./ft.<sup>2</sup> sec. the graphs actually attain an approximately symmetrical shape about the axis of the pipe, Fig. 25, 26.

It could be noted that higher concentration values are obtained than for the  $\frac{1}{2}$ " I.D. pipe but again they are not proportional either to air or to water flow rates.

#### Effect of Surface Tension Reduction.

Reducing surface tension from 71.5 dynes/cm. to 40 dynes/cm. the values of concentration show a decrease as shown in Figs. 27, 29; also the shape of concentration distribution changes from the nearly symmetrical to the exponential form.

It was not possible to use water with lower surface tension than 40 dynes/cm. due to excessive foaming in the pipe and in the sampling apparatus.

#### Horizontal Traverses.

A few horizontal traverses for both  $\frac{1}{2}$ " and 1" pipes were made and the results are shown in Fig. 31.

All of them reveal approximately symmetrical distribution. It will be seen that the ratio of the concentration at the wall to that at the centre of the pipe vary, but obtain a ratio of 1.8 at the highest flows.

#### 45° Traverses.

These traverses reveal no new phenomenon and the forms of the concentration curves shown in Fig. 32 are what might be expected.

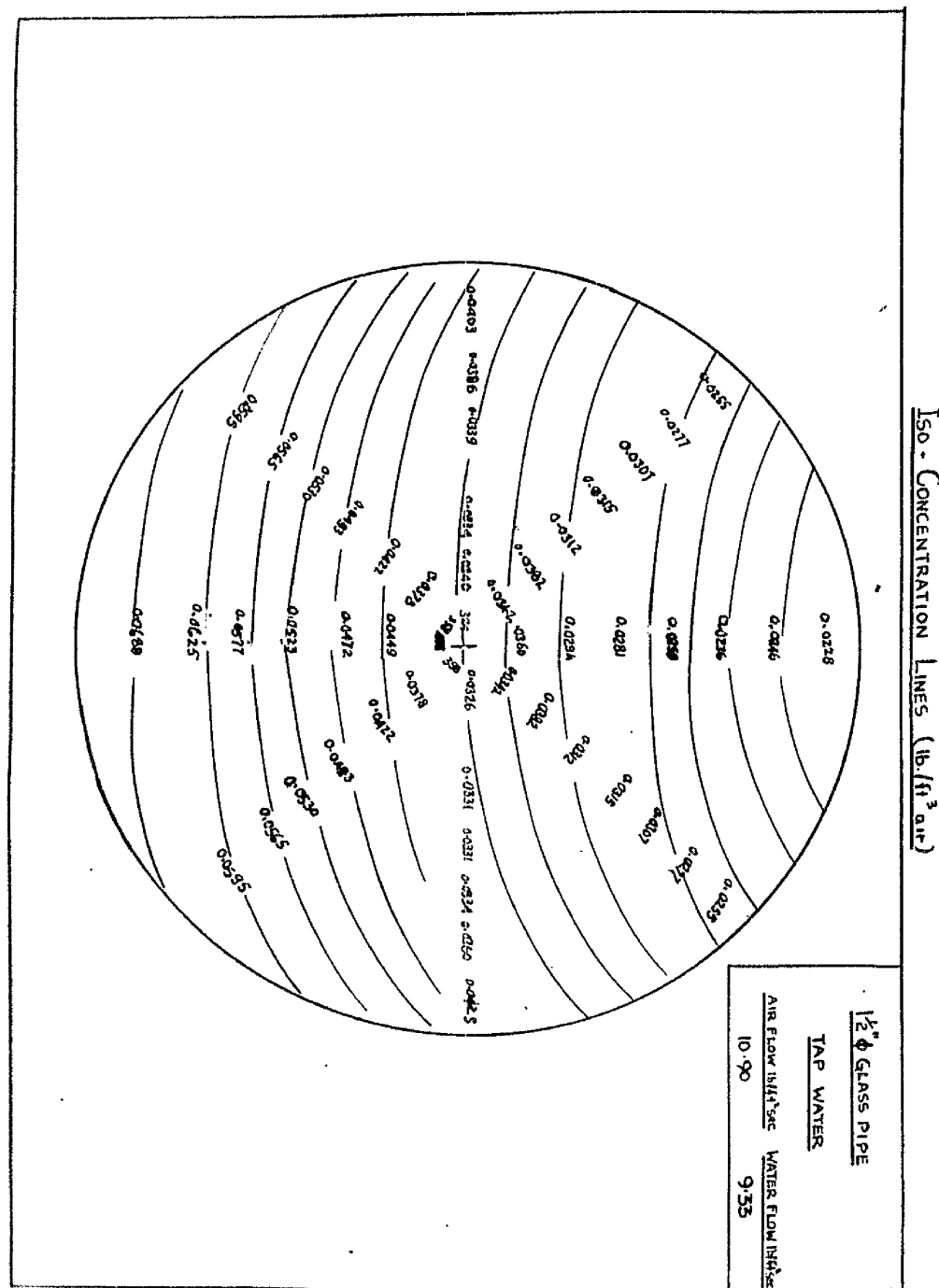


Fig. 33

Iso-Concentration Lines (lb/ft<sup>3</sup> air)

1½"  $\phi$  GLASS PIPE  
TAP WATER  
AIR FLOW lb/SEC. WATER FLOW gal/sec.  
6.30 19.0

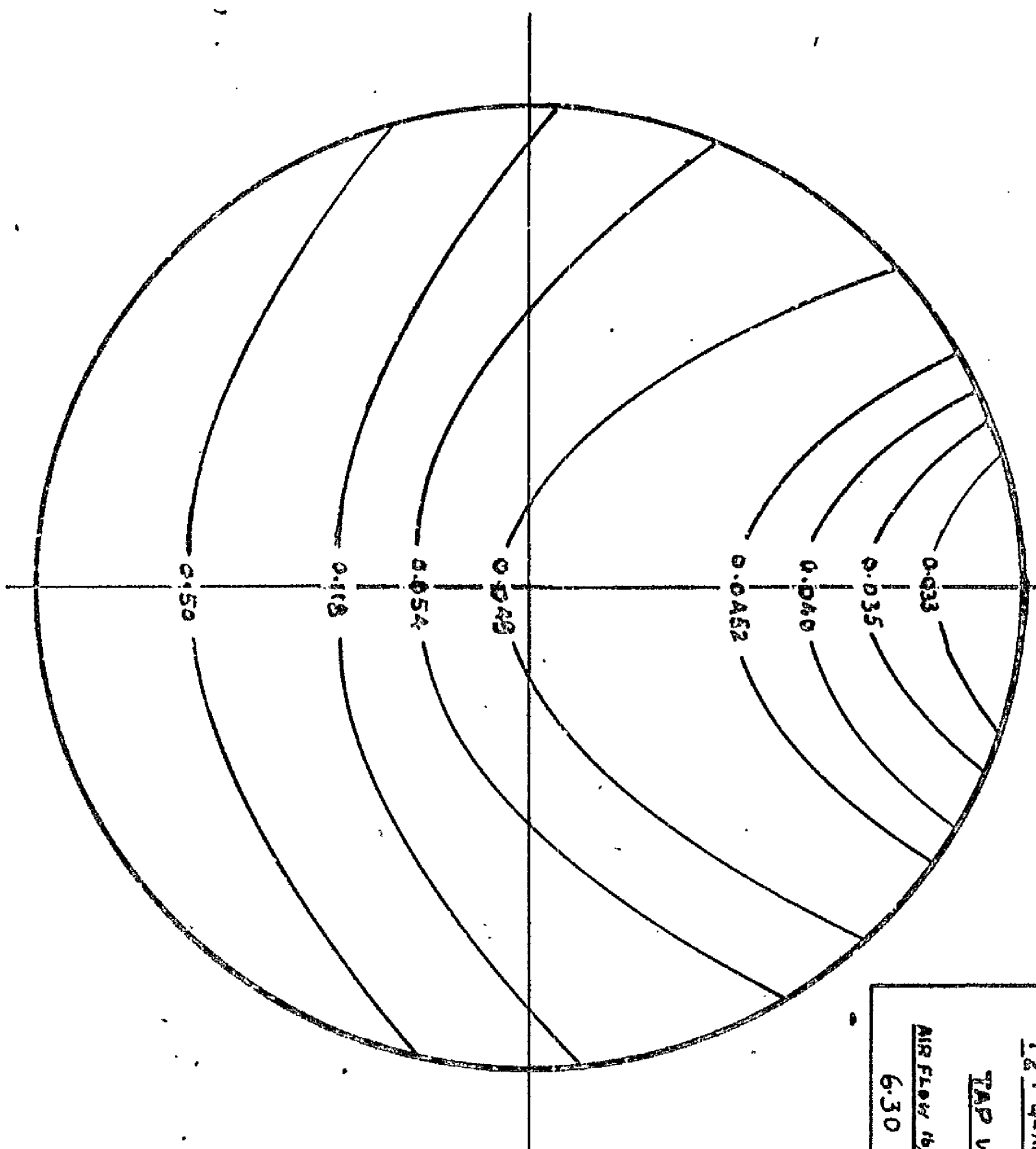


Fig. 33A

General Picture of Concentration Distribution.

Plotting the concentration values on a polar diagram, i.e., values at different points in the cross section, are shown in Figs. 33, 33A. It was considered that  $45^\circ$  traverses on both sides of the vertical axis are the same.

The general shape of the iso-concentration lines indicates that in the upper region there is a little change of concentration values from walls to the centre due to a small thickness of water layer, but as the bottom half is approached this difference increases which is due to a larger layer on the walls. Also, the values of concentration increase from top to bottom until the water layer was reached.

Discussion of Experimental Results on Entrainment.

- I. The direct measurement of water flow using the sampling tube provides a picture of the distribution of water throughout the air stream, showing that the actual quantity of water flowing varies considerably at different points in the gas stream and that variation follows a fairly definite pattern.

This is in marked contrast to the findings of Armand who concluded that the distribution of water flow was uniform across the air stream. A possible explanation of Armand's failure to note this variation is that his sampling tube was relatively large, compared to the tube diameter and therefore, any one reading taken, represented the average flow over a large fraction of the air flow area. Having regard to the velocity profile in the air stream and the need for balance

between the turbulence mass transfer and the gravitational settling, it would be unlikely that uniform distribution of the water flow could exist.

II. The presentation of the results in the form of concentration curves is new to the field of gas-liquid two-phase flow.

Again the pattern is very well defined. The development of the curve form is well established. At low velocities the exponential form holds. As the flow velocities increase the concentration increases but at a continually decreasing rate. A point is reached beyond which the shape of the curve for the lower part of the tube remains nearly constant while the concentration in the upper zone increases towards the top and the curve tends to a symmetrical form about the tube axis.

It is interesting to note that in liquid-solid two phase flow the method of plotting of concentration has already been adopted(31). The curves obtained in this field are all of the exponential type but the influence of particle size is noteworthy. As the size is reduced the curves become steeper and in the limit, tend towards uniform concentration over the section. The essential difference between the gas-liquid and the liquid-solid cases should be emphasized. In the latter the particle size in any one experimental series is predetermined and is obviously constant throughout. In the former, however, the size of the entrained particles vary with velocity. Comparison of the present results with those from the liquid-solid field suggests that droplet size decreases with air-velocity but only to a limited extent.

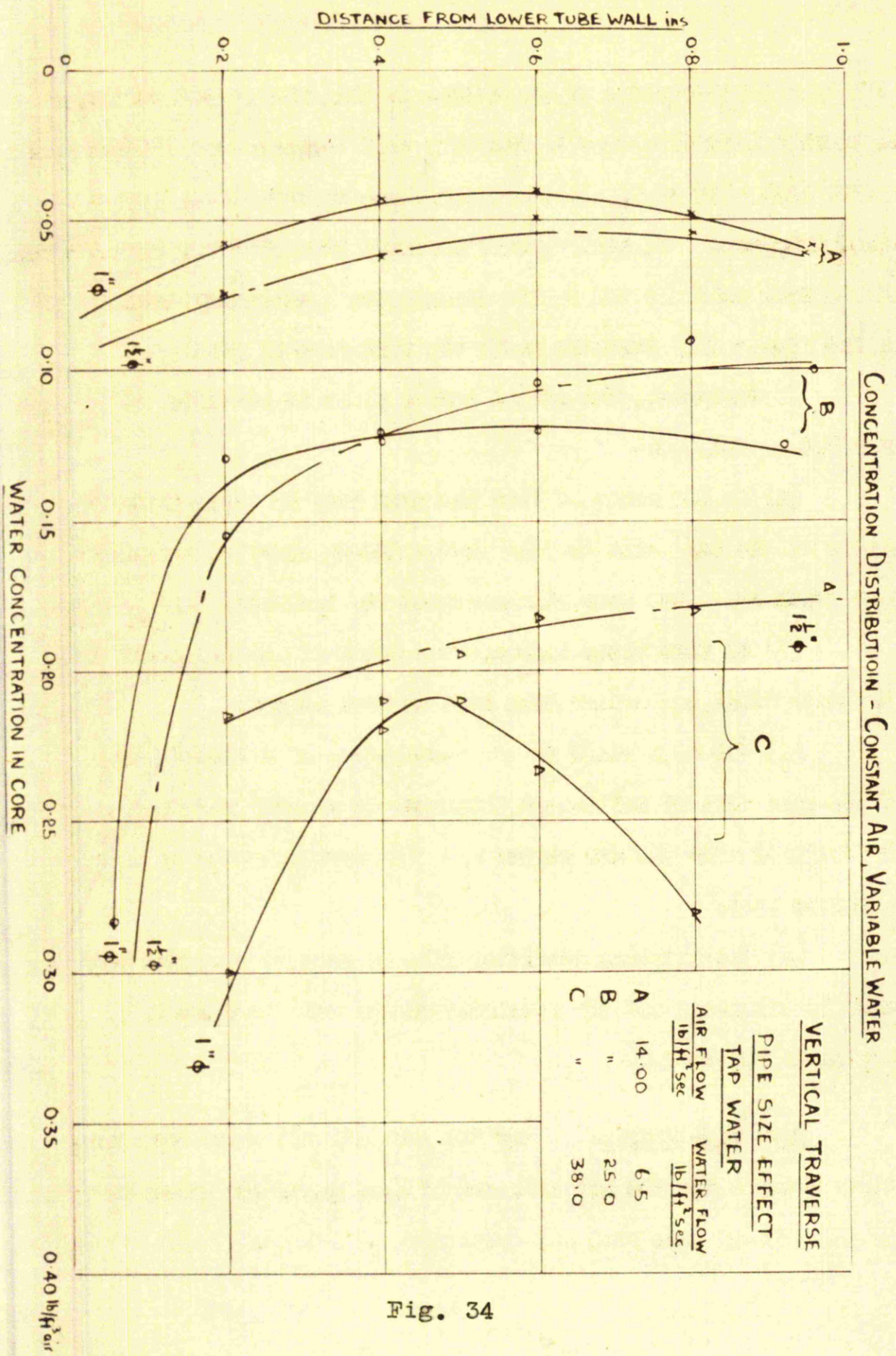


Fig. 34

A further point of difference is that the liquid particles due to surface tension adhere to the tube wall forming a continuous film which with high flow rates, thickens and forms an additional source of entrained droplets. It also appears probable that when the liquid layer around the tube wall assumes finite dimensions, a secondary downward flow within the liquid will commence under the influence of gravity.

To summarise, the action taking place in air-water flow might be described as follows:-

- (a) At low rates of flow the main body of water flows on the bottom of the tube with the air stream above, carrying entrained droplets which are acted upon simultaneously by turbulence and gravity.
- (b) As flow rates increase the depth of the turbulent zone will increase until the entire tube wall becomes wetted.
- (c) The next stage is the development of a liquid layer around the tube wall of sufficient thickness to promote rediffusion of liquid particles into the air stream and also recirculation of water down the tube wall.
- (d) The limiting condition will be reached when the bulk of the water is entrained and the remainder on the wall is reduced to boundary layer thickness.

III. Pipe Size Effect. For the same air and water mass flow velocities results for the  $1\frac{1}{2}$ " I.D. and 1" I.D. pipes are shown together in Fig. 34. It appears that pipe size only affects the shape of the

concentration distribution curves. The symmetrical form occurred only in the case of 1" I.D. pipe at water flow rates in excess of 38 lb/ft.<sup>2</sup>. sec. Fig. 23.

When the total amount of liquid entrained expressed in lb/ft.<sup>2</sup>. sec., is calculated it shows little variation with the small water flow rate but increases appreciably with water above 38 lb/ft.<sup>2</sup> sec.

#### Effect of Reduction in Surface Tension of the Liquid Phase.

A limited number of testing, as previously mentioned, were made at reduced surface tension. In the case of  $\frac{1}{2}$ " diameter glass or steel pipe the concentration values increase, a phenomenon that can be attributed to the reduction in drop size due to more effective atomization.

Unexpectedly, however, it is noted from the results of tests made on the 1" I.D. steel pipe, that at high water or air flow rates, when the shape of the curve for normal water would be nearly symmetrical, the form of distribution now takes exponential form.

This emphasises the importance of the layer of liquid at the top from which diffusion normally takes place. If adherence is small due to reduction in surface tension the build up of the layer

at the top is reduced and its thickness is insufficient to promote diffusion back into the main gas stream due to turbulence."

### Theoretical Analysis of Phase Distribution.

#### Introduction.

So far no attempt has been made to account for the variation of concentration of water in air in the case of horizontal pipes and this important fundamental effect must have a bearing on the characteristics of the flow and energy lost in the two-phase flow of air and water.

Very little work has been done on dispersed flow, apart from a few recent papers by Alexander and Goldren(2), and Longwell and Weiss (45) as already mentioned by Hughes(30), who in his survey states that the mechanism characteristics can be treated with the help of analysis made of "Fluidised transport of solids phenomenon".

The following theoretical analysis was made on the basis of the turbulent diffusion concept and Prandtl momentum transport theory.

According to Prandtl(53), the amount of mechanical admixture of concentration  $c$  which can be transferred across unit area in unit time is given by

$$M = - \epsilon_s \left( \frac{\partial c}{\partial y} \right) \quad (1)$$

where  $\epsilon_s$  is the coefficient of exchange of mass analogous to the molecular exchange coefficient.

The apparent shear stress is given by

$$\begin{aligned} \tau' &= \rho \cdot \ell^2 \cdot \left( \frac{du}{dy} \right)^2 \\ &= \epsilon \frac{du}{dy} \\ \text{i.e. } \epsilon &= \rho \cdot \ell^2 \cdot \left( \frac{du}{dy} \right) \end{aligned} \quad (2)$$

putting

$$\ell = Ky \quad (3)$$

then

$$\frac{du}{dy} = \frac{U_f}{Ky}$$

thus

$$\frac{U_{max} - U}{U_f} = \frac{1}{K} \log \frac{y}{r_0} \quad (4)$$

The expression

$$\epsilon = \rho U_f K \left[ r \left( 1 - \frac{r}{r_0} \right) \right] \quad (5)$$

indicates a parabolic curve of distribution, with zero values at the wall end at the centre of the pipe.

Experiments of Nikuradse(47) showed that the value of  $\epsilon$  is not zero at the centre and equation(5) can only be valid at a section away from the centre.

In order to correct further the fact that  $\epsilon$  is not zero at  $\frac{du}{dy} = 0$  Prandtl(52) suggested a modification of his original formula (2) of the form

$$\epsilon = \ell^2 \left[ \left( \frac{du}{dy} \right)^2 + \ell'^2 \left( \frac{d^2 u}{dy^2} \right)^2 \right]^{\frac{1}{2}}$$

But the lack of information about  $\ell'$ , makes its application doubtful.

The recent, although not an absolutely satisfactory approach, which was given by Kolmogoroff(35), was based on his hypothesis that "Motion associated with equilibrium range of wave-number is uniquely determined statistically by parameters  $E$  and  $\nu$  where  $E$  is the energy dissipation rate per unit mass evaluated from the pressure drop and  $\nu$  is the kinematic viscosity",

$$D' = \ell'_k = \nu^{-\frac{3}{4}} E^{\frac{1}{4}}$$

However, much work has recently been done on the turbulence problem in single phase flow by Batchelor(8) and Pai(50) but until a more satisfactory explanation and a better solution of this phenomenon is available, Prandtl's concepts may be accepted as the best.

Now, according to Taylor's(60) suggestion, we might take

$$\epsilon_M = \beta \epsilon_s \quad (6)$$

where  $\beta$  = constant.

#### Concentration Distribution in Circular Pipes.

Dealing with the problem in hand, the following simplifying assumptions are made:-

1. Steady conditions in the test length, i.e., no acceleration and no change of concentration distribution along the length or

$$\epsilon \frac{\partial c}{\partial z} = 0 \quad , \quad \epsilon \frac{\partial c}{\partial t} = 0$$

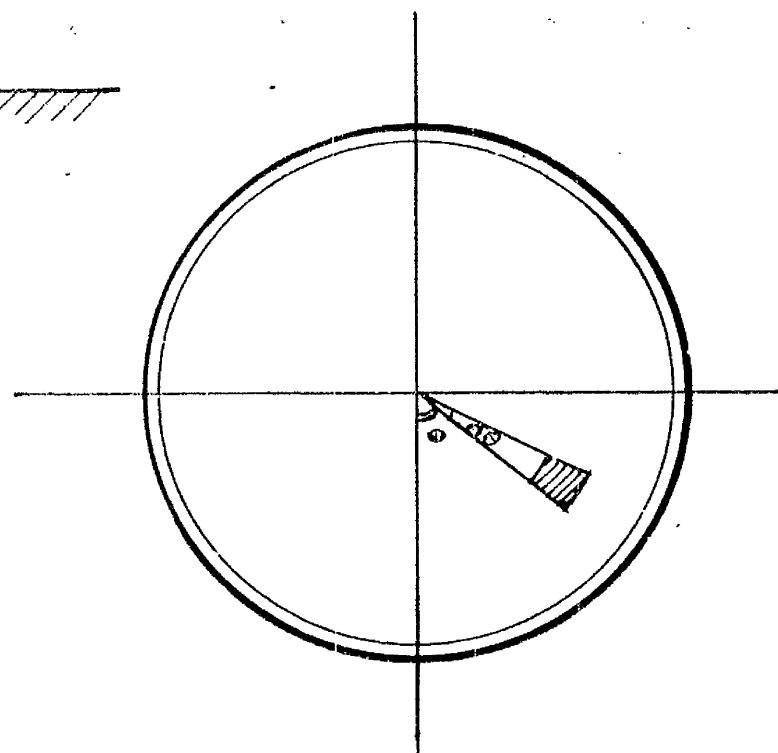
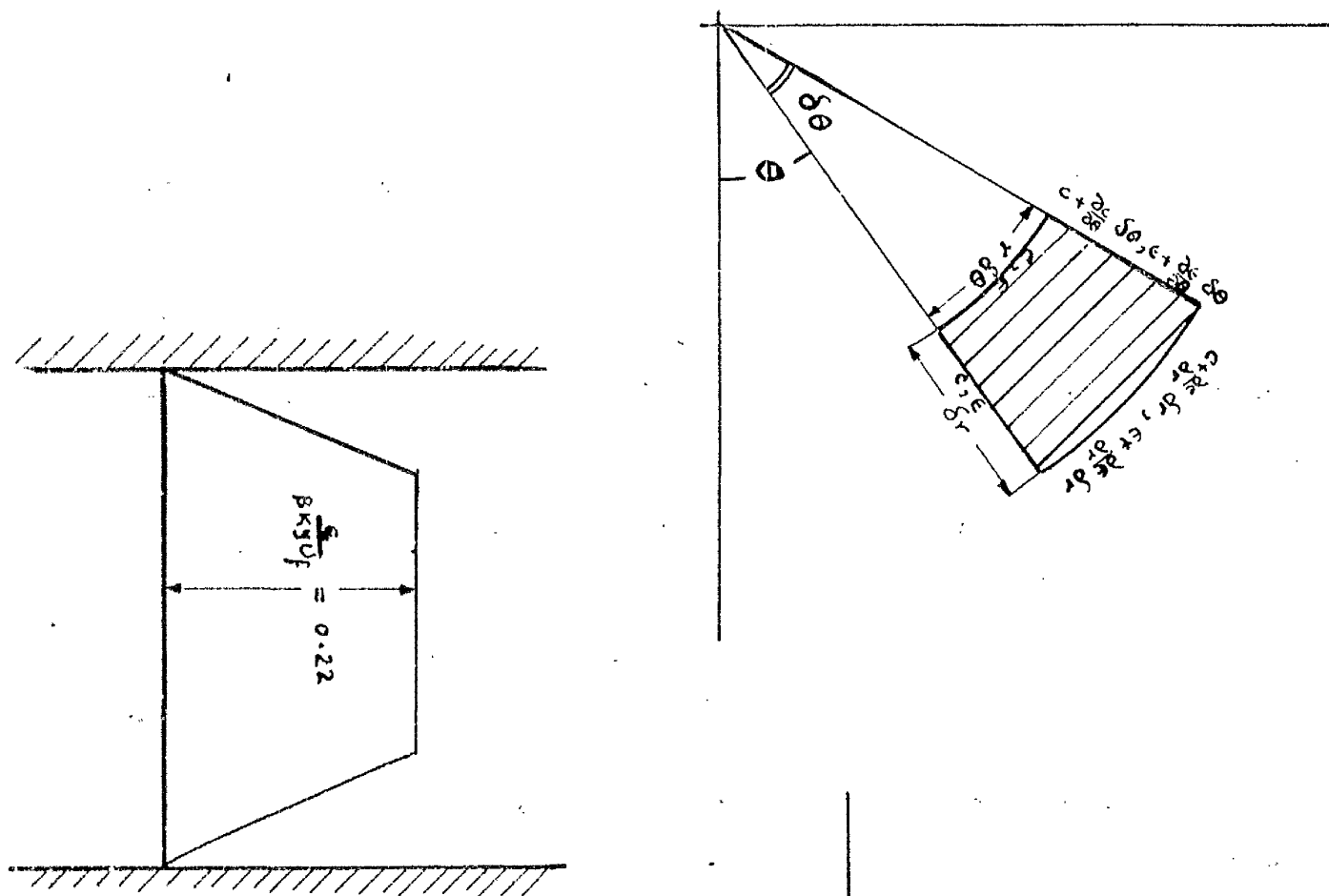
where  $z$  and  $t$  are the distance along the axis and time respectively.

2. Equal size distribution among the entrained water particles which are assumed spherical.

3. No appreciable adherences of the water particles on the walls of the pipe.

However, the central core of the flow is different from the flow of suspended sediment due to:-

(a) The ratio of densities of water/air is much higher than solids/water.



TURBULENCE COEFFICIENT  $\epsilon$   
DISTRIBUTION ALONG TUBE SECTION  
ACCORDING TO ISMAIL (31)

BALANCE OF FORCES  
FOR SUSPENSIONS IN  
CIRCULAR PIPES

(b) Fluid surface tension and capillary waves that take place at the interface.

In the development of the following theory, consideration is given to the two distinctive patterns of concentration distribution observed in the present experimental work.

(a) The exponential form at low flow rates of both phases, and

(b) The nearly symmetrical shape which hold for higher flow rates.

Referring to Fig.35, the forces taking place are in the dispersed air stream, i.e.,

(1) Turbulence effect in  $r$  direction:-

$$\begin{aligned} -\epsilon \frac{\partial c}{\partial r} r \delta\theta + (\epsilon + \frac{\partial \epsilon}{\partial r}) (\frac{\partial c}{\partial r} + \frac{\partial^2 c}{\partial r^2} \delta r) \times \\ (r + \delta r) \delta\theta \\ = r \delta r \delta\theta [\epsilon \frac{\partial^2 c}{\partial r^2} + (\frac{\epsilon}{r} + \frac{\partial \epsilon}{\partial r}) \frac{\partial c}{\partial r}] \end{aligned}$$

(2) Turbulence effect in  $\theta$  direction:-

$$\epsilon \frac{\partial^2 c}{\partial \theta^2} \delta r \delta\theta = r \delta r \delta\theta (\frac{\epsilon}{r^2} \frac{\partial^2 c}{\partial \theta^2})$$

(3) Effect of settling velocity  $w$  :-

$$\begin{aligned} w(c + \frac{\partial c}{\partial r} \delta r)(r + \delta r) \delta\theta \cos\theta - w c r \delta\theta \cos\theta \\ - w(c + \frac{\partial c}{\partial \theta} \delta\theta) \delta r \sin(\theta + \delta\theta) + w c \delta r \sin\theta \\ = r \delta r \delta\theta w (\frac{\partial c}{\partial r} \cos\theta - \frac{1}{r} \frac{\partial c}{\partial \theta} \sin\theta) \end{aligned}$$

For equilibrium we have:

$$\epsilon \frac{\partial^2 c}{\partial r^2} + \left( \frac{\epsilon}{r} + \frac{\partial \epsilon}{\partial r} \right) \frac{\partial c}{\partial r} + \frac{\epsilon}{r^2} \frac{\partial^2 c}{\partial \theta^2} + \omega \left( \frac{\partial c}{\partial r} \cos \theta - \frac{1}{r} \frac{\partial c}{\partial \theta} \sin \theta \right) = 0 \quad (7)$$

Considering  $\epsilon$  as constant in the main part of the stream with the assumption of  $\epsilon$  as given in Fig. b, equation 7 becomes

$$\epsilon \left[ \frac{\partial^2 c}{\partial r^2} + \frac{1}{r} \frac{\partial c}{\partial r} + \frac{1}{r^2} \frac{\partial^2 c}{\partial \theta^2} \right] + \omega \left[ \frac{\partial c}{\partial r} \cos \theta - \frac{1}{r} \frac{\partial c}{\partial \theta} \sin \theta \right] = 0 \quad (8)$$

Changing the equation to cartesian coordinates

$$\frac{\partial^2 c}{\partial x^2} + \frac{\partial^2 c}{\partial y^2} + \frac{\omega}{\epsilon} \frac{\partial c}{\partial y} = 0 \quad (9)$$

Solving this equation as shown in Appendix III we get

$$c = [A' e^{m_1 y} + B' e^{m_2 y}] \sin \left( \frac{n x}{\sqrt{\epsilon}} + \alpha \right) \quad (10)$$

where  $A'$ ,  $B'$ ,  $m_1$ ,  $m_2$ , are constants and  $n$ ,  $x$ , are the roots of

$$m^2 + \omega m - n^2 = 0$$

Unfortunately the number of boundary conditions are not enough to give a full solution of the equation.

Nevertheless, the equations may be used to give an idea of the possible distribution of concentration in the cartesian form in the case of a circular pipe.

The boundary conditions that can be applied in equation 10  
 $\alpha = 90^\circ$  (symmetry about  $yy$ )  
the expression becomes

$$C = (A e^{m_1 y} + B e^{m_2 y}) \cos\left(\frac{n x}{\sqrt{\epsilon}}\right) \quad (11)$$

It can be deduced from equation 11, that the shape of concentration distribution could be either of the form

$$C = C_a e^{m_1 y} \quad (12)$$

or

$$C = C_a (e^{m_1 y} + K e^{-m_2 y}) \quad (13)$$

One boundary condition which is available, viz., under steady conditions there are in effect no particles leaving or entering the layer on the wall. This could only be applied in the case of the circular channel by using polar coordinates.

$$\text{Writing } C = e^{-\frac{\omega}{2\epsilon} y} \times v \quad (14)$$

where  $v$  is a function of  $x$  and  $y$  and substituting in equation 8, we get

$$\frac{\partial^2 v}{\partial r^2} + \frac{1}{r} \frac{\partial v}{\partial r} + \frac{1}{r^2} \frac{\partial^2 v}{\partial \theta^2} - \frac{\omega^2}{4\epsilon^2} v = 0 \quad (14)$$

Solving this equation as shown in Appendix III, we get

$$C = e^{-\frac{\omega}{2\epsilon} r \cos \theta} \sum I_k \left( \frac{\omega}{2\epsilon} r \right) C_k \cos k\theta \quad (15)$$

The boundary condition as given above means that at  $r = r_0$  near the boundary no transport of liquid takes place, i.e.,

$$\frac{\partial C}{\partial r} = - \frac{\omega}{2\epsilon} r \cos \theta \quad (16)$$

the effect of this boundary condition on the solution is again detailed in Appendix III, which gave the final shape of the equation as

$$c = c_0 e^{-\frac{\omega}{\epsilon} r \cos \theta} \quad (17)$$

One important conclusion from this equation appears to be that the application of boundary conditions previously stated yields an exponential concentration distribution curve.

No theoretical treatment of suspensions in circular pipes was made before, and it could be applied to the case of solid-liquid as well as air-solid suspensions. It may be also of interest to note that the application of two dimensional rectangular channels by Durand(17) yielded very satisfactory results in his work on flow of suspensions in circular pipes.

Modification of the theoretical treatment as suggested by the shape of the concentration distribution.

Equation 6 was obtained by assuming a balance between turbulent mass transfer and settling velocity. Applying the boundary condition of no exchange of particles yielded a solution in exponential form as given by equation 17. Such a solution proved to be correct in the case of large pipes but at high air flow in the smaller pipes the concentration distribution undergoes a radical change as discussed when considering the experimental results.

This phenomenon could only be explained by the effect of secondary flow along the tube walls.

Referring to equation 9, which is

$$\frac{\partial^2 c}{\partial x^2} + \frac{\partial^2 c}{\partial y^2} + \frac{\omega}{\epsilon} \frac{\partial c}{\partial y} = 0$$

a third factor of the same nature as settling effect must be added.

Bearing in mind the experimental observations, it would be possible to come to the following tentative conclusions:

(a) The rate of precipitation of water drop is a function of concentration, i.e.,  $\Gamma c$  where  $\Gamma$  is a constant which in turn depends on:

(i) surface tension of the liquid  
 (ii) surface roughness and its characteristics

for adherence.

(iii)  $\frac{1}{r_0}$  where  $r_0$  is the radius of the pipe

(iv) Rate of air flow or water flow.

Introducing this new factor  $\Gamma c$  into equation 9, we have

$$\epsilon \frac{\partial^2 c}{\partial x^2} + \epsilon \frac{\partial^2 c}{\partial y^2} + \omega \frac{\partial c}{\partial y} + \Gamma c = 0 \quad (18)$$

Solution of this equation by the ordinary methods proved to be very difficult. An arithmetic solution suggested by Thomas et al (61) for a similar equation may be used here. They gave a solution

$$c = \frac{2 C_0}{1 + \sqrt{1 + \frac{4 \Gamma \epsilon}{\omega^2}}} e^{-j} \quad (19)$$

where

$$j = \pm \left[ \frac{\sqrt{1 - \frac{\Gamma \epsilon}{\omega^2}} - 1}{2} \right] \frac{\omega y}{\epsilon}$$

If  $\Gamma = 0$  when no secondary flow takes place, the curve would be of the form given by the solution of the equation previously, which is

$$c = C_0 e^{-\frac{\omega y}{\epsilon}}$$

If  $\Gamma$  has a value due to secondary circulation on the walls, then the distribution may be taken of the shape

$$C = \frac{2 C_0}{1 + \sqrt{1 + \frac{4\Gamma\epsilon}{\omega^2}}} \left[ e^{+ \frac{\sqrt{1 + \frac{4\Gamma\epsilon}{\omega^2}} - 1}{2} \frac{\omega y}{\epsilon}} \right] \left[ e^{- \frac{\sqrt{1 + \frac{4\Gamma\epsilon}{\omega^2}} - 1}{2} \frac{\omega y}{\epsilon}} \right] \quad (20)$$

which would give a shape of curve that confirms the increase of concentration distribution observed near to the top wall. The degree of curvature in the upper part will depend on the value of  $\Gamma$ .

Quantitative calculations cannot be made until something is known of the values to be given to  $\Gamma$ . Before this is possible more experimental work on the annular flow will be necessary.

Correlation of Theory and Experimental  
Results on Concentration Distribution.

With reference to the theoretical approach based on the analogy between the present problem and the flow of fluidized suspensions, the concentration distribution is shown to be of the form

$$C = C_0 e^{-Z \cos \theta} \quad (21)$$

$$\& Z = \frac{w}{\epsilon} r \\ \text{when } \epsilon \text{ is assumed constant.}$$

Plotting the concentration distribution obtained from experiments, on a log-log scale, the graphs indicate that a general equation which has been used previously with a two-dimensional rectangular channel, with variable  $\epsilon$ , could be applied satisfactorily.

This equation becomes

$$C = C_0 \left( \frac{r_0}{r_0 - r \cos \theta} \right)^{\frac{w}{\beta K u_f}} \quad (22)$$

The determination of the value of  $C$  in the above equation at any radius  $r$  depends on the evaluation of  $w$ ,  $\beta$ ,  $K$ ,  $u_f$  and  $C_0$ .

A general discussion of the evaluation of these individual factors follows.

(A) Fall or Terminal Velocity  $w$ .

The value of  $w$  is mainly a function of the drop size.

Drop Size It was found unpractical to measure the average size of the water drops in two-phase flow. Flash photographs of the issuing flow from the outlet of the pipe, Fig. 14, were magnified under a powerful microscope but they yielded no results due to the fineness of

the drop and the grain size of the photographic plate. Thus recourse to previous work was necessary for prediction of the drop size.

Numerous authors have studied the breakup of freely falling droplets in gases. Hinze(28) and Lane(39) found that the maximum stable drop diameter could be estimated in terms of a critical Weber number.

$$We_c = \frac{\rho_g v^2 D_d}{g \sigma}$$

The mechanism suggested previously for dispersion, namely the break off from the surface, indicates that the Weber-number concept should apply with  $D_d$  taken as the amplitude of the wave and  $v$  as a function of the average velocity in the pipe. Turbulence in the air stream may influence the breakup of the particles.

The distribution of drop sizes in spray devices was given by the correlation mentioned by Hughes and Evans(30)

$$\frac{dv'}{dy} = \frac{\delta}{\sqrt{\pi}} e^{-\delta^2 y^2}$$

where

$$y = \log \frac{aD}{D_m - D}$$

and

$$a, \delta = \text{const.}$$

In a circular pipe the range of  $a$  and  $\delta$  will be considerably narrower than in sprays and it is suggested that in our case the drop size might reasonably be considered uniform.

Nakayama and Tanasawa(48) studied the breakup of drops in venturi throats, a problem related in some measure to our gas-liquid system.

CONCENTRATION DISTRIBUTION

log - log plot

VERTICAL TRAVERSE

TAP WATER  
 $\frac{1}{2}$ " Glass Pipe  
 Air Flow 1b/lb-sec  
 Water Flow 1b/lb-sec

o	10.73	17.1
x	10.90	25.7
+	10.62	11.3

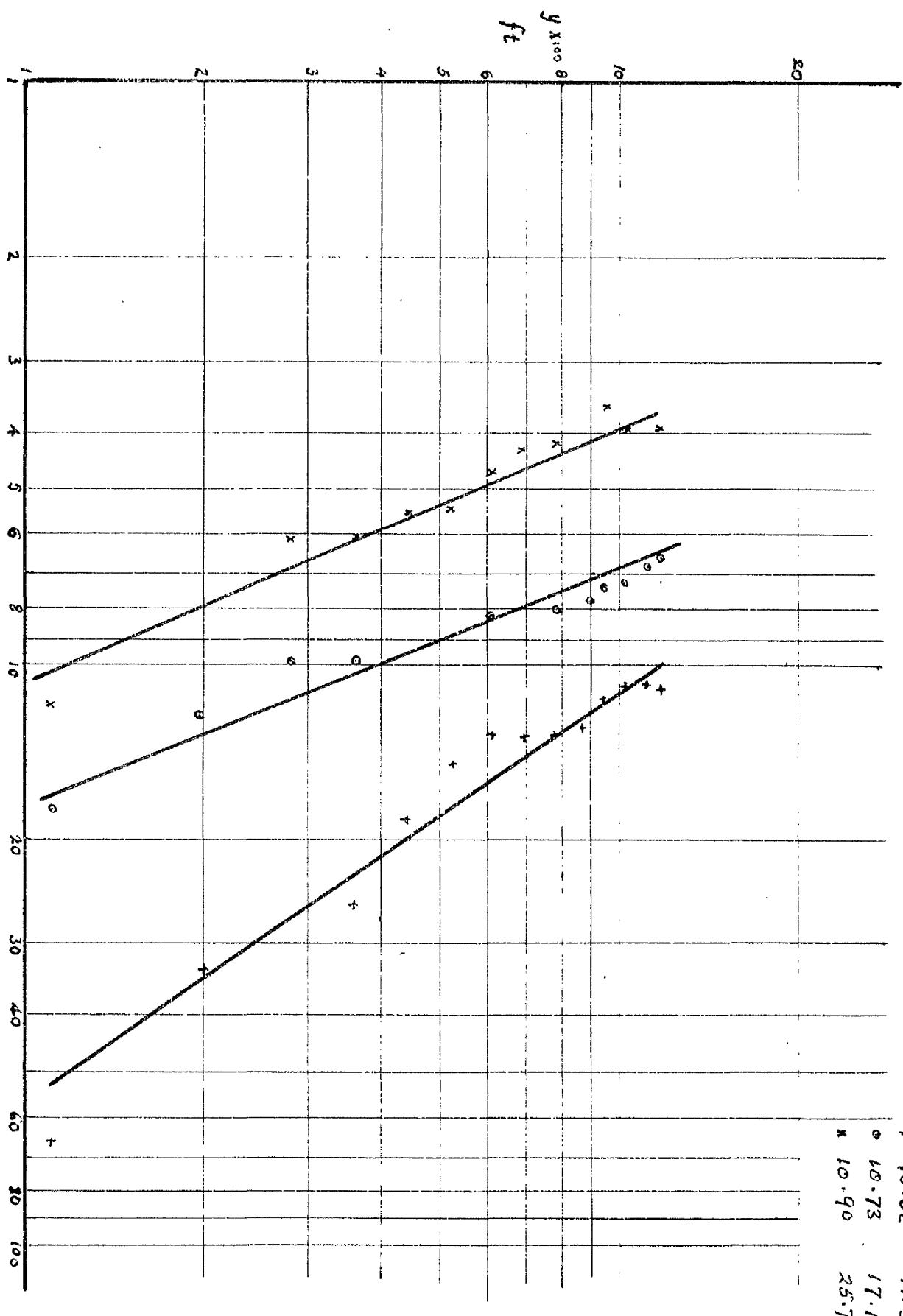


Fig. 36

$Z \times 10$

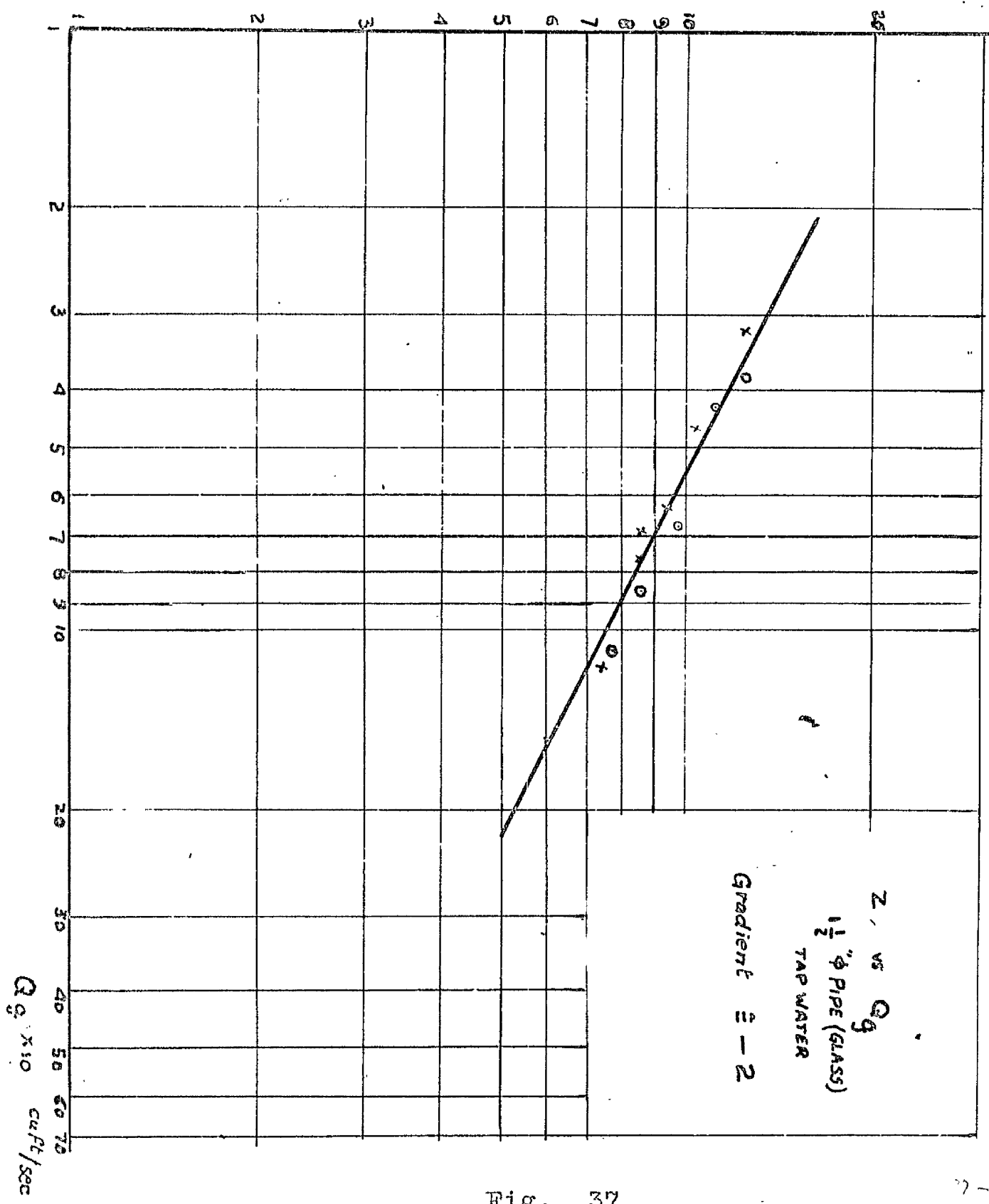


Fig. 37

Their empirical equation

$$D_d = \frac{585 \sqrt{\sigma}}{v_g \sqrt{\rho}} + 597 \left( \frac{\mu}{\sigma \rho} \right)^{0.45} \left[ 1000 \left( \frac{Q_g}{Q_\ell} \right) \right]^{1.5} \quad (23)$$

was a correlation of a large number of results and although dimensionally inconsistent it proved to be satisfactory according to Lewis *et al.* (41),

where  $D_d$  = average drop size in microns.

$\sigma$  = liquid surface tension in dynes/cm.

$\rho$  = liquid density gm/cc.

$\mu$  = liquid viscosity poises.

$v_g$  = relative velocity in the duct m/sec.

$Q_\ell$  = volume flow of the liquid.

$Q_g$  = volume flow of the gas.

This equation was valid for liquids of density range of 0.7 ~ 1.2 gm/cc., surface tension 19 ~ 73 dynes/cm. and viscosity of 0.003 ~ 0.50 poises.

To check the applicability of equation 23, the values of  $Z$  were obtained from the gradients of log-log plots given in Fig. 36. The value of  $Z$  varies little from minimum to maximum water flow for a fixed air flow.

This confirms the experimental finding that the shape of the concentration curves does not change radically over the main range of experiments, a fact that can be attributed to drop size.

When the values of  $Z$  are plotted against air flow on a log-log scale as shown in Fig. 37, a straight line relationship is obtained with a gradient of -2, i.e.,

In the expression  $Z = \frac{w}{\beta K u_f}$  considering that  $\beta$ ,  $K$  are constants and,

$$u_f \propto u_g \sqrt{\frac{f}{2}} \propto u_g$$

$$\text{or } w \propto \frac{1}{u_g}$$

it might be concluded that the first term of equation 23, viz.,  $\frac{585 \sqrt{\sigma}}{v_a \sqrt{\rho}}$  may be assumed valid in our case.

Modification of the second term is based on :

- (i) the fact that all of the water  $Q_f$  is not carried as a spray, and
- (ii) on the fact that  $Z$  varies only slightly for constant air and variable water flows.
- (iii) treating  $(\frac{Q_f}{Q_g})$  as one term, which should be kept intact, to indicate the ratio between the flow rates of the two phases.

By this tentative method of modification and by fixing the appropriate constants by trial, the modified drop size equation would read

$$D_d = \frac{585 \sqrt{\sigma}}{v_g \sqrt{\rho}} + 840 \left( \frac{\mu}{\sqrt{\sigma \rho}} \right)^{0.45} \left( 1000 \frac{Q_f}{Q_g} \right)^{0.5} \quad (24)$$

Fall velocity of Water Drops in Air:

For drop size less than 100 microns, Stokes' formula should hold

$$\omega = \frac{g}{16} \cdot \frac{\rho_p}{\rho_g} \cdot \frac{D_d^2}{v_g}$$

for air as the continuous medium and water as the entrained liquid, it can be written that

$$\omega = 102 D_d^2$$

Experimental values given by Richardson (55) confirmed the failure of Stokes' formula for droplets in excess of 100 microns.

For the drop sizes evaluated from equation 24, that lie in the range of 100-1000 microns, Newtonian forces would appear, and Prandtl (52), suggested that terminal velocity could be expressed by

$$\omega = 13.2 D_d \quad (25)$$

(B) Values of  $\beta = \frac{\rho_s}{\rho_m}$ .

Ismail(31) in his work on suspended solids in water streams gave  $\beta$  as 1.6 for small particles (0.1 mm.) and 1.3 for 0.16 mm. particles. Values given by Sherwood and Woerts(59), and by Corcoran confirmed that  $\beta > 1$ . Garsbans(31), as well as Laursen and Lin(31) suggested that

$$0 < \beta < 1.0 \quad \text{if} \quad \frac{\rho_s}{\rho_m} > 1$$

when  $\frac{\rho_s}{\rho_m}$  is the density of suspended particles to that of the continuous phase.

Because of the uncertainty of the value of  $\beta$ , it appears to be reasonable to take  $\beta = 1$ , as originally introduced by Von Kerman (64) for heat and mass transfer.

(C) Value of Universal Constant K

Von Karman's universal  $K$  was found theoretically to be 0.4 which was in very good agreement with the results of Nickuradse(47) and others.

In the case of two-phase flow, however, the value of  $K$  was indicated by Ismail(31) to vary substantially due to the presence of solids in the water stream. In a discussion of that paper, Lin(31) pointed out the scatter in Ismail(31) results and disputed his conclusions on the grounds that  $K$  is a factor which cannot define clearly turbulent flow. Indeed, this major point requires further study.

For the present work  $K$  will be accepted as 0.4.

So the general equation used for correlation would become

$$C = C_0 \left( \frac{r_o}{r_o - r \cos \theta} \right)^{\frac{0.4 U_f}{U}} \quad (26)$$

(D) Value of Friction Velocity  $U_f$ 

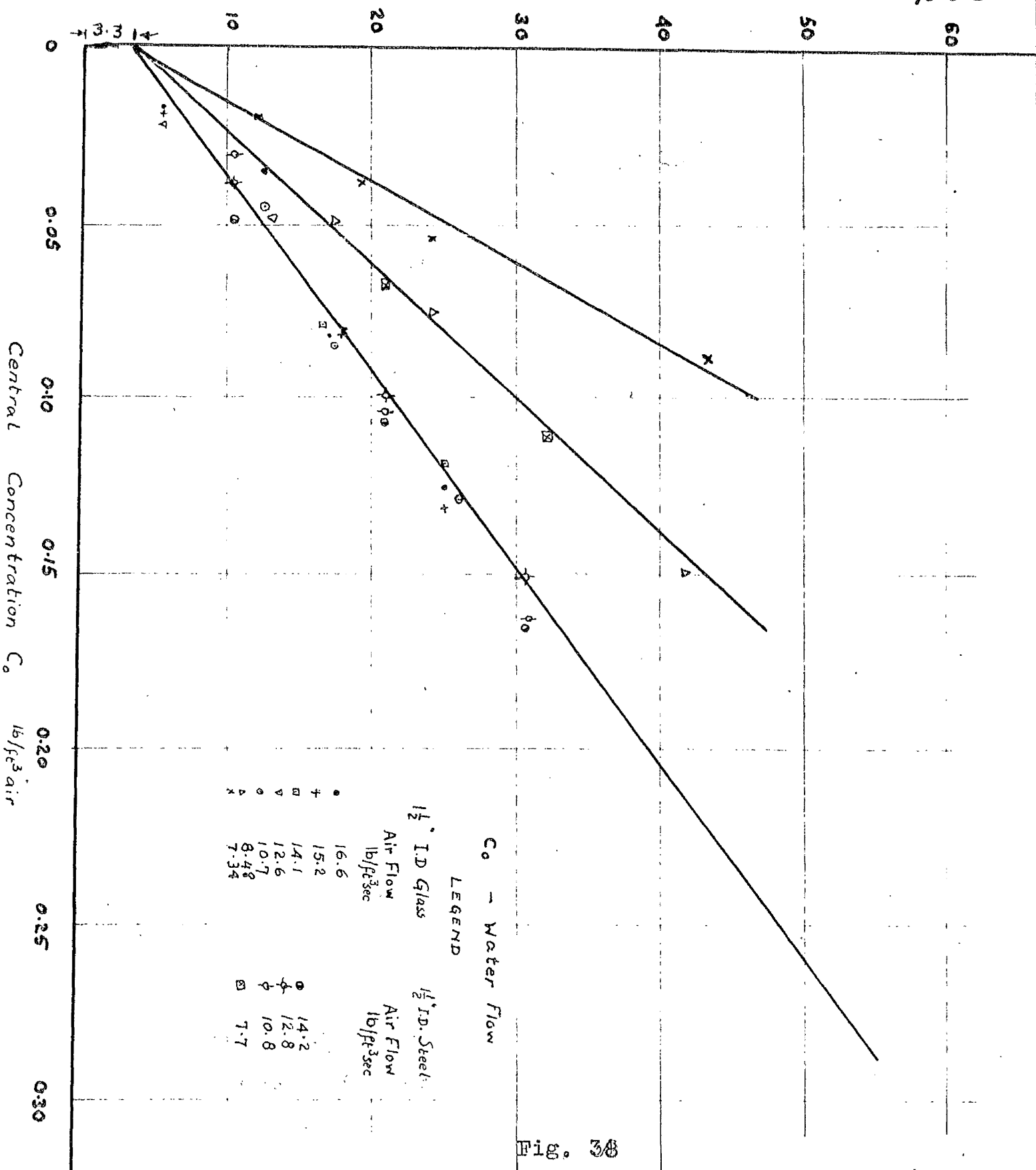
By definition the mean value of friction velocity

$$U_f = \sqrt{\frac{\tau_0}{\rho_m}}$$

The factors affecting the evaluation of  $U_f$  is wall shear stress  $\tau_0$ , and mean density  $\rho_m$ .

The actual shear stress distribution has to be predicted before  $U_f$  can be calculated, which adds to the complexity of the problem. Accepting the concept of straight line shear stress distribution, and, in this case, the idea that zero shear takes place at  $\frac{du}{dy} = 0$  (the discussion of this point is analysed in Chapter VI), would make it possible to predict the concentration distribution and hence the entrained liquid.

WATER FLOW  $\text{lb}/\text{ft}^2 \text{sec.}$



Following the lines given by Imaill, which seem reasonably applicable to the present case, the tube would be divided into two parts which could be treated separately.

$$\left. \begin{aligned} U_{ft} &= \bar{U}_f \sqrt{1 - \frac{y_m}{y_b}} \quad \sqrt{\frac{P_{av}}{P_t}} \\ U_{fb} &= \bar{U}_f \sqrt{\frac{z y_m}{y_{bb}}} \quad \sqrt{\frac{P_{av}}{P_b}} \end{aligned} \right\} \quad (27)$$

and giving a definition to  $U_f = U \sqrt{\frac{f}{2}}$  where the value of  $f$  is discussed later in Chapter VII. For theoretical prediction, however, it is considered ample to use the value of  $U_f$  for top and bottom parts without introducing serious error.

#### (E) The Value of Concentration at the Centre Co.

The concentration at the centre  $C_0$  is taken as a criterion for the rate of entrainment in the gas stream. Examining  $C_0$  values from experimental results it is noted that:

(a) for each air flow the value of central concentration  $C_0$  decreases or increases proportionally with water flow.

(b) Above a certain air flow rate, the value of  $C_0$  does not depend on the air flow, a characteristic noted previously in discussion of experimental results.

Plotting values of  $C_0$  against water flow rates yielded straight line relationship as shown in Fig.38. They intersect the  $W_w$  ordinate at a fixed value of 3.4 lb/ft.<sup>2</sup> sec. This value shows a remarkable agreement with Armand's results. The main criterion for this amount of water left on the wall is the thickness of the laminar

sub-layer. This is discussed fully later and it indicates a possible method of estimating directly the water entrained in the gas stream at high air rate.

For  $1\frac{1}{2}$ " I.D. and 2" I.D. pipes the same characteristics were noted but scatter in the case of 1" pipe was larger. Since prediction by the suggested formulae is only applicable to large pipes, the values corresponding to 1" I.D. were not included in Fig. 38.

From consideration of graphs,  $C_o$  can be deduced approximately to be given by

$$C_o = \frac{W_w - 3.4}{173} \left[ 2 - \frac{W_a'}{W_a} \right]^n \quad (28)$$

where  $W_w$  is the water mass flow velocity in  $\text{lb./ft.}^2 \text{ sec.}$

$W_a$  is air mass flow velocity in  $\text{lb./ft.}^2 \text{ sec.}$

$W_a'$  is a fixed value for air flow at which  $C_o$  does not change, apparently from our results it is  $10.7 \text{ lb./ft.}^2 \text{ sec.}$

The value of  $n$  is found from the plotted results to be approximately 4 which confirms that the non-dimensional groups having most influence on entrainment are:

Weber No. and Froude No.

This criterion was used by Boulter and others (12) for expressing commencement of wave formation.

So, putting equation 28 as  $C_o = K V^2$  and equating to the product of Weber and Froude numbers,

$$k u^n \propto \frac{f d u^2}{g \sigma} \times \frac{u^2}{g d}$$

we get

$$n = 4$$

and thus equation (28) would be

$$C_o = \frac{W_w - 3.4}{173} \left[ 2 - \frac{W_a'}{W_a} \right]^4 \quad (29)$$

This empirical formula, although dimensionally inconsistent, agrees with the range of results covered and it may be conservatively assumed that it would hold, with different values of constants, for all pipe sizes and allow the prediction of  $C_o$ .

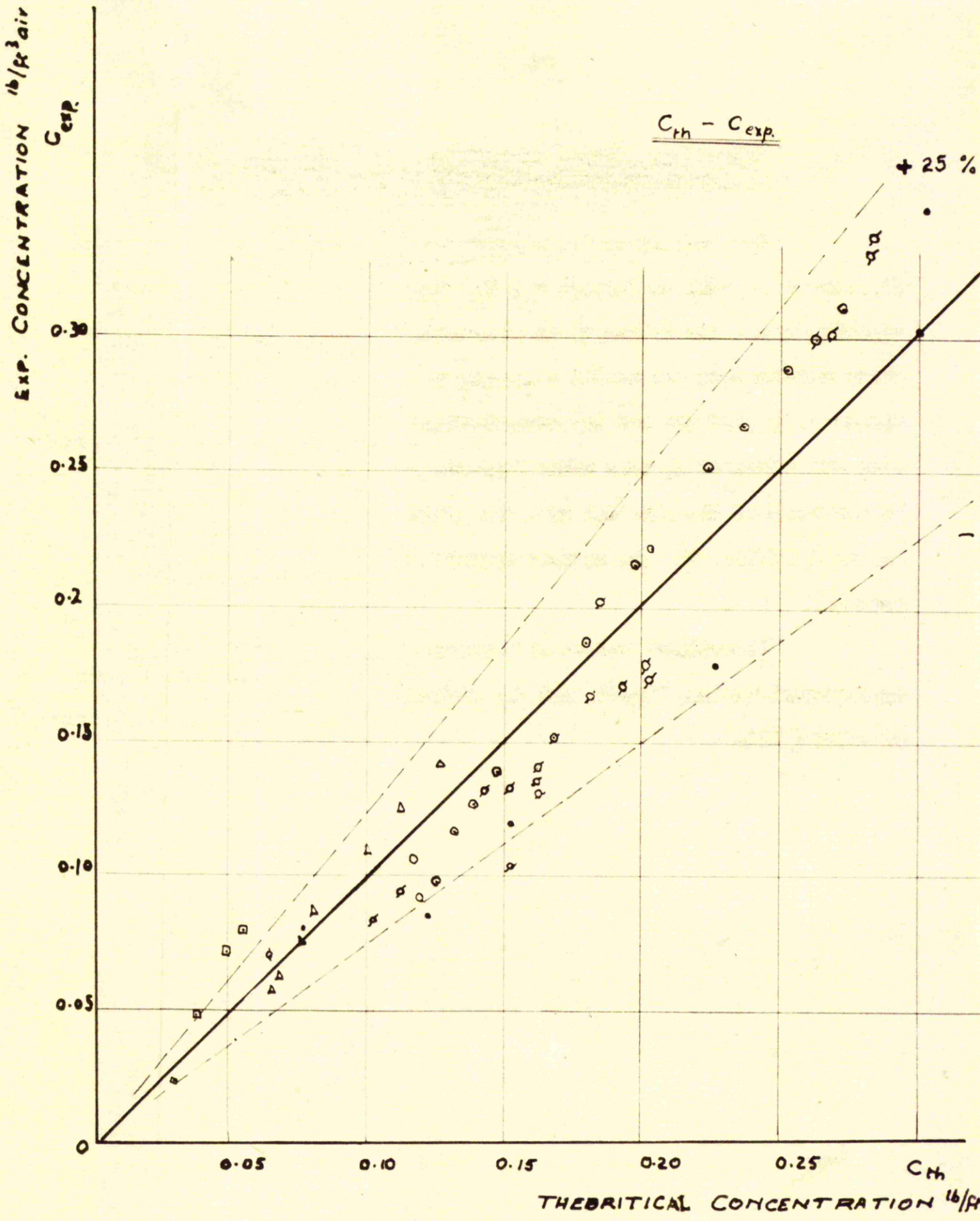


Fig. 39

Comparison between Theoretical and Experimental Values  
of Concentration Distribution in Two-phase Flow.

The results of the application of theory can be seen from Figs.16-19, as well as Figs.21 and 22, with the theoretical values superimposed. The values of  $C_0$  were taken from graph 38, and all the other factors were calculated according to the formulae given. The agreement is good for the exponential distribution. It should be noted that the values of  $U_F$  were taken from the equation 27, for top and bottom parts of the pipe but when the prediction of distribution is needed the value  $\bar{U}_F$  can be used without appreciably affecting the results.

Theoretical values of concentration were plotted against experimental values, Fig.39, and the deviation, as could be seen, never exceeded  $\pm 25\%$ .

WATER NOT ENTRAINED

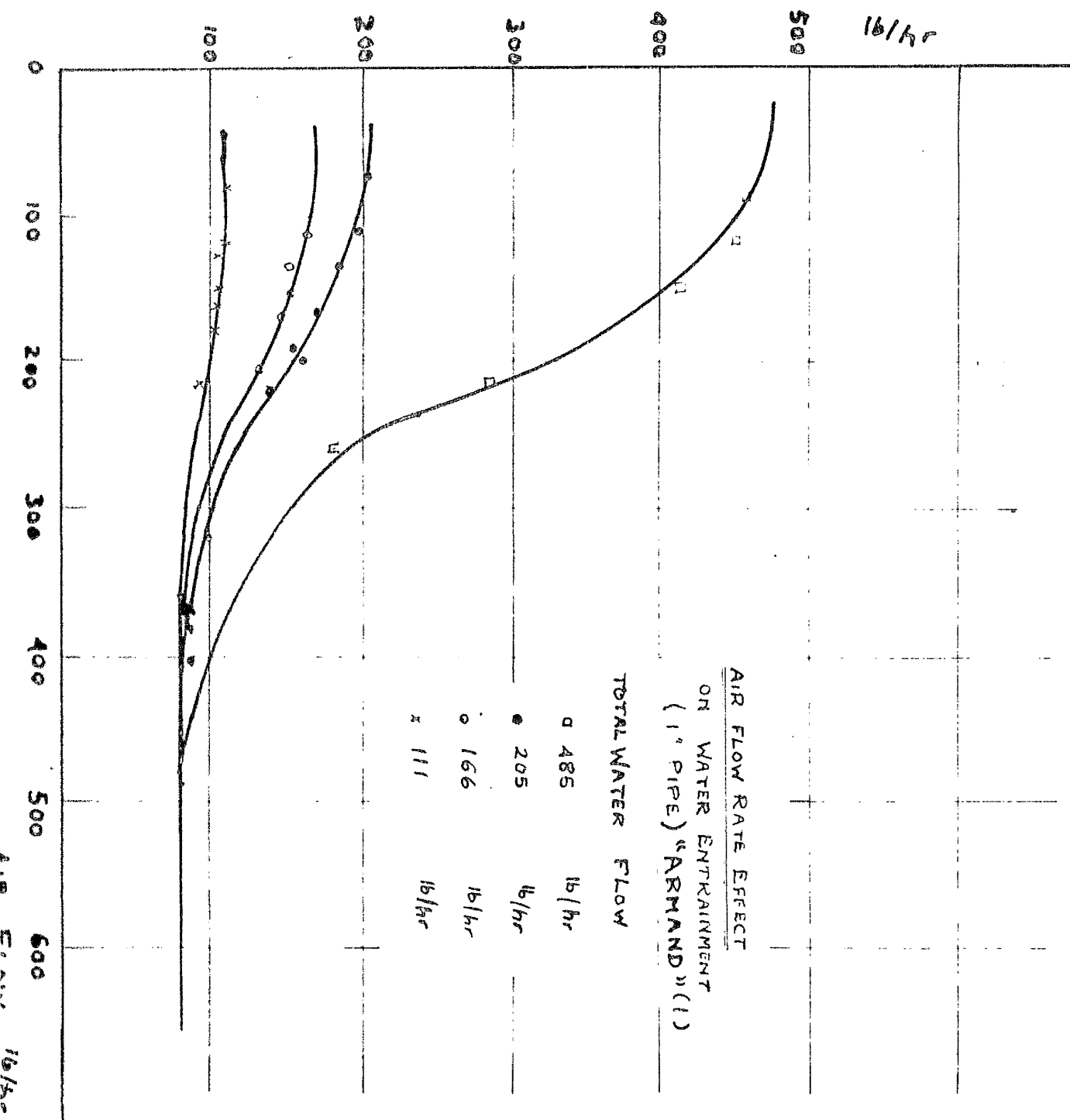


Fig. 40

Thickness of Laminar Sublayer and its relation to the Distribution of Phases.

As has been noted from Figs. 38, 40, there is a certain limiting flow where entrainment is zero, even at high air flow rates. This occurs when the thickness of the water film on the walls is reduced to the dimension of the laminar sublayer.

A careful consideration of how entrainment of liquid in the gas stream is due to the turbulence forces, indicates that this layer would not be affected by the turbulent mechanism.

Examining the laminar layer equations as given by Bakhmetoff(5), the boundary layer thickness is

$$t = N \frac{U_f}{U_f}$$

The velocity distribution in the sublayer can be taken as linear, i.e.,

$$U_w = N U_f$$

$U_w$  velocity at the boundary between the water and the air.

$$\begin{aligned} \text{Mass flow in this layer} &= \pi D \cdot t \cdot \frac{U_w}{2} \rho \\ &= \pi D \cdot N \frac{U_f}{U_f} \cdot \frac{N}{2} \cdot U_f \cdot \rho \\ &= \frac{1}{2} \pi D \rho N^2 U_f \\ &= \text{Const.} \quad (30) \end{aligned}$$

This confirms the fact that this layer will always exist independent of air or water flow rates (in the high range of air flow).

Calculated values of this constant for the pipes tested are given in Appendix IIIB. These show good agreement with the experimental results. This method renders it possible to obtain the amount of vapor entrained directly.

### Conclusions

1. The correlation between the experimental and theoretical results is satisfactory for the conditions of exponential distribution of phases, i.e., in the case of large pipe diameters. Hence, from this distribution the amount of entrained liquid can be calculated.
2. The values of concentration in symmetrically shaped graphs, which existed in the case of 1" I.D. pipe, were only given a mathematical explanation, but due to lack of evaluation of certain factors no calculations were made. These factors need further investigation.
3. At high air flow rates a method based on evaluation of laminar sublayer is used to calculate the amount of entrained liquid with reasonable results.

CHAPTER VI.  
VELOCITY DISTRIBUTION.

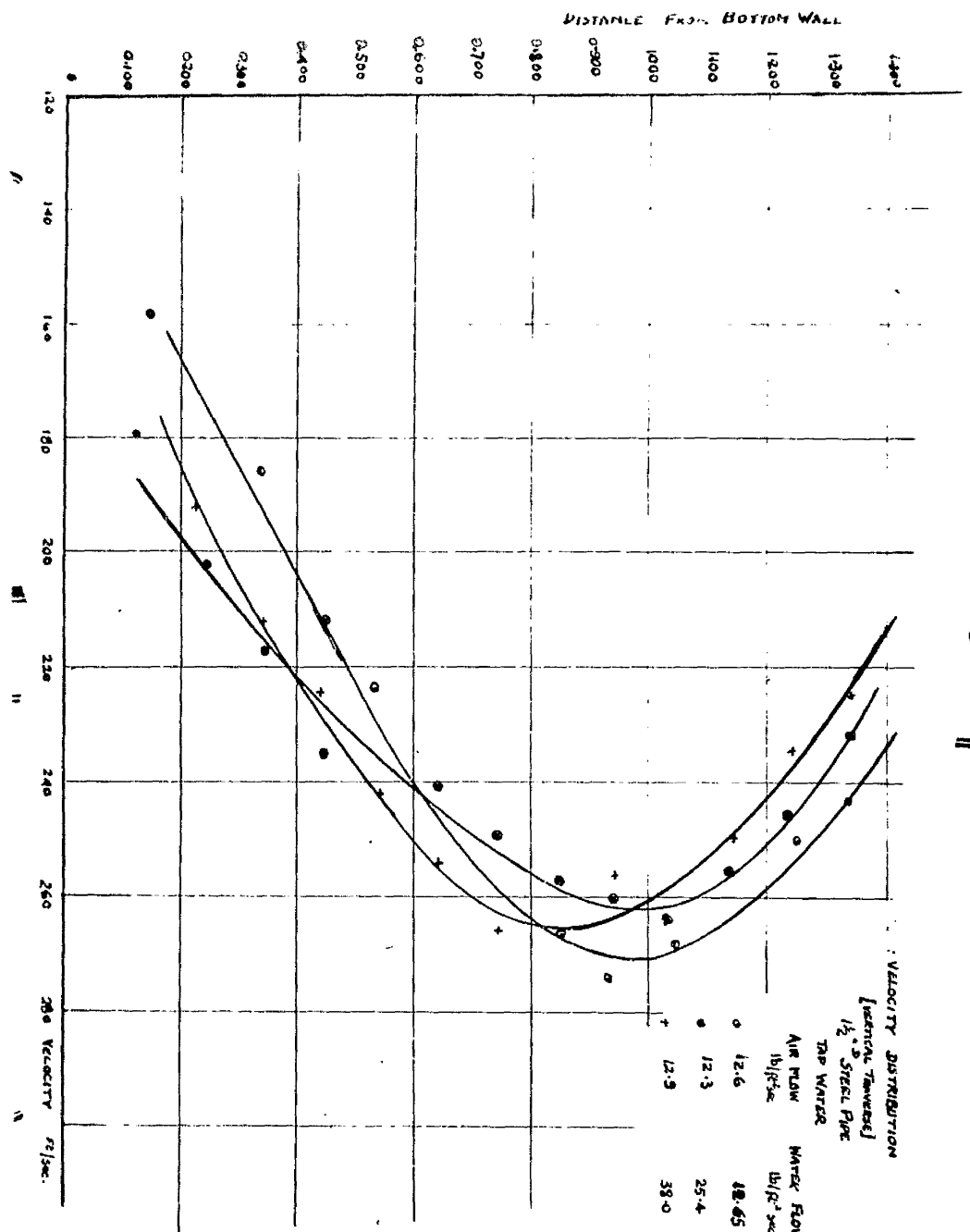


Fig. 41

VELOCITY PROFILES - CONSTANT AIR, VARIABLE WATER.

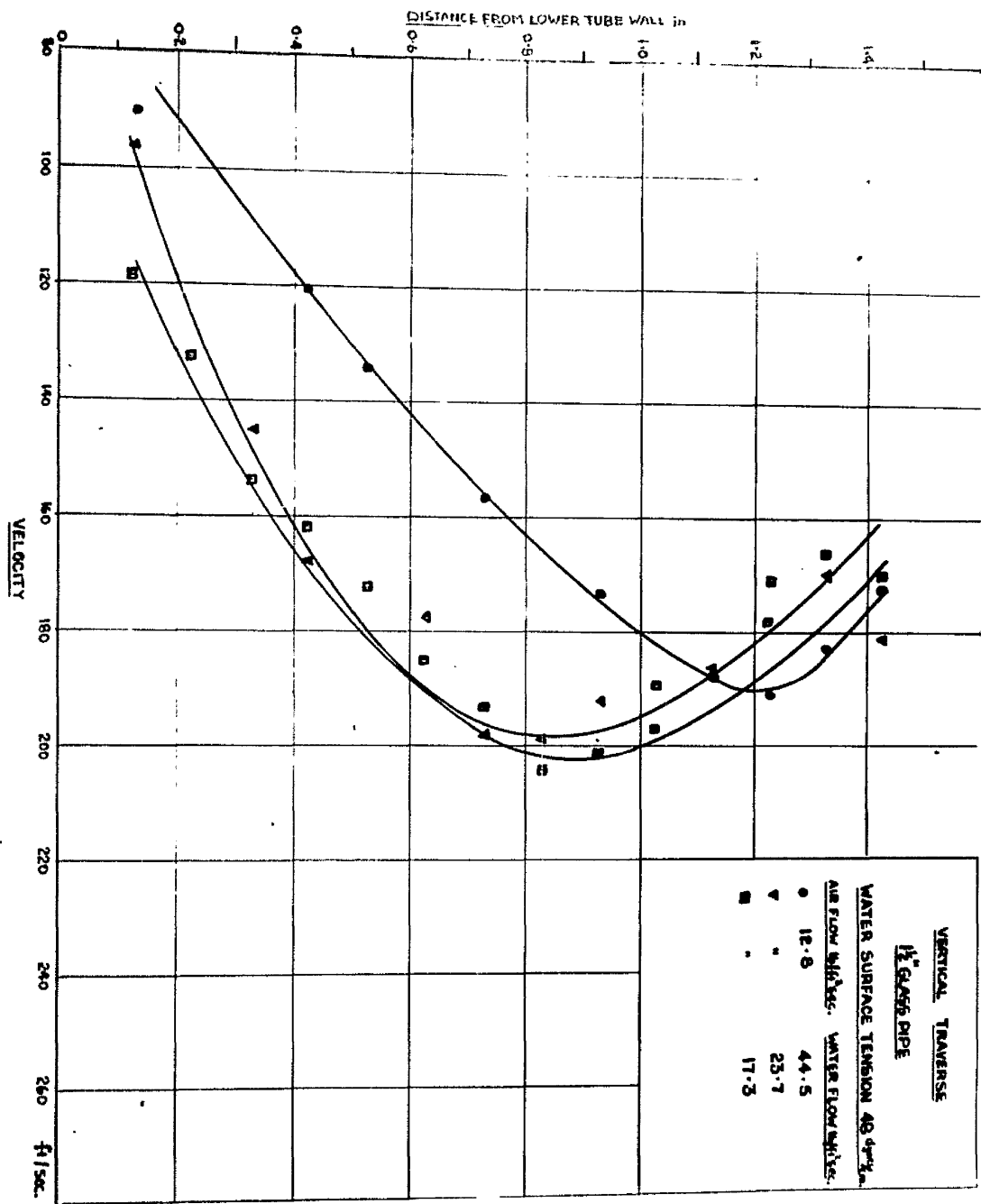


Fig. 42

### Velocity Distribution in Two-Phase Flow.

#### Introduction:

In Chapter III, the subject of relative velocities between the phases in two phase flow was discussed. Consideration of experimental findings and the results of calculations made to determine the relative velocity led to the conclusion that no great error was introduced by using the simple Pitot tube equation for estimating the mean velocity at the test point. Consequently the values of velocity plotted in the following figures have been obtained in this way.

#### Experimental Results.

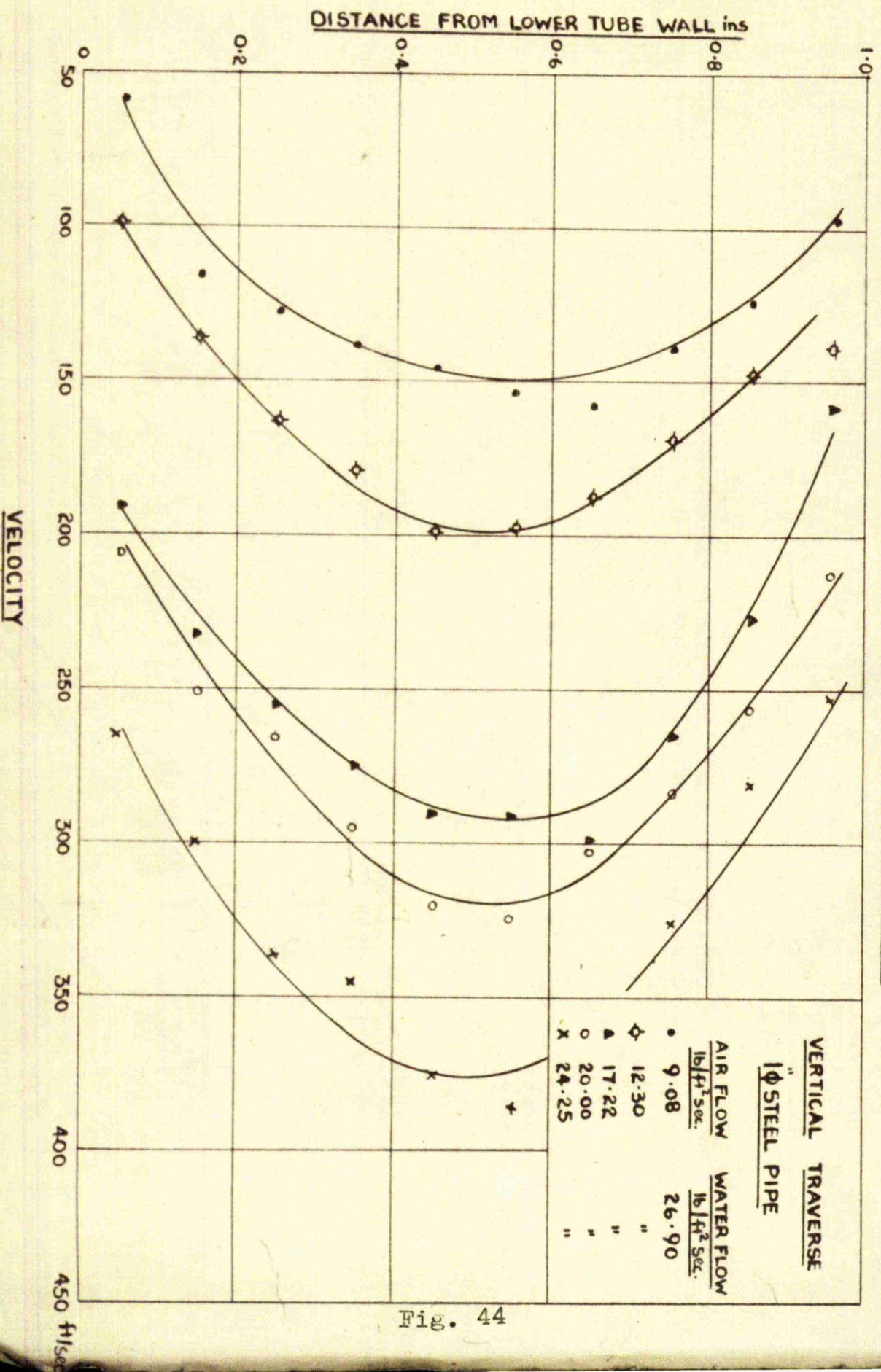
The velocity profiles for the air streams shown in Figs. 41 and 42, and Fig. 43, for  $1\frac{1}{2}$ " glass and  $2\frac{1}{2}$ " steel pipes respectively. Close to the water layer, results were rather erratic due to splashing from the break up of the waves there.

These profiles were plotted for constant air flow of 12.8 lb./ft.<sup>2</sup> sec. and variable water rates.

The points fall on reasonably uniform curves and the degree of scatter is surprisingly small which inspires confidence in the method of measurement.

Maximum velocity value does not vary very much but the point of maximum velocity, i.e.,  $\frac{dv}{dy} = 0$ , moved upwards as the water flow rate increased.

VELOCITY PROFILES - CONSTANT WATER, VARIABLE AIR



**VELOCITY PROFILES : CONSTANT WATER, VARIABLE AIR**

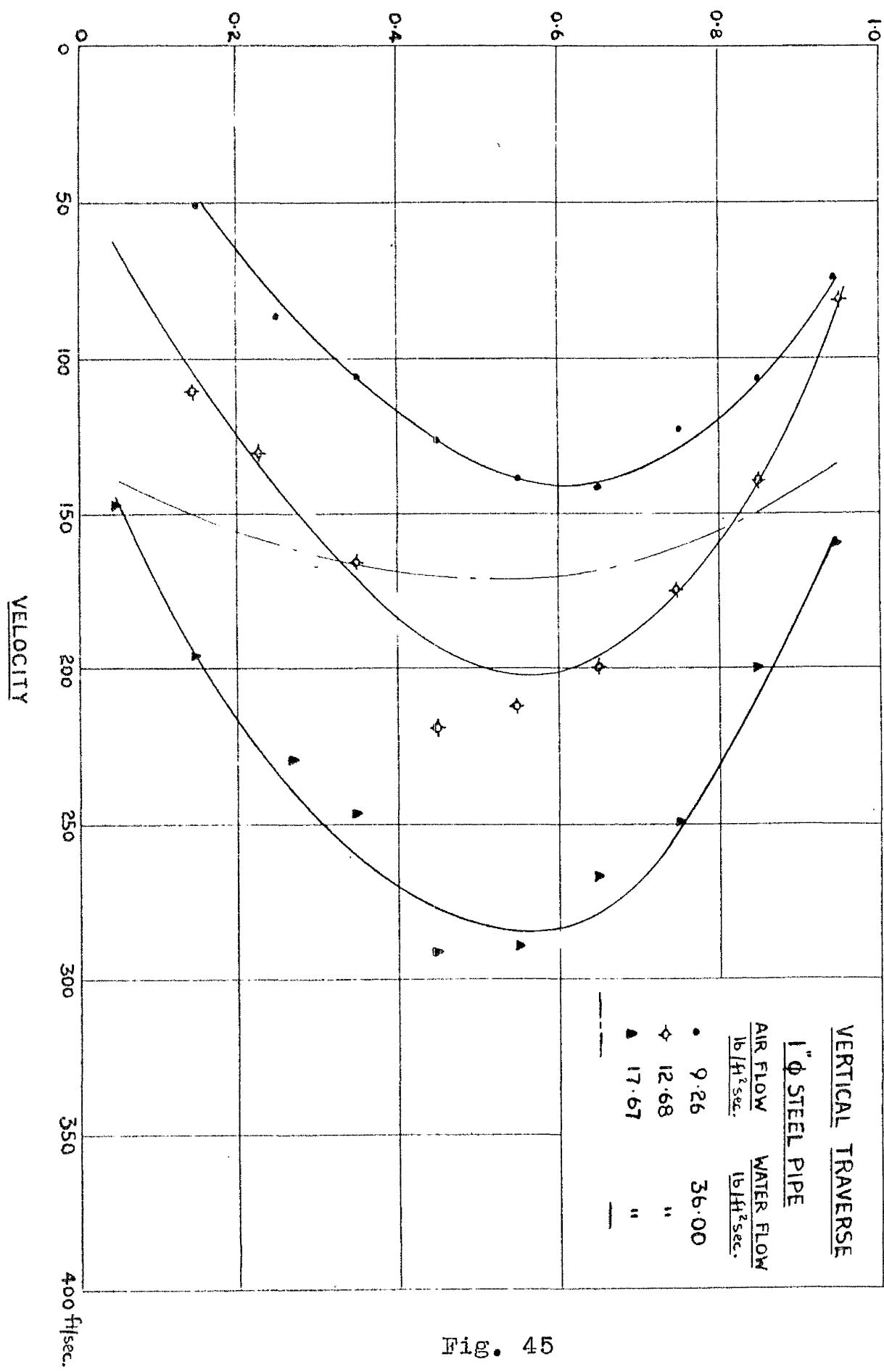
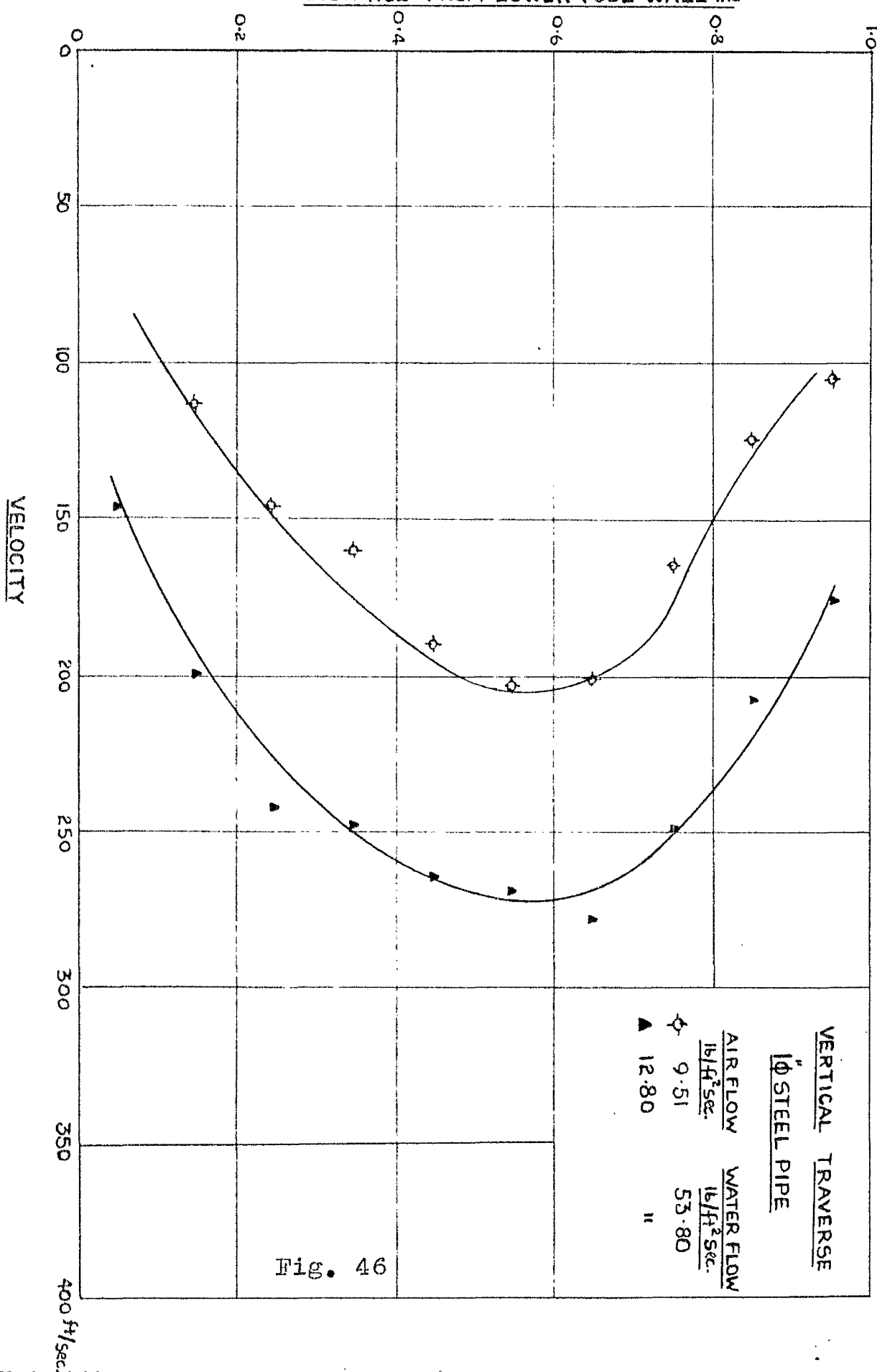


Fig. 45

VELOCITY PROFILES - CONSTANT WATER VARIABLE AIR



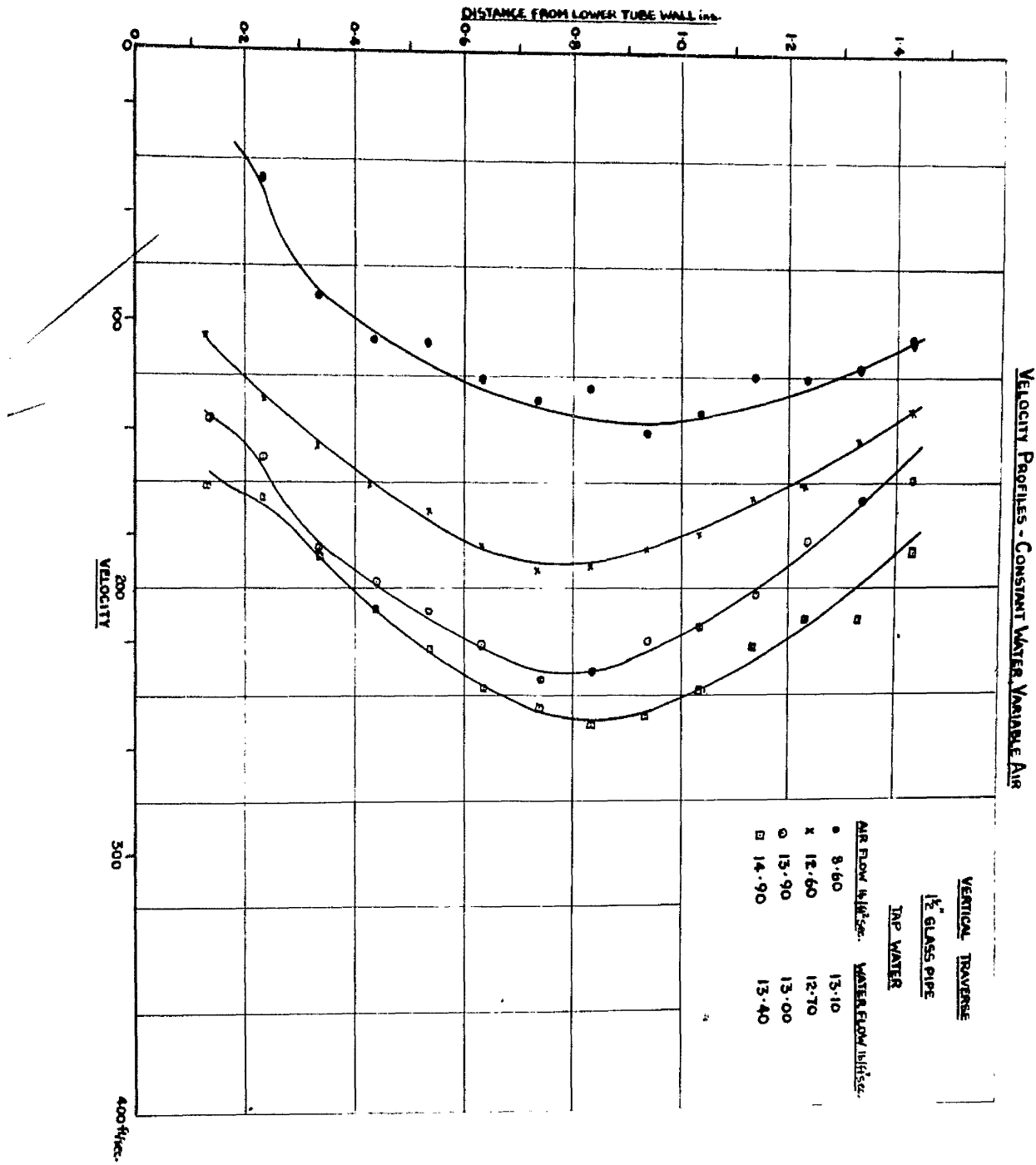


Fig. 47

**VELOCITY PROFILES - CONSTANT WATER, VARIABLE AIR**

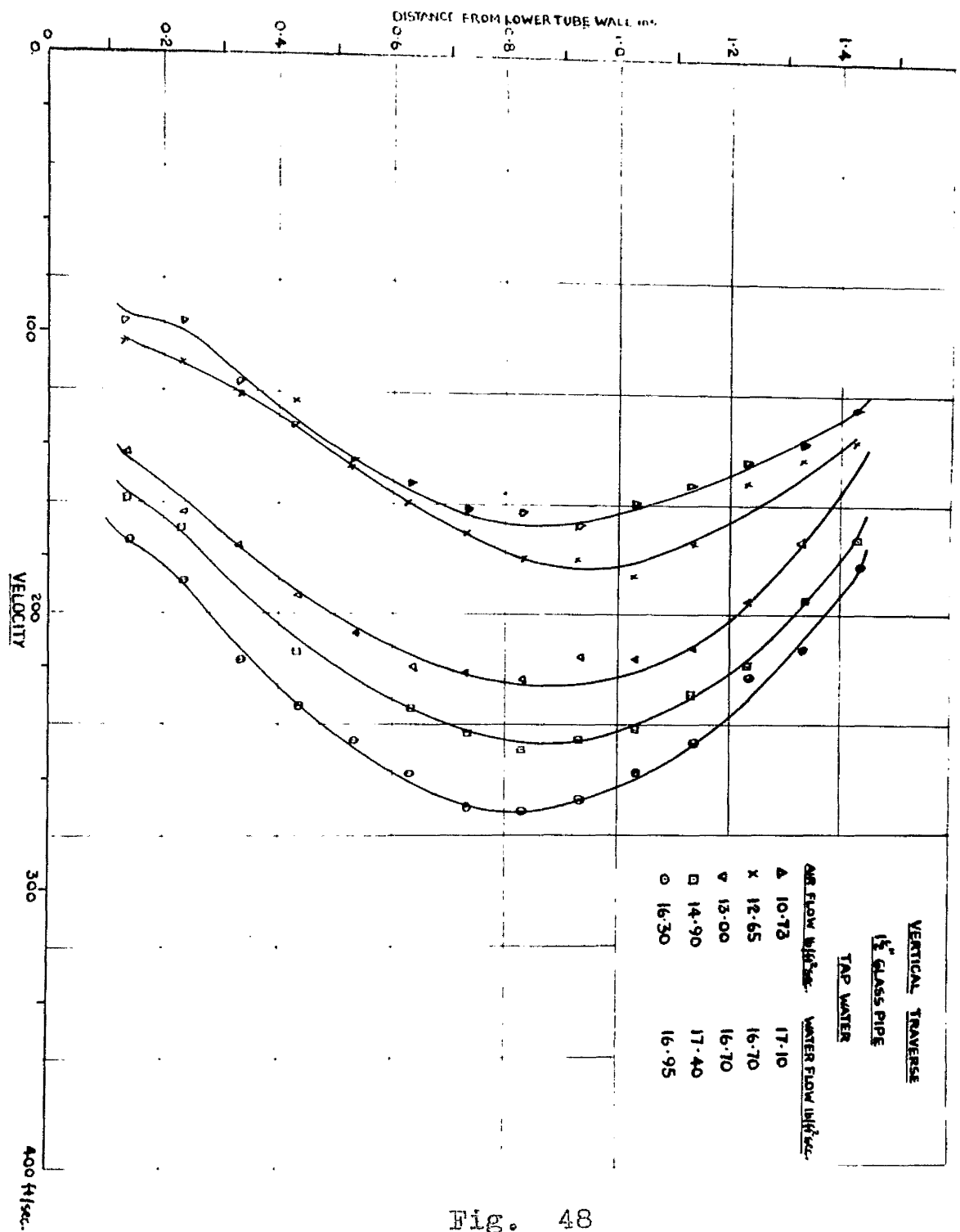
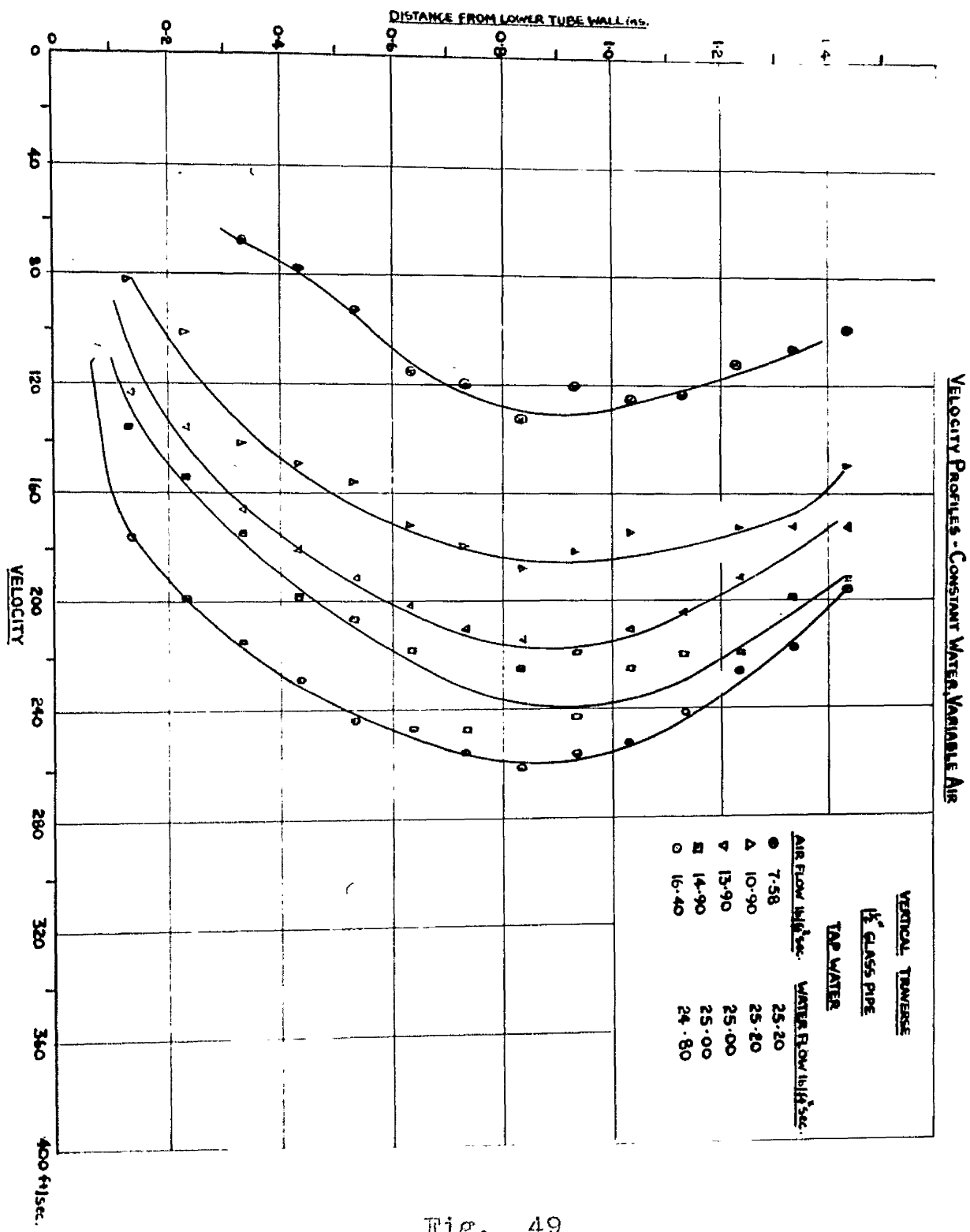
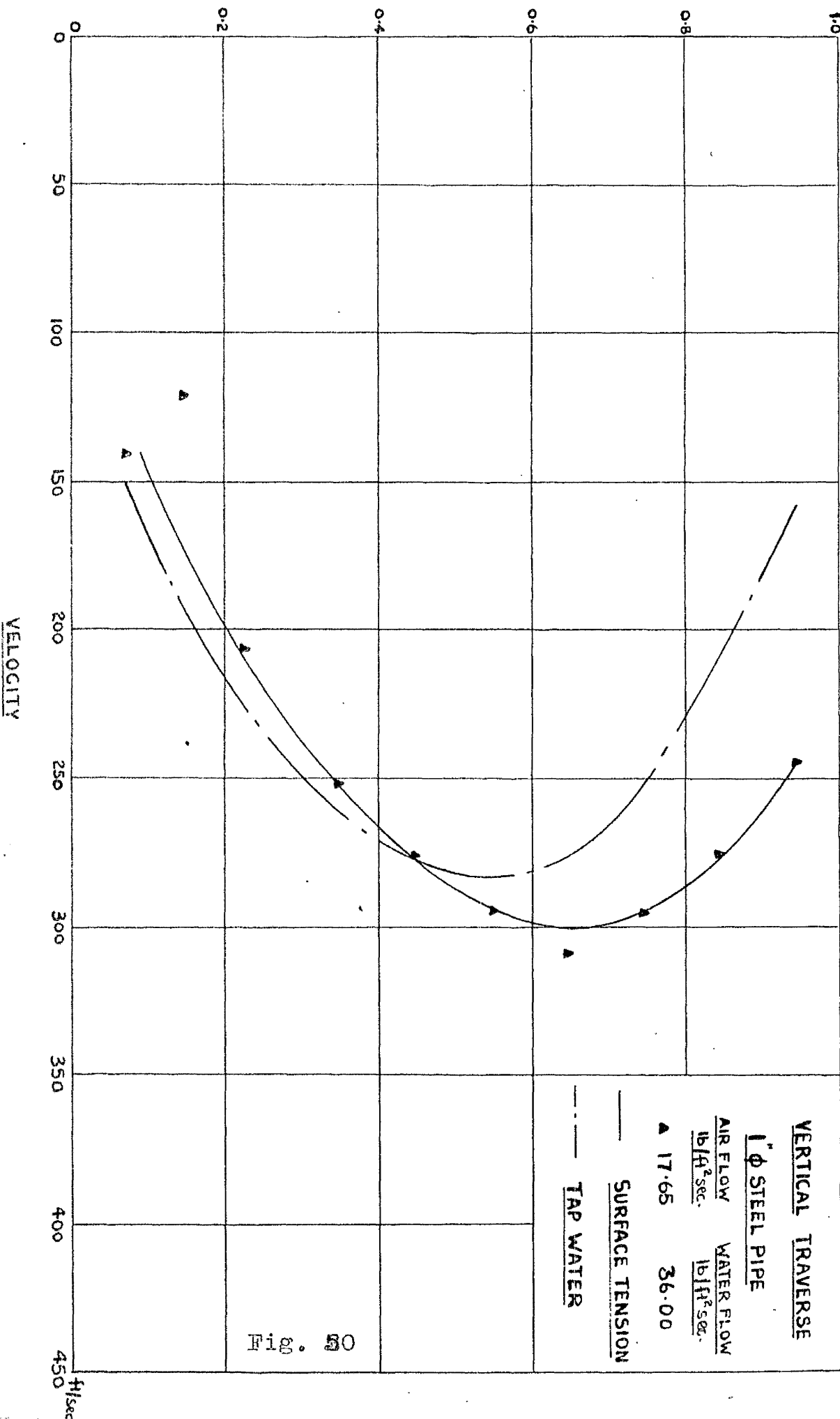


Fig. 48



VELOCITY PROFILES : TAP WATER & SURFACE TENSION



VELOCITY PROFILES : TAP WATER & SURFACE TENSION

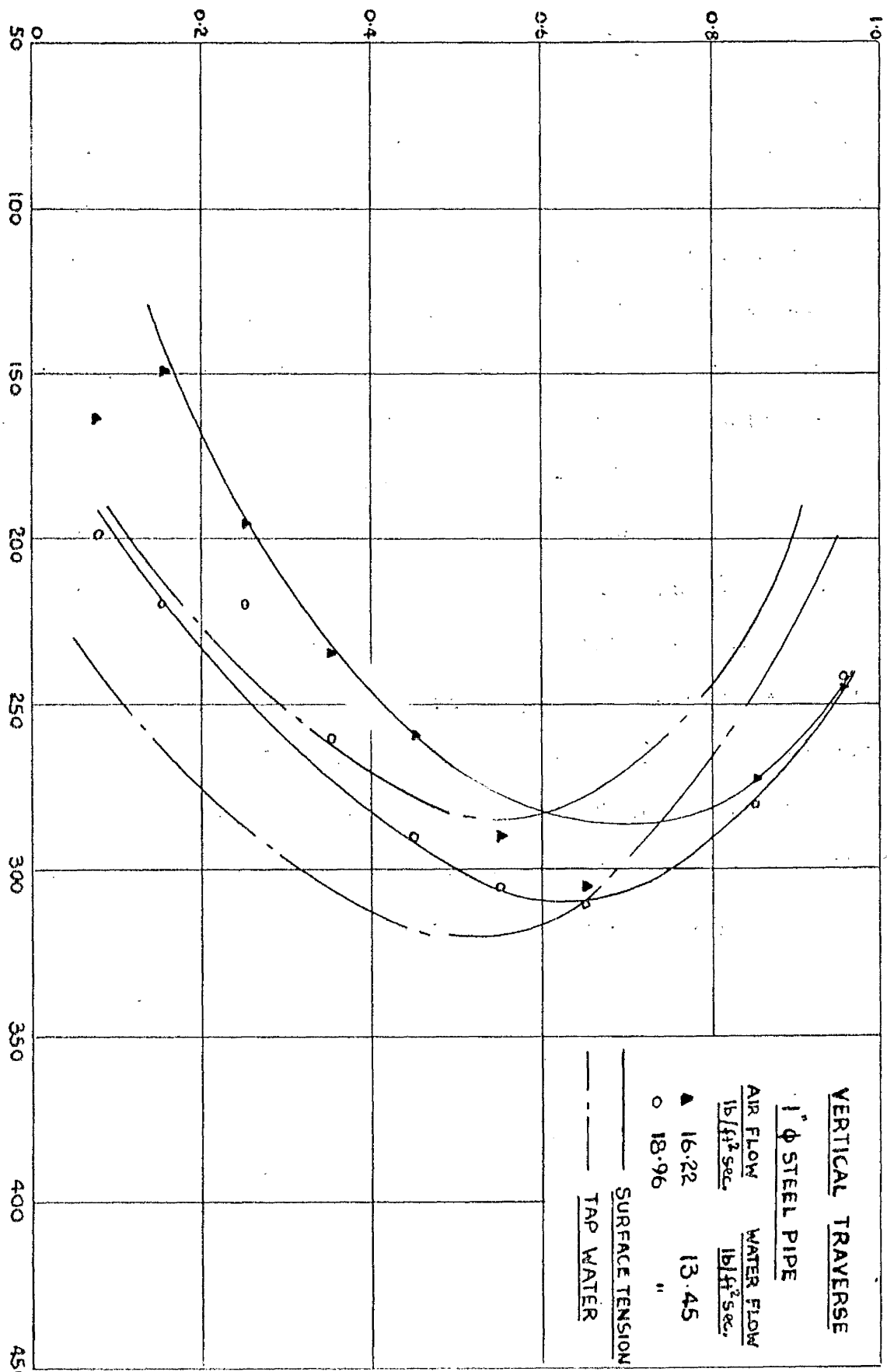


Fig. 51

450 ft/sec.

Figs. 44-46 show the velocity profiles for the 1" I.D. steel pipe for constant water variable air flow rates. Again little variation in the velocity profiles is apparent within the experimental range, while the point of maximum velocity is practically constant.

On some of these graphs the velocity profiles obtained when using air only at the same flow rate are superimposed and it is noteworthy that the difference between the two sets of curves.

The results with constant water and variable air flow rates are shown in Figs. 47, 48 and 49. These show a remarkable consistency and similarity. The maximum velocity changed according to the air flow but the point at which maximum velocity occurred remained almost unchanged; the characteristics persisted at all the different air flow rates used.

All the foregoing curves were plotted <sup>vertical</sup> for traverses.

For reduced surface tension the velocity distribution is shown in Figs. 50, 51, as compared with that obtained when tap water was used.

VELOCITY - LOG PLOT

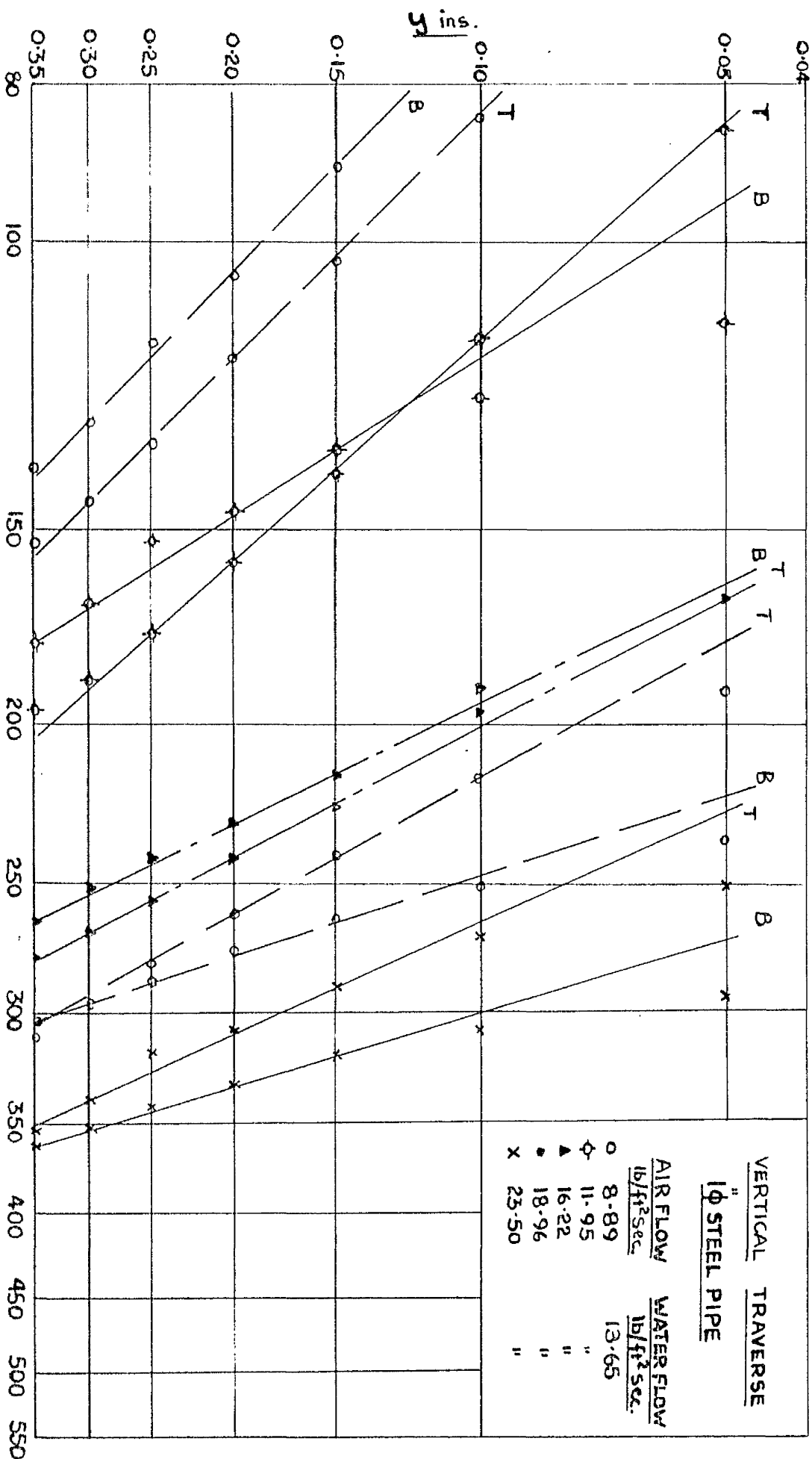
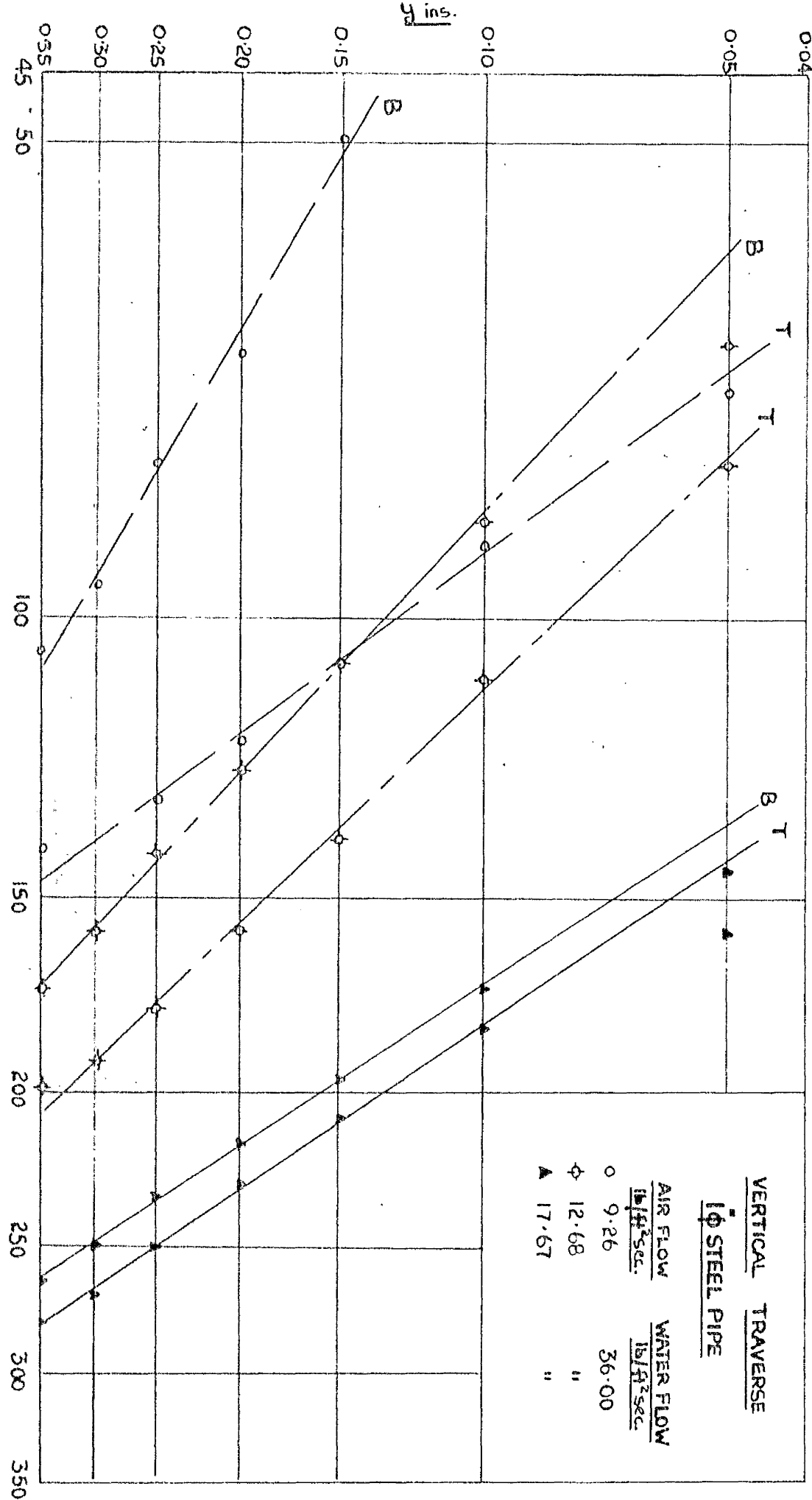


Fig. 52

VELOCITY - LOG PLOT



Discussion of Results.

The point of maximum velocity is shown to shift upwards as the water flow is increased in the case where exponential concentration distribution takes place.

It is interesting to note that when the surface tension was reduced the velocity profile varied from that of tap water. This could be explained by referring back to the concentration distribution which had undergone a definite change.

Correlation of Results.

Velocity values calculated were plotted against distance from the walls and they are somewhat similar to the limited number of curves given by Azmand(3). It ought to be noted that Azmand's results were based on mixture velocity in a horizontal section which is an indication of the velocity values.

The velocity values were plotted on log-log scale and show straight line relationships - Figs. 52 and 53. Thus a correlation of the form

$$v = A^* y^{\frac{1}{n}}$$

is applicable in such a case. This formula could be written as

$$v = A^* \left(\frac{\tau_0}{\rho} g\right)^{\frac{1}{n}} \left(\frac{y}{D}\right)^{\frac{1}{n}} \quad (31)$$

Values of  $n$  are given in Tables IV, IVa.

This is a satisfactory correlation for velocity distribution. Values of  $n$  varied appreciably for the top and bottom parts of the pipe. For example, in the case of  $1\frac{1}{2}$ " I.D. pipe, when the concentration distribution is definitely exponential, the value of  $n$  for the top half lies between 6 and 9, values that correspond to turbulent flow velocity distribution in single phase flow. For the bottom part of the velocity profiles  $n$  varied from 2.96 to 3.56 with different water flow rates. It is noteworthy that the small values of  $n$  are found where the maximum entrainment occurs.

In the case of nearly symmetrical concentration distribution, the values of  $n$  approach each other at the average of about 5.5.

Comparing these results with those of Nikuradse(47) where the friction criterion  $\frac{r_0}{k}$  varied, the minimum value of  $n$  was 4 for  $\frac{r_0}{k} = 10$ . The fact that in the present case, the values of  $n$  may go as low as 2, would indicate that capillary waves existing at the surface of the water layer have an important influence. Laird(38) has shown that for an air stream passing through a rubber tube whose surface moves sinusoidally, the friction losses are appreciably greater than with a stationary tube. No extension of this work has been done in the turbulent region, yet it might throw some light on the effect of the waves, which is due to irreversible exchange of energy.

In addition to the effect produced by the wave action there is also the fact that the values of  $n$  increase as the air flow rates increase. Associated with this is the evidence that concentration distribution suffers a radical change which may suggest a suppression of turbulence due to the presence of the liquid particles - a phenomenon observed by Prandtl(58) who compared this effect with the suppression of air gusts due to rain drops.

Mixing Length Calculations

By analogy to the kinetic theory of gases, Prandtl introduced the idea of mixing length to define turbulence momentum transfer due to crosscurrents between the layers. This has been mentioned before in Chapter V in the general discussion of turbulence.

$$\text{mixing length } \ell = \sqrt{\frac{T}{\rho}} \frac{du}{dy}$$

but  $T = T_0 \left( 1 - \frac{y}{r_0} \right)$

therefore,

$$\ell = \sqrt{\frac{T_0}{\rho_m}} \sqrt{1 - \frac{y}{r_0}} \frac{du}{dy} \quad (32)$$

due to the variation of  $\rho_m$  from top to bottom, we have to accept an average in the top and bottom parts of the pipe. This procedure has been adopted by H.A. Einstein(18) and others in connection with water channels.

Equation 32, gives zero mixing length at the pipe centre which contradicted the experimental results.

As mentioned in Chapter V page 58 the relation  $\ell = Ky$  was used satisfactorily to correlate the concentration distribution results. However, it was felt that a study of the actual values of  $\ell$  distribution calculated by the use of equation(32), would be of values.

To evaluate  $\frac{du}{dy}$  the method of difference was used.

MIXING LENGTH  
DISTRIBUTION  
 $1\frac{1}{2}$ " Steel Pipe  
Tap Water

Air Flow  
lb/ft<sup>2</sup> sec.

-□- 12.6  
-○- 12.3

$\frac{l}{d}$

0.20  
0.16  
0.12  
0.08  
0.04

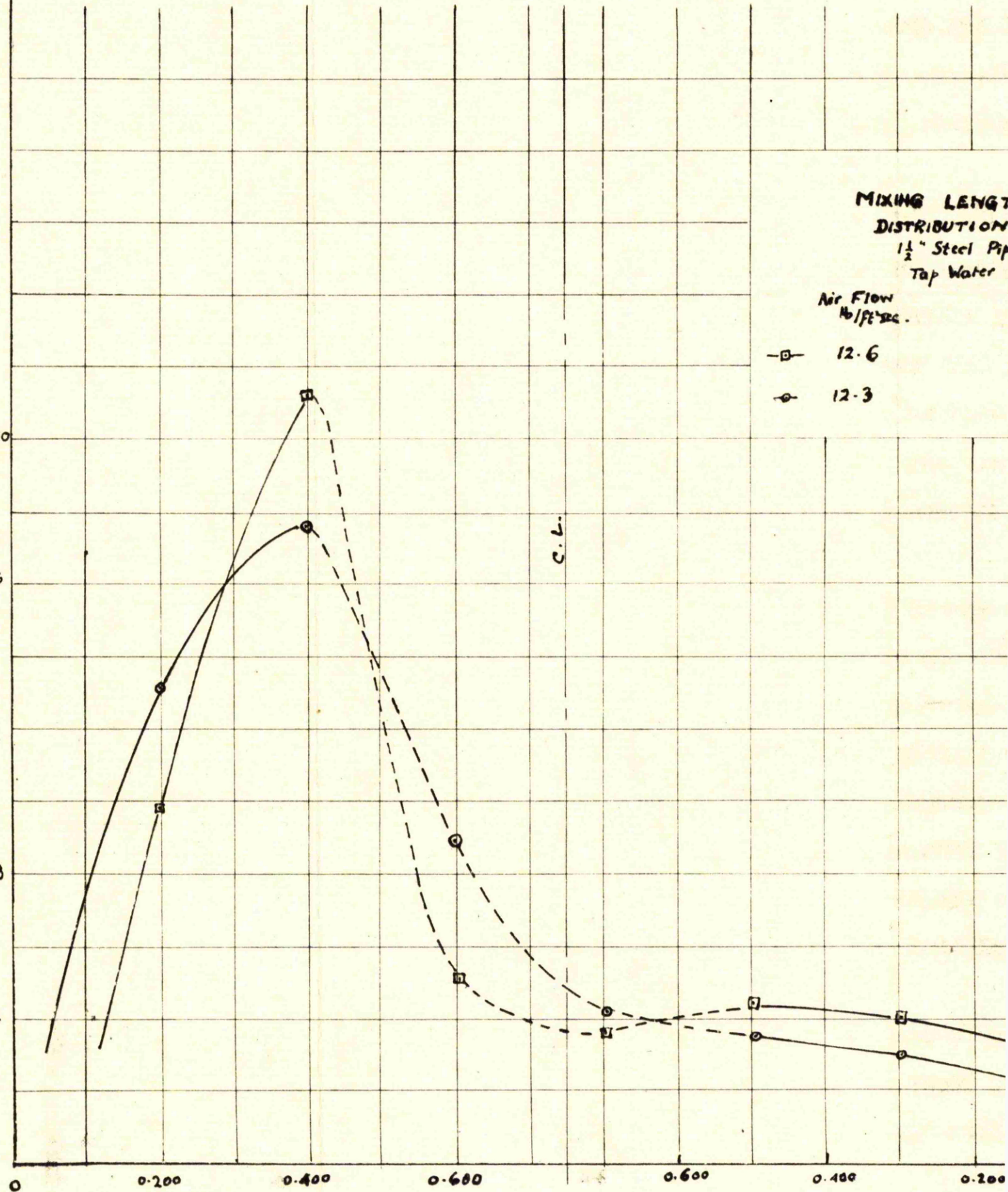


Fig. 54

Curves thus obtained would not give any quantitative estimation of mixing length, which is feasible since some of the assumptions made are still questionable from the point of their applicability to two-phase flow.

Some qualitative conclusions could be made with reference to Fig. 54. Discarding the middle part of the curves, which has been shown by many previous authors to be incorrect, the values of  $\lambda$  at the top are much higher than those at the bottom half of the pipe.

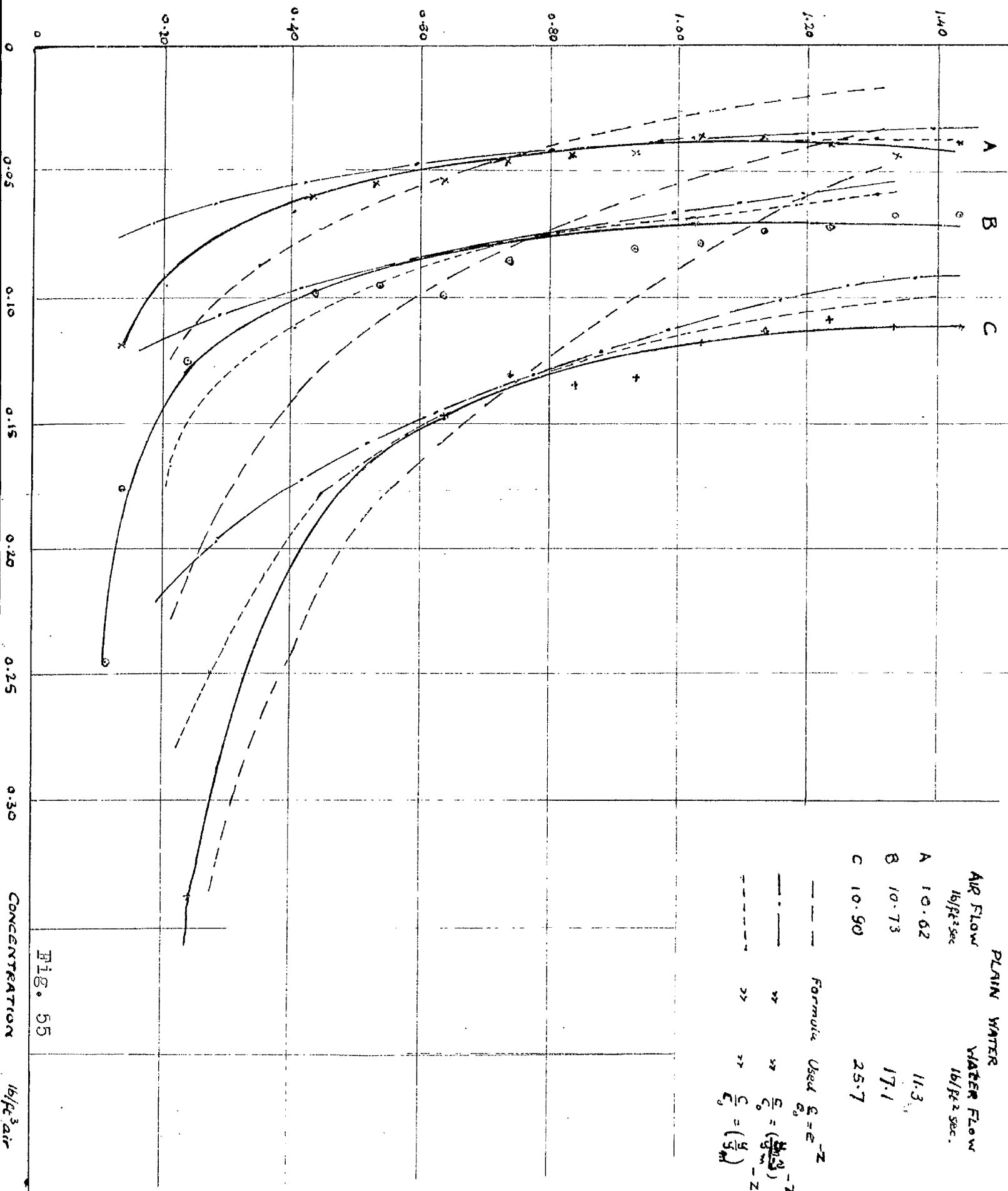
The assumption of Chisholm(16) who assumed equal mixing length for single and two-phase flows is not valid and it may explain, among other factors, the discrepancies between his theory and the experimental results.

In the case of the "symmetrical" type of concentration little difference between top and bottom could be found, thus confirming the previous conclusion of water particles effect.

It was found by Iqbal(32) that when most of the solid charge is carried in suspension by the liquid at high velocities, the point of maximum velocity occurred at the centre. Such a phenomenon was also confirmed in the present work. The only explanation would be a decrease in turbulence indicated by a value of  $K < 0.4$  for bottom part of the tube.

Prondzel(53) discussed this point and suggested that in a horizontal flow, where the density diminishes rapidly upwards, the process of turbulent mixing must cause heavier layers to move above

DISTANCE FROM LOWER TUBE WALL  
(in.)



the lighter and vice versa. That is, part of the store of work available for the maintenance of turbulence is used against gravity, hence turbulent motion is diminished and may die out all together.

Formula used to express  $\epsilon$ .

In the course of development of theoretical analysis for phase-distribution, as shown in Chapter IV, the turbulent viscosity coefficient was estimated first as being constant according to the assumptions of Tissail (31) but considerable lack in agreement with the experimental curves appears.

When  $\epsilon$  was calculated from

$$\epsilon = \rho \cdot l^2 \frac{du}{dy}$$

and using  $\frac{U_{max} - U}{U_f} = \frac{l}{k} \log \frac{y}{y_{max}}$ .

which gave an expression for concentration distribution of the form

$$c = C_0 \left( \frac{h}{h_a} \right)^z$$

where  $h = \frac{y - y_a}{y_{max}}$

still lack of agreement persists Fig. 55.

The best possible correlation was obtained by applying the formula

$$l = k_y$$

and this gave  $c = C_0 \left( \frac{y}{y_{max}} \right)^{-z}$

The three methods were applied for all experimental results and a sample of the effect of varying the theoretical expression for  $\epsilon$  is shown in Fig. 55.

Plane of Zero Shear in Two Phase Flow.

So long as the average density of the mixture is constant the plane of zero shear would take place at the point of maximum velocity, i.e.,

$$\frac{dv}{dy} = 0$$

Once the change in density becomes appreciable, however, can no longer be treated as a constant in determining the apparent shear due to the mixing process at any depth. So the shear stress resulting from momentum transport will vary with the gradients of both density and velocity(56).

$$\tau = \epsilon \rho_m \frac{dv}{dy} + \epsilon v \frac{d\rho_m}{dy}$$

Thus  $\tau = 0$  when  $\rho_m \frac{dv}{dy} = -v \frac{d\rho_m}{dy}$

For exponential distribution it found the  $\frac{d\rho_m}{dy}$  varied but very little from zero in the neighbourhood of  $\frac{dv}{dy}$  so it is concluded that for exponential concentration distribution zero shear takes place at the plane where

$$\frac{dv}{dy} = 0$$

But for the case of the nearly symmetrical distribution, application of the above equation should be taken into account.

CHAPTER VIII.

PRESSURE DROP.

Pressure Drop  $\frac{\Delta P}{\Delta L}$  for  $1\frac{1}{2}$ " I.D Glass & Steel

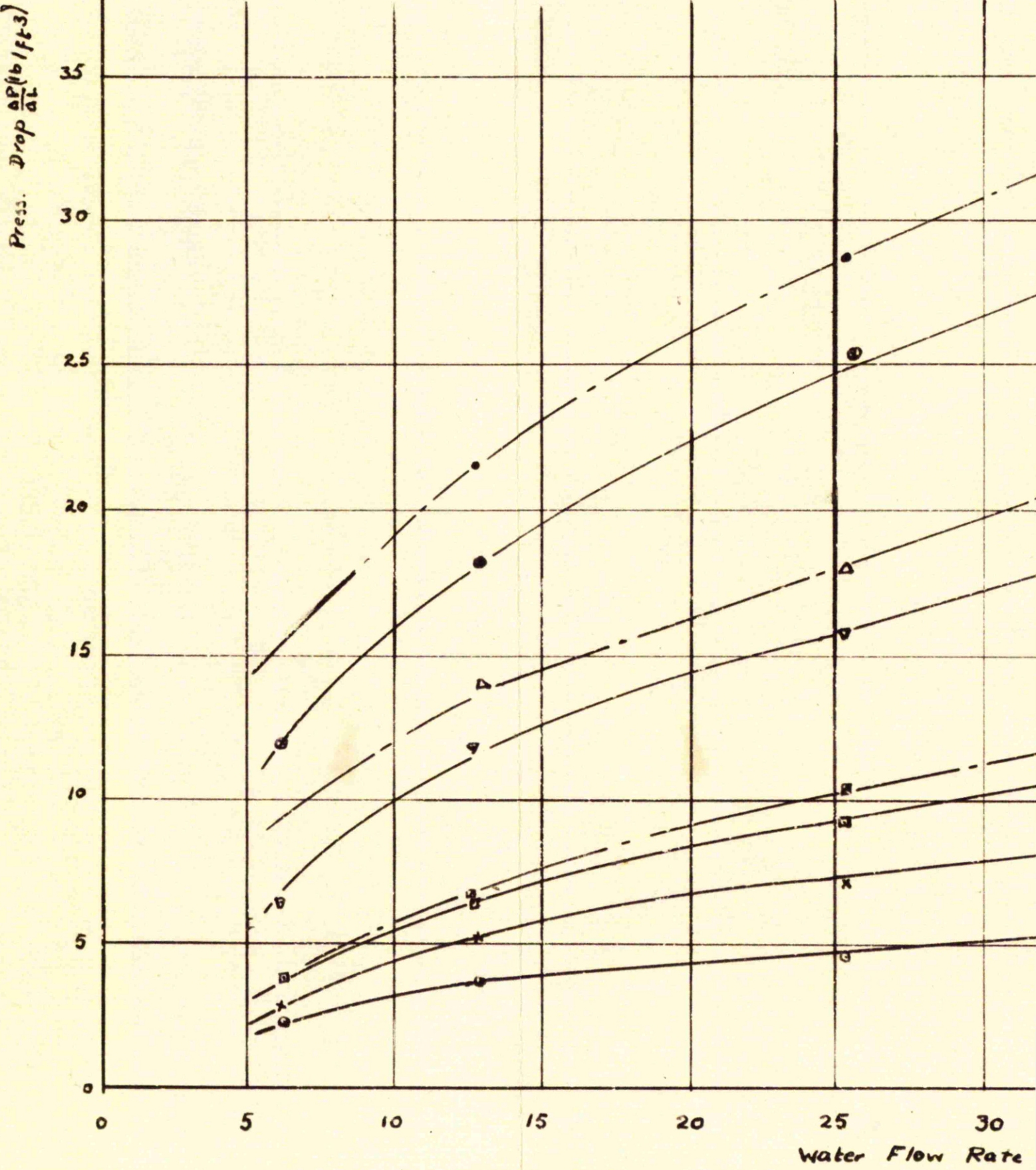
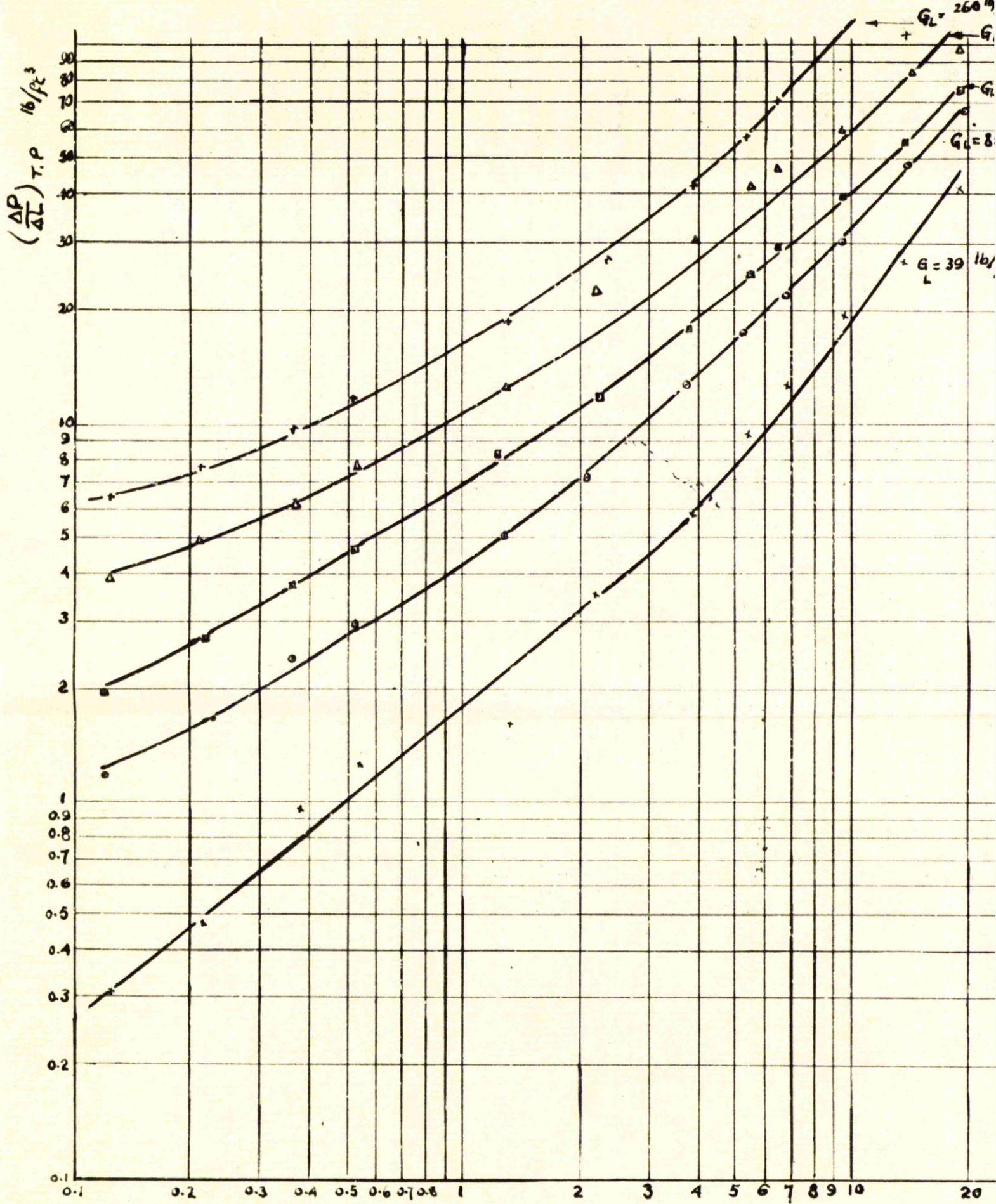


Fig. 56

Pressure Drop in 1" I.D. Steel Pipe



## Pressure Drop in Two-Phase Flow.

### Introduction:

Previous work done on two-phase flow as reviewed in Chapter I dealt mainly with the formulation of means for predicting pressure drops without any careful study of the mechanism of such a flow or without due consideration of several factors that would affect the problem.

Undoubtedly the phenomena involved are so complex that only empirical or semi-empirical solutions were possible. The effect of the flow pattern is also important. Martinelli's equation, even if it is still accepted as the classical approach to the prediction of pressure drops, has its serious limitations.

Armand's method based on "the slip" that takes place between the two phases, was fundamentally the same.

Kosterlin and Bergelin put forward some correlations based on the evaluation of the coefficient of friction for two-phase flow.

### Experimental Results.

Pressure drop  $\frac{\Delta P}{L}$  is plotted against air flow and water flow rates Figs. 56, 57, for the three pipes. All the curves obtained exhibit the same characteristics.

For constant air flow the pressure drop is proportional to water flow rate, the gradient increasing as the water flow rates increase.

For constant water flow variable air flow the pressure drops were not directly proportional but the curves remain fairly consistent in shape.

Comparing the present results with those of Boelter, Martinelli and Gooley, it can be seen that they are similar in form, although the air flow rates used here are higher.

#### Evaluation of Slip Velocity.

The method of measurement of the area of the cross section occupied by each phase individually has been discussed previously in Chapter III, and the results are tabulated in Table VI, Appendix VI. It should be noticed that these measurements were made only in the case of 1" I.D. steel pipe.

#### Pressure Drop Prediction.

##### 1. Friction coefficient concept.

As an approximation the air stream with its entrained water droplets can be assumed a homogeneous mixture of air and water with an average density

$$\rho_m = \frac{Q_w \cdot \rho_w + Q_a \rho_a}{Q_w + Q_a}$$

$$\text{or } \rho_m \approx \frac{Q_w \rho_w + Q_a \rho_a}{Q_a}$$

neglecting the volume of water.

Using the Fanning formula for friction-drop of a homogeneous mixture and assuming that the relative velocity between the water particles and air to be small we can write

$$\frac{\Delta P}{L} = \frac{\lambda}{D} \cdot f_m \cdot \frac{V^2}{2g} \quad (33)$$

$\lambda - R_{eq}$  for 3 tested pipes

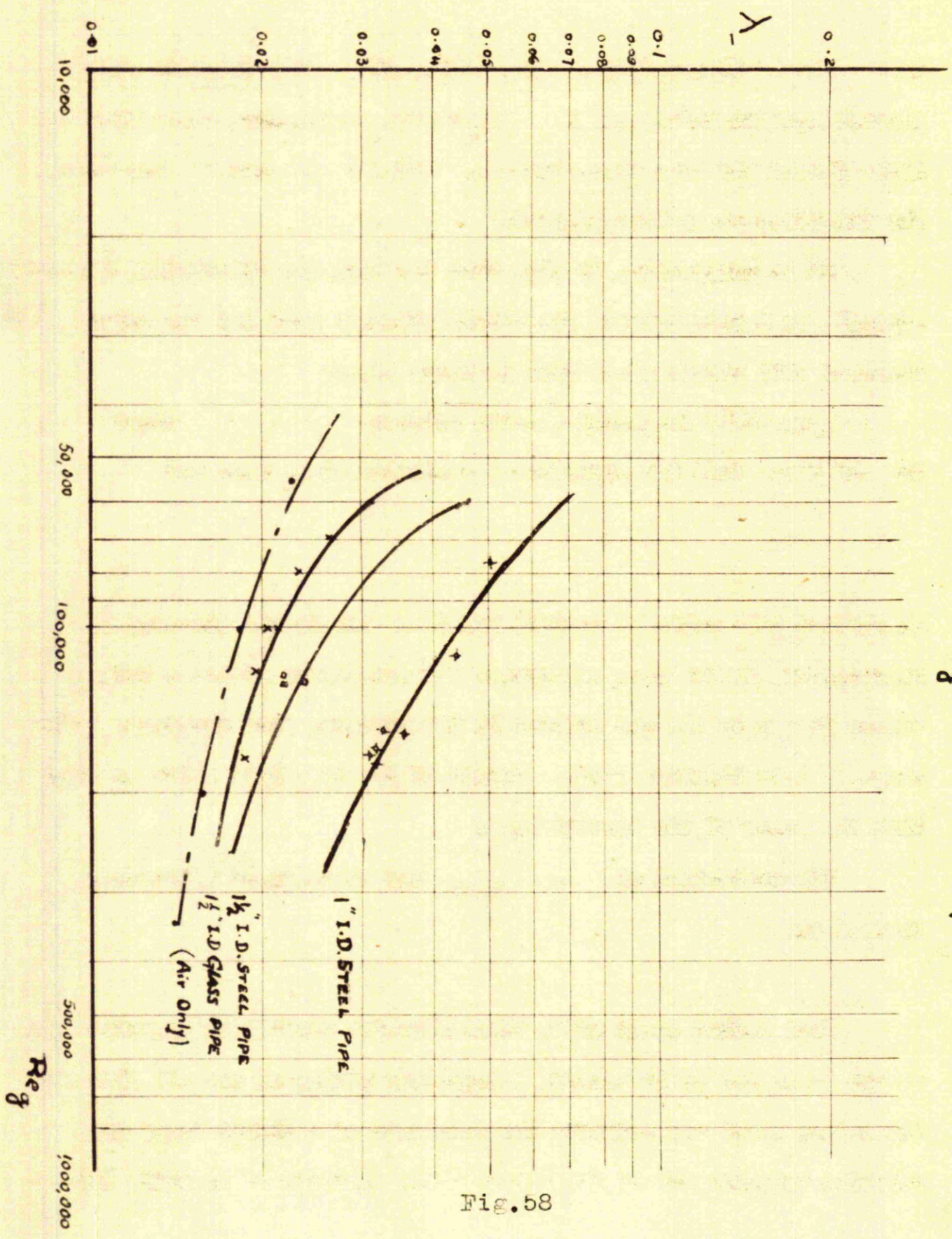


Fig. 58

thus  $\lambda$  could be evaluated. The values of  $\lambda$  thus obtained were plotted against values of  $R_{e_a}$  calculated on the assumption that air alone filled the tube cross section. Fig. 58 illustrates the results for the three pipes investigated.

It is interesting to note that for high air velocities, a marked resemblance exists between the values obtained here and the values measured with single phase flow in rough pipes.

Koestenin's suggested a ratio between  $\frac{\lambda_{mix}}{\lambda} = \gamma$  where  $\lambda$  is the air phase friction coefficient evaluated at  $R_{e_{mix}}$  and

$$R_{e_{mix}} = \frac{4 G_{mix}}{\pi D g \mu_{mix}}$$

He plotted this ratio  $\gamma$  against Froude number Fr and obtained a relationship in the form of curves. These curves indicate that  $\gamma$  values rise with the gas content in the mixture, then decrease. The range of investigation covered values of Fr 10 - 2000 which is lower than the range of the present work.

For evaluation of  $\lambda$ ,  $\rho_{mix}$  was substituted in Fanning formula as

$$\rho_{mix} = c_v \rho_w + (1 - c_v) \rho_a$$

Such method seems quite reasonable for predicting pressure drops except in so far as it assumes homogeneous mixing of the air flow and the entire water and neglects the existence of a liquid layer, of relative velocity and of the irreversible exchange of momentum between

the phases. The method used in the present analysis which is already mentioned is a better one and gives more rational results.

For air mass velocities of 8 lb/ft.<sup>2</sup> sec., the value of  $\lambda_{mix}$  was approximately 0.04 dropping to 0.02 for air flow 16.4 lb/ft.<sup>2</sup> sec. This drop can be explained by the existence of truly annular flow at high air flow rates with layer on the walls so thin that the effect of surface waves is small. This is confirmed by Kosterin's work at high Froude numbers. At low air velocities the water layer is thicker and the waves are higher, thus values of  $\lambda$  are higher.

### II. Prediction of Pressure Drop by Analogy with Prandtl Mixing Length.

In turbulent flow, according to the Prandtl mixing length theory, the shear stress at any point in the flow can be expressed by

$$\tau = \rho \ell^2 \left( \frac{du}{dy} \right)^2 \quad (34)$$

These conceptions are widely applied for the theoretical analysis of turbulent flow in pipes and in free expanding jets.

In Chapter V, page 50, the application of such concepts was given. Even in single phase flow - gas or liquid - this theory was found to have restricted application.

In applying this formula to two phase flow it was accepted as the simplest and probably the only tool to express the distribution of suspended liquid particles. It was intended, to examine more closely the application of the equation to the present problem and to obtain the

fundamental relationships between the factors affecting the flow, namely

$$\tau, \ell, \rho_m, \frac{dv}{dy}$$

In the field of single phase flow, the work by Nukradse<sup>47)</sup> seems to be the best available. He investigated the effect of variation of the turbulence on friction.

In adopting the same method as Nukradse, which would be to consider all the factors affecting the flow, one has to bear in mind the appearance of a third variable in equation 34, due to density variation.

The present results were checked by eliminating the factor  $\rho_m$  from the equation by taking values of  $\tau$  and  $\frac{dv}{dy}$  at equal densities.

It was hoped that a certain universal relationship similar to the mixing length  $\ell$  could be obtained.

For  $\tau$ , according to the balance between the pressure along distance  $\Delta L$  and shear stress distribution, the fundamental relations

$$\tau = \frac{\Delta P}{\Delta L} \times \frac{r}{2} \quad (35)$$

$$\tau = T_0 \times \frac{r}{r_0} \quad (35a)$$

still hold.

Applying this to different tests at fixed values of concentration  $C$ , values of  $(\frac{T}{dy})^2$  were calculated and are shown in Table V. Comparing the corresponding values of  $(\frac{T}{dy})^2$  for fixed densities, it can be seen that there is a trend similar to that found with the mixing length  $\ell$  in single phase flow, but still more experimentation is required before a definite relationship can be stated.

It is interesting to notice, however, that there is not a universal type of relationship between  $\ell$  and  $r$  that would hold directly for air-water mixtures at any constant density value. For the range where annular flow appears to exist (air flow range in the case of  $1\frac{1}{2}$ " I.D. pipe of  $10 - 17$  lb./ft.<sup>2</sup> sec. and varying water rates) there is a certain relationship, but it breaks down at lower air rates.

The factors which lead to this breakdown might well be:

- (a) Effect of the distribution of the water phase and in particular the inert layer of water on the walls,
- and (b) The inaccuracy of velocity measurement near tube walls where wave action prevails.

The number of points was not enough to yield any concrete correlation but it appears that the application of the ordinary concepts of turbulence would be permissible in the case of two-phase flow.

The general relationship for shear stress in this case, adopting equation 34, and putting

$$\ell = Ky$$

$$\text{d} \quad K = \text{const.}$$

is given by

$$\tau = \rho_c \left( \frac{u}{g_o} \right)^{-\frac{\omega}{PKU_f}} (Ky)^2 \left( \frac{du}{dy} \right)^2 \quad (36)$$

where  $\rho_c$  = density at central point.

$\left( \frac{u}{g_o} \right)^{-\frac{\omega}{PKU_f}}$  = expression for distribution of density at any point.

$Ky$  = expression for mixing length  $\ell$

On the other hand

$$\tau = \tau_0 \left( 1 - \frac{y}{y_0} \right)$$

$$\text{and } \tau_0 = \frac{\Delta P}{\Delta L} \times \frac{y_0}{z}$$

from equations 35, 36

$$\rho_c \left( \frac{y}{y_0} \right)^{0.40f} k^2 y^2 \left( \frac{dy}{dy} \right)^2 = \frac{\Delta P}{\Delta L} \frac{y_0}{z} \left( 1 - \frac{y}{y_0} \right) \quad (37)$$

putting  $\beta = 1$  and  $K = 0.4$  as has been suggested before.

From equation 37, the velocity relationship that proved to be applicable in this case is

$$v = A' \left( \frac{\tau_0}{\rho} g \right)^{1/n} \left( \frac{y}{y_0} \right)^{1/n}$$

The value of  $n$  for the lower part of the tube section has been given in Chapter VI in relation to the rate of flow. The value of  $n$  within the range of experimental investigation may be given empirically as:

$n = 3 - 3.36$  with an average of approximately 3.3 and for the top an average value of 7 which corresponds to single phase flow.

So from equation 37 above, and applying the formula

$$U_f = \sqrt{v} \sqrt{\frac{\lambda}{g}} , (\lambda = 4f)$$

all the components in the above equation are known and hence  $\frac{\Delta P}{\Delta L}$  can be calculated

Deviations as cited in methods I, II; when applying the fundamental equations of fluid flow to two phase flow may be explained by a further consideration of some more fundamental concepts to the problem.

It could be stated that the mechanics of gas-liquid flow in cylindrical conduits is far from being understood at present.

- (a) For any fluid flowing in steady state through a distance  $\Delta L$ , continuity equation

$$\frac{d(U \cdot \rho)}{dL} = 0$$

and the mechanical energy balance for a system can be written as

$$\frac{1}{\rho} \frac{dP}{dL} + \frac{V}{g} \frac{dv}{dL} + \frac{dF}{dL} = 0$$

These are applicable and are independent of the boundary shape.

However, when an attempt was made by Ward and Delavelle to apply them, complications such as the determination of the respective flow channels, the effect of interfacial roughness, entrainment, and others arise.<sup>(67)</sup>

- (b) When applying fundamental equations such as Newton's Law which can be expressed by

$$\rho \frac{du}{dL} dv = - dV \left[ \frac{\partial}{\partial x} T_{xx} + \frac{\partial}{\partial y} T_{yx} + \frac{\partial}{\partial z} T_{zx} \right]$$

where  $T_{xx}$ ,  $T_{yx}$ ,  $T_{zx}$  are the shear stresses. For application of this formula, among others such as Navier—Stokes equation, for two-phase flow,  $dV$  must be large enough to incorporate a statistical part of the dispersed fluid and small enough to allow integration of

$$\rho = \delta V \lim_{\delta m} \frac{\delta m}{\delta V}$$

where  $\delta V > \delta V_{min}$ .

$$\text{so } F_{xx} = -\delta V \left[ \frac{\partial}{\partial x} T_{xx} + \frac{\partial x}{2} \frac{\partial^2}{\partial x^2} T_{xx} \right]$$

putting  $\frac{\partial x}{2} \ll \frac{\partial^2}{\partial x^2}$  [if small  $T_{xx}$  is linear and  $\frac{\partial^2}{\partial x^2} = 0$ ]

$$\text{we get } F_x = \delta V \cdot \frac{\partial}{\partial x} T_{xx}$$

from which  $T_{xx}$  may be expressed.

Happol and Byrne(25) suggested a mathematical solution for expressing relations of Navier-Stokes equation for a flow of a single sphere in a flowing fluid.

The method is quite interesting although it is tedious and gave expressions of pressure drops in the system.

All these considerations would illustrate the complexities which such a flow would entail and also may explain why, when applying the two fundamental equations 35, 37, in our case the results show a rather wide scatter.

However, this initial exploration of the subject is hopeful enough to justify further investigation.

### III. Determination of Relative Velocity.

The quick closing cocks were used to determine  $X_f$ . The values determined from these tests are shown in Table VI, and the method of calculation is detailed in Appendix VI.

Slip between Phases  $\frac{v_2}{v_1}$

12

10

8

6

4

2

0

0

2

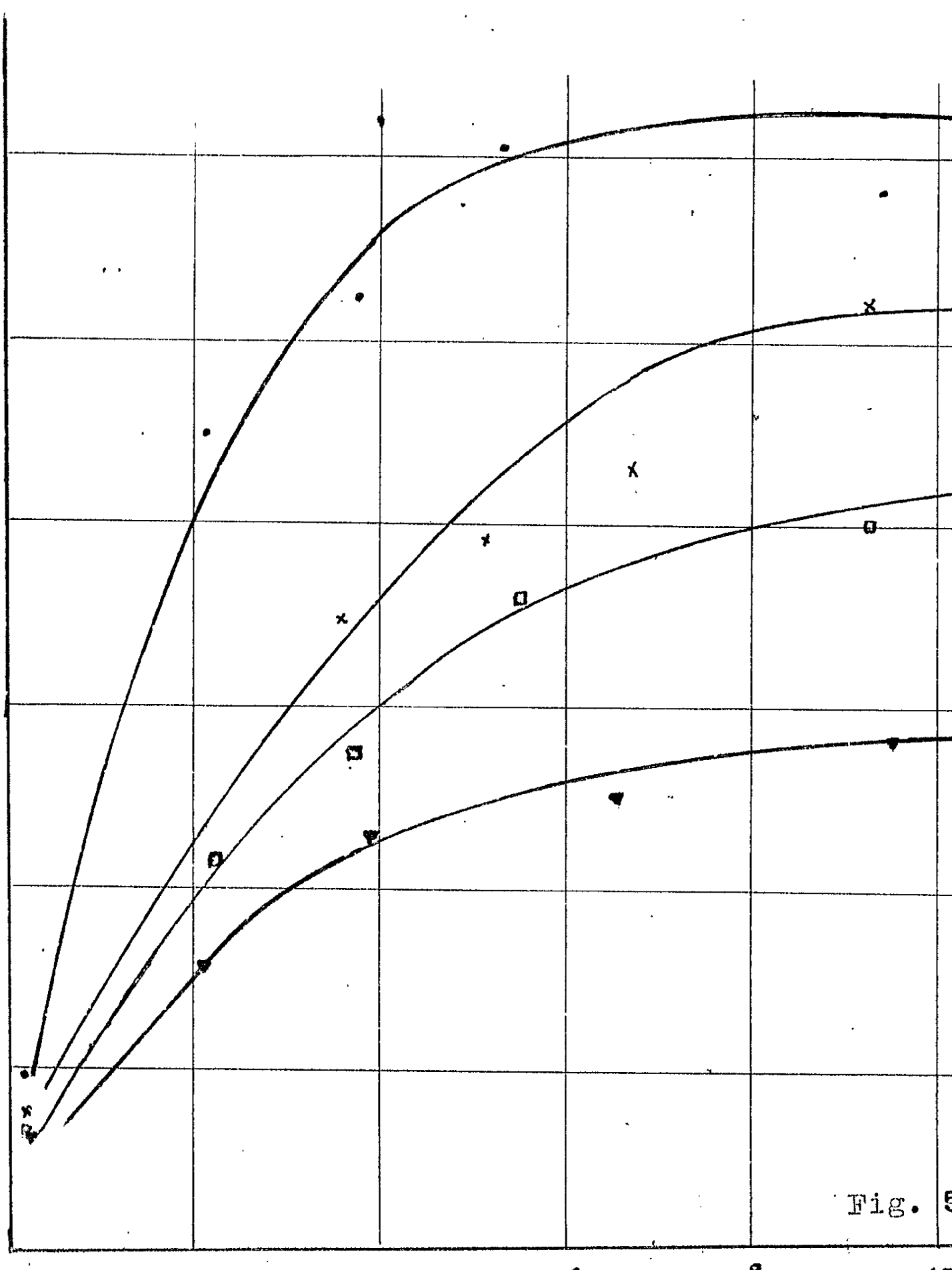
4

6

8

10

Fig. 5



The results compare favorable with those according to Johnson and Abu Salé.

Slip or the relative velocity increased as the air flow increased and after reaching a maximum at a certain air flow, it decreases slightly and maintains almost a constant value. The results are shown in Fig. 59 and Tables VI, in Appendix VI, and a sample of the calculation is presented there. "Slip" varies with air flow rates and also with the water flow rates which also show similarity with the results presented by Johnson for non-isothermal flow.

The rising characteristic of the curves may be explained by the variation in the flow patterns which ends with a form of annular form.

For calculation of slip, however, the ideal form was assumed, i.e., no entrainment, which has been shown in Chapter V to be far from the actual case.

Ghoshal considered this entrained liquid effect and gave expressions for the value of "slip" when dispersed water particles are taken into consideration.

If  $\theta$  is the slip, given as the ratio between velocities of gas stream and water layer, then by taking entrained liquid effect we get

$$\frac{x_e}{x} = \frac{\frac{w_e - w_e}{\rho_e v_e} + \frac{w_e}{\rho_e s \cdot v_e}}{\frac{w_g}{\rho_g s v_e} + \frac{w_e - w_e}{\rho_e v_e} + \frac{w_e}{\rho_e s v_e}}$$

$$s = \frac{\frac{w_e - w_e}{\rho_e} - \frac{x_e}{x} \left[ \frac{w_e - w_e}{\rho_e} \right]}{\frac{x_e}{x} \frac{w_g}{\rho_g} + \frac{w_e}{\rho_e} \left[ \frac{x_e}{x} - 1 \right]}$$

$$\alpha = (\Delta \rho_L)^{T.P.} / (\Delta P)_L$$

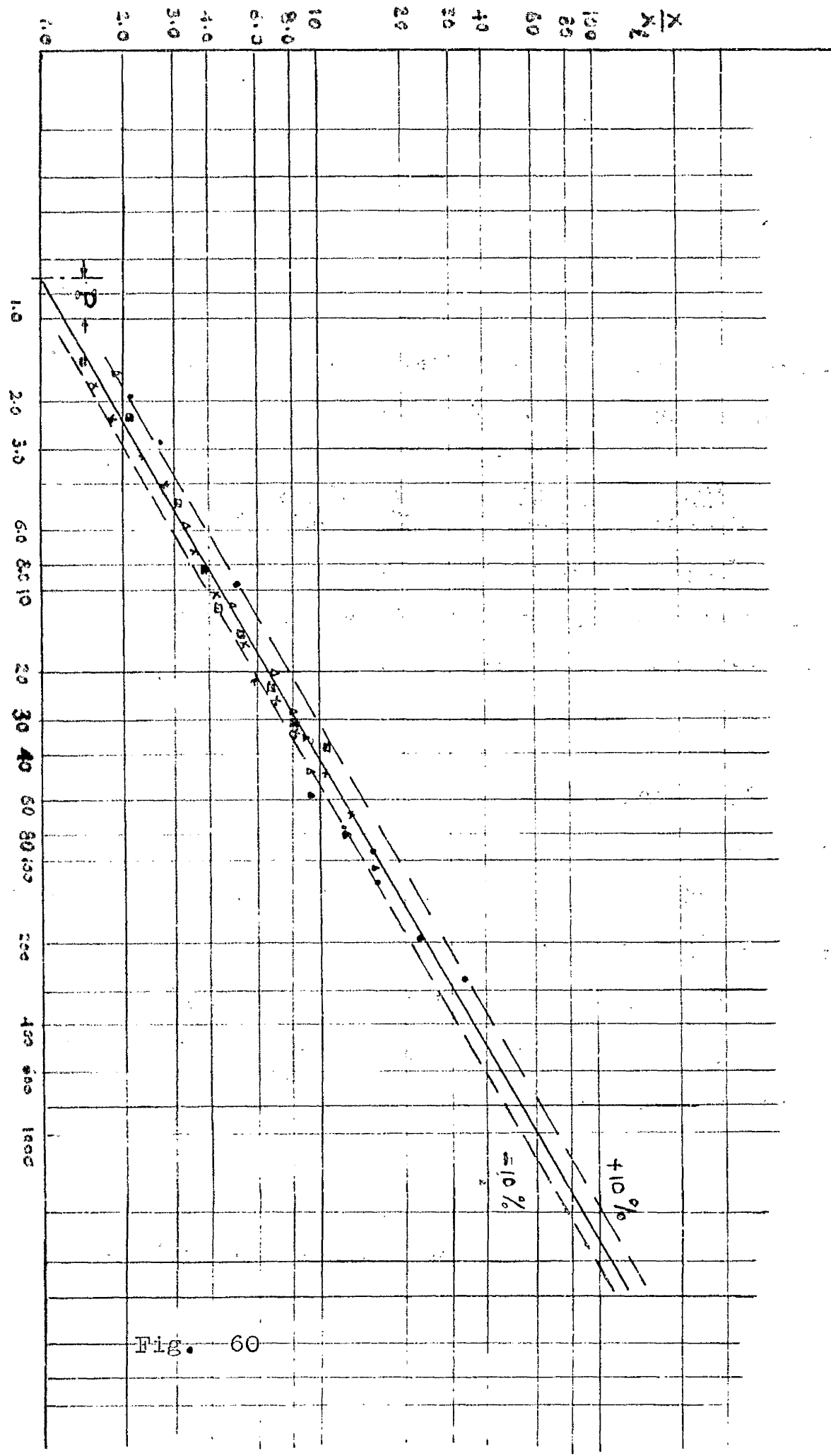


Fig. 60

or

$$S = \frac{\frac{w_e - w_f}{P_e} \left[ \frac{x_g}{x} \right]}{\frac{x_g}{x} \left( \frac{w_g}{P_g} \right) - \frac{w_e}{P_e} \left( \frac{x_g}{x} \right)} \quad (38)$$

values of  $\frac{x_g}{x}$  were obtained by using the quick closing cocks and  $w_f$  values are calculated from sampling.

Correlation of pressure drop results by a method analogous to one-solid formula.

Vogt and White(63) gave an interesting paper on the pressure drops in pneumatic conveying of solids. The method was based on Gasterstadt's formula (21), and reads as

$$\alpha - 1 = P \left[ \frac{w_g}{w_s} \cdot \frac{R}{R_e} \right]^s$$

where  $P, s$ , are constants

and  $\alpha = (\frac{\Delta P}{\Delta L})_{T,P} / (\frac{\Delta P}{\Delta L})_g$ ,  $R$  is taken as specific loading  $= \frac{w_s}{w_g}$

Plotting values of  $\alpha$  against  $\frac{x_g}{x_L}$  as shown in Fig.60, gave a very good correlation with values of  $s = 1.7$  and  $P = 0.8$

The deviation for the range covered was nearly  $\pm 10\%$ .

Applying the method of Vogt and White(63) for the expression of pressure drop of a mixture of gas and solids

$$P_{s,s} = f \left[ \frac{(\rho_s - \rho_g)}{3 \mu_g^2} \rho_g g D_a^2 \right]^{0.5}$$

so the formula applicable in the present problem should read

$$\alpha = 0.8 \left( \frac{x_g}{x_L} \right)^{1.7} \quad (39)$$

GENERAL DISCUSSION AND CONCLUSIONS.

General Discussion of Results and Conclusions.

The object of this work has been to develop a technique which would allow measurement of distribution of water content, velocities and pressure drops with a view to building up the pattern of two phase air-water flow in a pipe, and to proceed with the analysis of the results aimed at the prediction of water entrainment and pressure drop for any given air-water flow rates. The problem calls for an understanding of turbulence mechanism and mass transfer which are the outstanding features of this type of flow.

Flow Patterns.

With any given water flow rate, as the air flow increases the progressive development of the flow pattern may be summarised as follows:-

- (a) Stratified flow with a definite interface between air and water.
- (b) Incidence of waves on water surface.
- (c) Breaking of the wave surface and entrainment commenced.
- (d) Spreading of water layer around tube wall and wetting of copper wall due to increased turbulence and entrainment.
- (e) Growth of water film giving imperfect annular flow form.
- (f) Complete annular flow with decreasing water layer.
- (g) Fully dispersed flow with water layer reduced to sub-laminar thickness.

To the above may be added the surmise that as soon as the water layer on the upper wall is of sufficient thickness, secondary circulation due to gravity will affect the water flow on the wall.

#### Concentration Distribution.

For the vertical traverses of the tube cross section the graphs showing water concentration in the air stream plotted to a base of distance from the tube wall at the bottom of the section fall into two main groups. In the first, the graphs have an exponential form which are comparable with those obtained in liquid-solid two phase flow. This group covers the major part of the experimental range.

In the second, which is associated in general with the high air flow rates, the graphs show a minimum concentration followed by increasing values as the tube wall at the top is approached. In the limit at very high air rates the curve is almost symmetrical about the centre of the tube. The larger the pipe diameter the more persistent is the exponential form. It would appear that for pipes larger than  $1\frac{1}{2}$ " I.D. the exponential form alone would occur within the present experimental flow range. For the 1" I.D. pipe on the other hand, the exponential form holds only up to certain water flow rates in the low air flow range and persisted for the air flow range above  $38 \text{ lb}/\text{ft}^2 \text{ sec.}$ .

It might be noted that this is the first use of the concentration graphs in gas-liquid flow although it has been used previously in liquid-solid flow, when the concentration invariably has the exponential form.

This, therefore, is the first appearance of concentration curves of the approximately symmetrical type. The form is attributable to surface tension of the entrained medium and so to the possibility of the secondary circulation of the liquid on the walls.

For the exponential form an equation (page 63) based on mass transfer concept and a modified formula for drop size was applied to the prediction of phase distribution and hence the calculation of entrained water. The agreement with experiment attained was within  $\pm 25\%$ . At the other end of the scale with fully dispersed annular flow, by first estimating the water quantity in the laminar sublayer, the amount of entrained liquid has been evaluated and compared with the measured quantities. The same method was applied to Armand's (3) results. In both cases satisfactory agreement between calculated and experimental values was obtained.

It seems reasonable to expect that the effects of entrainment upon velocity distribution, mixing length, shear stress and so upon turbulence characteristics will be of importance.

#### Velocity Distribution.

From the various formulae available for analysing the velocity curves the well known equation  $\frac{V}{U_f} = A^* \left( \frac{y U_f}{\mu} \right)^{\frac{1}{n}}$  was chosen as being the most readily applicable.

For cases in which exponential concentration distribution held, each velocity curve gave two quite definite values of  $n$ , one for the bottom part of the tube section and the other for the top, the former

being definitely smaller than the latter which corresponded closely to the single phase value of 7 . The small value in the lower part of the tube section is attributed to the increased turbulence damping due to larger concentration of entrained water. For the cases in which the concentration distribution approached the symmetrical form, the value of  $n$  was practically the same for top and bottom. Calculation of mixing lengths in various cases supported the idea of the increased turbulence damping in the lower part of the tube due to increased concentrations.

The point of maximum velocity shifts as the concentration distribution changes, which means that the position of the zero shear plane also moves as the concentration distribution changes. Shear stress distribution around the circumference cannot be uniform due to the lack of symmetry in the velocity curve. Shear stress is assumed linear between the wall and the point of maximum velocity. It is also affected by the density of the mixtures.

#### Pressure Drop Prediction

Throughout the present work, the aim has been to study all the fundamental principles used in the study of the flow problem and to test their application to two-phase flow. In applying the Fanning formula the values of  $\lambda$  obtained from the test results showed reasonable correlation within the range of tests. It should be born in mind, however, that the range of water flow rates was limited.

In the second approach, which is more fundamental, the simple Prandtl hypothesis used may have implied an over simplification of the problem. It is still considered to be the best approach to the problem, since it incorporates the fundamental concepts of internal shear and leads to a better interpretation of the flow characteristics.

The third method, based on the conception of slip between the phases and upon an expression developed by previous workers for gas-solid flow, led to equation 39, which gave a reasonable correlation of the results. For predicting pressure drops, this appears to be the best and the simplest method at present.

R E F E R E N C E S.

1. Abramson, A.E.: Investigation of Annular Liquid Flow in Horizontal Tubes. App.Mech.(Trans.A.S.M.E.) Vol.74, p.267 (1952).
2. Alexander, L.G.: Droplet Transfer from Suspending Air to Duct Walls. Industrial and Engineering Chemistry, Vol.43, p.1325 (1951).
3. Armand, A.A.: Resistance to Two-phase Flow in Horizontal Tubes. Investia, W.T.I. USSR, I, p.16 (1946).
4. Armand, A.A. and Tredichew, G.G.: Investigation of Resistance during the Motion of Steam-water mixtures in heated boiler tube at high pressure. Investia, W.T.I. No.4, (1947).
5. Bakhmeteff, B.: The Mechanics of Turbulent Flow. Princeton Univ. Press, 1936.
6. Baldina, D.M. and Peterson, D.F.: The application of dimensionless co-ordinates for the generalization of experimental results of circulation in steam boilers. Koltoturbostraenie No.2, (1949).
7. Baron, T., Sterling, G.S., and Schweler, A.P.: Viscosity of Suspensions. Proceeding of Third Mid-western Conference of Fluid Mechanics, Univ. of Minnesota, p.103-128, (1953)
8. Batchelor, G.K.: Notes on Free Turbulent Flow. J.Aero.Sciences V.17, p.44 (1950).
9. Bergelin, O.P.: Chem. Eng., 104-6 (May, 1949).
10. Bergelin, O.P., Kegel, Carpenter, Gazley, G.: Co-current Gas-Liquid Flow in Vertical Tubes. Heat Transfer and Fluid Mechanics Institute. p.19, (June 1949).
11. Bergelin, O.P., and Gazley, G.: Co-current Gas-Liquid Flow - Flow in Horizontal Tubes. Heat Transfer and Third Mechanics Institute. American Soc. of Mech. Engineers. p.5, June, (1949).

12. Boelter, L.M.K.,  
Kepner, R.H.  
Pressure Drop Accompanying Two Component Flow  
Through Pipes. Industrial and Eng. Chemistry.  
(1939), Vol. 31, p.436.
13. Bottomley, W.T.  
Flow of Boiling Water through Orifices and Pipes.  
North East Coast Institute, p.65 (1936).
14. Burnell, E.G.,  
Flow of Boiling Water through Nozzles, Orifices,  
and Pipes. Engineering, p.572, V.164(1947).
15. Chisholm, D.  
Circulation in Water Tube Boilers.  
Ph.D. Thesis (Glasgow University) (1953).
16. Cramp, W., and  
Priestly, A.  
Pneumatic Transport Plants. Chem. and Industry.  
207-112, (1925).
17. Durand, R.  
Hydraulic Transportation of Solids in Pipes.  
Houille Blanche, p.384, (1951).
18. Einstein, H.A.  
Formula of Transportation of Bed Load. Trans.  
A.S.C.E., V.107, p.575, (1942).
19. Engineers Digest, Oct. 1953. Dust Content of Flowing Gases, p.347.
20. Fage, A. and  
Townsend A.  
Proceedings of Royal Society, V.135, p.656  
(1932).
21. Gastlaestadt,  
Experiments on Pneumatic Transportation (German)  
Zeit. V.D.I., V.68, p.617-24 (1924).
22. Gazley, G.  
Interfacial Shear and Stability in Co-current  
Gas Liquid Flow. Heat Transfer and Third  
Mechanics Institute, p.29-40 (1949).
23. Goldstein, S.  
Modern Developments in Fluid Dynamics.  
Oxford Press. Report(1952).
24. Halbrane, G.  
The measurement of concentrations and of  
velocities in a current of air and water.  
La Houille Blanche , p.394,(May-June 1951)
25. Happel, J.,  
Byrne, B.J.  
Motion of a Sphere and Fluid in a Cylindrical  
Tube. Industrial and Engineering Chemistry.  
V.46, No.6, p.1181 (1954).

26. Marin, and Molstad, Pressure Drop in Vertical Tubes in Transport of Solids by Gases. *Ind. Eng. Chemistry.* V.41, p.1148-50 (1949).
27. Hinckle, Barron, L. Acceleration of Particles and Pressure Drops encountered in Horizontal Pneumatic Conveying. Ph. D. Thesis to Georgia Institute of Technology, (1953).
28. Hinze, J.O. Transfer of Heat and Matter in the Turbulent Mixing Zone of an Axially Symmetrical Jet. *Applied Scientific Research.* Vol. 41, 435-461, (1949-1950).
29. Howard, G.W. Transportation of Sand and Gravel in a 4 inch Pipe. *Trans. A.S.C.E.*, V.104, p.1334-1380, 1939.
30. Hughes, R.R., and Evans, Fluid Vaporisation. *Chemical Engineering Progress.* V.49 p. 78 (1953).
31. Ismail, H.M. Turbulent Transfer Mechanism and Suspended Sediment in Closed Channels. *Amer. Soc. of Civil Engrs.* V.117, p.409, (1952).
32. Jenkins, R. Two-phase Two-Cont. Flow of Air and Water. M.Ch.E. Thesis, University of Delaware (1949).
33. Johnson, A.A., and Abou-Sabé, A.H. Heat Transfer and Pressure Drop for Turbulent Flow of Air-Water Mixtures in a Horizontal Pipe. *Trans. A.S.M.E.* V.74, p.977 (1952).
34. Keulegan, G.H. Laminar Flow at the Interface of Two Liquids. *Journal of Research of the National Bureau of Standards* V.32, p.303, (1944).
35. Kolmogoroff, A.N. Local Structure of Turbulence in Incompressible Viscous Liquids. *G.R. Acad. Sc. (USSR),* V.30, p.301, (1941).
36. Korn, A.H. New Solids Flow in Pneumatic Handling Systems. *Chem. Eng.* V.57, No.3, p.108-111 (1950).
37. Kosterin, S.J. Investigation of the Influence of Diameter and Layout of the Pipe on Hydr. Resistance and from the Flow of a Mixture of Gas and Liquid. *Investig-Akad. Nauk. USSR.* No.12, p.1024 (1949).

38. Laird, A.K. Stability of Gas Flow in a Tube as related to Vertical Annular Gas-Liquid Flow. Trans. A.S.M.E., V.76, No.7, P.1005-1010, (1954).
39. Lane, W.R. Shatter of Drop in Streams of Air. Ind. and Eng. Chem. V.43, p.1312 (1951).
40. Lapple, C.E. Fluid and Particle Mechanics. Univ. of Delaware, (1954).
41. Lewis and others. Atomization of Liquids in High Velocity Gas Streams. Industrial and Eng. Chemistry, V.40, p.67, (1948).
42. Lin Discussion on Paper (31)
43. Lüning, D. The Adiabatic Flow of Evaporating Fluids in Pipes of Uniform Bore. Proc. Institution of Mechanical Engineers. (1952)
44. Lockhard, R.W. and Martinelli, R.C. "Proposed Correlation of Data for Isothermal Two-Phase, Two Compt. Flow in Pipes" Chemical Enging Progress, V.45, p.67, (1949).
45. Longwell, L. and Weiss, M. Industrial and Engineering Chemistry, V.45, p.607 (1953).
46. Martinelli, R.C. and Isothermal Pressure Drop for Two-Phase, Two-component Flow in a Horizontal Pipe. Trans. Amer. Soc. Mech. Engineers. V.66, p.39, (1944).
47. Nikuradse, J. V.D.I. Forschungslift, V.21, p.356 (1932).
48. Nukiyama, S., and Tanasawa, Y. Trans. Soc., Mechn. Eng. (Japan). V.4, No.14, p.86 (1938), V.5, No.15, p.136(1939). V.6, No.19, p.69, No.22, p.11-7, No.22, p.11-8 (1949).
49. Owen, H. The Measurement of Air Flow. Chapman and Hall Rep. (1949).
50. Pai, S.T. Turbulent Flow in Circular Pipe. Journal of Franklin Institute. Vol.256, p.357,(1953).
51. Pinkins, O. Press Drop. in Pneumatic Conveyance of Solids. Journal of App. Mech. V.74, p.425 (1952).
52. Prandtl, L. Ref. (8)

53. Prandtl, L. The Essentials of Fluid Dynamics. Blackie and Son Ltd. Rep. (1953).
54. Prandtl, L. Z.A.M.M. V.5, p.116, p.137, (1925)
55. Richardson, E.G. Dynamics of Real Fluids. Arnold, 1950.
56. Rouse H. Fluid Mechanics for Hydraulic Engineers. McGraw Hill Book Co., 1936.
57. Shchutsh, V.A. Hydraulics of Two-Phase Flow in a Vertical Branch of a Free Circulation Boiler. Kotloturbo Stroenie, No.4, 1947.
58. Sherwood, T.K. Heat and Mass Transfer and Fluid Friction. Industrial and Engineering Chemistry. V.42, p.2077 (1950).
59. Sherwood T.K. and Woeritz, B.B. Mass Transfer Between Phases. Industrial and Engineering Chemistry. Vol.31, p.1034 (1939).
60. Taylor, G.I. The Statistical Theory of Turbulence. Proc. of Roy. Soc. Vol. A, 156, p.307 (1936).
61. Thomas, A.A., and Archibald, R.A. Analysis of the Die-away Curve in Turbulent Flow. Proceedings of A.S.C.E. V.77, No.84 (1951).
62. Towle, W.L. and Sherwood, T.K. Mass Transfer in the Central Position of a Turbulent Air Stream. Industrial and Chemical Engineering. V.31, p.457 (1939).
63. Vogt, E.G. and, G. White, R.R. Friction in the flow of suspension - Granular Solids in Gases through pipe. Industrial and Engineering Chemistry. V.40, p.1733 (1948).
64. Von Karman, T. Turbulence and Skin Friction. Journal of the Associated Sciences. V.1-2, 1934, p.1-20.
65. Vanoni, V.A. Transportation of Suspended Sediment by Water. Trans. A.S.C.E. V.111, p.67-133, 1946.
66. Widdel, T. Pressure Losses in the Flow of Gas-Liquid Mixtures in Horizontal Pipes. I.V.A. (Sweden). V.20, No.2, p.60-74 (1949).
67. Ward H.C., and Dallavalle J.M. Chem. Eng. Progress Symposium Series 10. Vol. 50 (1954)

APPENDIX E

The flow rates covered in the present work were chosen according to the following factors:-

(a) Full range of air flow rate as determined by the discharge of the compressor.

(b) The water range was determined in the case of  $1\frac{1}{2}$ " I.D. pipes by the maximum head available from the overhead tank, also the range that gave steady flow.

(c) In the case of 1" I.D. pipe the full water range was covered within the limits of the measuring instruments.

Hereafter the test ranges are detailed for the three pipes.

TABLE I ATests for  $1\frac{1}{8}$ " I.D. Glass Pipe. Vertical Traverse. Tap Water.

Air Flow lb/min.	Water Flow lb/min.	Air Flow. lb/ft <sup>2</sup> sec	Water Flow. lb/ft <sup>2</sup> sec
11.95	4.66	16.2	6.25
12.1	8.25	16.3	11.3
12.2	12.5	16.3	17
12.3	16.4	16.4	25.2
12.8	25.0	16.4	35
10.9	4.66	14.8	6.32
11.03	9.9	14.9	13.45
11.1	12.8	14.9	16.85
11.1	16.4	14.9	24.8
11.2	28.0	15.05	37.9
10.22	9.6	13.9	13.0
10.25	12.5	13.9	16.5
10.3	16.7	13.9	25.0
10.35	29.5	14.0	39.0
9.3	9.6	12.5	12.9
9.37	12.5	12.65	17
9.4	20.0	12.7	27.1
9.5	23.6	12.85	47
7.84	8.82	10.62	11.3
7.85	12.6	10.73	17.1
8.08	19.2	10.9	25.7
8.05	32.4	10.9	43.8
6.35	5.6	8.7	7.6
6.5	12.7	8.85	17.8
6.7	18.7	9.2	23.3
6.9	30.5	9.4	41.4
6.56	9.3	7.62	12.65
6.59	14.8	7.65	19.8
6.57	16.3	7.66	24.8
6.61	32.3	7.6	43.8

## 10B.

Tests for 1<sup>1/2</sup>" I.D. Glass Pipe.    Horizontal Traverse.    Tap Water.

<u>Air Flow</u> <u>lb/min.</u>	<u>Water Flow</u> <u>lb/min.</u>	<u>Air Flow</u> <u>lb/ft<sup>2</sup> sec</u>	<u>Water Flow</u> <u>lb / ft<sup>2</sup> sec</u>
6.41	9.52	6.75	12.98
6.44	21	6.76	26.5
6.5	26	6.85	36
9.1	12.8	13.36	19.4
9.18	16	12.42	21.7
9.1	30	12.36	40.7
11.03	9.5	16	12.9
11.1	12.6	16.1	17.1
11.3	33.7	16.2	45.8

Average Surface Tension at 50    dyne/cmVertical Traverse.

9.37	12.7	12.7	17.3
9.3	17.6	12.6	23.7
9.58	33.7	13	44.3
10.9	9.33	14.0	12.68
10.9	12.5	14.9	17
10.93	16.8	14.9	20.8

TABLE I BTests for 1 $\frac{1}{2}$ " I. D. Steel Pipe. Vertical Traverse. Tap Water.

Air Flow lb/min.	Water Flow lb./min.	Air Flow lb./ft. <sup>2</sup> sec	Water Flow lb./ft. <sup>2</sup> sec
12.0	9.33	16.3	12.65
12.17	18.66	16.45	25.3
12.46	28.0	16.9	38
10.92	9.33	14.7	12.65
11.05	18.66	14.9	25.3
11.4	28.0	15.42	38
9.8	9.33	12.6	12.65
9.07	18.66	12.9	25.3
9.52	28.0	12.9	38
6.47	9.33	8.75	12.65
6.45	18.66	8.72	25.3
6.47	28.0	8.70	38
3.94	18.66	5.34	25.3

45° Traverse. Tap Water.

6.3	9.33	8.42	12.65
6.45	28	8.72	38
10.9	9.33	14.68	12.65
11.2	28	15.2	38

Horizontal Traverse. Tap Water.

6.34	9.33	8.62	12.65
10.86	9.33	14.8	12.65
11.2	28	15.2	38

104.  
TABLE Ic.

Tests for 1" O.D. Steel Pipe.	Vertical Traverse.	Tap Water.	
Air Flow. lb/min	Water Flow. lb/min	Air Flow. lb/ft <sup>2</sup> /sec	Water Flow. lb/sec ft <sup>2</sup>
2.05	12.5	6.05	30
2.07	16.7	6.82	56.5
2.09	20	6.4	85
2.1	37.8	6.8	114
3.08	4.66	8.95	13.5
3.15	9.33	9.15	27
3.21	12.5	9.8	36
3.3	18.7	9.55	54
3.9	12.5	12	38
3.9	18.7	12	56.7
3.92	20	12.1	85
3.95	37.4	12.15	114
4.15	4.66	12	13.5
4.27	9.33	12.4	27
4.4	12.5	12.7	36
4.45	18.7	12.9	54
5.97	4.66	17.3	13.5
6	9.33	17.3	27
6.12	12.5	17.0	36
6.32	18.7	18.5	54
6.6	4.66	19	13.5
6.95	9.33	20.2	27
7.05	12.5	20.4	36
7.5	18.7	21.7	54

N.B. More tests were carried out mainly for pressure drops (Appendix VI) and not shown above.

APPENDIX II.A. Observed Results.

For each test, as has been detailed in Chapter III, pressure and temperature for air and water were measured and the sampling quantities were noted. An example of these results appear in the following tables which are specimens for the three pipes.

B. Calculated Results.

Orifice Meter Calculations. According to Owen(49) page 113, Air flow can be expressed by the formula

$$W_a = 8.76 C \propto a_2 \sqrt{h_1 - h_2} \sqrt{\frac{b + p}{460 + t}} \quad \text{II(1)}$$

where  $b$  = barometric pressure in Hg

$p$  = pressure at the orifice in Hg

$t$  = temperature \* \* °F

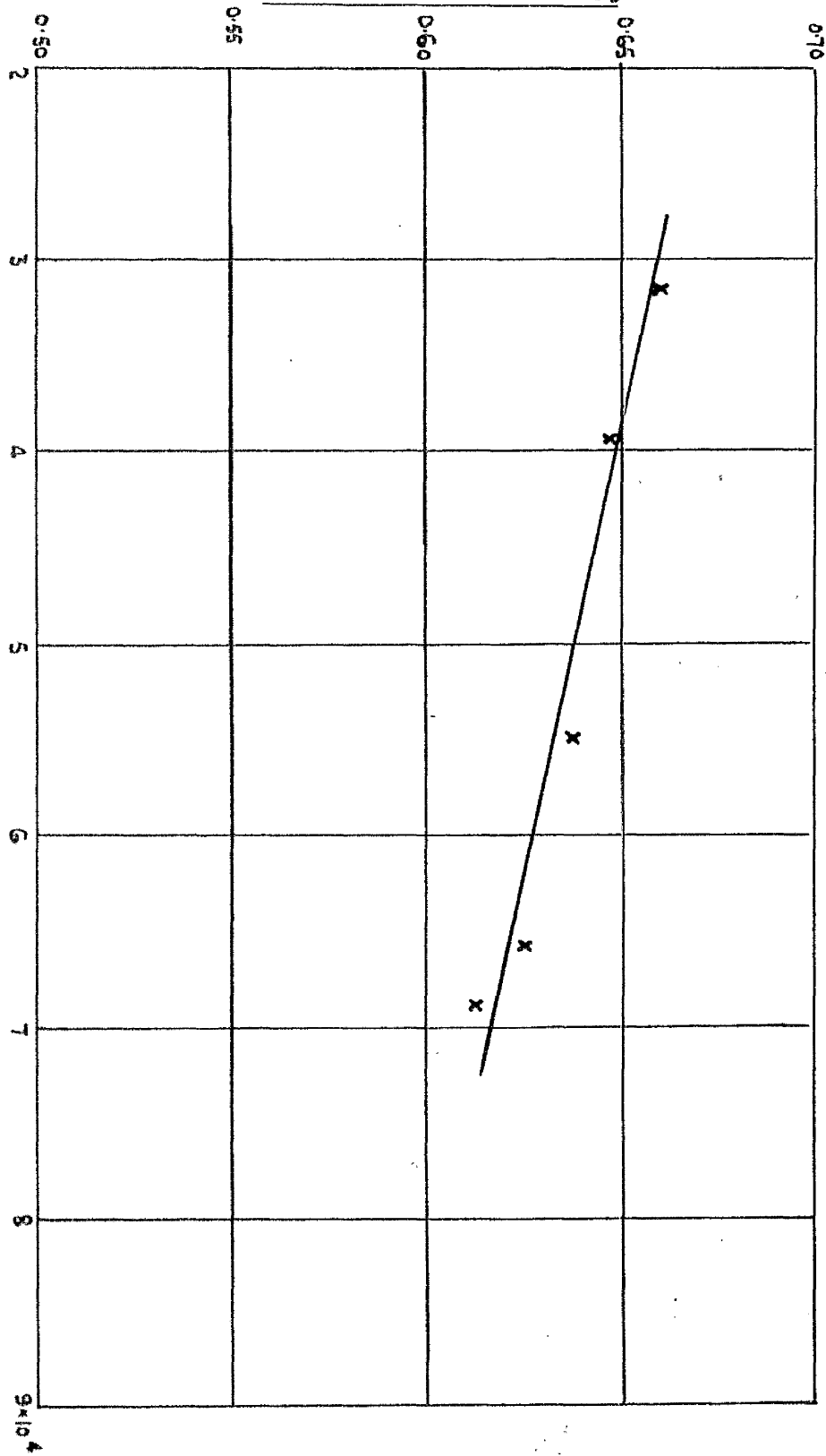
$h_1 - h_2$  = pressure drop across the orifice.

For an orifice plate  $\frac{1}{2}$ " diameter and for a value of

$$R_e \approx 50,000$$

we get  $C_d \approx 0.635$  from the calibration chart shown in Fig. 61.

COEFFICIENT OF DISCHARGE  $C_d$



ORIFICE CALIBRATION ( $C_d$  AVE 0.635)

REYNOLDS NUMBER  $R_e$

Fig. 61

Thus formula II<sub>(1)</sub> will read

$$W_a = 6.9 \sqrt{h_1 - h_2} \sqrt{\frac{b + p}{160 + t}} \quad \text{II (2)}$$

Referring to Table A:

$$\begin{aligned} h_1 - h_2 &= 19 \quad " \text{Hg} \\ p_a &= 11 \quad 1b/\square" \\ &= 22.4 \quad " \text{Hg} \\ t_a &= 87 \quad ^\circ \text{F} \end{aligned}$$

substituting in Equation II<sub>(2)</sub> we get

$$\begin{aligned} W_a &\approx 9.27 \text{ lb/min.} \\ &\approx 12.65 \text{ lb/ft}^3 \cdot \text{sec.} \end{aligned}$$

Considering station 400 thous. says:-

$$\begin{aligned} \text{Actual mano reading} &= \text{"Experimental Pitot Reading"} \times 45^\circ \\ &\approx 60.5 \text{ cm H}_2\text{O} \times 0.707 \\ &\approx 42.7 \text{ cm H}_2\text{O} \end{aligned}$$

$$\begin{aligned} \text{Air content in the sample} &= \text{Air in the sample} \\ &\approx 0.1 \text{ ft}^3 / 16.1 \text{ sec} \times 60 \text{ sec.} \\ &\approx 0.372 \text{ ft}^3 / \text{min.} \end{aligned}$$

$$\begin{aligned} \text{Water content in the sample} &= 73.0 \text{ c.c. / 5 min.} \\ &\approx 0.0322 \text{ lb/min.} \end{aligned}$$

$$\begin{aligned} \underline{\text{Concentration}} &\approx \frac{\text{Water flow (lb/min.)}}{\text{Air flow (ft.}^3/\text{min.)}} \\ &\approx \frac{0.0322}{0.372} \\ &\approx 0.0866 \text{ lb./ft.}^3 \end{aligned}$$

10%.

$$\text{Density} = \frac{\text{Air flow(lb./min.) + water flow(lb./min.)}}{\text{Air flow (ft.}^3\text{/min.)}}$$
$$= \frac{0.372 \times 0.0765(\text{lb./ft.}^3) + 0.0322}{0.372}$$
$$= 0.163 \text{ lb./ft.}^3$$

$$\text{Concentration} = \frac{0.0322}{0.372} = 0.0866 \text{ lb./ft.}^3$$
$$\text{Velocity} = K \sqrt{\frac{h}{\rho_m}}$$
$$= 19.2 \sqrt{\frac{h}{\rho_m}}$$
$$= 185 \text{ ft./sec.}$$

The calculated results are tabulated in Table B.

TABLE 2.

Cast Observations.

Test No.	Sec	Pipe dia. Steel.	Pressure.	Vertical.	Water.	Temp.	Bar.
Water 2100.	28 15.1/2 min.	Nature 2000.	60%	Max. Angle 45°	Mr. Flon (b, c, d)	10.5°	
12-1000. 21	37.2	At Press. 2. H. P.	Atmos. Press. 3.25	Press. At 3.	0.3750.		
Press. 1000. 1-21	20.91 D. 0.	Press. Dens. 2-3.	3.375.				
Station.	0	200	300	400	500	600	700
inches.							
Total.							
Water. Pending	37.0	32.0	55.5	56.0	60.5	63.0	58.0
en. H. O.							
Water 12							
Sample	36.0	43.2	57.0	54.2	73.0	81.0	82.0
0.275 min.							
Kit 12							
Sample	27.6	27.5	26.8	26.2	25.1	25.8	26.0
sec. 0.1 min.							

卷之三

Carteret et al. / Environmental Resuscitation 3

APPENDIX III.

Concentration distribution in a circular pipe was expressed by Equation 9 on page 110. Solution of this equation in cartesian co-ordinates is detailed here.

Solution of the Equation 9.

$$\epsilon \frac{\partial^2 c}{\partial r^2} + \frac{1}{r} \frac{\partial c}{\partial r} + \frac{1}{r^2} \frac{\partial^2 c}{\partial \theta^2} + w \left[ \frac{\partial c}{\partial r} \cos \theta - \frac{\partial c}{\partial \theta} \sin \theta \right] = 0$$

Put  $c = X \cdot Y$ ,  $X = f(x)$  &  $Y = f(y)$

with  $x = r \cos \theta$ ,  $y = r \sin \theta$

$$\begin{aligned}\therefore \frac{\partial c}{\partial r} &= \frac{\partial c}{\partial x} \cdot \frac{\partial x}{\partial r} + \frac{\partial c}{\partial y} \cdot \frac{\partial y}{\partial r} \\ &= \frac{\partial c}{\partial x} \cos \theta + \frac{\partial c}{\partial y} \sin \theta\end{aligned}$$

and

$$\frac{\partial c}{\partial \theta} = \left[ \frac{\partial c}{\partial x} (-\sin \theta) + \frac{\partial c}{\partial y} \cos \theta \right] \cdot r$$

Thus

$$\begin{aligned}\epsilon \nabla^2 c + w \left\{ \left[ \frac{\partial c}{\partial x} \cos \theta + \frac{\partial c}{\partial y} \sin \theta \right] \cos \theta - \sin \theta x \right. \\ \left. \left[ -\sin \theta \frac{\partial c}{\partial x} + \cos \theta \frac{\partial c}{\partial y} \right] \right\} = 0\end{aligned}$$

i.e.,  $\epsilon \nabla^2 c + w \left\{ \left[ \frac{\partial c}{\partial x} \cos^2 \theta + \frac{\partial c}{\partial y} \sin \theta \cos \theta \right] + \left[ \frac{\partial c}{\partial x} \sin^2 \theta - \frac{\partial c}{\partial y} \sin \theta \cos \theta \right] \right\} = 0$

or  $\epsilon \nabla^2 c + w \left( \frac{\partial c}{\partial y} \right) = 0$

$$\epsilon \frac{\partial^2 c}{\partial x^2} + \left( - \frac{\partial^2 c}{\partial y^2} + w \frac{\partial c}{\partial y} \right) = 0$$

which is the expression of concentration differential equation in cartesian coordinates, solution of which can be made as follows:-

put

$$C = X(x) \cdot Y(y) = x \cdot Y$$

then

$$\epsilon(Y \frac{\partial^2 X}{\partial x^2} + X \frac{\partial^2 Y}{\partial y^2}) + wX \frac{\partial Y}{\partial y} = 0$$

$$\therefore [(\epsilon \frac{\partial^2 Y}{\partial y^2}) + w(\frac{\partial Y}{\partial y})] X = -\epsilon Y \frac{\partial^2 X}{\partial x^2}$$

$$\frac{1}{Y} (\epsilon \frac{\partial^2 Y}{\partial y^2} + w \frac{\partial Y}{\partial y}) = -\frac{\epsilon}{x} \frac{\partial^2 X}{\partial x^2}$$

taking both sides to be  $\approx n^2$  (positive)

$$\therefore \frac{\epsilon}{x} \frac{\partial^2 X}{\partial x^2} = n^2$$

and

$$\frac{1}{Y} (\epsilon \frac{\partial^2 Y}{\partial y^2} + w \frac{\partial Y}{\partial y}) = n^2$$

but from:

$$\epsilon \left( \frac{\partial^2 X}{\partial x^2} \right) = -n^2 X$$

so

$$X = A \cos \frac{nx}{\sqrt{\epsilon}} + B \sin \frac{nx}{\sqrt{\epsilon}}$$

$$\epsilon \frac{\partial^2 Y}{\partial y^2} + w \frac{\partial Y}{\partial y} - n^2 Y = 0$$

i.e.,

$$Y = C' e^{m_1 y} + D' e^{m_2 y}$$

where

$(m_1, m_2)$  are roots of

$$\epsilon m^2 + w m - n^2 = 0$$

Thus the solution is

$$C = Y \cdot X$$

and

$$C = [D_1 e^{m_1 y} + D_2 e^{m_2 y}] \sin \left( \frac{nx}{\sqrt{\epsilon}} + \alpha \right)$$

Solution of concentration equation 9 in polar coordinates.

$$\epsilon \frac{\partial^2 c}{\partial y^2} + \epsilon \frac{\partial^2 c}{\partial x^2} + w \frac{\partial c}{\partial y} = 0$$

Writing down

$$c = e^{-\frac{w}{2\epsilon} y} \times U$$

where  $U$  is a function of  $x$  and  $y$  and substituting in equation 9, we obtain

$$\frac{\partial^2 U}{\partial x^2} + \frac{\partial^2 U}{\partial y^2} - \frac{w^2}{4\epsilon^2} U = 0$$

The first part is Laplace's equation

thus

$$\frac{\partial^2 U}{\partial r^2} + \frac{1}{r} \frac{\partial U}{\partial r} + \frac{1}{r^2} \frac{\partial^2 U}{\partial \theta^2} - \frac{w^2}{4\epsilon^2} U = 0$$

putting  $U = R \Theta$

where  $R$  is a function of  $r$  only and  $\Theta$  is a function of  $\theta$  only, we get

$$\frac{R''}{R} + \frac{1}{r} \frac{R'}{R} + \frac{1}{r^2} \frac{\Theta''}{\Theta} - \frac{w^2}{4\epsilon^2} = 0$$

$$\therefore r^2 \frac{R''}{R} + r \frac{R'}{R} - r^2 \frac{w^2}{4\epsilon^2} = K^2 = - \frac{\Theta''}{\Theta}$$

putting  $\frac{\Theta''}{\Theta} = -K^2$

we get  $\Theta = C_K \cos K\theta$  [symmetry about  $y-y$ ]

and

$$r^2 \frac{R''}{R} + r \frac{R'}{R} - r^2 \frac{w^2}{4\epsilon^2} = K^2$$

$$R'' + \frac{1}{r} R' - \left( \frac{w^2}{4\epsilon^2} + \frac{K^2}{r^2} \right) R = 0$$

which is a modified Bessel function of the first kind, giving

$$R = C_2 I_K \left( \frac{w}{2\epsilon} r \right) + C_3 K_K \left( \frac{w}{2\epsilon} r \right)$$

but  $K_k \left( \frac{\omega}{2\epsilon} r \right)$  goes to infinity at  $r = 0$  thus  $K$  must be zero.

$$\therefore R = C_2 I_k \left( \frac{\omega}{2\epsilon} r \right)$$

thus

$$c = e^{-\frac{\omega}{2\epsilon} r \cos \theta} \leq I_k \left( \frac{\omega}{2\epsilon} r \right) C_k \cos k\theta$$

put

$$z = \frac{\omega}{2\epsilon} r$$

$$\text{therefore } c = e^{-z \cos \theta} \leq I_k(z) C_k \cos k\theta$$

putting the boundary condition of no transport of suspensions near the walls at  $r \approx r_0$

$$\begin{aligned} \frac{\partial c}{\partial r} &= -\frac{\omega}{\epsilon} c \cos \theta \\ \frac{\partial c}{\partial r} &= -\frac{\omega}{2\epsilon} \cos \theta \cdot c + \frac{\omega}{2\epsilon} e^{-z \cos \theta} \sum_k C_k \cos k\theta I'_k(z) \\ &\leq \frac{C_0}{2} [\cos(k-1)\theta + \cos(k+1)\theta] I_k(z\omega) \\ &= \sum_k C_k \cos k\theta I'_k(z\omega) \end{aligned}$$

$$\text{where } z_0 \approx z \quad \text{at the wall} \approx \frac{\omega}{2\epsilon} r_0$$

for  $k$  integers

$$\begin{aligned} -\frac{C_1}{2} I_1(z\omega) &= C_0 I'_0(z\omega) \\ -C_0 I_0(z\omega) - \frac{C_1}{2} I'_0(z\omega) &= C_1 I'_1(z\omega) \end{aligned}$$

But

$$I_1(z) = I'_0(z)$$

and

$$I_{k-1}(z) + I_{k+1}(z) = 2 I'_k(z)$$

or

$$C_1 = -2 C_0$$

and

$$C_1 = -C_2 = C_3 = -C_4$$

thus the general solution will be

$$c = c_0 \left[ e^{-2 \cos \theta} (I_0(z) + 2 \sum_{k=1}^{\infty} (-1)^k \cos k\theta I_k(z)) \right]$$

which will add up to

$$c = c_0 \left( e^{-2 z \cos \theta} \right)$$

or

$$c = c_0 \left( e^{-\frac{\omega}{\epsilon} r \cos \theta} \right)$$

the Equation quoted on page 55 as 17.

APPENDIX III(b)Thickness of Laminar Boundary Sublayer  
and its Relation to Distribution of Phases.

As shown on page 68, the liquid mass flow through the layer left on the walls even at high air flow, was proved to be constant.

$$\begin{aligned}\text{Mass flow through this layer} &= \pi d \cdot t \cdot \frac{\sigma_w}{2} \cdot \rho \\ &= \pi d \cdot N \frac{\omega}{U_f} \cdot N \cdot U_f \cdot \rho \\ &= \pi \rho d N^2 \omega\end{aligned}$$

Substituting the values for water,

$$W = 0.000108 \text{ ft.}^3/\text{sec.}$$

and an average  $N = 11.1(5)$  for the range of Reynold's number covered in the experiments.

$$\begin{aligned}\text{Mass flow through the layer} &= \pi \times \frac{1}{2} \times 0.000108 \times 11.1^2 \times 62.4 \times 3600 \\ &= 117 \text{ lb./hr.} \\ &= 2.86 \text{ lb./ft.}^3 \text{ sec.}\end{aligned}$$

This value compares favourably with the value found from Fig. 38, viz., 3.3 lb./ft.<sup>3</sup> sec.

Also, for 1" tube the value of sublayer flow is 85 lb/hr. which is nearly equal to Armand's findings of 83.5 lb./hr.(3)

This calculated value will indicate a means of determining the amount of liquid entrained by subtracting this fixed amount of liquid from the liquid flow rates.

APPENDIX IV.Calculated Results for Concentration Distribution  
in a Vertical Traverse.(a) Drop Size.

The modified expression for the drop size

$$D_d = \frac{585 \sqrt{\sigma}}{v \sqrt{\rho}} + 840 \left( \frac{u}{\sqrt{\sigma \rho}} \right)^{0.45} \left( 1000 \frac{Q_f}{Q_a} \right)^{0.5}$$

The following quantities are considered constant for the tests:-

Surface tension of (tap) water  $\approx 71.5$  dynes/cm.

(as determined by Du Noy Surface tension apparatus)

Viscosity of tap water  $\approx 0.01$  poises

Density of water  $\approx 1$  gm./c.c.

Other values are derived, for example for the test detailed previously,

$$\approx \frac{\text{Water mass rate}}{62.4}$$

$$\approx 0.398$$

Air volume  $Q_a$  calculated as follows:

$$\text{Air pressure} = \frac{b + \text{pressure drop } 1 - 3}{2}$$

$$= 29.3 + \frac{2.3}{2} = 30.95 \text{ Hg.}$$

$$= 15.3 \text{ lb/in}^2.$$

$$\text{Air temperature} = 460 + 67 = 547^\circ\text{Fols.}$$

$$\text{Air specific volume } V_a = \frac{R T_a}{P_a} = 13.37 \text{ cu ft/lb}$$

$$\text{Air volume rate } Q_a = 13.37 \times 9.27$$

$$= 124 \text{ cu ft/min}$$

$$\text{Then } (1000 \frac{Q_e}{Q_a}) = 2.405$$

$$\text{also } (\frac{\mu}{V_a P})^{0.45} = \frac{1}{20.7}$$

$$\text{thus the second term } 840 (1000 \frac{Q_e}{Q_a}) (\frac{\mu}{V_a P})^{0.45} = 62.5 \text{ microns}$$

and the first term

$$= \frac{585 \sqrt{\sigma}}{V_a T_a}$$

$$= \frac{4950}{V_a}$$

$$\text{Velocity of air can be taken as } = \frac{W V_a}{Q_a}$$

where  $a$  = cross sectional area of the pipe m/sec.

i.e.,  $V_a = 0.414 Q_a \text{ m/sec}$

then the first term  
 $= \frac{11950}{Q_a}$   
 $\approx 109.0 \text{ microns.}$

thus  $D_d = 109 + 62.5$   
 $\approx 171.5 \text{ microns.}$

The fall velocity  $w = 18.1 D_d / 1000$   
 $\approx 2.25 \text{ ft/sec}$

Calculation of  $Z_t \rightarrow Z_b$ 

Applying Equation 27, and considering the same test we have

$$\tau_0 = \frac{\Delta P}{\Delta L} \cdot \frac{\pi}{2} \quad (\text{test length of pipe} = 12\text{ft. } \frac{1}{2}\text{ in.})$$

$$= \frac{232}{152.5} \cdot \frac{0.75}{2}$$

$$= 0.575 \text{ lb./ft.}^2$$

$$U_f = \sqrt{\frac{\tau_0 g}{\rho}}$$

$$= 9.80 \text{ ft./sec.}$$

$$U_{f_t} = U_f \sqrt{2 \left( 1 - \frac{r}{r_0} \right) s} \sqrt{\frac{\rho_m}{\rho_t}}$$

$$= 9.80 \sqrt{2 \left( 1 - \frac{1.16}{1.30} \right)} \sqrt{\frac{0.193}{0.123}}$$

$$= 8.87 \text{ ft./sec.}$$

$$U_{f_b} = U_f \sqrt{2 \left( \frac{r}{r_0} \right)} \sqrt{\frac{\rho_m}{\rho_b}}$$

$$= 9.60 \text{ ft./sec.}$$

but  $w = 2.25 \text{ ft/sec}$

$$Z_b = \frac{w}{0.044 U_{f_t}}$$

$$= 0.60$$

$$\text{and } z_b = \frac{w}{0.044 U_f b}$$

$$= 0.53$$

### Calculation of $C_0$ .

According to Equation 29, the value of  $C_0$  for the sample test is  $= 0.110 \text{ lb/ft}^3$

$$\text{thus } C = C_0 \left( \frac{y_o}{y} \right)^{0.6} \quad \text{top}$$

$$C = C_0 \left( \frac{y_o}{y} \right)^{0.53} \quad \text{bottom}$$

is calculated.

The values are tabulated in Tables **III** and **IV**.

TABLE IIIA.

DROP SIZE CALCULATIONS.

Average Pipe Diam. 1.500"

1/2" Glass Pipe.

$$D_d = \frac{585 \sqrt{\sigma}}{\sqrt{a} \sqrt{f}} + 840 \left( \frac{u}{\sqrt{af}} \right)^{0.45} \left( 1000 \frac{Qe}{Qa} \right)^{0.5}$$

Air Flow Rate W <sub>a</sub> ft <sup>3</sup> /min.	Liquid Flow Rate Q <sub>e</sub> ft <sup>3</sup> /min.	1/2" Glass Pipe.					
		1000 $\frac{Qe}{Qa}$	$(1000 \frac{Qe}{Qa})^{0.5}$	$840 \left( \frac{u}{\sqrt{af}} \right)^{0.45}$	$\frac{585 \sqrt{\sigma}}{\sqrt{a} \sqrt{f}}$	D <sub>d</sub> microns	
11.95	157	0.0746	0.475	0.69	28	76	104
12.10	159	0.1325	0.835	0.915	37	75	112
12.20	159.5	0.200	1.255	1.12	45.4	75	120.4
12.30	161.5	0.295	1.83	1.35	54.7	74	128.7
12.30	162	0.414	2.56	1.60	64.8	73.7	138.5
10.9	144.5	0.0746	0.510	0.72	29.2	82.7	111.9
11.08	147.5	0.159	1.09	1.04	42.2	81	123.2
11.1	145.5	0.207	1.43	1.19	48.4	82.2	130.6
11.1	149	0.298	2.00	1.41	57.1	80.2	137.3
11.2	149	0.459	3.03	1.756	71.2	80.2	151.4
10.22	137	0.153	1.112	1.00	43	87.2	130.2
10.25	136.8	0.195	1.43	1.195	48.4	87.8	136.2
10.3	135	0.298	2.21	1.49	60.4	88.5	148.9
10.35	135.6	0.473	3.50	1.87	75.7	88	163.7
9.2	122	0.746	0.611	0.784	31.8	93	129.8
9.30	123	0.153	1.25	1.12	45.4	97.2	142.6
9.35	123.5	0.301	1.64	1.38	51.8	97.0	148.8
9.50	125.5	0.655	4.45	2.11	65.5	95.4	180.9
7.84	104	0.134	1.29	1.135	46.0	114.8	160.8
7.85	104	0.20	1.92	1.38	55.9	114.8	170.7
8.02	106	0.298	2.53	1.66	65.0	114.9	180.9
8.05	105	0.54	5.1	2.25	61.0	113.9	204.9
7.2	95	0.139	1.46	1.21	49	126	175
7.2	95	0.293	3.03	1.76	71	126	197
6.50	85	0.09	1.05	1.025	41.8	142.5	184.3
6.50	86	0.15	1.74	1.322	54.0	142.5	196.5
6.50	86	0.205	2.37	1.54	62.4	139	201.4

Air Flow Rate No.	Q <sub>a</sub> ft <sup>3</sup> /min.	Liquid Flow Rate Q <sub>l</sub> ft <sup>3</sup> /min.	$\frac{1000 Q_l}{Q_a}$	$(\frac{1000 Q_l}{Q_a})^{0.5}$	$840 \left( \frac{\mu}{\sqrt{P_o}} \right)^{0.45}$		$D_q$ microns
					$\lambda \left( \frac{1000 Q_l}{Q_a} \right)^{0.5}$	$\frac{5870}{v_a \sqrt{P}}$	
6.7	88.5	0.296	3.36	1.83	74.2	135	209.2
6.90	91	0.49	5.4	2.32	94.0	131	225
6.90	94	0.192	2.4	1.55	62.7	142	204.7
6.96	94	0.356	4.89	2.46	63.5	142	225.5
6.96	84	0.501	6.00	2.46	98	142	240
6.04	80	0.228	3.85	2.69	69.5	149.5	218
6.04	80	0.344	4.80	2.87	83.7	149.5	233.2
6.04	80	0.462	5.76	2.40	97	149.5	246.5
5.5	72.5	0.15	2.00	1.44	50.3	164.8	223.1
5.55	73	0.235	3.21	1.79	72.6	163.7	236.2
5.55	73	0.294	4.09	2.01	81.3	163.7	244.9
5.56	73.8	0.52	7.1	2.67	100	163.3	271.2

TABLE III B.  
CALCULATIONS OF Z VALUES.  
(1 1/2" I. D. Glass Pipe)

Test No.	0.4 U <sub>sp</sub>	0.4 U <sub>cp</sub>	Drop Size	Refl. Vel.	Z <sub>g</sub>	Z <sub>b</sub>
	w	w			0.40 ft.	0.40 ft.
V <sub>x</sub>	A 5.9	5.9	104	1.37	0.231	0.231
	B 5.9	5.95	112	1.48	0.250	0.250
	C 5.53	5.9	120.4	1.60	0.278	0.27
	D 6.55	5.45	128.7	1.7	0.26	0.311
	E 5.22	5.65	136.5	1.82	0.347	0.322
V <sub>xI</sub>	A 5.45	5.63	111.0	1.46	0.27	0.26
	B 5.45	5.63	123.2	1.62	0.297	0.287
	C 5.05	5.63	130.6	1.72	0.34	0.305
	D 4.85	5.63	137.3	1.81	0.378	0.36
	E 4.75	5.60	151.4	1.90	0.42	0.36
V <sub>xII</sub>	A 5.27	5.27	130.2	1.73	0.39	0.33
	B 5.20	5.16	136.2	1.79	0.326	0.334
	C 5.22	4.67	148.9	1.95	0.372	0.418
	D 5.05	5.13	163.7	2.15	0.423	0.413
V <sub>xIV</sub>	A 5.31	5.05	129.6	1.7	0.33	0.330
	B 4.25	4.5	142.6	1.86	0.427	0.413
	C 4.8	4.4	148.6	1.95	0.455	0.443
	D 3.68	3.18	160.9	2.47	0.642	0.768
V <sub>y</sub>	A 3.50	3.67	104.3	2.42	0.703	0.660
	B 3.62	4.45	190.7	2.335	0.585	0.503
	C 3.67	7.38	199.9	2.37	0.648	0.554
	D 3.47	3.09	204.9	2.605	0.772	0.863
V <sub>xy</sub>	A 3.45	3.67	184.3	2.42	0.703	0.660
	B 2.70	3.68	196.5	2.575	0.920	0.700
	C 2.04	-	201.4	2.64	0.920	-
	D -	-	82.5	0.69	-	-
	E -	-	88	0.79	-	-

Test No.	0.4 $U_{fb}$	0.4 $U_{fb}$	Drop Size	Fall Vel.	$Z_b$ $w$	$Z_b$ $w$
					$0.40 ft$	$0.40 ft$
VIII A	3.51	3.04	228.1	3.92	0.832	1.030
B	3.49	3.54	236.3	3.99	0.867	1.218
C	3.57	1.96	244.9	3.21	0.918	1.635
D	2.840	2.36	271.8	3.54	1.245	1.5
A	4.47	3.32	175.7	3.29	0.51	0.69
D	4.31	3.11	297	3.57	0.60	0.83
A	3.82	1.64	204.7	3.68	0.81	1.05
B	3.68	1.86	225.5	3.95	0.91	1.59
C	4.4	2	200	3.15	0.72	1.59
A	3.4	3.2	210	3.86	0.845	0.9
B	3.56	2	233.2	3.05	0.86	1.52
C	3.1	2.4	246.5	3.22	1.04	2.30

TABLE III.C.

## PHASE DISTRIBUTION. CALCULATED RESULTS.

<sup>1</sup>" Glass Pipe. Pep Kebab. Vertical Traverses.

$\frac{D}{D_2}$	Water Flow	$\frac{P}{P_2}$	$\frac{V}{V_2}$	$\frac{P_m}{P_2}$	$\sqrt{\frac{P_m}{P_2}}$	$y_m$	$\sqrt{\frac{y_m}{y_b}}$	$U_f$ ft/ sec.	$U_h$	$U_{f,b}$
1.0	0.054	0.0345	0.0895	0.132	0.93	0.963	0.80	1.032	14.9	14.8
1.2	0.352	0.1198	0.124	0.134	0.93	0.945	0.780	1.02	15.4	14.9
1.3	1.1	0.1705	0.177	0.20	0.93	0.925	0.800	1.032	14.4	14.8
1.4	25.2	0.1085	0.1865	0.233	0.92	0.910	0.810	1.057	14.3	13.6
1.5	35	0.2295	0.217	0.275	0.927	0.910	0.900	1.095	13.1	14.2
1.6	6.25	265	0.62	0.102	0.960	0.170	1.02	0.85	0.800	1.032
1.7	31.3	345	0.353	0.139	0.130	0.157	0.92	0.800	1.032	14.1
1.8	17	448	1.11	0.177	0.167	0.138	0.985	0.94	0.860	1.07
1.9	25.2	500	1.287	0.195	0.201	0.202	0.95	0.950	1.082	12.6
2.0	35	590	1.43	0.217	0.243	0.295	1.02	0.933	0.940	1.32
2.1	6.25	6.32	250	0.62	0.102	0.130	0.170	0.95	0.770	1.032
2.2	31.3	13.45	350	0.353	0.139	0.130	0.157	0.94	0.780	1.02
2.3	17	16.85	368	0.360	0.167	0.165	0.138	0.985	0.920	1.045
2.4	25.2	24.8	445	1.10	0.243	0.201	0.202	0.95	0.880	1.085
2.5	35	37.9	522	1.462	0.256	0.243	0.295	1.02	0.933	1.32
2.6	6.25	13	325	0.752	0.1335	0.132	0.153	1.017	0.95	0.770
2.7	31.3	36.5	362	0.392	0.162	0.150	0.170	1.04	0.95	0.780
2.8	17	25	356	0.375	0.195	0.1685	0.250	1.035	0.895	1.045
2.9	25.2	39	558	1.380	0.2576	0.242	0.295	1.021	0.932	0.880
3.0	35	12.8	210	0.520	0.10	0.093	0.109	1.02	0.96	0.76
3.1	6.25	17	234	0.578	0.134	0.151	0.157	0.942	0.925	0.80
3.2	31.3	27.2	286	0.520	0.186	0.155	0.242	1.10	0.895	1.02
3.3	17	47	325	1.30	0.324	0.234	0.372	1.18	0.695	1.06
3.4	25.2	35	12.35	12.35	12.35	12.35	12.35	12.35	12.35	12.35

/.

$\Delta P$	$T_0$	$\frac{P_b}{P_e}$	$T_e$	$P_b$	$\sqrt{\frac{P_e}{P_b}}$	$U_e$	$\sqrt{\frac{P_e}{P_b}}$	$U_b$	$\frac{dP}{dt}$	$U_{fr}$	$\frac{dP}{dt}$	$\frac{dP}{dt}$
in.	deg	cm. <sup>2</sup> /cm. <sup>2</sup>	deg.	cm. <sup>2</sup> /cm. <sup>2</sup>		cm.		cm.	cm. <sup>2</sup> /sec.	cm.	cm. <sup>2</sup> /sec.	cm. <sup>2</sup> /sec.
10.62	17.2	0.458	0.385	0.317	0.197	2.09	0.36	0.320	1.046	10.2	0.36	10.6
10.73	23.9	0.563	0.187	0.140	0.250	1.064	0.813	0.349	1.06	10.45	0.05	10.6
6.9	25.7	0.592	0.216	0.170	0.295	1.13	0.537	0.329	1.06	10.15	0.20	10.7
20.9	43.8	0.342	0.288	0.233	0.593	1.19	0.32	1.00	1.155	9.70	0.37	7.72
8.7	76	0.24	0.092	0.083	0.116	1.05	0.89	0.349	1.06	0.24	0.17	0.71
9.2	17.2	0.359	0.134	0.117	0.370	1.37	0.705	0.559	1.066	9.25	0.22	6.95
9.4	25.3	0.437	0.267	0.139	0.228	1.39	0.54	0.369	1.13	7.24	0.12	4.42
9.4	21.4	0.720	0.205	0.160	0.608	1.33	0.315	1.00	1.16	9	0.35	7.15
7.32	12.65	109	0.247	0.048	0.306	0.306	0.1	0.226	1.055	0.82	1.045	8.9
7.55	19.8	123	0.394	0.148	0.44	0.44	0.55	0.577	0.98	1.11	6.12	6.7
7.56	22.3	136	0.336	0.135	0.109	0.55	1.23	1.23	0.90	1.10	8.10	6.9
7.60	23.8	205	0.50	0.259	0.188	0.535	1.18	1.07	1.39	7.38	7.1	5.9

TABLE IX.Calculation of Theoretical Phase Distribution

Air Flow 12.5 lb./ft.<sup>2</sup> sec. Motor Flow 12.9 lb./ft.<sup>2</sup> sec.  
 $C_0 = 0.020 \text{ lb./ft.}^2 \text{ (air).}$

Section	Bottom Half: $Z_b=0.336$					Top Half: $Z_t=0.320$		
y ins.	0.1	0.2	0.4	0.6	0.8	1.00	1.20	1.30
$y_0/y$	7.5	3.75	1.875	1.25	0.94	0.75	0.625	0.58
$(y_0/y)^2$	5.625	1.5625	1.325	1.073	0.93	0.92	0.87	0.84
$C_0 \left(\frac{y_0}{y}\right)^2$	0.032	0.0332	0.0347	0.0315	0.0196	0.0184	0.0174	0.0168

Air Flow 12.65 lb./ft.<sup>2</sup> sec. Water Flow 17 lb./ft.<sup>2</sup> sec.  
 $C_0 = 0.045 \text{ lb./ft.}^2 \text{ (air).}$

Section	Bottom Half: $Z_b=0.419$					Top Half: $Z_t=0.487$		
y ins.	0.10	0.20	0.40	0.60	0.80	1.00	1.20	1.30
$y_0/y$	7.5	3.75	1.875	1.25	0.94	0.75	0.625	0.58
$(y_0/y)^2$	5.625	1.5625	1.325	1.073	0.941	0.88	0.822	0.782
$C_0 \left(\frac{y_0}{y}\right)^2$	0.1035	0.078	0.0662	0.0493	0.0493	0.396	0.0370	0.0352

Air Flow. 12.7 lb./ft.<sup>2</sup> sec. Water Flow 27.1 lb./ft.<sup>2</sup> sec.  
 $C_o = 0.083 \text{ lb./ft.}^3 \text{ (air)}$

Section	Bottom Half: $Z_b=0.143$					Top Half: $Z_t=0.456$		
y in.	0.1	0.2	0.4	0.6	0.80	1.00	1.20	1.30
$\frac{y}{y}$	7.5	3.75	1.875	1.25	0.94	0.75	0.625	0.56
$(\frac{y_0}{y})^2$	2.44	1.6	1.322	1.104	0.973	0.876	0.803	0.765
$C_o (\frac{y_0}{y})^2$	0.202	0.149	0.11	0.0855	0.061	0.0725	0.067	0.066

Air Flow 12.65 lb./ft.<sup>2</sup> sec. Water Flow 47 lb./ft.<sup>2</sup> sec.  
 $C_o = 0.20 \text{ lb./ft.}^3 \text{ (air)}$

Section	Bottom Half: $Z_b=0.769$					Top Half: $Z_t=0.642$		
y in.	0.10	0.20	0.40	0.60	0.80	1.00	1.20	1.30
$\frac{y_0}{y}$	7.5	3.75	1.875	1.25	0.94	0.75	0.605	0.53
$(\frac{y_0}{y})^2$	4.7	2.76	1.62	1.186	0.98	0.827	0.756	0.700
$C_o (\frac{y_0}{y})^2$	0.94	0.552	0.324	0.237	0.192	0.1655	0.147	0.140

APPENDIX V.Velocity Curves:

According to Chapter VI, page 72, velocity was plotted against distance  $y$  on log-log scales and the values of the gradients  $n$  were obtained. These values are tabulated for the  $1\frac{1}{2}$ " I.D. and 2" I.D. pipes.

For the  $1\frac{1}{2}$ " I.D. pipes the values of  $n$  were nearly constant for water flow rates, thus the average values were tabulated.

Average Values for  $1\frac{1}{2}$ " I.D. Glass and Steel PipesTop Part of Pipe.

Average Water Flow rate $lb/ft.^2 sec.$	12.7	17.3	24.8
Value of ( $n$ )	3.20	3.56	3.96

Bottom Part of Pipe.

Average Water Flow $lb/ft.^2 sec.$	12.7	17.65	24.8
Value of ( $n$ )	3.03	3.39	3.89

Water Flow lb/hr.	Air Flow (Orifice "Hg)									
	15	11	8.6	5	3	Top	Bottom	Top	Bottom	Top
280	6.32	6.14	6.63	6.14	3.72	4	3.22	3.08	2.00	1.90
560	6.70	3.70	4.6	4.60	3.14	4.70	3.64	2.76	4.44	2.42
743	-	-	*	*	2.86	2.96	2.05	1.82	2.62	1.14
1120	-	-	*	*	3.00	3.48	1.93	1.90	-	-

It can be noted from the Table for 1" I.D. steel pipe that because of the change of flow pattern, the value of  $n$  changes correspondingly and  $n$  does not attain any constant values for a certain particular water flow.

APPENDIX VI.

It has been pointed out in Chapter VII, page 82, that a fundamental relationship between the main values affecting turbulent characteristics in a two-phase flow was sought and a universal relationship was sought similar to that conception of mixing length in single phase flow.

The different curves obtained of velocity and phase distribution were correlated by

$$\tau = \rho \ell^2 \left( \frac{du}{dy} \right)^2$$

The values of  $\frac{du}{dy}$  were obtained by the method of differences from the velocity diagrams at constant values of (i.e., constant value of concentration  $C$ ) and the value of  $\tau$  was calculated from

$$\frac{\Delta P}{\Delta L} \cdot \frac{r}{2} = \tau_0$$

$$\tau = \tau_0 \left( \frac{r}{r_0} \right)$$

The values were so calculated to give a relationship between

$$y \quad \text{and} \quad \frac{\tau}{\left( \frac{du}{dy} \right)^2}$$

Sample of calculation.

For 12" I.D. Steel pipe (1.690" actual I.D.)

for  $C = 0.125 \text{ lb/ft.}^3$  air.

$$y = 0.34 \text{ ft.}$$

$$P = 129 \text{ lb/ft.}^2$$

$$\frac{du}{dy} = 1800$$

$$T_0 = \frac{\Delta P}{\rho L} \cdot \frac{f}{2} = \frac{120}{12.85} \cdot \frac{0.75}{212} = 0.322 \text{ lb./in.}^2$$

$$T = T_0 \left( \frac{r}{r_0} \right)$$

$$\text{but } \approx 1.2$$

$$\approx 0.322 \times \frac{0.75}{1.1}$$

$$\approx 0.23 \text{ lb./in.}^2$$

$$\approx 0.0705$$

The results for 1/2" glass and steel pipe are tabulated in the following tables.

The inconsistency of the relationships can be attributed to the difficulty in the calculation of  $\frac{du}{dy}$  particularly near the boundary.

TABLE VIIA.Pressure Drop for  $\frac{1}{2}$ " I.D. Glass Pipe.

Actual I.D. = 1.500

Length between pressure points = 12.71 ft.

Test	Air Flow lb./ft. <sup>2</sup> .sec.	Water Flow lb./ft. <sup>2</sup> .sec.	Pressure Drop 1 - 2	Pressure Drop 2 - 3
V <sub>1</sub>	16.2	6.23	156	265
	16.3	11.30	171	343
	16.3	16.95	244	440
	16.4	25.20	356	500
	16.4	35.0	395	500
V <sub>1.2</sub>	14.8	6.32	170	350
	14.9	13.40	203	388
	14.9	16.65	220	446
	14.9	24.80		
	15.05	37.0	206	592
V <sub>1.2.2</sub>	13.9	13	160	305
	13.9	16.5	176	362
	13.9	25	209	396
	14	39	265	558
V <sub>1.7</sub>	12.5	6.30		210
	12.6	13.9		234
	12.65	17		296
	12.85	47		486
V <sub>7</sub>	10.7	11.3	88	182
	10.73	17.1	113	230
	10.9	25.7	146	281
	10.9		176	342
V <sub>7.4</sub>	8.6	6.4	47	95
	8.6	13.65	-	141
	8.6	17.9	-	156
	8.6	25.3	91	177
	8	41.0		300
V <sub>7.5.2</sub>	7.62	12.65	84	104
	7.55	19.0	101.5	129
	7.56	24.6	667	136
	7.60	43.0	108.5	209

TABLE VFriction Coefficient with 2-Phase Flow for  $1\frac{1}{2}$ " Glass Pipe.

Actual Diam. = 1.500"

Length between measuring points = 12.71 ft.

Air Flow lb./ft. <sup>2</sup> sec.	Water Flow lb./ft. <sup>2</sup> sec.	Pressure			Average Velocity ft./sec.	$\lambda$	Reg.
		Dry lb./ft. <sup>2</sup>	Average Density lb./ft. <sup>3</sup>				
16.4	35	590	228	0.2295	0.031	173500	
16.4	25.8	500	228	0.1935	0.0309	173500	
16.3	17	446	232	0.1705	0.0315	172200	
16.3	11.8	346	241	0.1198	0.030	171000	
15.05	37.9	592	202.3	0.256	0.032	158000	
14.90	24.8	445	202	0.2143	0.035	157000	
14.90	16.85	390	213	0.1617	0.036	157000	
14.90	13.45	352	214	0.139	0.035	156000	
12.85		480	166	0.324	0.0393	134000	
12.7	17.1	307	143	0.188	0.04	134000	
12.6	12.9	234	168	0.134	0.0300	133000	
10.9	43.8	342	136.5	0.2880	0.0407	111000	
10.9	25.7	261	123	0.235	0.0500	111000	
10.73	17.1	230	139	0.1670	0.0445	114000	
10.62	11.8	182	143	0.1385	0.0407	116000	

TABLE V A

Friction Coefficient with 2-Phase Flow,  
for 1 $\frac{1}{2}$ " Steel Pipe.

Actual Diam. = 1.032" Length between Measuring Points = 11.5 ft

Air Flow lb./ft. <sup>2</sup> sec.	Water Flow lb./ft. <sup>2</sup> sec.	Pressure Drop lb./ft. <sup>2</sup>	Average Velocity ft./sec.	Average Density lb./ft. <sup>3</sup>	$\lambda$	Reg.
9.8	36	304	112.8	0.329	0.03	57700
9.15	27	247	132	0.2364	0.031	69500
8.95	13.5	210	130	0.1496	0.040	69500
12.9	54	605	152.6	0.373	0.0385	80600
12.7	36	446	158.5	0.3427	0.036	83500
12.4	27	380	159.3	0.2193	0.032	84200
12	13.5	156.6	156.6	0.1267	0.036	82600
16.8	54	727	220.8	0.3479	0.02	121,700
17.8	36	620	241.1	0.2484	0.0203	127,000
17.3	27	501	245.8	0.1891	0.0211	126,000
17.3	13.5	330	239.9	0.1215	0.0236	126,000
20.2	27	620	270.5	0.2193	0.020	143,000
19.0	13.5	436	274.5	0.1315	0.02	143,500
24.8	27	911	321.6	0.2049	0.0186	17,500
23.6	13.5	564	329.5	0.1376	0.0196	17,500

135.  
1 $\frac{1}{2}$ " I.D. Steel Pipe.

Values of  $(\frac{\partial v}{\partial y})^2$  at  $G = 0.1$  lb./ft.<sup>3</sup> (air).

Water Flow lb./ft. <sup>2</sup> sec.	Air Flow lb./ft. <sup>2</sup> sec.	$\Delta F$	$\frac{du}{dy}$	$\frac{v}{y}$	1 $\frac{1}{2}$ " ft.	$y$ , in.	T lb./ ft. <sup>2</sup>	$(\frac{\partial v}{\partial y})^2$ $\times 10^6$
9.4	25.2	0.4	129	1600	0.832	1.1	0.212	0.0313
9.4	41.4	0.8	155.5	0	0.40	1.26	0.146	-
12.7	27.1	0.35	233	744	0.57	1.14	0.415	0.721
12.85	47.0	1.37	290	1360	0.746	1.24	0.044	0.360
14.9	24.8	0.75	263	1070	0.69	1.2	0.465	0.410
15.05	37.0	1.10	403	514	1.04	1.26	0.132	0.044
16.3	17	0.12	277	2690	0.707	0.76	0.60	0.138
16.4	25.2	0.6	367	1080	0.95	0.705	0.355	0.305
16.4	35	1.27	439	1440	1.15	1.04	0.140	0.0677

Values of  $(\frac{\partial v}{\partial y})^2$  at  $G = 0.125$  lb./ft.<sup>3</sup> (air).

Water Flow lb./ft. <sup>2</sup> sec.	Air Flow lb./ft. <sup>2</sup> sec.	$\Delta F$	$\frac{du}{dy}$	$\frac{v}{y}$	1 $\frac{1}{2}$ " ft.	$y$ , in.	T lb./ ft. <sup>2</sup>	$(\frac{\partial v}{\partial y})^2$ $\times 10^5$
9.4	25.2	0.34	129	1600	0.832	1.1	0.23	0.0705
9.4	41.4	0.55	155.5	915	0.400	1.26	0.225	0.048
12.7	27.1	0.56	233	1360	0.57	1.02	0.310	0.127
12.85	47.0	1.04	290	0	0.746	1.08	0.703	-
14.9	24.8	0.42	263	1690	0.69	1.20	0.23	0.067
15.05	37.0	0.62	403	1630	1.04	1.26	0.53	0.200
16.3	17	0.4	367	1440	0.95	1.04	0.535	0.282
16.4	25.2	0.60	439	1920	1.15	0.96	0.43	0.116

1. D. Steel Pipe

Values of  $(\frac{\bar{w}}{w_0})^2$  at  $G = 0.15 \text{ lb.}/\text{ft.}^3$  (air)

Water Flow Air Flow	$\Delta P$	$\frac{r_o}{r}$	$\frac{T}{T_0}$	$\frac{\bar{w}}{w_0} \times 10^6$				
lb./ft. <sup>2</sup> sec.	lb./ft. <sup>2</sup> sec.	y	lb./ft. <sup>2</sup>	$\frac{dr}{dy}$	lb./ft. <sup>2</sup>	y <sub>m</sub>	lb./ft. <sup>2</sup>	$(\frac{\bar{w}}{w_0})^2$
9.4	26.3	0.3	139	2160	0.332	1.10	0.242	0.051
9.4	41.4	0.38	155.5	246.0	0.40	1.26	0.28	0.045
12.7	27	0.4	233	2100	0.60	1.240	0.194	0.042
12.85	27	0.67	290	1610	0.746	1.16	0.315	0.122
14.9	24.8	0.26	263	2400	0.78	1.2	0.153	0.265
15.05	37.9	0.60	403	1540	1.04	1.26	0.47	0.198
16.4	25.2	0.39	367	1320	0.95	0.96	0.563	0.325
16.4	35	0.75	439	1040	1.15	1.04	0.32	0.295

Values of  $(\frac{\bar{w}}{w_0})^2$  at  $G = 0.175 \text{ lb.}/\text{ft.}^3$  (air).

Water Flow Air Flow	$\Delta P$	$\frac{r_o}{r}$	$\frac{T}{T_0}$	$\frac{\bar{w}}{w_0} \times 10^6$				
lb./ft. <sup>2</sup> sec.	lb./ft. <sup>2</sup> sec.	y	lb./ft. <sup>2</sup>	$\frac{dr}{dy}$	lb./ft. <sup>2</sup>	y <sub>m</sub>	lb./ft. <sup>2</sup>	$(\frac{\bar{w}}{w_0})^2$
9.4	26.3	0.28	139	2940	0.332	1.1	0.245	0.285
9.4	41.4	0.32	155.5	1800	0.40	1.26	0.3	0.363
12.7	27	0.3	233	3120	0.57	1.16	0.422	0.435
12.85	27	0.65	290	1440	0.746	1.24	0.358	0.173
14.9	24.8	0.12	263	4600	0.69	1.2	0.622	0.27
15.05	37.9	0.52	403	1680	1.04	1.26	0.6	0.213
16.4	25.2	0.08	367	360	0.95	1.04	0.89	0.068
16.4	35	0.30	439	2280	1.15	0.96	0.79	0.152

TABLE V

Evaluation of  $(\frac{T}{\frac{du}{dy}})^2$  -  $1\frac{1}{2}$ " Glass Pipe

Constant  $\theta = 0.076 \text{ lb/ft.}^2 \text{ (air).}$

Air Flow lb/ft. <sup>2</sup> sec.	Water Flow lb/ft. <sup>2</sup> sec.	$y$	$\frac{du}{dy}$	$T$ lb/ft. <sup>2</sup>	$(\frac{T}{\frac{du}{dy}})^2$ $\times 10^6$
16.3	16.95	0.82	665	0.0328	0.747
14.9	13.4	0.50	1300	0.32	0.099
14.9	16.85	0.84	630	0.0219	0.54
13.9	13	0.4	1970	0.357	0.092
13.9	16.5	0.85	900	0.0355	1.06
12.6	12.9	0.22	2000	0.41	0.102
12.65	17	0.75	600	0.0206	0.572
10.73	17.1	0.27	2260	0.388	0.076
10.9	25.7	0.89	335	0.016	1.44
6.7	17.3	0.38	1640	0.232	0.063
6.7	25.3	0.68	1040	0.159	0.146
7.50	24.0	0.56	1400	0.129	0.0655

TABLE Y.

Evaluation of  $(\frac{T}{(dy)^2})$  - 1½" Glass Pipe

Constant  $C = 0.126 \text{ lb/ft.}^2 (\text{dy})$ .

Air Flow lb/ft. <sup>2</sup> sec.	Water Flow lb/ft. <sup>2</sup> sec.	y	$\frac{dy}{dy}$	T lb/ft. <sup>2</sup>	$(\frac{T}{(dy)^2}) \times 10^6$
16.3	16.95	0.14	3700	0.93	0.066
16.3	25.2	0.50	1450	0.8	0.36
16.3	35	1.05	900	0.285	0.31
14.9	16.85	0.240	2500	0.755	0.113
14.9	24.80	0.75	477	0.173	0.76
12.6	16.5	0.5	760	0.582	1.00
12.6	22.9	0.08	6500	0.55	0.013
11	17.3	0.2	2520	0.355	0.056

Calculation of "Slip" between the phases.

"Slip" is defined as the ratio between gas and liquid velocities. It was determined by the use of the quick closing cocks which would determine the cross sectional area occupied by each phase and hence by knowing the rates of flow of each phase  $\frac{V_g}{V_L}$  was calculated.

Sample of Calculation:

For test carried on 1<sup>1/2</sup> I.D. Pipe.

$$\text{Rate of liquid flow.} \approx 39 \text{ lb./ft.}^2 \text{ sec.}$$

$$\text{* * air flow.} \approx 0.122 \text{ lb./ft.}^2 \text{ sec.}$$

$$\text{Average air temperature.} \approx 67^\circ\text{F.}$$

$$\text{Air pressure.} \approx 15.9 \text{ lb./in.}^2.$$

$$\text{Quantity of water trapped.} \approx 856 \text{ c.c.}$$

$$\text{Distance between cocks} \approx 11.5 \text{ ft.}$$

$$R_L = \frac{39 \times 144}{453.4 \times 62.4 \times 11.5 \times 31.032} \\ \approx 0.456$$

$$R_g = 0.504$$

$$\text{Water velocity} = \frac{39}{0.456} \approx \frac{1}{62.4}$$

$$\approx 1.87 \text{ ft./sec.}$$

$$\text{Air volume} = \frac{58.3 \times (460+67)}{15.9 \times 144}$$

$$\approx 12.2 \text{ ft.}^3/\text{lb.}$$

Air velocity.	= $\frac{0.121}{0.554} \times 12.3$
	= 2.66
Slip	= 1.94 $\text{ft.}/\text{sec.}$

The results thus calculated are shown in the following Tables.

TABLE VI.

Liquid flow rate = 39 lb./ft.<sup>2</sup> sec.

Gas Flow G <sub>g</sub> lb./ft. <sup>2</sup> sec.	Air Pressure lb/in <sup>2</sup> abs.	R <sub>L</sub> = $\frac{x_L}{V_L}$	Liquid Vol. V <sub>L</sub> ft/sec.	R <sub>G</sub> = $\frac{x_G}{V_G}$	Gas Velocity V <sub>G</sub> ft/sec.	Slip = V <sub>G</sub> / V <sub>L</sub>
0.121	19.9	0.456	1.37	0.554	2.66	1.94
0.31	15.8	0.339	1.623	0.661	3.90	2.14
0.361	15.6	0.290	2.16	0.71	6.12	2.84
0.536	15.6	0.267	2.34	0.738	8.90	3.80
1.30	15.8	0.199	3.14	0.801	19.50	6.2
2.16	15.6	0.172	3.64	0.828	32.40	8.9
3.0	16.2	0.124	5.05	0.876	53.0	10.42
3.96	16.6	0.107	5.84	0.893	70	12
6.61	16.6	0.070	8	0.932	84.5	10.5
9.43	17.1	0.064	9.75	0.936	115	11.8
13.88	17.8	0.042	11.40	0.958	159.5	13.8
19.23	19.1	0.03	20.8	0.97	203	9.9

Liquid Flow rate 85 lb./ft.<sup>2</sup> sec.

0.118	16	0.596	2.28	0.404	5.56	1.57
0.224	15.8	0.400	2.91	0.532	5.12	1.76
0.357	15.7	0.383	3.5	0.612	7.10	2.03
0.519	15.7	0.344	3.96	0.656	9.6	2.43
1.28	15.8	0.256	5.27	0.742	21	4
2.07	16.0	0.199	6.93	0.801	31.5	4.6
3.61	16.4	0.175	7.8	0.825	53.5	6.85
5.16	16.7	0.148	9.2	0.852	71.5	7.76
6.68	17.4	0.124	11	0.876	91.3	8.36
9.29	18.1	0.104	13	0.896	133	10.3
13.9	19.6	0.077	17.6	0.923	173	9.9
19.7	22.3	0.062	22	0.936	233	10.8

Liquid Flow Rate 119 lb./ft.<sup>2</sup> sec.

Gas Flow G <sub>G</sub> lb./ft. <sup>2</sup> . sec.	Liq. Pressure lb/in. <sup>2</sup> abs.	R <sub>G</sub> $\frac{V_L}{V_G}$	Liquid vol. V <sub>L</sub> ft. <sup>3</sup> /sec.	R <sub>L</sub> $\frac{V_G}{V_L}$	Gas Velocity V <sub>G</sub> ft./sec.	Slips $\frac{V_G}{V_L}$
0.119	16.1	0.628	9	0.362	4	1.33
0.213	16	0.599	8.58	0.461	6	1.70
0.353	15.9	0.419	4.54	0.589	7.56	1.66
0.53	15.9	0.351	5.40	0.640	9.0	1.83
1.23	16.2	0.275	6.90	0.724	22	3.18
2.20	16.5	0.224	8.15	0.768	35	4.29
3.75	17.0	0.184	10.8	0.813	55.5	5.4
5.46	17.5	0.171	11.1	0.829	79	7.1
6.52	18	0.143	13.3	0.857	90	6.8
9.20	18.5	0.12	15.8	0.880	121	7.6
14.0	20.4	0.093	30.4	0.907	173	8.4
19.1	23.1	0.077	24.7	0.939	227	9.2

Liquid Flow Rate 185 lb./ft.<sup>2</sup> sec.

0.122	16.5	0.732	4.05	0.268	5.4	1.33
0.206	16.5	0.614	4.82	0.386	6.3	1.8
0.361	16.5	0.489	6.07	0.511	6.82	1.38
0.526	16.5	0.445	6.65	0.556	11.20	1.68
1.30	17	0.316	9.40	0.684	22	2.34
2.18	17.5	0.258	11.40	0.742	38.4	2.93
3.89	18	0.234	12.70	0.765	57	4.5
5.6	19	0.187	15.80	0.813	70	4.42
6.55	19.7	0.181	16.40	0.819	80	4.87
9.45	20.4	0.148	20	0.852	106	5.3
14.1	23.6	0.123	24.3	0.876	134	5.4
19.8	25.0	0.098	30.8	0.902	168	5.55

TABLE VII.

Pressure Drop Correlation.

$$G_L = 39 \text{ lb/ft.}^2 \text{ sec.} \quad (\frac{\Delta P}{\delta L})_L = 0.16267 \text{ lb/ft}^3$$

$G_L$ lb/ft. <sup>2</sup> sec.	$(\frac{\Delta P}{\delta L})_{T.P.}$ lb/ft. <sup>2</sup>	$R_L = \frac{x_L}{X}$	$\frac{1}{R_L} = \frac{X}{x_L}$	$(\frac{\Delta P}{\delta L})_{T.P.}$ $(\frac{\Delta P}{\delta L})_L$
0.121	0.31	0.456	2.19	1.00
0.210	0.47	0.389	2.95	2.08
0.360	0.94	0.290	3.45	5.78
0.536	1.25	0.267	3.75	7.70
1.30	1.56	0.199	5.02	9.60
2.16	2.96	0.172	5.82	18.20
3.60	5.77	0.124	8.06	35.40
5.36	9.20	0.107	9.35	56.50
6.61	13.00	0.070	12.82	78.70
9.42	19.80	0.064	15.60	122.00
13.88	31.17	0.042	23.80	195.00
19.22	43.7	0.030	33.30	268.00

$$G_L = 85 \text{ lb/ft.}^2 \text{ sec.} \quad (\frac{\Delta P}{\delta L})_L = 0.60763 \text{ lb/ft}^3$$

$G_L$ lb/ft. <sup>2</sup> sec.	$(\frac{\Delta P}{\delta L})_{T.P.}$ lb/ft. <sup>2</sup>	$R_L = \frac{x_L}{X}$	$\frac{1}{R_L} = \frac{X}{x_L}$	$(\frac{\Delta P}{\delta L})_{T.P.}$ $(\frac{\Delta P}{\delta L})_L$
0.116	1.17	0.596	1.68	1.00
0.224	1.64	0.468	2.14	2.69
0.357	2.34	0.386	2.58	4.00
0.519	2.96	0.344	2.90	4.86
1.26	5.0	0.250	3.88	6.20
2.67	7.03	0.199	5.02	11.60
3.61	12.5	0.175	6.28	20.6
5.16	17.2	0.148	7.24	28.30
6.68	21.5	0.124	8.06	35.50
9.29	29.8	0.104	9.62	49.20
13.9	48.4	0.077	13.00	80
19.7	66.4	0.062	16.10	109

$$G_L = 119 \text{ lb/ft}^2 \text{ sec. } \left( \frac{\Delta P}{\delta L} \right)_L = 1.1189 \text{ lb/ft}^2$$

$G$ lb/ft. <sup>2</sup> sec.	$\left( \frac{\Delta P}{\delta L} \right)_{T.P.}$ lb.ft. <sup>2</sup>	$R_L \cdot X$	$\frac{1}{R_L} \cdot \frac{X}{X_L}$	$\left( \frac{\Delta P}{\delta L} \right)_{T.P.}$ $\left( \frac{\Delta P}{\delta L} \right)_L$
0.119	1.25	0.638	1.565	1.745
0.213	2.65	0.539	1.855	2.370
0.353	3.67	0.419	2.39	3.28
0.520	4.59	0.351	2.85	4.11
1.230	8.12	0.276	3.68	7.27
2.20	11.85	0.384	4.27	10.60
3.75	17.90	0.184	5.43	16.0
5.46	24.60	0.171	5.85	22.0
6.53	29	0.143	7.0	26.0
9.28	38.4	0.120	8.95	34.4
14.0	54.6	0.093	10.75	48.8
19.10	77.2	0.077	13.0	69.10

$$G_L = 165 \text{ lb/ft}^2 \text{ sec. } \left( \frac{\Delta P}{\delta L} \right)_L = 2.68280 \text{ lb/ft}^2$$

$G$ lb/ft. <sup>2</sup> sec.	$\left( \frac{\Delta P}{\delta L} \right)_{T.P.}$ lb.ft. <sup>2</sup>	$R_L \cdot X_L$	$\frac{1}{R_L} \cdot \frac{X}{X_L}$	$\left( \frac{\Delta P}{\delta L} \right)_{T.P.}$ $\left( \frac{\Delta P}{\delta L} \right)_L$
0.122	3.82	0.732	1.37	1.42
0.206	4.84	0.614	1.63	1.60
0.361	6.00	0.489	2.055	2.26
0.526	7.80	0.445	2.23	2.90
1.30	12.50	0.316	3.16	4.65
2.18	22.30	0.258	3.93	8.30
3.98	30.1	0.234	4.27	11.30
5.59	42.7	0.187	5.35	15.90
6.55	46.1	0.161	6.47	17.20
9.45	60	0.148	6.75	23.30
14.10	83.5	0.122	8.20	31
19.30	99.5	0.098	10.20	37.0

ADDENDUM TO THESIS ON

" PHASE DISTRIBUTION AND FLOW CHARACTERISTICS OF  
ISOTHERMAL CO-CURRENT TWO-PHASE FLOW IN HORIZONTAL PIPES"

BY

SHAWKY ASSAAD HARKLY

B. Sc., A.R.T.C

Use of non-dimensional parameters in correlating the  
results of two phase experiments.

Introduction:

In experimental work on fluid flow, the direct plotting of test results provides graphs which show the relationship between the measured quantities.

The application of these relationships is strictly limited to the conditions obtaining in the particular experiments involved. No wider interpretation of the results is permissible.

To obtain more general correlation of the results taken from widely varying sets of conditions, it is helpful to carry out dimensional analysis of all the relevant physical quantities and then either by the application of the  $\pi$  theorem or by inspection, to collect these quantities into independent non-dimensional groups.

Graphs obtained by plotting two independent non-dimensional groups against one another then have quite general application provided the remaining groups involved are held constant. This process has proved of inestimable value in correlating results obtained in widely different branches of fluid flow.

It must be stressed that a rational treatment is only possible if all the physical quantities involved in the problem/



/problem are included in the dimensional analysis.

As an example, in single phase incompressible viscous fluid flow in a pipe, it has been shown that

$$F = \rho V^2 D^2 f \left( \frac{\rho V D}{\mu} \right)^n$$

where

$$F = \text{friction force} \quad \text{lb ft/sec}^2 (\text{MLT}^{-2})$$

$$\rho = \text{fluid density} \quad \text{lb/ft}^3 (\text{ML}^{-3})$$

$$V = \text{velocity of flow} \quad \text{ft/sec} (\text{LT}^{-1})$$

$$D = \text{pipe diameter} \quad \text{ft} (\text{L})$$

$$\mu = \text{fluid viscosity} \quad \text{lb/ft sec} (\text{ML}^{-1}\text{T}^{-1})$$

A close examination would show that this relationship is dimensionally valid.

Writing

$$\frac{F}{\rho V^2 D^2} = f \left( \frac{\rho V D}{\mu} \right)^n$$

the non-dimensional group  $\frac{\rho V D}{\mu}$  is the well known Reynolds number  $R_e$  and  $\frac{F}{\rho V^2 D^2} = \lambda$  the coefficient of friction.

A single graph relating  $\lambda$  and  $R_e$  is universally used for pressure drop calculations.

This example illustrates the great use of dimensional analysis.

Application of dimensional analysis to Two phase flow:

The difficulty in treating gas-liquid flow is due on one hand to the different properties of gas and liquid and on the other to the complex flow patterns which the combination of the phases makes possible.

This is evidenced by the treatment given to the problem. An attempt to correlate pressure drop test results was given by Martinelli and co-workers (46)<sup>\*</sup> who assumed four possible combinations of either viscous and turbulent flow of each phase.

Even this seems to be an over-simplification of the problem as it was shown by Gazley (11) to lack general application and it was evident that each mode of flow would require different treatment. For every form of flow it appears important to define the channel occupied by each phase.

The three distinct modes of flow to consider are bubble, stratified, and annular flow. For the first the liquid is definitely the continuous phase wetting the entire surface of the pipe, with air bubbles being dispersed throughout. In this case therefore it would seem reasonable in the dimensional analysis to use parameters associated with the liquid. In the case of stratified flow each phase would be treated separately as /

---

\* Numbers between brackets refer to the bibliography as mentioned in the thesis and compiled at the end of this addendum.

/as has been shown by Gazley (11) and simple hyrdrodynamics formulae applied for each phase with its respective channel. These two simple cases are not very common in practice and are associated with small flow rates either of gas relative to the liquid or of both gas and liquid.

In annular flow interfacial surface irregularities, entrainment of liquid and variation in the shape of annulus complicate the problem considerably as was emphasized in chapters 4 and 5 of the thesis. For the annular flow mode the liquid wets the pipe circumference. Flow conditions would appear to be controlled by turbulence i.e., inertia forces in the core and by viscous forces at the wall i.e., the liquid film. Subsequent analysis shows that the liquid flow reflects the core conditions sufficiently to allow liquid properties to be considered as the physical quantities that control the two phase flow.

Thus we can write

$$\Delta P = f (\rho_l, V_l \text{ or } W_l, W_g, \mu_l, \sigma, g)$$

where  $\rho_l$  liquid density lb/ft

$W_l$  liquid flow rate lb/sec

$W_g$  gas flow rate lb/sec

$V_l$  liquid velocity based on ft/sec total pipe area.

D pipe diameter ft

$\mu_l$  liquid viscosity lb/sec·ft

$\sigma$  liquid surface tension lb/ft

g gravitational acceleration ft/sec<sup>2</sup>

grouping/

/grouping these quantities in non-dimensional parameters we get

$$\Delta P = \rho V^2 \phi \left[ \frac{\rho V_l^2 D}{\sigma}, \frac{V_l^2}{gD}, \frac{\rho V_l D}{\mu_l}, \frac{W_g}{W_l} \right] \quad (1)$$

dividing by appropriate length quantities, equation (1) can be written as:

$$\left( \frac{\Delta P}{\Delta L} \right)_{T.P.} / \frac{\rho V_l^2}{D} = \phi \left[ W_e, F_r, R_e, \frac{W_g}{W_l} \right] \quad (2)$$

where  $W_e$  = Weber number

$F_r$  = Froude number

$R_e$  = Reynolds number

It may be that pipe roughness would play an important part, so to generalise equation (2) roughness factor  $\frac{k}{D}$  may be added to the parameters where

$k$  = mean wall roughness

Thus equation (2) reads

$$\left( \frac{\Delta P}{\Delta L} \right)_{T.P.} / \frac{\rho V_l^2}{D} = \phi \left[ W_e, F_r, R_e, \frac{W_g}{W_l}, \frac{k}{D} \right] \quad (3)$$

Assuming that we are working with similar pipes (i.e.,  $\frac{k}{D}$  is constant) this factor can be dropped.

For complete dynamical similarity it is essential to keep  $W_e$ ,  $F_r$ ,  $R_e$  and  $W_g/W_l$  all constant which is physically impossible.

Thorough examination of the problem should however decide which of these groups are important in relation to particular modes of flow.

#### 1. Weber Number :

Weber number is the ratio between inertia forces and surface tension.

For/

TABLE I  
EFFECT OF SURFACE TENSION ON  $(\Delta P)_{T.P.}$   
 $1 \frac{1}{2} \Phi$  Steel Pipe

Air Flow $lb/Ft^2 sec$	Water Flow $lb/Ft^2 sec$	$(\Delta P)_{T.P.}$ $lb/Ft^2$ (TAP WATER)	$(\Delta P)_{T.P.}$ $lb/Ft^2$ (S.T. Reduced)
8.95	14.2	210	208
9.15	28.5	247	254
9.30	38.0	304	312
12.0	14.2	269	255
12.40	28.5	360	353
12.70	38.0	446	453
17.30	14.2	339	328
17.80	28.5	501	510
17.80	38.0	620	613
19.0	14.2	438	422
20.2	28.5	623	618
20.4	38.0	785	773

Air Flow $lb/Ft^2 sec$	Water Flow $lb/Ft^2 sec$	$(\Delta P)_{T.P.}$ $lb/Ft^2$ (Tap Water)	$(\Delta P)_{T.P.}$ $lb/Ft^2$ (S.T. Reduced)
6.25	39	159	163
6.32	56.5	193	204
6.40	85	252	143
6.50	119	360	357

/For two phase flow Martinelli and co-workers (46) reported that pressure drops measured in the case of co-current air and water-nekal mixtures proved that reduction of surface tension has no effect on pressure drop. In the present experimental work, during the course of phase distribution examination, when lissapol was added to water, pressure drops were noted. Some of the results as compared with the same tests using plain water are given in Table (1) which confirms Martinelli's conclusion. The fact that surface tension has no effect on pressure drop may be explained by reference to phase distribution. When surface tension was reduced the distribution of entrained liquid changes but not the quantity; thus the thickness of the water layer does not vary. Thus the interfacial shear forces remain constant.

It can be concluded that surface tension has little effect on pressure drop and Weber group can be ignored and equation (2) becomes

$$\frac{(\Delta P)}{AL}_{T.P.} / \frac{\rho V^2}{D} = \phi [ Fr, Re, \frac{Wg}{W_l} ] \quad (4)$$

2. Froude Number;

Froude number is the ratio between inertia forces and gravity forces. For the present analysis it is based on the mean velocity of the liquid over the pipe cross section using the pipe diameter as parameter.

In two phase flow in a horizontal pipe, with low flow velocities, gravity is an important factor since it plays some part in establishing the different flow patterns. It affects entrainment which depends on the balance between the aerodynamic turbulent/

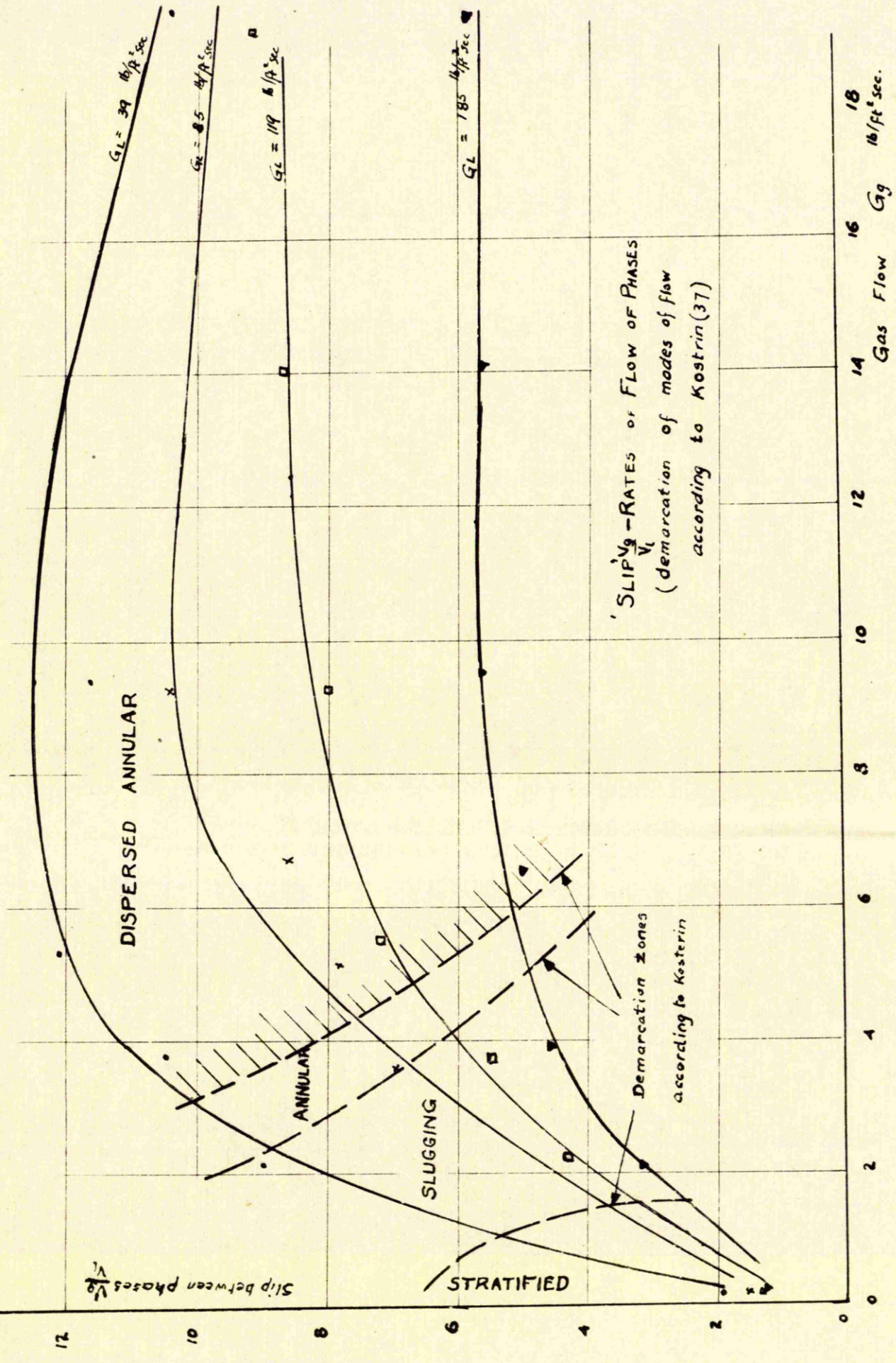


Fig. 62

/turbulent forces and the settling velocity due to gravity. At low velocities when large drops of liquid form, its influence is significant. At high velocities, however, the major portion of the liquid is carried as a suspension of fine particles. Thus due to the combination of high velocities and the small particle size the influence of gravity is very much reduced and settling effect is small as compared with turbulent forces.

Confirmation of this argument is shown by the constancy of 'slip' between phases at high air flow rates. Fig. (59) from the thesis has been reproduced in Fig. (62). It shows 'slip' being plotted against gas flow rate for constant values of water flow rates. Upon this graph has been superimposed lines of demarcation between the different forms of flow, which have been derived from the work of Kosterin (37). From Fig. (62) it is clear that 'slip' is only constant in the case of dispersed annular flow form which occurs at high gas flow rates.

It can therefore be concluded that provided these flow rates are high Froude number need not be included and equation (4) becomes

$$\left(\frac{\Delta P}{\Delta L}\right)_{T.P.} / \frac{\rho v_l^2}{D} = \phi [R_e, \frac{W_g}{W_l}] \quad (5)$$

### 3. Reynolds Number:

Reynolds number expresses the ratio between inertia forces and viscous forces acting on fluid particles.

In turbulent flow the forces existing at the wall through the laminar sublayer are due to viscous shear. For single phase flow this layer diminishes in thickness as  $R_e$  increases and viscous/

/viscous forces diminish with respect to inertia forces. Rough walls would cause a quicker decrease in laminar sublayer effect. These two facts are illustrated by nearly constant coefficient of friction at very high values of Reynolds number for smooth pipes and the marked increase of friction coefficient for rough pipes as well as the extension of the zone of constancy to lower values of  $R_e$  as shown by Nikuradse's observations (47).

The significance of  $R_e$  in two phase flow may be discussed for the three modes of flow.

In bubble flow, the pressure drop may be correlated by the familiar  $R_e - \lambda$  relationship.

In stratified flow Gazley(11) has shown that the two phases could be treated separately with their individual values of  $R_e$ . In this case the hydraulic diameter is given by

$$d = \frac{4(\text{area occupied by the phase})}{\text{wetted perimeter}}$$

He also pointed out that when waves occur at the interface,  $\lambda$  values increase considerably due to the expenditure of work for wave making.

In annular flow, if the total water is assumed to run as an annulus on the tube wall, then the characteristics of the flow in this annulus will be comparable with those for single phase liquid flow and consequently Reynolds number for the liquid would be used. In this case the hydraulic diameter can be expressed as  $d = 4 y_o$ .

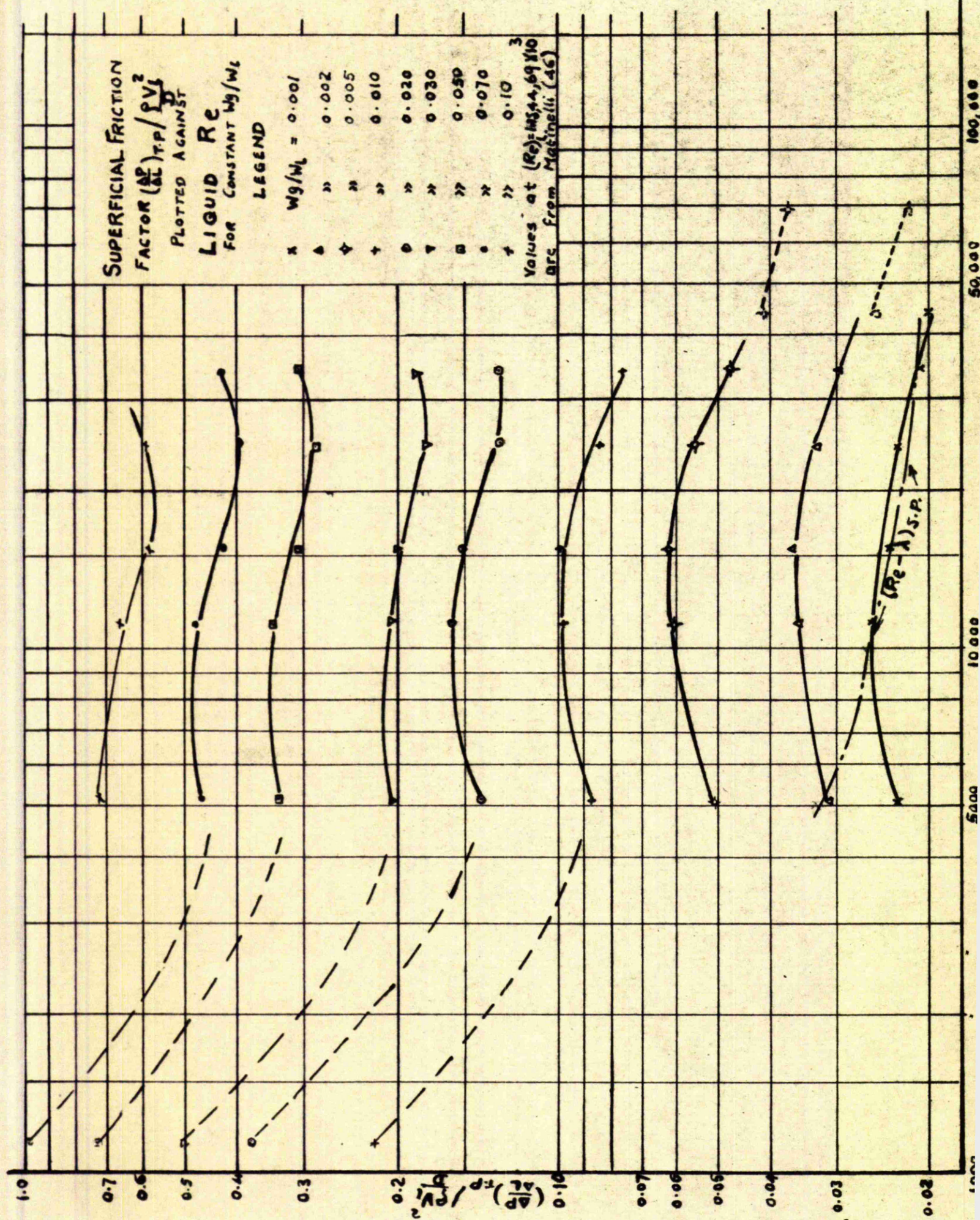


Fig. 63

where

$y_0$  = thickness of the annulus.

Thus

$$\begin{aligned} (R_e)_l &= \frac{G_l \cdot \frac{\pi}{4} D^2}{\pi D y_0} \cdot \frac{4 y_0}{\mu_L} \\ &= \frac{G_l \cdot D}{\mu_L} \end{aligned} \quad (6)$$

where

$G_l$  = mass velocity of the liquid  $\text{lb}/\text{ft}^2 \text{sec}$

$(R_e)_l$  is the same as for liquid flow when it occupies the total cross section of the pipe.

It should be noted however that this is only precise when the total liquid is contained in the annulus. In the present work it has been found that varying amounts of liquid are entrained in the gas stream, hence the values of  $R_e$  obtained on the above basis will be approximate.

The graph obtained by plotting  $(\frac{\Delta P}{L})_{T.P.} / \frac{\rho v_l^2}{D}$  against  $(R_e)_l$  for constant values of  $W_g/W_l$  are shown in fig. 63.

Due to the limitations of the apparatus the experimental results are confined to a range of water flow from 39 to 260  $\text{lb}/\text{ft sec}$ . The range of  $W_g/W_l$  covered in these tests is from 0.001 to 0.100. To extend the range of  $R_e$  values, the results of Martinelli (46) were analysed and plotted on the presented curves.

From these curves the first point of importance to note is that there is a separate curve for each particular value of  $W_g/W_l$ . This emphasises at the outset, the marked difference between single phase and two phase flow. The second point/

point is that the form of the curve changes progressively as the value of  $W_g/W_1$  increases, a fact which again emphasises the importance of the ratio of the flow rates of the two phases. These two observations together underline the difficulty of finding suitable non-dimensional parameters for correlating the results of experiments in two phase flow.

A curve has been added at the bottom of fig. 63 showing  $\lambda - R_e$  relationship for the pipe as obtained from tests carried out by using air only. As would be expected it lies close to the two phase flow curve for  $W_g/W_1 = 0.001$  representing the closest approach to single phase flow. The divergence at values of  $R_e < 10,000$  may be attributed to the transition to stratified flow in this range and friction forces would be smaller due to decreased liquid wetted perimeter.

In the graphs obtained where  $W_g/W_1 > 0.02$  it will be seen that  $(\frac{\Delta P}{\Delta L})_{TP} / \frac{\rho v^2}{D}$  falls to a minimum value and then rises. This characteristic may be explained by the influence of entrained liquid particles on the water layer flowing over the tube wall. The entrained particles may bombard the water annulus and so disturb the laminar sublayer. It is analogous to an increase in pipe roughness. A similar phenomenon was reported by Ismail (31) in the case of liquid-solid suspension.

The dispersal of the curves shows that the use of Reynolds number based on liquid properties is not sound.

To explore the possibilities of non-dimensional parameters/

TABLE II

$$Re_g - \left(\frac{\Delta P}{\Delta L}\right)_{T.P} / \frac{\rho V_g^2}{D}$$

$\frac{W_g}{W_L}$	$G_t = 39 \frac{lbf}{ft^2 sec}$		$G_t = 85 \frac{lbf}{ft^2 sec}$		$G_t = 119 \frac{lbf}{ft^2 sec}$		$G_t = 185 \frac{lbf}{ft^2 sec}$	
	Reg	$\left(\frac{\Delta P}{\Delta L}\right)_{T.P} / \frac{\rho V_g^2}{D}$	Reg	$\left(\frac{\Delta P}{\Delta L}\right)_{T.P} / \frac{\rho V_g^2}{D}$	Reg	$\left(\frac{\Delta P}{\Delta L}\right)_{T.P} / \frac{\rho V_g^2}{D}$	Reg	$\left(\frac{\Delta P}{\Delta L}\right)_{T.P} / \frac{\rho V_g^2}{D}$
0.001	290	30	660	34	920	31	1500	29.5
0.002	580	9.8	1300	11.7	1800	12.1	2900	10.7
0.005	1450	2.72	3100	3.2	4300	3.25	6900	3.0
0.010	2950	1.15	6000	1.29	8400	1.36	13500	1.36
0.020	5900	0.45	12000	0.532	16500	0.54	26500	0.628
0.050	14500	0.216	28500	0.195	39200	0.185	64000	0.180
0.070	20500	0.139	40000	0.139	55000	0.136	80000	0.136
0.10	30000	0.102	56000	0.097	76300	0.095	120000	0.133
0.160	48500	0.092	103000	0.083	141500	0.081		
0.230	68000	0.063	146000	0.061				
0.350	127000	0.042						
0.50	145000	0.0365						

parameters based on the gas phase physical properties, values of  $(R_e)_g$  and  $(\frac{\Delta P}{\Delta L})_{T.P.} / \frac{\rho V_g^2}{D}$  were calculated, where

$$(R_e)_g = G_g \cdot D / \mu_g$$

$G_g$  = mass velocity of the gas      lb/ft<sup>2</sup> sec

The values obtained are tabulated in Table (2) and clearly show the lack of relationship between the two functions.

As already stated, the main difficulty in employing Reynolds number for two phase flow lies in the choice of the appropriate physical values for the mixture over the wide range of complex modes of flow. Even if the gas stream in the core, dispersed with liquid particles, is assumed to be homogeneous and the gas itself is taken as the continuous phase, yet changes in mass velocity ( $\phi V$ ) and viscosity ( $\mu$ ) for the mixture would be subject to change due to varying degrees of entrainment.

It appears therefore that  $R_e$  for either of the two phases has secondary significance in gas-liquid flow characteristics and equation(5) may be written as

$$(\frac{\Delta P}{\Delta L})_{T.P.} / \frac{\rho V_i^2}{D} = \phi [ \frac{W_g}{W_l} ] \quad (7)$$

#### 4. Phase weight ratio $W_g/W_l$ :

Having shown that  $W_e$ ,  $F_e$ ,  $R_e$  in turn fail as significant parameters for correlating pressure drops, it remains only to test the importance of the phase weight ratio  $W_g/W_l$ .

To do this, values of  $(\frac{\Delta P}{\Delta L})_{T.P.} / \frac{\rho V_i^2}{D}$  were plotted against/

Variation of Superficial Friction  
Coefficient  
 $(\frac{\Delta P}{\Delta L})_{TP} / \rho V_L^2$  with  $\frac{Wg}{W_L}$

LEGEND

▲	$G_L$	3.9	$16/\text{ft}^2\text{sec}$
□	$G_L$	8.5	$16/\text{ft}^2\text{sec}$
+	$G_L$	11.9	$16/\text{ft}^2\text{sec}$
○	$G_L$	18.5	$16/\text{ft}^2\text{sec}$
×	$G_L$	26.0	$16/\text{ft}^2\text{sec}$

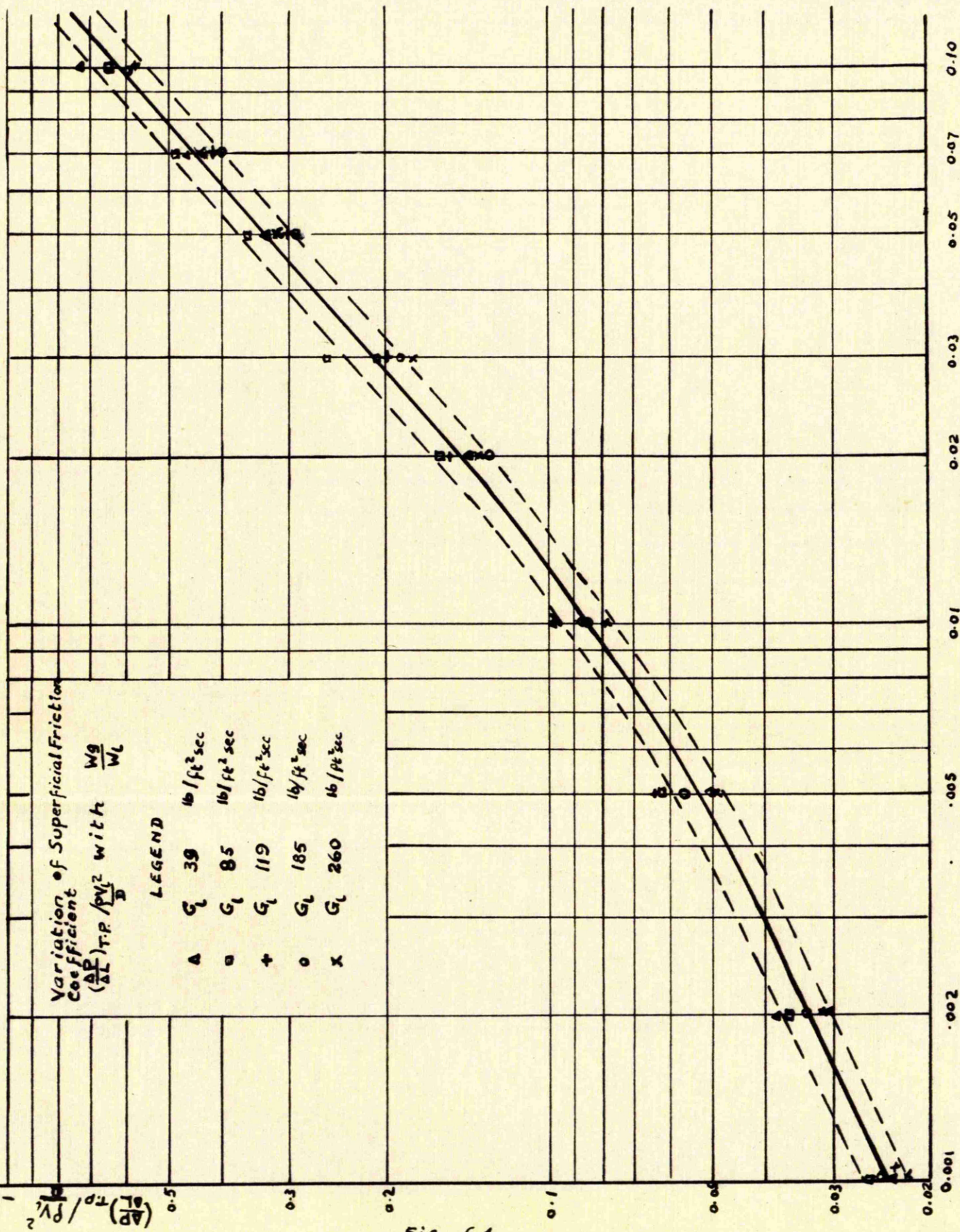


Fig. 64

$Wg / W_L$

Fig. 64

against  $W_g/W_l$ . The graph obtained is shown in fig. 64 in which the dotted lines indicate the band within which the experimental points fall.

From this graph it is evident that the dominant parameter is the weight ratio of the two phases. The relationship could be written as

$$\left(\frac{\Delta P}{\Delta L}\right)_{T.P.} / \frac{\rho V_l^2}{D} = K_1 + K_2 \left(\frac{W_g}{W_l}\right)^n \quad (8)$$

When there is only single phase liquid flow i.e.  $W_g/W_l = 0$  the value  $K_1 = \lambda$ . Thus with suitable constants for  $K_2$  and  $n$  equation (8) reads

$$\left(\frac{\Delta P}{\Delta L}\right)_{T.P.} / \frac{\rho V_l^2}{D} = 0.022 + 6.2 \left(\frac{W_g}{W_l}\right) \quad (9)$$

It should be noted that equation (9) obtained from dimensional analysis resembles equation (39) in the thesis viz.

$$\left(\frac{\Delta P}{\Delta L}\right)_{T.P.} / \left(\frac{\Delta P}{\Delta L}\right)_l = 0.80 \left(\frac{x}{x_l}\right)^{1.7}$$

since both are dependent on the ratio of flow rates of the phases. Equation (9), however, has a certain advantage that the weight ratio is more easily obtained than the ratio of cross sectional areas occupied by the phases. It is interesting also to note the similarity between this equation and that already developed by Gasterstadt (21) for the case of gas-solid flow.

#### Conclusions:

This further analysis of the results using non-dimensional parameters has proved to be of value in that it has shown more clearly the relative importance of the various non-dimensional groups. It has established that in annular

dispersed two phase flow, the weight ratio of the two phases assumes greater importance than the other groups i.e.  $W_e$ ,  $F_r$  and  $R_e$  and has produced a correlating formula in terms of the weight ratio which is applicable to the case of annular dispersed two phase flow.

References.

N.B. The numbers refer to those as quoted in the thesis

3. Armand A. A. 'Resistance to two phase flow in horizontal pipes' Izvestia W.T.I. USSR (1946) p.16
11. Berglin O.P. & Gazley C. 'Co-current gas-liquid flow in horizontal pipes' Heat transfer & Fluid mech. Inst. A.S.M.E. (1949) p.5
21. Gasterstadt 'Experiments on pneumatic transportation' Zeit. V.D.I. vol. 68 (1924) p.617-24
31. Ismail H.M. 'Turbulent transfer mechanism of suspended sediment in closed channels' Amer. Soc. of Civil Engrs. vol.117(1952)p409
37. Kosterin S.I. 'Investigation of the influence of diameter and layout of pipe on hydraulic resistance and form of flow of a mixture of gas and liquid' Izvestia Akad.Nauk.USSR vol.12(1949)
46. Martinelli R.C. and others 'Isothermal pressure drop for two phase, two component flow in a horizontal pipe' Trans.A.S.M.E. vol.66(1944) p.39
47. Nikuradse J. 'V.D.I. Forschungsheft vol. 21(1932)p.356



